uOttawa

L'Université canadienne
Canada's university

FACULTÉ DES ÉTUDES SUPÉRIEURES ET POSTOCTORALES

uOttawa

L'Université canadienne
Canada's university

FACULTY OF GRADUATE AND POSDOCTORAL STUDIES

Lisa Bevilacqua
AUTEUR DE LA THÈSE / AUTHOR OF THESIS

Ph.D. (Biochemistry)
GRADE / DEGREE

Department of Biochemistry, Microbiology and Immunology
FACULTÉ, ÉCOLE, DÉPARTEMENT / FACULTY, SCHOOL, DEPARTMENT

The Effects of Aging and Calorie Restriction on Whole-body and Mitochondrial Energetics

TITRE DE LA THÈSE / TITLE OF THESIS

Mary-Elen Harper
DIRECTEUR (DIRECTRICE) DE LA THÈSE / THESIS SUPERVISOR

CO-DIRECTEUR (CO-DIRECTRICE) DE LA THÈSE / THESIS CO-SUPERVISOR

EXAMINATEURS (EXAMINATRICES) DE LA THÈSE / THESIS EXAMINERS

Douglas Gray

Steven Smith

Michael McBurney

Jean-Marc Renaud

Gary W. Slater
Le Doyen de la Faculté des études supérieures et postdoctorales / Dean of the Faculty of Graduate and Postdoctoral Studies

The effects of aging and calorie restriction on whole-body and mitochondrial energetics

LISA BEVILACQUA

In partial fulfilment of requirements for the degree of Doctor in Philosophy

Department of Biochemistry, Microbiology and Immunology

Faculty of Medicine

May 2007

Your file Votre référence
ISBN: 978-0-494-41604-4
Our file Notre référence
ISBN: 978-0-494-41604-4

ABSTRACT

It has been well documented that calorie restriction (CR) without malnutrition is an effective strategy to improve health and extend lifespan in a variety of species. The mechanisms underlying CR are unclear. We proposed that a reduction in proton leak-dependent respiration could play a central role in the action of CR by inhibiting reactive oxygen species (ROS) production. In support of this hypothesis, we found that CR resulted in a rapid and sustained reduction in both maximum leak-dependent respiration and ROS production in skeletal muscle mitochondria. We also demonstrated that CR appears to decrease ROS production by different mechanisms in the acute and chronic settings. To further pursue the mechanism governing these adaptations, we also examined the effect of acute CR in Uncoupling Protein-3 knockout mice (*Ucp3*-KO mice) and wild-type mice. We found that CR decreased skeletal muscle mitochondrial proton leak-dependent respiration in the wild-type, but not in the *Ucp3*-KO mice. The kinetic response of the proton leak reactions in *Ucp3*-KO mice subjected to CR indicated increased proton conductance, whereas no CR-induced differences were observed in wild-type mice. Further assessment of these differences suggest that alterations in proton leak with acute CR occur via a UCP3-independent mechanism, that to some extent, involves the Adenine Nucleotide Translocator (ANT). In summary, this dissertation demonstrates that the benefit of CR is mediated, at least in part, by a decrease in the production of ROS. However, the mechanisms underlying the action of CR are complex and involve several processes, including hypometabolism and mitochondrial proton leak. Further *in vitro* and *in vivo* research is warranted to better understand these mechanisms. Research in this area has important implications as it may lead to novel treatment strategies (*e.g.*, nutraceuticals or pharmaceuticals) that could improve the quality of life for an increasing aging population.

DEDICATION

This thesis is dedicated to my parents and sister. Thank you for all your constant encouragement and support throughout my studies.

Dedico questa tesi ai miei genitori e alla mia sorella. Grazie del vostro incoraggiamento ed appoggio continuo durante questi anni di studio. Ti amo!

ACKNOWLEDGEMENTS

I would like to take the opportunity to thank everyone who has supported me throughout my time at the University of Ottawa and who has helped bring this project to fruition.

- I am extremely grateful to my supervisor Dr. Mary-Ellen Harper. She has always been there as a constant source of guidance, encouragement, support and enthusiasm. Mary-Ellen has provided me with invaluable opportunities that have made my Ph.D. experience extremely rewarding. *Mary-Ellen, I will never be able to thank you enough for being such an amazing mentor, friend and inspiration.*

- I would like to acknowledge our collaborators in these studies: Dr. Jon Ramsey (University of California, Davis) and Dr. Richard Weindruch (University of Wisconsin, Madison). Thank you for allowing me to be part of such interesting and fulfilling body of work.

- I would like to acknowledge OGS, NSERC and the University of Ottawa, Department of Biochemistry, Microbiology and Immunology for their financial support throughout my graduate studies.

- To my thesis advisory committee, Drs. Steffany Bennett (University of Ottawa, Department of BMI) and Jean-Michel Webber (University of Ottawa, Department of Biology). Thank you for your time, insight, and support throughout this thesis.

- I would like to thank Dr. Shadi Monemdjou. Thank you for providing me with the technical training that I needed to complete this project. I wish you the best of luck in your career and life!

- I simply could not have made it through the last few years without the guidance and friendship of Dr. Martin Gerrits (a.k.a McGuyver). Thank you for never activating the "3 questions/day" rule. Thank you for your constant technical assistance and more importantly for your encouragement whenever I needed it.

- To Dr. Veronic Bezaire and Dr. Erin Seifert. Thanks for making the last few years in the lab so enjoyable. I have learned so much from both of you. Erin, I am extremely grateful for all the help you have provided me during the writing of my dissertation. Your editorial comments and suggestions have been very useful.

- To my fellow Harper lab graduate students, Sheila Costford and Adrienne Gowing. Thanks for the good times in and out of the office! Sheila best of luck as you finish up your degree and then at your post-doc! I'm confident that you'll be a terrific P.I. Adrienne, I wish you the best in whatever path you choose! You both deserve the best!

- To Mahmoud Salkhordeh. Ahh, Mahmoud! What would we do without you! Thanks for being a great technician and thanks for making the lab so much fun! I'll miss your funny jokes and stories! Remember, if your "Labmates" TV show ever gets a television deal, I want a cut! Seriously, I wish you and your family a lifetime of health and happiness!

- Over the years, I have been fortunate to work with a terrific group of technicians and students in the Harper Lab. Thanks for making the lab an intellectually motivating and fun place to work.

- To Shelley, Rosalie, Ola and Kathy. I could not have made it through undergrad and graduate school without our weekend getaways and vacations. I am glad to be part of such an amazing circle of friends! I wish the best for each of as you complete your PhDs and MDs. I look forward in continuing to share all the important moments of our lives together.

- To my cousins, Elizabeth, Angelo, and Gloria. Thanks for your encouragement, and friendship. I also want to thank your mom, for providing a great example of living life to its fullest everyday. I know she is looking down upon us smiling and guiding us in the right direction. To my Zia Beatrice, you are truly missed.

- To the Pavone family. You are all such wonderful people! Thanks for making me feel so welcome in your family. I look forward to Pavone family fun night every Tuesday! Thanks for your support, friendship, Greys Anatomy and Sequence.

- I would like to extend a huge thank you to my grandparents. They have instilled in me the importance of family and respect. I would like to dedicate this to the memory of my Nonno Domenico, Nonna Giuditta and Nonno Rocco. To my Nonna Carmela, thank you for providing me with a quite place to work when I needed to focus. You have taught me so many lessons that I will hopefully carry through to my children. Grazie per tutto! Ti voglio molto bene!

- Last but not least, I would like to thank Cris. There is nothing I could say to even come close to properly expressing my gratitude for your unwavering support, encouragement and patience over the last few years. I look forward to sharing the rest of our lives together... SO, now that my thesis is submitted I have one thing to say ... My ring size is... 5 (wink, wink)! Love you!

TABLE OF CONTENTS

LIST OF TABLES

LIST OF FIGURES

LIST OF ABBREVIATIONS

A

ACS	acyl-coenzyme A synthase
ADP	adenosine 5'-diphosphate
ADP:O	number of ADP molecules phosphorylated for each oxygen molecule reduced
AGE	advanced glycation end-products
AIN	American Institute of Nutrition
ANOVA	analysis of variance
ANCOVA	analysis of covariance
ANT	adenine nucleotide translocase
ATP	adenosine 5' –triphophate

B

ß-oxidation	beta oxidation
BAT	brown adipose tissue
BHT	butylated hydoxytoluene
BMI	body mass index
BMR	basal metabolic rate
BSA	bovine serum albumin
BWt	body weight

C

$CaCl_2$	calcium chloride
CAT	carboxyatractylate
CO_2	carbon dioxide
CoA	coenzyme A
Complex I	NADH-CoQ reductase or NADH dehydrogenase
Complex II	succinate dehydrogenase
Complex III	cytochrome bc1 complex or CoQ-cytochrome c reductase
Complex IV	cytochrome c oxidase
Complex V	ATP synthase
CR	calorie restriction
CRON	calorie restriction with optimal nutrition
CRS	calorie restriction society
CPT1	carnitine palmitoyl transferase 1
$CuSO_4.H_2O$	copper sulphate pentahydrate
Cyt c	cytochrome c

D

d	day
ddH_20	deionized distilled water
DNA	deoxyribonucleic acid
DR	dietary restriction

E

ECL	enhanced chemilunescence
EDTA	ethlenediamine tetraacetic acid
EE	energy expenditure
e.g.,	example
EGTA	ethylene glycol-bis tetraacetic acid
ETC	electron transport chain
ER	energy restriction
EWAT	epididymal white adipose tissue

F

$FADH_2$	flavin adenine nucleotide dinucleotide (reduced form)
$FBNF_1$	cross between Brown Norway X Fisher 344 rat strains
f.c.	final concentration
FCCP	carbonyl cyanide *p*-(trifluoromethoxy)-phenylhydrazone
FFA	free fatty acid
FMN	flavin mononucleotide
FR	food restriction

G

g	centrifugal force
g	gram
GDP	guanosine diphosphate
GH	growth hormone
GPx	gluthathione peroxidase
GSH	reduced glutathione
GSSG	oxidized glutathione
GTP	guanosine triphosphate

H

4-HNE	4-hydroxy-2,3,-trans-nonenal
8-oxodG	8-hydroxy 2-deoguanosine
h	hour

H_2O_2	hydrogen peroxide
HCl	hydrochloric acid
HDL	high density lipoprotein
HEPES	hydroxyethyl piperazine ethane sulphonic acid
Hsp	heat shock protein
Ucp3	human uncoupling protein gene, or its mRNA transcript
UCP3	human uncoupling protein (protein form)

I

i.e.,	in other words
IGF-1	insulin-like growth factor 1
IgG	immunoglobulin G

K

K_2HPO_4	dipotassium phosphate
KCl	potassium chloride
kDa	kilodalton
KH_2PO_4	potassium dihydrogen orthophosphate
KOH	potassium hydroxide

L

l	litre
LCFA	long-chain fatty acid anion
LDL	low density lipoprotein
Log	logarithm (base 10)

M

M	moles/litre
mg	milligram
$MgCl_2$	magnesium chloride
$MgSO_4$	magnesium sulphate
MIM	mitochondrial inner membrane
min	minute
ml	milliliter
MLSP	maximum lifespan
mm	millimeter
mM	millimole/litre
mo	month
MOM	mitochondrial outer membrane
mole	mole
mRNA	messenger ribonucleic acid

mtDNA	mitochondrial DNA
MTE-1	mitochondrial thioesterase-1
mV	millivolt

N

Na_2EDTA	ethylenediamine tetraacetic acid (disodium salt)
NAD	nicotinamide adenine dinucleotide
NADH	nicotinamide adenine dinucleotide (reduced form)
NEFA	non-esterified free fatty acid
nDNA	nuclear DNA
ng	nanogram
NIA	National Institute of Aging
nm	nanometer
NST	non-shivering thermogenesis
NO	nitric oxide
NO_2	nitrate
NO_3	nitrite

O

O	monoatomic oxygen
O_2^-	superoxide
O_2	molecular (diatomic) oxygen
OH^-	hydroxyl radical
ONOO	peroxynitrite

P

P_i	inorganic phosphate
PAGE	polyacrylamide gel electrophoreseis
PGC-1α	peroxisome-proliferator-activated receptor-gamma co-activator, 1 alpha
PHPA	p-hydroxyphenylacetate
PMF	protonmotive force
PPAR	peroxisome proliferators-activated receptor
PPRE	PPAR-response element
PRCF	percent relative cumulative frequency
PRX	peroxireductase

R

RCR	respiratory control ratio
RER	respiratory exchange ratio
RMR	resting metabolic rate

RNA	ribonucleic acid
RNS	reactive nitrogen species
ROS	reactive oxygen species
Rpm	revolutions per minute
RT-PCR	real-time polymerase chain reaction

S

SDS	sodium dodecyl sulphate
SEM	standard error of the mean
SIRT1	mammalian homolog of silent mating type information regulation 2
SMR	standard metabolic rate
SOD	superoxide dismutase
State 3	maximal phosphorylating respiration
State 4	maximal non-phosphorylating respiration

T

T_3	triiodothyronine
T_4	thyroxine
TBARS	thiobarbituric acid reactive substance
TCA	tricarboxylic acid cycle
TIM	translocator inner membrane
TOM	translocator outer membrane
$TPMP^+$	triphenylmethylphosphonium cation
TPMP-Br	triphenylmethylphosphonium bromide
TSH	thyroid stimulating hormone
TRE	thyroid response element

U

U	units
Ubiquinone	ubiquinol or coenzyme Q10
Ucp	uncoupling protein gene, or its mRNA
Ucp3-knockout	mice lacking UCP3
UCP	uncoupling protein (protein form)
UCP-3Tg	transgenic mice overexpressing UCP3

V

v/v	volume per volume
V	volts
VDAC	voltage dependent anion channel

W

WAT	white adipose tissue
wt/vol	weight per volume

Symbols

~	approximately
$\Delta\Psi m$	mitochondrial membrane potential
Δp	mitochondrial proton motive force
ΔpH	pH gradient
°C	degrees Celsius
µg	microgram
µL	microlitre
µm	micrometre
µM	micromole/litre

CHAPTER 1
INTRODUCTION AND LITERATURE REVIEW

1.1 INTRODUCTION

Throughout history humans have been preoccupied with increasing lifespan, slowing or even reversing the process of aging (Masoro, 2002). Alexander the Great (356-323 B.C.) wrote about encountering the "fountain of life". In 1512, the Spanish explorer, Ponce de Leon (1460-1521) led an expedition around the Caribbean searching for the mystical fountain of youth, which was described by local Indian folklore as a magical spring that could make older people young again (Finkel, 2003). Over time numerous substances have been purported as "magic bullets" or elixirs that prevent aging. In addition, various lifestyle changes such as good hygiene and dietary practices have also been supposed methods for slowing aging. The 14th century Italian author, Luigi Cornaro wrote in "Discorsi Della Vita Sobria (Discourse of a Sober Life)" that good hygienic and dietary practices would increase longevity. He lived to be 102 years old. Anecdotally, it was thought that his long life was a result, of following two rules: 1) eat what agrees with your digestion (i.e., quality foods) and 2) eat as little as possible (i.e., reduce the quantity) (Masoro, 2002).

Life expectancy, which is also referred to as mean lifespan, is defined as the age at which there is a 50% survival in the population studied. Over the last hundred years it has increased significantly in developed countries due to improvements in environmental factors such as hygiene, nutrition and medical care. The outcome has been that the life

expectancy of Canadians has increased from 47.3 years of age in 1900 to 79.7 years of in 2002 (St-Arnaud J., 2005).

However, it is still not entirely clear how changes in environment and lifestyle have truly delayed the aging process since many of these changes have increased lifespan by preventing early deaths. Factors that affect the rate of aging should affect the maximum lifespan (MLSP), as well as life expectancy. MLSP is defined as the maximum age that a species can live (i.e., the age at which there is 0% survival of a population under study). Interventions that increase MLSP are thought to be mediated through changes in the fundamental biological mechanisms of aging (Weinert and Timiras, 2003).

Nonetheless, it has been very difficult to validate many of the claims about manipulations that improve lifespan in mammals. The only exception to this is the experimental intervention involving reductions in the amount of dietary energy intake while maintaining adequate intake of essential nutrients. This intervention is most commonly termed calorie restriction (CR), but can also be referred to as dietary restriction (DR), energy restriction (ER) or food restriction (FR). CR is the only intervention that has markedly and consistently increased lifespan in all species tested. While CR has been shown to be effective, the biological mechanisms are as yet poorly understood and as a result CR remains an important area of aging research.

This doctoral dissertation fundamentally concerns the elucidation of the metabolic mechanisms underlying the anti-aging effects of CR. It has been suggested that the mechanism of CR may involve a state of hypometabolism resulting in decreased oxygen consumption and/or oxygen radical production. In this dissertation we have addressed this issue by investigating the effect of CR on whole body and skeletal muscle energetics. The

following sections provide an overview of the current literature relevant to understanding CR as a life-extending strategy.

1.2 AGING

Aging is not a disease but a complex universal biological process. Aging involves progressive changes at the molecular, cellular and organ level, which result in the deterioration of physiological function. The compounded effects impair the ability of an organism to maintain homeostasis, which altogether increase the likelihood of disease and death. All organisms are subject to a functional decline as a result of aging, however there is intra-species and inter-species variation in the sequence and characteristics of these declines.

Human aging is characterized by a number of changes in body composition and physiological function. Such changes include the loss of muscle mass and bone density, decreased strength, and increased body fat, insulin resistance, and increased circulating levels of LDL, cholesterol, and triacylglycerides. Declines also occur in memory function, reaction times, sexual activity, hearing, vision, and immune system function. Therefore the general phenotype of aging is one in which any system, tissue or organ can fail. It is clear that a number of pathologies increase with age such as diabetes, heart disease, cancer, arthritis and kidney disease. However, the incidence of some disorders, such as sinusitis, remains constant, while that of other disorders, such as asthma, decline with age. This suggests that aging is not a collection of diseases and disorders but involves a declining ability to respond to stress by increasing homeostatic imbalance and incidence of pathology (Weinert and Timiras, 2003).

1.2.1 THEORIES OF AGING: AN OVERVIEW

It is widely acknowledged that aging is a complex and multifactorial process with many etiologies. Numerous theories have been proposed to explain the biological mechanisms of aging. A detailed discussion of these theories is beyond the scope of this literature review, but many of the theories are described in detail in a review by Weinert and Timiras (2003). Overall, theories of aging can be divided into two classes: 1) intrinsic or "programmed" and 2) extrinsic or "wear and tear". Intrinsic factors refer to the genomic mechanisms that control aging. In other words, the regulation of life through growth, development, maturity and time depends on genes switching on and off signals to nervous, endocrine and immune systems responsible for maintance of homeostasis and activation of defence responses (Weinert and Timiras, 2003). Extrinsic aging refers to various external environmental influences on the organism. These processes are not programmed, but occur as the net result of numerous environmental impacts or assaults such as damage by radiation, chemical toxins and free radicals. The cumulative effect is damage to cells and the tissues they make up (Weinert and Timiras, 2003).

1.2.2 OXIDATIVE STRESS THEORY OF AGING

Oxidative stress is a general term that describes the amount of oxidative damage to a molecule, cell, organ or tissue caused by reactive oxygen species (ROS). Oxidative stress can also include damage inflicted by reactive nitrogen species (RNS) and reactive aldehydic species. The main types of ROS include the superoxide anion ($^{\bullet}O_2$), the hydroxyl radical ($^{\bullet}OH$), hydrogen peroxide (H_2O_2), and fatty acid hydroperoxides (FAOOH), whereas RNS include nitric oxide ($^{\bullet}NO$), peroxynitrite ($ONOO^-$), and N-nitrosamines. Most endogenous

ROS arise as by-products of oxidative metabolism in mitochondria (described in section 1.3.3).

Environmental stimuli known to increase ROS production and oxidative stress include exposure to pollutants such as cigarette smoke or automobile emissions, ionizing radiation and bacterial or viral infections (Finkel and Holbrook, 2000). The level of oxidative stress in a system is a balance between the rate at which endogenous ROS and/or RNS are produced and the rate at which these species are repaired and removed. Low levels of ROS/RNS have important roles in signalling, translational control and in other cellular processes (Droge, 2002; Shigenaga et al., 1994; Sohal and Weindruch, 1996; Yu, 1996). Conversely, high levels of these oxidants increase the probability of abnormal function and disease (Figure 1). The *oxidative stress theory of aging* proposes that the age-associated loss of function is due to the progressive accumulation of oxidative damage to proteins, lipids and DNA (Sohal and Weindruch, 1996). The accumulated damage leads to declines in cellular, tissue and eventually organismal function. Furthermore, it has been proposed that a longer lifespan can be achieved by decreasing the level of oxidative damage incurred over time (Sohal and Weindruch, 1996). The oxidative stress theory was first proposed in 1957 as the "free radical theory of aging" as it directly implicated free radicals in the oxidative stress process (Harman, 1956). This hypothesis was extended in the 1970s to implicate mitochondria as the main source of free radicals (Harman, 1972; Pak et al., 2003). The role of the mitochondria was thus described at this time in the "mitochondrial theory of aging", proposing that mitochondrial oxidative stress results in a "vicious cycle" in which damaged mitochondria progressively generate more ROS, resulting in progressively more damage (Harman, 1972).

FIGURE 1: THE ROLE OF OXIDANTS IN CELLULAR HOMEOSTASIS.

The majority of endogenous oxidants are produced as by-products of oxidative metabolism in mitochondria and peroxisomes. ROS are also produced to a lesser extent by a variety of cytosolic oxygen consuming enzymes. Moreover, ROS production can be triggered by exogenous sources such as environmental toxins. The detoxification of ROS occurs by several enzymatic and non-enzymatic systems including superoxide dismutase and antioxidant vitamins. ROS are important for many life-sustaining processes within the cell thus cellular homestasis is important to maintain ROS at a certain level. ROS levels below the homeostatic set-point may impair physiological processes including host defenses and translational control. Conversely, if ROS levels within the cell are not controlled, then the detrimental effects of oxidative stress can occur. Impairment by ROS can result in random damage to cellular macromolecules in addition to activation of specific redox-sensitive signaling pathways that can in turn cause more damage. Oxidative stress is thought to be involved in many aging processes, and the oxidative stress theory of aging is one of the most widely acknowledged theories of aging. Figure adapted from (Finkel and Holbrook, 2000)

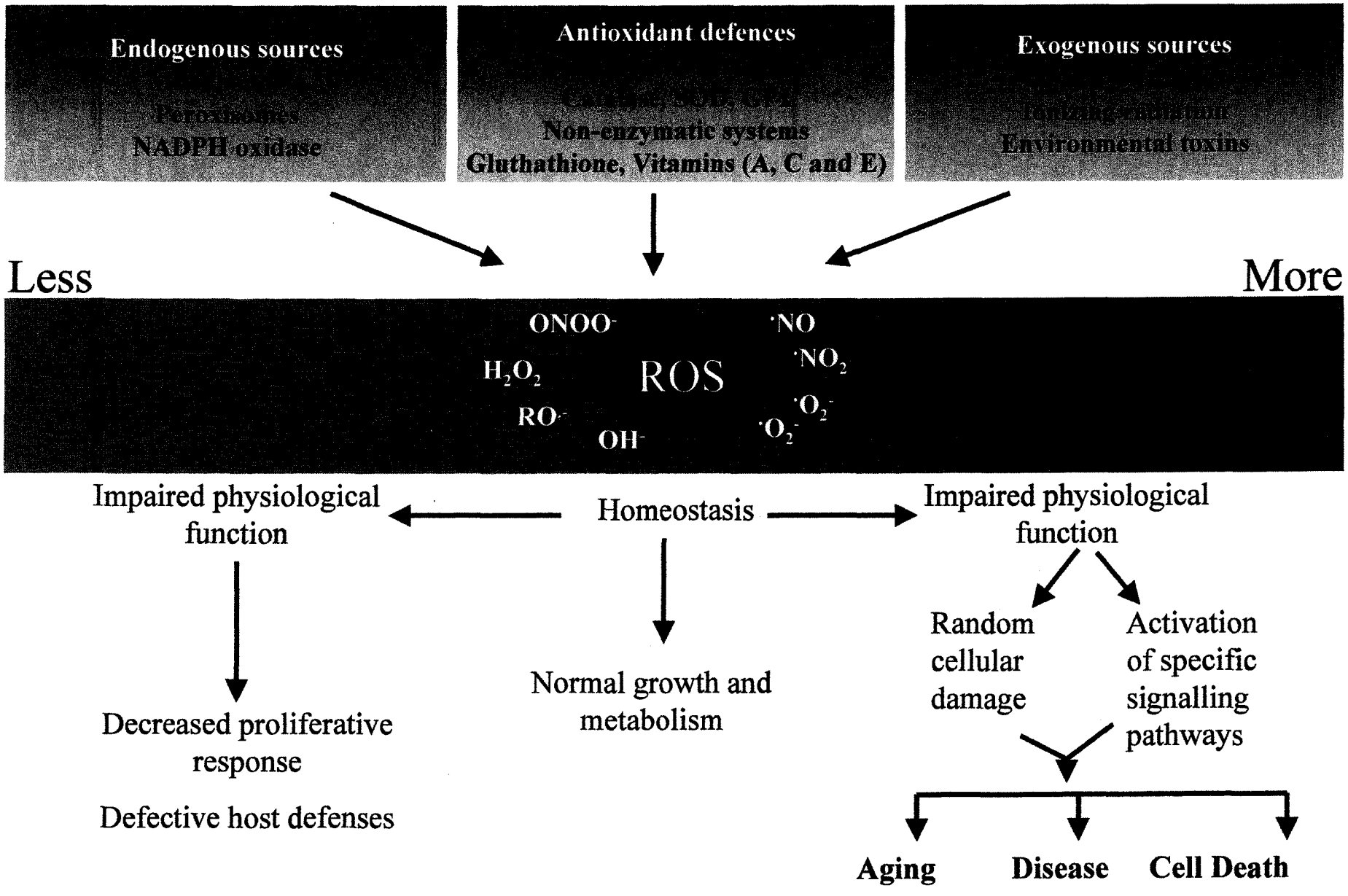

1.3 MITOCHONDRIA AND OXIDATIVE STRESS

The accumulation of oxidative damage and mitochondrial dysfunction have been proposed to lead to several age-related pathological conditions, including insulin resistance (Petersen et al., 2003), exercise intolerance (Conley et al., 2000), and sarcopenia (Bua et al., 2002). Evidence supporting the mitochondrial theory of aging indicates that the loss of mitochondrial function compromises the ability of the mitochondria to meet ATP demands, which in turn limits the oxidative capacity of the tissue, thereby disrupting cellular energetics, and sensitizing cells to apoptosis or necrosis. The combination of reduced oxidative capacity and increased cell death results in tissue degeneration and loss of functional capacity, particularly in post-mitotic tissues like skeletal muscle (Marcinek et al., 2005).

Mitochondria are commonly described as cellular "powerhouses" because they transduce energy into forms that can be effectively used. Mitochondria are double membrane-enclosed organelles involved in fatty acid beta-oxidation (β-oxidation), the urea cycle and adenosine triphosphate (ATP) production via the respiratory chain. In addition to a role in cellular energy metabolism, mitochondria are involved in calcium homeostasis, intracellular signaling, and apoptosis.

Traditionally, mitochondria have been thought of as discrete organelles when in fact they are budding and fusing networks very similar to the endoplasmic reticulum (Mannella et al., 1997). The outer and inner membranes are composed of phospholipid protein bilayers, each with their own specific functional characteristics. The outer membrane phospholipid composition is similar to that of the plasma membrane and contains numerous integral membrane proteins termed porins. Porins are permeable to molecules of 5000

daltons or less. The transport of larger molecules requires active transport processes. The outer membrane also contains enzymes that are involved in the activation and elongation of fatty acids, the oxidation of epinephrine, and the degradation of tryptophan. The outer membrane surrounds the organelle while the highly folded inner membrane surrounds the matrix space that contains proteins and DNA. The intermembrane space is located between the two membranes and contains proteins including the mobile electron carrier, cytochrome c, which is weakly associated with complex IV of the respiratory chain. The inner membrane has a very high protein to phospholipid ratio (3:1 by weight) and is rich in the phospholipid cardiolipin. The inner membrane is far less permeable than the outer membrane; it does not contain porins. In fact, to traverse the inner membrane, almost all ions and molecules need specialized transporters. The inner membrane is compartmentalized into numerous pleomorphic invaginations called cristae (Mannella, 2006). The cristae contain the complexes of the electron transport chain (ETC), the phosphorylation apparatus, and various membrane transporters. The cristae increase the surface area of the inner mitochondrial membrane, which enhances its capacity for ATP production. Contact sites are formed by portions of the inner and outer membranes, which participate in the import of proteins, adenine nucleotides, and fatty acid substrates into the mitochondria (Nicolay et al., 1990). Constituents of these transport sites include the translocase import proteins such as TOM (translocase outer membrane), and TIM (translocase inner membrane), and the adenine nucleotide translocator (ANT), (Brdiczka et al., 1990).

1.3.1 OXIDATIVE PHOSPHORYLATION

The ETC, also referred to as the mitochondrial respiratory chain, is composed of five transmembrane, multi-subunit enzyme complexes, all of which are located in the mitochondrial inner membrane. Reduced cofactors or equivalents (NADH and $FADH_2$), produced from the oxidation of carbohydrates, proteins and fats, donate electrons to complex I (NADH-Coenzyme Q reductase or NADH dehydrogenase) and complex II (succinate dehydrogenase). These electrons flow between the complexes down a redox gradient and are shuttled by complexes III (cytochrome bc1 complex, CoQ-cytochrome c reductase), complex IV (cytochrome c oxidase) and by two mobile electron carriers, ubiquinone (ubiquinol, coenzyme Q10) and cytochrome c. The ability of complexes I-IV to shuttle electrons is accomplished through their subunits, which contain prosthetic groups (iron-sulphur groups in complex I-III and heme iron in cytochrome c and complex IV). Complex IV transfers electrons to the ultimate electron acceptor, oxygen, resulting in the production of water. It is currently thought that the ETC complexes are likely organized into larger protein complexes termed respirasomes, which optimize the channelling of reducing equivalents (Schagger et al., 2004; Schagger and Pfeiffer, 2000).

The energy released from the transfer of electrons is used by complexes I, III and IV to pump protons out of the mitochondrial matrix into the intermembrane space generating a pH and electrochemical gradient. The sum of the pH gradient (ΔpH) and the electrochemical potential gradient ($\Delta\psi$) is the protonmotive force (PMF). Complex V (ATP synthase) harnesses the potential energy stored in the PMF to generate adenosine triphosphate (ATP) from adenosine diphosphate (ADP) and inorganic phosphate (P_i). This mitochondrial process of using energy from fuel oxidation to synthesize ATP underlies

oxidative phosphorylation (Figure 2). ATP is the most common energy source for all active metabolic processes within a cell and is exported by ANT from the mitochondrial matrix in exchange for cytosolic ADP.

The rate of oxidative phosphorylation is determined by the energy needs of the cell. It is slow when the energy demand is low (decreased availability of ADP). Mitochondria in this state are said to be respiring at, or near, state 4 (non-phosphorylating) respiration. When the return of protons to the matrix through ATP synthase has stopped, state 4 respiration results in a rise in the PMF and a reduction in the rate of electron transport (i.e., oxygen consumption). When the cellular energy demand is increased, ADP concentrations are augmented due to increased ATP hydrolysis. This, in turn, enhances the rate of phosphorylation by complex V. The rise in phosphorylation dissipates the PMF, and as a result, electron transport is stimulated and oxygen consumption is increased. Oxygen consumption at the point of maximal ATP production rate is termed state 3 respiration or maximal phosphorylating respiration (Nicholls, 2002b). The ADP:O ratio, which is defined as the number of ADP molecules phosphorylated for each oxygen atom reduced, provides an estimate of the efficiency of oxidative phosphorylation. Complex I substrates were thought to have an ADP:O ratio of 3.0 since complexes I, III and IV are actively translocating protons. However this value has recently been re-evaluated and is likely to be as low as 2.4 (Brand, 2005). Complex II-linked substrates traditionally have been thought to have an ADP:O ratio of 2.0, as only two proton pumping centers (complex III and IV) are active. However, again it is likely that a value of approximately 1.5 is more accurate (Brand, 2005).

FIGURE 2: SCHEMATIC DIAGRAM OF THE MITOCHONDRIAL INNER MEMBRANE SHOWING THE OXIDATIVE PHOSPHORYLATION PATHWAY AND MITOCHONDRIAL PROTON LEAK.

Oxidative phosphorylation is a process through which the energy from reduced substrates is used to produce ATP. The reduced substrates generated in the Krebs cycle supply the electrons to the complexes of the electron transport chain (shown in blue in the mitochondrial inner membrane). The transport of electrons (yellow arrows) from one complex to another along the chain is associated with the translocation of protons (orange arrows) from the mitochondrial matrix into the mitochondrial inter-membrane space. This generates an electrochemical gradient known as the protonmotive force (PMF). The energy stored in the PMF drives protons back into the mitochondrial matrix through ATP synthase (purple) and in combination with the adenine nucleotide translocator (red) and the phosphate carrier (green), results in the production of ATP. The coupling of proton translocation and ATP production is not perfect. Protons can leak back into the mitochondrial matrix bypassing ATP synthase and this results in the PMF dissipation in the absence of ATP synthesis. This process is referred to as the 'mitochondrial proton leak' (turquoise arrows). The mechanism of proton leak is unclear, however it is thought that proton return is a general property of mitochondrial membranes and/or mediated by inner membrane proteins such as Uncoupling Proteins (UCPs) and the Adenine Nucleotide Translocase (ANT). The mechanism of uncoupling caused by UCP1 in brown adipose tissue is however well understood.

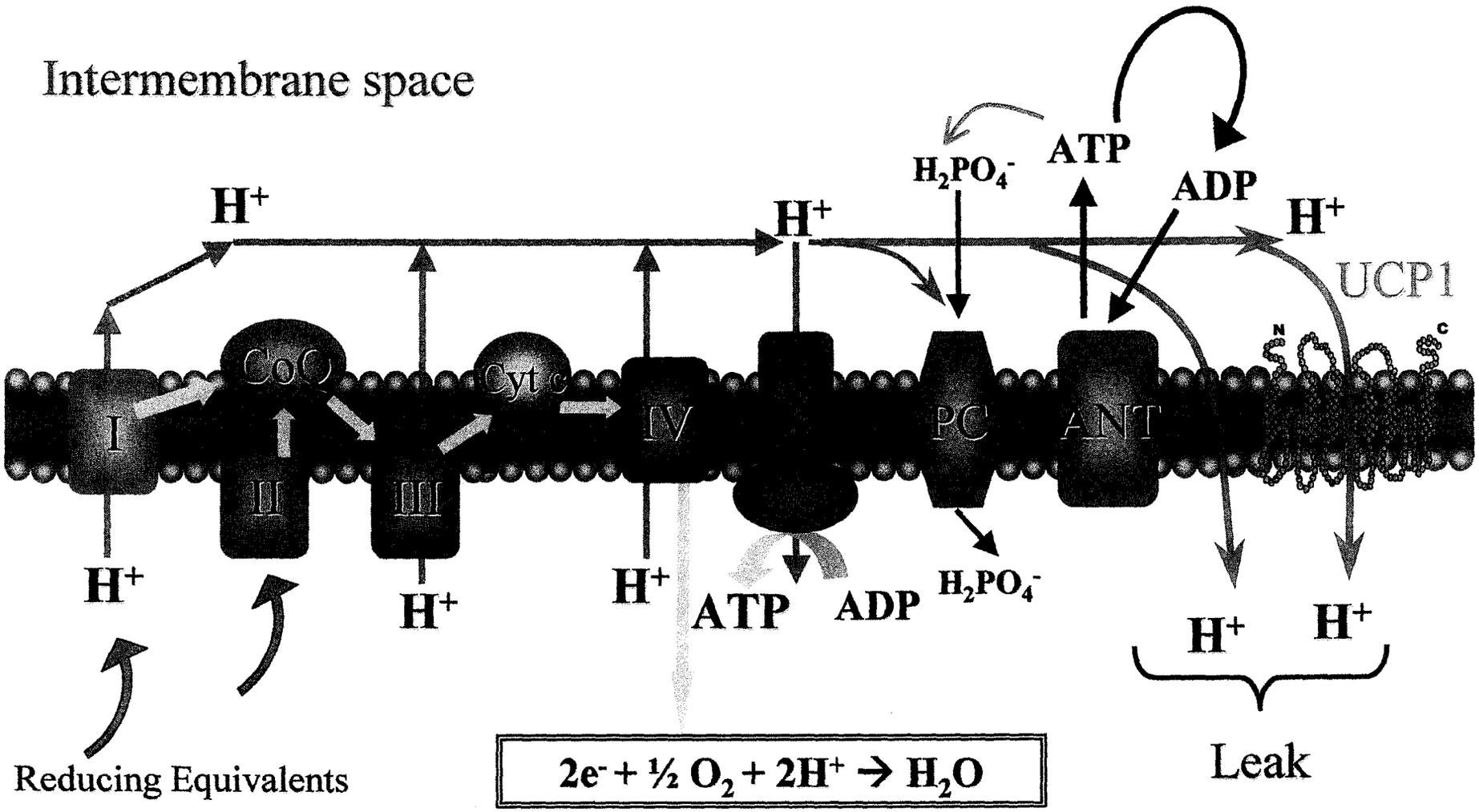

1.3.2 UNCOUPLING OF OXIDATIVE PHOSPHORYLATION

The uncoupling of respiration from ADP phosphorylation impairs the efficiency of oxidative phosphorylation. Under certain conditions, ATP synthase is not the only route by which protons can return into the matrix. Protons can return or "leak" back to the mitochondrial matrix and thus bypass ATP synthase. This route of proton return clearly does not contribute to the production of ATP. As a result, the energy stored in the PMF is wasted by its release as heat (Brown, 1992; Brown and Brand, 1986; Nicholls, 1974). The flux of protons through this non-productive proton conductance pathway is termed 'proton leak' or 'mitochondrial uncoupling'.

The proton leak rate has a non-linear ("non-ohmic") relationship with its driving force, PMF; proton leak rates increase exponentially at high PMF values. Proton leak is not an artifact of mitochondrial isolation as it has been quantified not only in isolated mitochondria, but also in intact cells (e.g., hepatocytes, thymocytes) and perfused tissues such as skeletal muscle. The proportion of resting oxygen consumption that is estimated to be due to leak ranges from 20-30% (Buttgereit et al., 1992; Buttgereit et al., 1991; Nobes et al., 1990). At the level of the whole body, proton leak is estimated to account for up to 20-25% of standard metabolic rate in the rat (Rolfe and Brown, 1997). Proton leak is greatest under nonphosphorylating conditions (i.e., state 4 respiration). Conversely, under phosphorylating conditions (i.e., state 3 respiration), proton leak is essentially non-existent as proton return is primarily through ATP synthase. Suggested functions for mitochondrial proton leak include: (1) thermogenesis (heat production), (2) protection from free radical generation, and (3) regulation of energy metabolism (Rolfe and Brand, 1997). The

mechanism of proton leak remains unclear; however, it is currently thought that there are two main pathways: basal proton leak and inducible proton leak.

1.3.2.1 BASAL PROTON LEAK

The exact mechanism of basal proton leak is not entirely understood. The activity of this pathway in mitochondria varies within different tissues, within mammals and birds having different body masses, and with both phylogeny and thyroid status from different tissues (Brand et al., 1994; Harper and Brand, 1993; Nobes et al., 1990; Porter and Brand, 1993; Rolfe et al., 1994). Mitochondrial inner membrane fatty acid composition and surface area are thought to affect the permeability of the membrane (Porter et al., 1996). The amount of very long chain n-3 polyunsaturated fatty acids, particularly docosahexaenoic acid ($C_{22:6,n-3}$), has been shown to be positively correlated with the rate of proton leak whereas the amount of the n-6 polyunsaturated fatty acid, linoleic acid ($C_{18:2,n-6}$), and monounsaturates, particularly oleate ($C_{18:1,n-9}$), have been correlated with decreased proton leak (Brand et al., 1994; Brookes et al., 1998; Porter et al., 1996).

In fact, there has been much debate as to whether proton leak is protein-mediated or simply a diffusion of protons through the lipid bilayer. These ideas have been tested using reconstituted liposomes. Early studies have shown that liposomes made from mitochondrial phospholipids had a 20-fold lower proton leak rate than that in the mitochondria from which the phospholipids were isolated (Brookes et al., 1997a; Brookes et al., 1997b). Also, proton leak rates were not different in liposomes derived from mitochondrial phospholipids from liver of a variety of species; whereas, it has been shown that leak in liver mitochondria is directly associated with mass-specific metabolic rate in a variety of species (Brookes et al.,

1997a). These results indicated that the intrinsic proton conductance was lost in reconstituted liposomes, and suggested that leak is not simply affected by membrane lipid phospholipid composition. Indeed the mitochondrial inner membrane protein, ANT, has recently been demonstrated to catalyze a significant portion (approximately 33-50%) of basal proton leak (Brand et al., 2005).

1.3.2.2 INDUCIBLE PROTON LEAK

Inducible proton leak, unlike basal proton leak, can be stimulated by many physiological and pathological conditions and can also be catalyzed by specific proteins such as uncoupling proteins (UCPs). The original uncoupling protein (a.k.a. UCP1 or thermogenin) is expressed exclusively in brown adipose tissue (BAT) and is responsible for the cold-induced thermogenesis in this tissue (Nicholls and Locke, 1984). UCP1-mediated proton leak is activated by free fatty acids, which are liberated in brown adipocytes as a result of adrenergic activation. Several putative homologues of UCP1 (UCP2-5) were discovered in other tissues and have been given the name uncoupling protein simply based on their high amino acid similarity to UCP1 (Boss et al., 1997; Fleury et al., 1997; Gimeno et al., 1997; Mao et al., 1999; Sanchis et al., 1998; Vidal-Puig et al., 1997). Recently, it has been proposed that the leak catalyzed by UCPs is activated by ROS or alkenals from lipid peroxidation products and is purine nucleotide-sensitive (Brand et al., 2004b; Esteves and Brand, 2005). However, the physiologic relevance or probability of such a mechanism has recently been questioned (Nicholls, 2006). The complex role of UCPs in the inducible proton leak will be discussed further in section 1.6.4. In addition to UCPs, ANT can also mediate the inducible proton leak. This leak has been demonstrated to be activated by fatty

acids, AMP or alkenals, and inhibited pharmacologically by carboxyatractylate (CAT) (Andreyev et al., 1989; Andreyev et al., 1988; Cadenas et al., 2000; Echtay et al., 2003; Skulachev, 1998).

1.3.3. CELLULAR AND MITOCHONDRIAL REACTIVE OXYGEN SPECIES (ROS) PRODUCTION

Mitochondria use 85-90% of cellular oxygen to support oxidative phosphorylation. The vast majority of cellular reactive oxygen species (ROS) is generated by the mitochondria (Figure 3). Approximately, 0.2-2% of cellular oxygen consumption is thought to generate ROS production, mainly superoxide, as a by-product of oxidative phosphorylation (Chance et al., 1979; Han et al., 2001a). The generation of ROS occurs at several sites along the ETC as electrons from the reducing equivalents that "escape" and interact with oxygen or other electron acceptors (Balaban et al., 2005).

In addition to the mitochondria, ROS can also be generated in other cellular compartments. Approximately 10-15% of cellular oxygen consumption is used to support non-mitochondrial reactions by various oxidases, oxygenases and other non-enzymatic reactions. Important contributors to non-mitochondrial ROS production include plasma membrane proteins such as the NADPH oxidases (Lambeth, 2004), xanthine oxidase, P450 cytochromes, acyl-CoA oxidases and cytosolic cyclooxygenases involved in peroxisomal lipid metabolism (Balaban et al., 2005).

1.3.4. SITES OF MITOCHONDRIAL ROS PRODUCTION

The relative importance of different sites of ROS production in the mitochondrial ETC is unclear. However, it is generally agreed that the two main sites of ROS production

are at complexes I and III (Barja, 1999). These are sites associated with large changes in redox potential (Balaban et al., 2005). Studies have shown that experimental manipulations (e.g., adding inhibitors of the complexes) that increase the redox potential of complexes I and III, in turn increase the production of ROS (Chen and Yu, 1994; Kushnareva et al., 2002) demonstrating the importance of these sites for ROS production.

Complex I is the least understood of the ETC complexes involved in ROS production (Yagi and Matsuno-Yagi, 2003). Complex I is a multi-subunit enzyme composed of approximately 46 proteins that have a combined molecular weight of over 1 MDa. It is thought to contain at least one bound flavin mononucleotide (FMN) and eight iron-sulfur groups (Balaban et al., 2005). The specific sites in complex I for ROS production are thought to be the iron-sulphur centers (Genova et al., 2001; Herrero and Barja, 1997) or the active site flavin (Liu et al., 2002a).

The electron carriers of complex III are the cytochromes b_L, b_H and c_1, the Rieske iron-sulfur center, and the ubisemiquinones (Turrens et al., 1985). The specific ROS production site in complex III is thought to be the ubisemiquinone at the inner or outer membrane surfaces of centers "*i*" or "*o*" (Aguilaniu et al., 2003; Turrens et al., 1985). Some reports have suggested that cytochrome b, rather than ubisemiquione, is the main site of superoxide production at complex III (Nohl and Stolze, 1992). However, evidence against cytochrome b involvement has been provided by several independent studies (Barja, 1999; Turrens, 1997; Turrens et al., 1985).

Moreover, in regard to the membrane localization of ROS production, complex I is thought to release ROS exclusively on the matrix side of the inner membrane, as this is where the iron-sulfur centers and the active flavin sites are located. Complex III was

originally believed to release superoxide towards the matrix (Turrens, 1997). The determination of the crystal structure of complex III suggested that ROS can be released into the intermembrane space since the center 'o' is oriented toward the intermembrane space and not the matrix (Iwata et al., 1998; Zhang et al., 1998). The release of superoxide by complex III in the intermembrane space is further supported by studies showing increased ROS production by liver mitoplasts (mitochondria stripped of outer membrane portions) (Han et al., 2001a). A later series of experiments by St-Pierre *et al.* (2002) further examined the sites and topology of ROS production in the ETC. Their findings further corroborated the idea that superoxide from complex III can be released directly into the intermembrane space and showed that in the presence of inhibitors of complex III can generate more ROS than complex I (St-Pierre et al., 2002). Thus, complex III can release ROS into the matrix (approximately 70-80%) and intermembrane space (20-30%) (St-Pierre et al., 2002). Finally, it must be acknowledged that the relative importance of the generation of ROS by complex I and III is dependent on experimental conditions, tissue type and animal species (Barja, 1999).

1.3.5. REGULATION OF ROS PRODUCTION

There are many factors *in vivo* and *in vitro* that contribute to the regulation of ROS production. Experimentally, addition of electron chain inhibitors that increase the redox status of sites I or III greatly increases ROS production (Aguilaniu et al., 2003; Loschen et al., 1971; Staniek and Nohl, 2000).

Physiologically, ROS production is affected by the metabolic status of the mitochondria. Mitochondrial ROS is highest under state 4 conditions, when oxygen

consumption is low, protonmotive force is high, and the complexes of the electron transport chain are in reduced states. Under these conditions, the major factor underlying the protonmotive force-dependent production of ROS is the occupancy of the outer Q-site of complex III with the semiquinone anion (Nicholls, 2002a). Thus, PMF, rather than electron flux or oxgen consumption has been suggested to be the most important factor underlying ROS production (Miwa et al., 2003; Nicholls, 2004). However, under state 3 conditions (phosphorylating conditions) superoxide production is drastically reduced as PMF decreases and oxygen consumption increases (Boveris and Chance, 1973; Boveris et al., 1972; Loschen et al., 1971).

In vitro and *in vivo* studies have suggested that complex I may be the most important site for ROS production. Barja and colleagues assessed this idea by measuring complex I- and III- dependent superoxide production in heart and brain mitochondria. ROS production by complex I was detected under both states 3 and 4 conditions; however there was lower ROS production under state 3 conditions. Superoxide production by complex III was only detected under state 4 conditions indicating that complex I could be the only ROS generator when ATP is being synthesized at high rates (Barja, 1999; Herrero and Barja, 1997).

Miwa and Brand (2003) have proposed that reverse electron flow may be another important *physiological* mechanism for ROS production. With complex I-linked substrates, electrons flow from complex I to complex III and superoxide is produced at a lower rate than that associated with complex II-linked substrates. ROS production associated with complex II substrates is thought to be produced by reverse electron flow since rotenone (a complex I inhibitor) largely abolishes superoxide production (Liu et al., 2002b; Miwa et al., 2003). Reverse electron flow occurs when electrons provided by complex II-linked

substrates flow back from complex II to complex I (Aguilaniu et al., 2003; Loschen et al., 1971). This type of superoxide production requires tightly coupled mitochondria capable of maintaining a high membrane potential (Votyakova and Reynolds, 2001). Thus, reverse electron flow is highly dependent on membrane potential, and it disappears as the level of mitochondrial uncoupling increases, or in the presence of a complex I inhibitor, such as rotenone (Miwa and Brand, 2003; Miwa et al., 2003; Scholes and Hinkle, 1984). The production of ROS by reverse electron flow may be important to explain the high ROS levels during high rates of fatty acid oxidation when $FADH_2$ is generated and donates electrons to complex II (Boveris and Chance, 1973; Boveris et al., 1972). Superoxide production using glycerol-3-phosphate has been recently measured in *Drosophila* mitochondria and shown to occur by reverse electron flow (Miwa et al., 2003). Despite this interesting finding, the physiological relevance of reverse electron flow in other organisms is still unexplored.

1.3.6. ELIMINATION OF ROS

Cells and mitochondria contain many important enzymes to detoxify ROS and their downstream products. Within the cell, there are two important superoxide dismutase enzymes involved in scavenging superoxide. SOD1 (CuZnSOD) in the mitochondrial intermembrane space and the cytosol protects the cell against superoxide produced in the cytosol. SOD2 (MnSOD) protects mitochondria from superoxide produced in the mitochondrial matrix. Extracellular SOD3 (CuZnSOD) protects against superoxide that has escaped degradation in the mitochondria or cytosol, and has reached the extracellular space. These enzymes convert the superoxide anion to H_2O_2, which is then converted to water by catalase (Radi et al., 1991). Glutathione peroxidases can also scavenge ROS by using H_2O_2

to oxidize reduced glutathione (GSH) to produce oxidized glutathione (GSSG) and water. Glutathione reductase can then convert GSSH back to GSH. Peroxiredoxins, recently identified in mitochondria, offer additional protection from ROS (Chang et al., 2004; Taylor et al., 2003).

On a molecular level, the transcription factor Nrf2 (NF-E2-related factor 2) has been suggested to be involved in the induction of defense enzymes/proteins in response to ROS and other electrophilic intermediates. This electrophile-response mechanism has been observed in rats, mice and humans, in the form of a group of detoxifying enzymes and antioxidant proteins. Transcription of these antioxidant enzymes is coordinated through electrophile responsive element/antioxidant responsive element (EpER/ARE) (Itoh et al., 1999). Upon activation in the cytoplasm by ROS, Nrf2 dissociates from Keap1 (Kelch-like ECH associating protein), an actin cytoskeleton binding protein. Upon dissocation Nrf2 localizes to the nucleus and acts as a potent activator of dexoification enzymes and antioxidant stress proteins such as HO-1 (heme oxygenase 1) (Kang 2007). These numerous and efficient protection mechanisms allow cells and tissues to maintain a homeostatic balance enabling them to survive hazardous oxidative environments.

FIGURE 3: A SCHEMATIC DIAGRAM REACTIVE OXYGEN SPECIES PRODUCTION AND DETOXIFICATION.

In this diagram, the yellow arrows indicate electron flow. The complexes of the ETC are shown with increasing blue intensity to indicate increasing redox potential. Proton transport is omitted for simplicity. Figure adapted from (Jezek and Hlavata, 2005)

Superoxide anions are produced at sites I and III of the ETC as by-products of oxidative phosphorylation. Complex I releases superoxide into the mitochondrial matrix (by forward and reverse electron flow), whereas Complex III releases superoxide to both the matrix and the intermembrane space. Matrix superoxide is dismuted to H_2O_2 by mitochondrial MnSOD, while intermembrane CuZnSOD dismutes the superoxide that is released into the intermembrane space. The superoxide released into the intermembrane space and not scavenged by CuZnSOD can enter the cytosol (via VDAC) where it can be further scavenged by cytosolic SOD or go on to cause oxidative damage or participate in cell signaling pathways. H_2O_2 produced in the intermembrane space can easily diffuse to the cytosol due to its uncharged nature. H_2O_2 can be further converted to hydroxyl radical ($^{\cdot}OH$ by the Fenton reaction catalyzed by Fe^{2+}). The Fe^{2+} is released by the oxidation of the Fe-S cluster in aconitase rendering it inactive. The hydroxyl radical can react with proteins and lipids to cause oxidative damage to cellular and mitochondrial components. H_2O_2 can also be converted to water and oxygen by catalase or to water and reduced glutahione (GSSH) by glutathione peroxidase (GPX). Mitochondrial peroxireductase (PRX) can also deactivate H_2O_2. Reactive nitrogen species can be formed by the reaction of superoxide with NO (generated by mitochondrial nitric oxide synthase) to produce peroxinitrite, which subsequently can react with protein and lipids. Both ATP production and uncoupling can reduce superoxide production by decreasing PMF.

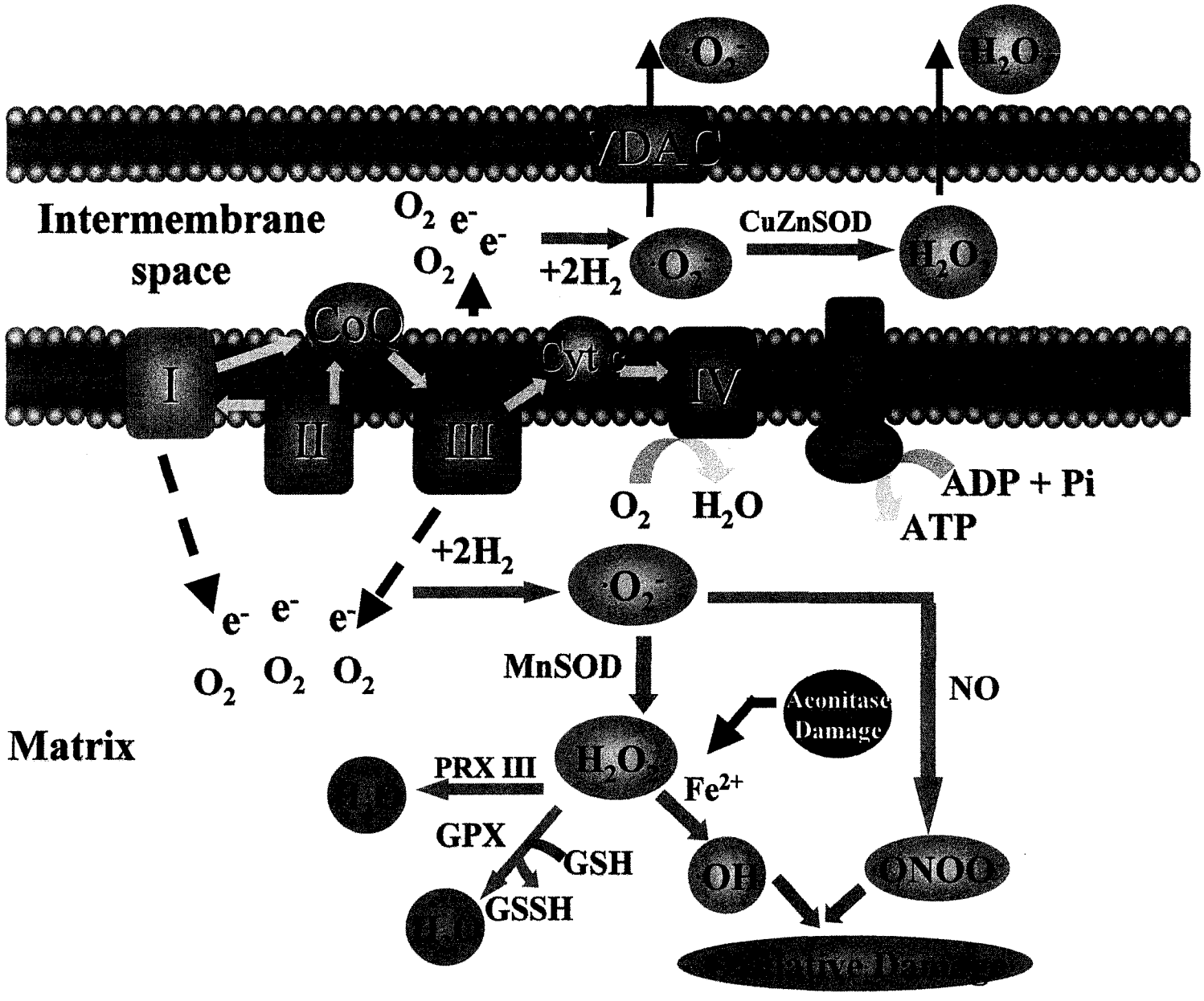

1.4 CALORIE RESTRICTION (CR) AS AN ANTI-AGING STRATEGY

Calorie restriction (CR) without malnutrition (i.e., adequate intake of vitamins, minerals and other essential dietary components) is the only intervention that has markedly and consistently been shown to increase lifespan as well as slow the intrinsic rate of aging in a wide variety of species. CR also delays the onset of many age-related diseases such as type 2 diabetes mellitus, hypertension and various forms of cancer. In addition, CR provides many health benefits including improved immune function and cognitive ability. Due to these medical implications, CR has been a very active subdiscipline in the field of aging research.

1.4.1 HISTORICAL PERSPECTIVE

The first reports of the anti-aging effect of CR were described in the 1930s by Charles McCay. He initially studied the effect of a low protein diet on the growth of fish. During these studies he observed that trout with slowed growth had longer lifespans than control trout (McCay, 1929). This observation led to a subsequent study, which directly tested the effect of growth on lifespan in three groups of rats. The first group of rats was allowed to grow at a normal rate. The other two groups had restricted intakes of all nutrients. Both restricted groups did not grow and began to deteriorate until food intake was increased. The restricted groups went through periods of no growth and periods of growth spurts. One of the two restricted groups was placed on a restricted diet for 700 days while the other group remained on the restricted diet for 900 days. The control rats had a mean lifespan of approximately 600 days but were outlived by both restricted groups (McCay,

1935). In his follow-up study McCay decreased the intake of calories but not that of vitamins, minerals or protein. Results from this study were very similar to the first in that the restricted rats outlived the control rats. McCay concluded that the length of life was a result of retarded growth (McCay, 1939).

The next 20 years of CR research focused on the effect of CR on age-related diseases. For example, CR was shown to delay the progression of chronic nephropathy in rats, a major disease in rats (Saxton, 1941), and the development of leukemia in mice (Saxton, 1944). Moreover, the possible effects of specific nutrients on lifespan were examined and it was concluded that a reduction in calories specifically increased lifespan and delayed the onset of disease (Ross, 1961; Ross and Bras, 1965).

1.4.2. STUDIES IN NON-HUMAN PRIMATES AND HUMANS

The anti-aging effect of CR has been demonstrated in invertebrates (protozoa, flies and water fleas), nematodes, rotifers, spiders and vertebrates such as hamsters, dogs and fish (Austad, 1989; Comfort, 1963; Fanestil and Barrows, 1965; Kirk, 2001; Klass, 1977; Sawada and Carlson, 1987; Weindruch et al., 1986). However, it is not yet know that CR protects against age-related diseases and extends lifespan in higher primates.

There are few long-term studies in higher species, such as human and non-human primates, as they are expensive and time-consuming (i.e., long lifespans and may surpass those of the investigator(s)). Long-term CR studies in non-human primates (e.g., rhesus and squirrel monkeys) are ongoing at the University of Wisconsin, University of Maryland and at the National Institute of Aging (Bethesda, MD). So far, it is too early in the data collection process to know how much lifespan is extended in these animals. It is important

to note that these studies are in the 16-17 year timepoint and monkeys normally live 25-30 years. However, each group has demonstrated that all monkeys treated with CR are healthier as they have improved biomarkers of aging (e.g., improved glucose tolerance and lipid profiles), consistent with CR effects in rodents (Kemnitz et al., 1994; Lane et al., 1996; Lane et al., 1995b).

Similar studies into the effects of long-term CR on human lifespan have not been completed because it is difficult to adhere to the rigorous CR regimen. Completed studies have involved short-term CR and have demonstrated many health benefits (Fontana et al., 2004; Heilbronn et al., 2006; Walford et al., 1999; Weyer et al., 2000). These studies have reported improvements in many aging biomarkers such as increased HDL cholesterol, reduced blood pressure and reduced body fat (Fontana et al., 2004; Heilbronn et al., 2006; Walford et al., 1999). Although not originally designed as a CR study, the Biosphere 2 experiments supported the concept that CR could increase lifespan in humans. This project was a two-year study led by Roy Walford and was conducted in a closed ecological space in the Arizona desert (Walford et al., 1995). During this study, eight people spent two years living in Biosphere 2 where a CR diet became necessary due to unexpected crop failures, and hence a limited food supply. The crew thus ate approximately 30% fewer calories than originally planned. Results demonstrated that many physiological and biochemical parameters were improved, similar to what had been observed in mice and rats. For example, crew members had decreased metabolic rate, body temperature, blood glucose, insulin and thyroid hormones. In addition, these positive effects continued up to 18 months after exiting the biosphere and returning to normal diets (Walford et al., 1999; Walford et al., 2002; Weyer et al., 2000).

The Japanese Okinawans are an interesting human population as they provide support for the anti-aging effect of CR. Okinawans have reduced morbidity and mortality and have the greatest percentage of centenarians worldwide (Heilbronn and Ravussin, 2003; Kagawa, 1978). Compared to North Americans, they have 50% lower mortality, compared to Japanese populations in other parts of Japan. Okinawans consume a diet composed mostly of vegetables, grains, fruit, fish, seaweed and soy. Importantly, however, the Okinawan diet has approximately 20% fewer calories than diets in other areas of Japan and 40% fewer calories compared to the average North American diet. The diet of the Okinawans thus seems to mimic the CR diets used in experimental animal studies (Heilbronn and Ravussin, 2003; Kagawa, 1978).

There is also an international society called the Calorie Restriction Society (CRS), whose members strive to follow CR with optimal nutrition (CRON). Studies of members who have been practicing CR for 3-15 years have again demonstrated improvements in many biomarkers of aging, such as lower glucose and insulin levels, as well as improvements in lipid profiles (Fontana et al., 2004). Theses findings suggest that the beneficial effects of CR in rodents and monkeys can be mimicked in human subjects. A recent clinical trial called CALERIE (Comprensive Assessment of Long-term Effects of Reducing Intake of Energy) was intitated recently to investigate the effects and possible mechanisms of CR on surrogate markers of longevity in nonobese humans. These studies are underway and preliminary evidence suggests that CR can improve many biomarkers of aging (Heilbronn et al., 2006).

1.4.3. VARIATIONS IN CR DESIGN CHARACTERISTICS

Compared to the study design used by McCay in the early 20th century, current CR studies use a less complicated study design. The most common method employs a control group that is fed *ad libitum* and one or more CR groups. Usually, CR groups are fed 30-50% fewer calories than the control groups, which results in a 30-40% increase in maximum lifespan (Weindruch et al., 1986). There are data from mouse studies to suggest that the greater the degree of CR without malnutrition and starvation, the greater the effect on lifespan (Weindruch et al., 1986). Interestingly, Seo *et al.*, (2006) demonstrated that even 8% CR had beneficial effects including reductions in biochemical and inflammatory biomarkers in rat. Variations in CR study design also often include slightly restricting the energy intake of the control group to prevent the development of obesity. Another CR regimen that has been effective is every-other-day feeding, where food is provided only on alternate days. Finally, the age at which CR is initiated is also important. Most rodent studies initiate CR early in life, i.e., 1-3 months of age. However starting CR at older ages (i.e., adulthood) has also been reported to increase lifespan and delay the onset of age-related diseases (Weindruch, 1996).

Results from most CR studies suggest that the life extension effect of CR is due to a reduction in total energy intake. However, results of recent studies have questioned whether or not caloric intake is truly the dietary factor responsible for life extension (Mair et al., 2005; Sanz et al., 2006). Mair *et al.*, (2005) demonstrated that life extension in *Drosophila* is not entirely due to CR. The reduction in the yeast or sugar components of the diet reduced mortality and increased lifespan by an amount that was unrelated to the amount of

calories provided. In addition, it was observed that reducing the yeast component had a greater effect on lifespan than reducing the sugar component (Mair et al., 2005).

Protein restriction in rats and mice has also been shown to increase maximum lifespan, although the magnitude of the increase was half of that observed with CR (Barrows and Kokkonen, 1975; Goodrick, 1978; Leto et al., 1976). It has been shown that restriction of the amino acid methionine has increased maximum lifespan in rats and mice (Miller et al., 2005; Richie et al., 1994). Interestingly, Sanz *et al.* (2006) demonstrated that methionine restriction decreases ROS production and oxidative stress; two factors implicated in aging. More studies are needed to clarify which dietary factor(s) are involved in the anti-aging effect of CR.

1.4.4 ORGANISMAL ENERGETICS AND CR

CR affects a wide variety of physiological, hormonal and biochemical processes including body weight and body composition. With CR, total body weight is reduced in response to the energy deficit. Lean body mass decreases, however the percent reduction is less than the percent reduction in body weight (Yu et al., 1982). The masses of most internal organs (liver, heart, kidney, lungs) are reduced with CR, but interestingly there are no decreases in the masses of the brain or the testes (Yu et al., 1982; Yu et al., 1984). While skeletal muscle mass is reduced, the age-associated rate of loss of function and mass/body weight is delayed (Aspnes et al., 1997; Payne et al., 2003). CR also reduces body fat, and for rodents, this is primarily visceral adipose tissue (Barzilai and Gupta, 1999; Bertrand et al., 1980; Garthwaite et al., 1986).

One hypothesis for the mechanism of anti-aging effect of CR suggests that CR involves a reduction in body fat content (Barzilai and Gupta, 1999). Evidence against this hypothesis includes the lack of correlation between lifespan and fat mass in rats and mice (Bertrand et al., 1980; Harrison et al., 1984; Masoro, 1995). For example, it has been demonstrated that CR ob/ob obese mice lived longer than *ad libitum* fed control mice despite having higher body fat percentage (48% vs 22%). Additionly, these mice lived as long as lean control mice with (15% body fat) (Harrison et al., 1984; Johnson et al., 1997). It must be acknowledged however that there are other differences between ob/ob mice and wild-type control mice (i.e., beyond the degree of adiposity such as altered lipid levels). Interestingly Masoro *et al.* (1995) demonstrated that rodents with higher levels of body fat often live longer. On the contrary, Speakman *et al,* (2003) demonstrated no correlation between lifespan and body mass, fat mass or lean body mass in dogs. Adipose tissue is now recognized as an endocrine organ, these observations are gaining renewed interest. The adipokines and cytokines secreted by adipose tissue may indeed play an important role in longevity (Barzilai and Gupta, 1999; Bluher et al., 2003; Tatar et al., 2003). In agreement with this, the adipose tissue-specific knockout of the insulin receptor was shown to decrease adiposity and increase lifespan in mice (Bluher et al., 2003).

It has long been hypothesized that, energy expenditure is decreased in animals that have been restricted over extended periods of time (*i.e.,* reduced metabolic rate/animal) (Masoro, 1990; Masoro, 2002). Metabolic rate per unit of fat-free mass, or per unit of metabolic mass, over the lifetime of long-term CR male rats has been found to be decreased (Dulloo and Girardier, 1993; Gonzales-Pacheco et al., 1993), similar (McCarter and Palmer, 1992) or increased (Selman et al., 2005). Also, studies in rhesus monkeys have shown that

mass-adjusted metabolic rate was either decreased (DeLany et al., 1999; Ramsey et al., 1997) or not changed (Blanc et al., 2003; Lane et al., 1995a; Ramsey et al., 1997). In humans, short term CR (6 mo) decreased 24-hour energy expenditure beyond the level expected from reduced metabolic body mass (Heilbronn et al., 2006). This is consistent with primate studies, which show reduced metabolic rate with short-term CR (Lane et al., 1995a; Ramsey et al., 1997). These discrepancies continue to fuel the debate on the effect of CR on energy expenditure. Much of the confusion surrounding the effect of CR on metabolic rate arises from the fact that CR results in a reduction in body mass and composition, both of which can affect metabolic rate. Therefore, the main debate is centered around how to best correct for these differences; including expressing energy expenditure data by body mass, by fat free mass, or by lean mass (Blanc et al., 2003; Ramsey and Hagopian, 2006).

It is also unknown whether creating an energy deficit by increasing physical activity without altering any other health behaviors will increase lifespan. Holloszy *et al.*, (1985) have shown in rats that increase in activity to attain an energy deficit of 30% did not extend maximal lifespan, although average lifespan was increased. Increases in exercise also resulted in many of the same traits of CR including improved insulin sensitivity, decreased fat mass and reduced tumor incidence. Therefore the combination of exercise and CR does not interfere in the CR effects on lifespan. Recently, Heilbronn *et al.*, (2006) have demonstrated that 12.5% CR in combination with exercise to achieve a combined energy deficity of 25% resulted in similar improvements in physiological parameters, compared to subjects following a 25% CR regimen. The latter corroborates the studies by Hollozsy in rodents (Holloszy, 1985). The addition of exercise to CR has the added benefit of improved

aerobic capacity. Thus, these results suggest that increasing physical activity to create a relative energy deficit may improve compliance for humans wanting the benefits of CR.

Body temperature decreases with CR in rodents (Duffy et al., 1989), monkeys (Lane et al., 1996), and humans (Heilbronn et al., 2006). These changes are thought to reflect decreases in basal thermogenesis and in fat stores that provide insulation and minimize heat loss. Moreover, changes in hormonal profiles (described in the following section) may in part underlie these decreases in basal thermogenesis.

1.4.5. HORMONAL RESPONSE TO CR

Thyroid hormones are major endocrine determinants of basal metabolic rate. CR reduces thyroid stimulating hormone (TSH), triiodothyronine (T_3) and thyroxine (T_4) levels in rats, monkeys and humans (Armario et al., 1987; DeLany et al., 1999; Han et al., 2001b; Heilbronn et al., 2006). This is consistent with the importance of thyroid pathways as a determinant of energy metabolism.

Type II diabetes mellitus is characterized by an inability of insulin-sensitive tissues (*e.g.,* skeletal muscle, adipose tissue and liver) to respond to normal levels of insulin and therefore results in a high level of circulating glucose. High blood glucose levels can lead to the accumulation of advanced glycation end-products (AGE) often seen with age. Lower glucose and insulin levels have been proposed as a potential mechanism for the improved health and increased lifespan seen with CR (Kalant et al., 1988). This idea is supported by the observation that CR animals have lower levels of glucose, insulin, and AGE products in addition to a reduced risk of diabetes and insulin resistance (Masoro et al., 1992).

While the activities of the thyroid, gonadotropic and somatotropic axes decline with CR, the activities of the hypothalamus-pituitary-adrenal axis are enhanced (Chacon et al., 2004; Sabatino et al., 1991; Zhu et al., 2004). Alterations in the activities of these axes have been proposed as potential mechanisms underlying the life-extension properties of CR. In fact, long lived mouse models with mutations in these endocrine axes share many phenotypic characteristics with CR animals, such as reduced plasma insulin, glucose and insulin growth factor 1 (IGF-1) (Longo and Fabrizio, 2002). For example, dwarf mice having spontaneous genetic alterations in the pit-1 and prop-1 genes, Snell and Ames mice respectively, are long-lived. The pit-1 gene is a pituitary-specific transcription factor that can activate growth hormone and prolactin promoters. Prop-1 is a transcription factor that is upstream of pit-1, and can also induce expression of the growth hormone and prolactin genes. Thus, Snell and Ames mice with abnormalities in pit-1 and prop-1 also exhibit stunting of the anterior pituitary, resulting in deficiencies in several endocrine factors including growth hormone (GH), prolactin, TSH and IGF-1. These mice show growth retardation, but live 25-65% longer in comparison to wild-type littermates (Bartke et al., 2001; Brown-Borg et al., 1996; Flurkey et al., 2002). The overall consensus from studies of these mouse models suggests that the increased longevity is due to decreased IGF-1 signaling (Bartke et al., 2003). However, it is still unclear if the mechanisms involved are relevant to the life extension resulting from CR.

1.5 AGING AND CR: TOWARDS A MECHANISTIC UNDERSTANDING

Any intervention that slows aging should affect molecular and cellular processes. CR has been demonstrated to affect many such processes, as described in the following section.

1.5.1. GENE EXPRESSION

DNA microarray approaches have been used as a tool to better understand the process of aging and the effects of CR. Gene expression profiles have been characterized in several tissues of rodents (and humans), including skeletal muscle (Kayo et al., 2001; Lee et al., 1999b; Welle et al., 2004; Welle et al., 2003), brain (Lee et al., 2000), heart (Lee et al., 2002), and adipose tissue (Higami et al., 2004). Results from skeletal muscle will be the focus here since it is susceptible to oxidative stress and has been the tissue of greatest interest in this disseration.

Before describing the changes in gene expression with age and CR, it should be pointed out that most studies to date have assessed mRNA transcript levels of only one, or just a few gene(s). Moreover, while some microarray studies have confirmed their results with RT-PCR, relatively few have gone beyond transcript levels to assess protein levels. Despite this, these findings from gene expression profiling provide valuable information that can be used as a platform for further studies.

Gene expression patterns from gastrocnemius muscle from five mo old and thirty mo old male mice revealed that aging is characterized by increases in the expression of genes involved in the stress response (e.g., Hsp71, Hsp27), oxidative stress inducible genes (e.g.,

protease Do), and DNA damage induced genes (*e.g.*, GADD45) (Lee et al., 1999a). Aging also resulted in the induction of genes associated with muscle injury and re-innervation, including the genes for neurotrophin-3, PEA and HIC-5. Genes involved in mitochondrial function and turnover were down-regulated including those encoding subunits of ATP synthase, NADP transhydrogenase, and LON protease (involved in mitochondriogenesis). Aging also suppressed the expression of genes involved in fatty acid and cholesterol synthesis, glucose and glycogen metabolism including stearoyl desaturase and glucose-6-phosphate. Genes involved in protein turnover such as the 20S proteosome subunit and ubiquitin thioesterase were also down-regulated with age. These results support the concept that mitochondrial dysfunction plays a major role in the aging of skeletal muscle.

Subsequent studies in mouse skeletal muscle revealed that CR partially prevented or completely prevented these age-related changes (Lee *et al.*, 1999a). CR resulted in a shift of gene expression profile toward one that would support increased protein turnover and biosynthesis. These findings contrast the evidence for reduced protein turnover and the accumulation of altered proteins in age-matched animals receiving the control diet. For example, CR enhanced the expression of genes such elongation factor-1 and 26S proteasome subuit TBP-1, both of which are involved in protein turnover. CR also induced the expression of PPAR-delta and PPAR-gamma, two potent genes involved in fat metabolism and insulin sensitization. Genes involved in glycolysis, gluconeogenesis and the pentose phosphate shunt were also up-regulated with CR. Interestingly, CR mice had reduced expression of genes involved in stress response and/or DNA repair systems (Lee et al., 1999b; Sreekumar et al., 2002). The decrease in mRNA encoding genes involved in metabolic detoxification, DNA repair and the oxidative stress response is consistent with the

idea that CR acts through a reduction in oxidative damage. These studies also reported that CR lowered the expression of the thyroid hormone receptor-alpha gene, providing support for a state of lower basal metabolic rate in CR mice (Lee et al., 1999a). Thus these studies provide transcriptional evidence for a central mechanism of action of CR in aging retardation of postmitotic tissues involving shifts in energy metabolism, increases in protein turnover and decreased macromolecular damage (Lee et al., 1999a).

Gene expression profiles were also conducted in quadriceps muscle of rhesus monkeys (Kayo *et al.*, 2001). Aging up-regulated the expression of genes involved in inflammation and oxidative stress and those involved in neuronal death. Down-regulated genes included those that encode proteins involved in mitochondrial bioenergetics, such as those in the ETC. *Ad libitum* fed and CR monkeys (adult onset CR, CR duration of 9 yr) were also profiled. CR induced genes encoding structural proteins, such as collagen and proteins involved in cellular growth such as Sox12 and cyclin I. CR also suppressed the expression of genes involved in electron transport and oxidative metabolism, such as the 51kDa subunit of complex I and pyruvate dehydrogenase kinase (Park and Prolla, 2005). However, adult onset CR did not have an inhibitory effect on the age-related changes in gene expression. It is possible that CR in larger mammals, such as monkeys, only affects gene expression if it is initiated early in life.

Age-related changes in the gene expression profiles of human vastus lateralis muscle included reductions in genes involved in electron transport and oxidative phosphorylation (Welle et al., 2004; Welle et al., 2003). Induction of gene transcripts encoding metallothioneins, heterogenous nuclear ribonucleoproteins, RNA binding/processing proteins and components of the ubiquitin-proteasome proteolytic pathway also increased

(Welle et al., 2004; Welle et al., 2003). Surprisingly, the authors did not observe up-regulation of genes associated with oxidative stress. To date, there are no published reports of the CR effects on gene expression profiles in human muscle.

1.5.2. NUCLEAR AND MITOCHONDRIAL DNA DAMAGE

Aging may in part be a result of nuclear and mitochondrial genomic instability. Several studies have demonstrated increases in genomic DNA damage with age (Hudson *et al.*, 1998; Mecocci *et al.*, 1999). In various rodent models CR has resulted in reduced levels of 8-hydroxy 2-deoguanosine (8-oxodG; a biomarker of oxidative DNA damage) in brain, heart, skeletal muscle, kidney and liver (Sohal *et al.*, 1994a). The age-related increases in nuclear DNA mutations and damage may be due to reductions in DNA repair mechanisms as well as enhanced DNA repair pathways.

Moreover, mitochondrial DNA (mtDNA) damage may also play an important role in aging (Beckman and Ames, 1998). Oxidative damage compromises mitochondrial integrity with age, despite mitochondrial turnover processes (Shigenaga *et al.*, 1994; Wei *et al.*, 2001). Efficient mitochondrial bioenergetics requires the maintenance of mitochondrial DNA integrity (Hunt *et al.*, 2006). Mitochondrial DNA is thought to be more vulnerable to oxidative stress than nuclear DNA (nDNA) due to the fact that histone proteins do not protect it. Also, mtDNA is in much closer proximity to the ETC, the main site of ROS production, than is nDNA. The greater sensitivity of mtDNA to oxidative stress has been confirmed by several studies (Barja and Herrero, 2000; de la Asuncion et al., 1996; Yakes and Van Houten, 1997). Richter *et al.*, (1988) reported that rat liver mtDNA damage was 10-fold higher than nDNA. Similar results were also observed in human brain tissue

(Mecocci *et al.*, 1999). MtDNA damage could be particularly detrimental, as most of the mitochondrial genome is transcribed to proteins, whereas nDNA codes for many genes that are not transcribed (Van Remmen and Richardson, 2001). The increased susceptibility of mtDNA to oxidative damage has led to the concept of a "vicious cycle" in which initial damage increases subsequent ROS production, thereby leading to further damage (Harman, 1972).

Prior to the seminal work of Bohr, it was thought that alterations in mitochondrial DNA damage with age were due to ineffective repair pathways. Bohr and colleagues (2002) demonstrated that mitochondria have effective base-excision repair (BER) pathways. In fact, this mitochondrial repair pathway may even increase with age (Bohr, 2002). Nuclear BER, however, has been reported to be decreased with age (Bohr, 2002). CR has been shown to thwart age-associated decreases in nuclear BER in several tissues including brain, liver and spleen (Cabelof *et al.*, 2003). This finding has been corroborated and extended by Stuart and colleagues who have shown that CR is associated with an up-regulation of nuclear BER, but is not associated with an up-regulation of mitochondrial BER (Stuart et al., 2004). Results from these studies are consistent with the idea that the anti-aging effects of CR are independent of mtDNA repair pathways.

1.5.3. MEMBRANE STRUCTURE AND FUNCTION

Cellular membranes are structural barriers that protect cellular integrity, regulate movement into the cytosol and function as signal transducers. Therefore, it is extremely important that the composition of the cell membrane remains stable and that its infrastructure remains intact throughout the lifespan of an organism. With age, cellular

membranes undergo compositional changes that could, in part, explain the loss of function over time (Masoro, 2002).

Mitochondrial membrane lipids, especially the long polyunsaturated fatty acids, are highly vulnerable to oxidative damage. ROS can oxidize lipids, resulting in the production of highly reactive aldehyde species, such as 4-hydroxy-2,3, trans-nonenal (4-HNE). These products can, in turn, cause other serious detrimental effects. Cardiolipin, which makes up the bulk of mitochondrial inner membrane phospholipid composition, is extremely susceptible to oxidative damage due to the high degree of unsaturation of its fatty acids (Laganiere and Yu, 1993). The content of cardiolipin in the inner membrane is important for mitochondrial energetics, affecting the activities of several mitochondrial proteins including ANT and cytochrome c oxidase (Hoch 1992). Some theories of aging are based on the correlation between membrane lipid composition and aging. Specifically, maximum lifespan inversely correlates with the amount of membrane polyunsaturated fatty acids (PUFAs). PUFAs are more susceptibile to peroxidation and this increase in sensitivity has been thought to underlie cellular damage with age (Pamplona et al., 2002). Aging is associated with changes in fatty acid composition of the inner membrane including increased proportions of polyunsaturated long-chain fatty acids (e.g., 20:4, 22:5, 22:6) and decreases in 18:2, 18:1 and 16:1 fatty acids. Linoleic acid (18:2) is needed to optimize the interactions of cardiolipin and inner membrane proteins. Thus the decrease in 18:2 with age may explain the observed decreases in mitochondrial respiratory control ratios with aging (Shigenaga et al., 1994).

CR delays many of the age-associated changes in membrane composition by redistributing the proportions of membrane lipids (i.e., increasing the amount of 18;2 and

16:1 while decreasing the amount of 22:4 and 22:5) (Laganiere and Yu, 1993). CR also reduces membrane lipid peroxidation and maintains membrane fluidity in rat liver, brain and heart (Choe *et al.*, 1995; Choi and Yu, 1995; Lee *et al.*, 1999b; Yu *et al.*, 2002). Thus alterations of the composition of the mitochondrial and cellular membranes may be responsible for some of the anti-aging effects of CR.

1.5.4. PROTEIN STRUCTURE AND FUNCTION

There are several different types of posttranslational modifications of cellular proteins that occur with aging, including oxidation, glycation, glycoxidation, deamination, S-nitrosylation and aggregation; all of which can alter protein function (Masoro, 2002). Damage to mitochondrial inner membrane proteins due to oxidative stress can result in membrane depolarization and impaired mitochondrial function. Several components of oxidative phosphorylation, including ANT (Yan and Sohal, 1998) and ATP synthase have been reported to be vulnerable to oxidative stress *in vitro* (Forsmark-Andree et al., 1997; Lippe et al., 1991). In addition, the mitochondrial matrix enzyme, aconitase, has been shown to have increased susceptibility to oxidative stress (Yan *et al.*, 1997). Mitochondrial protein carbonyl groups have also been shown to increase with age in houseflies (Sohal and Dubey, 1994). CR has been shown to decrease the age-associated increase in oxidative damage to mitochondrial proteins in various tissues including brain, heart and skeletal muscle (Lass et al., 1998; Leeuwenburgh et al., 1997; Sohal et al., 1994b).

CR also increases protein turnover and protein synthesis in a variety of mouse tissues including liver, kidney and brain (Goto et al., 2002). The increase in protein turnover may contribute to the decreased accumulation of damaged proteins often associated with CR

(Weindruch *et al.*, 2001). CR increases autophagy (sequestration and degradation of damage organelles) in the liver and attenuates its age-related decline (Cavallini *et al.*, 2001; Donati *et al.*, 2001). Thus the beneficial effects of CR may be a result of improved protein turnover.

1.5.5. MITOCHONDRIAL FUNCTION AND ENERGETICS

It is clear that mitochondrial dysfunction leads to several age-related pathological conditions. Mitochondiral function or capacity for ATP production is the product of structural (i.e. mitochondrial volume) and functional (P/O ratio and ETC defects) aspects of the mitochondria. Thus age-related increase in mitochondrial oxidative damage results in loss of mitochondrial function. If CR is involved in delaying the aging process, then it should prevent or delay much of the age-related loss of mitochondrial function.

Several studies have examined whether or not mitochondrial ROS production is increased with age, however results have been inconsistent. ROS have been reported to increase in flight muscles of houseflies and in mitochondria isolated from mouse kidney, heart and brain and in rat liver mitochondria (Sohal et al., 1994a; Sohal and Sohal, 1991). Other studies have not observed any differences in ROS production with age in rat liver or heart (Hansford *et al.*, 1997; Lopez-Torres *et al.*, 2002). In skeletal muscle, ROS have been reported to be higher in older (20 mo) mice compared to younger mice (4 mo) (Lass *et al.*, 1998). Most recently, H_2O_2 production was demonstrated to be increased in old (27-29 mo) hind limb muscle compared to young (6-8 mo) mice (Mansouri *et al.*, 2006). The inconsistencies in the determination of age-related ROS levels may be a result of several experimental variables such as difference in methods of ROS assessment, assay conditions

(*e.g.*, substrates/inhibitors used; type of biological preparation: intact mitochondria vs. sub-mitochondrial particles *vs.* intact cells), species differences and tissue-dependence. Despite these differences, it is generally accepted that aging does result in higher levels of oxidative damage due to increased ROS production.

The increase in oxidative damage with age could result in impaired ATP production. ATP production was significantly lower in hind limb skeletal muscle of older mice compared to young mice (Mansouri et al., 2006). These results are consistent with previous studies in isolated hepatocytes (Harper *et al.*, 1998), rat skeletal muscle (Drew *et al.*, 2003) and in human skeletal muscle (Conley *et al.*, 2000; Short *et al.*, 2005). Similarly, *in vivo* ATP content was 50% lower in quadriceps muscle from elderly subjects, compared to younger subjects (Conley *et al.*, 2000). Consistent with decreases in ATP production, there are age-related changes in the activity of the ETC complexes in a variety of tissues. For example, complexes I, III and IV seem to be most affected by age. These complexes have been reported to have significantly lower activity in the gastrocnemius muscle of 20 mo old mice compared to 10 mo old mice (Desai et al., 1996; Kumaran et al., 2004). In humans, the age-related reduction in ETC activity is not as clear. It was reported to be reduced for complex I, II and IV in muscle (19 vs. 91 yr) (Boffoli et al., 1994) whereas Capel *et al.* (2005) did not observe any decreases in the activity of any of these complexes. The reasons for the different outcomes are not known, but may be related to the fact that different muscle groups were studied. Complex II seems to be the least affected by age. Interestingly, many of the subunits comprising complex I, III and IV are encoded by mtDNA, whereas complex II is entirely encoded by nDNA (Van Remmen and Richardson, 2001).

In addition to age-related declines in ATP production, aging has been associated with increased mitochondrial proton leak. Specifically, our laboratory has reported that proton leak was higher in hepatocytes isolated from 30 mo old mice compared to those from 3 mo old mice (Harper et al., 1998; Lal et al., 2001). This is consistent with several studies that have demonstrated decreased mitochondrial membrane potential with age (Hagen et al., 1997; Sastre et al., 1996). Changes in mitochondrial lipid composition and lipid peroxidation are also consistent with the age-related increases proton leak.

Our laboratory has demonstrated that long-term CR prevented the age-related increase in proton leak-dependent oxygen consumption in skeletal muscle mitochondria from CR rats (Lal *et al.*, 2001). Similarly, CR prevented the age-related increase in state 4 (non-phosphorylating) respiration in brain, heart, and kidney mitochondrial isolated from 9, 17, and 23 mo old mice (Sohal *et al.*, 1994b). Long-term, but not short-term, CR lowered mitochondrial proton leak and decreased ROS production in liver mitochondria of 40% CR rats (Hagopian et al., 2005; Ramsey et al., 2004). This reduction in liver proton leak was not consistent with the results of Lambert *et al.*, (2004) who demonstrated a CR related increase in proton leak associated with decreased ROS production in rats. These differences may be a result of the variation in the experimental design. For example, Lambert and Merry used Brown Norway rats, and initiated CR at 2 months of age, and used body weight clamping rather than CR *per se*. Thus, the contributions to the proton leak differences could be due to differences in rat strain, age of CR initiation, and CR protocol (Ramsey et al., 2004). Interestingly, the increased leak with CR in these studies was reversed by 2 wk insulin replacement suggesting that insulin signalling may be important for the action of CR in decreasing ROS (Lambert *et al.*, 2004).

Most recently, Lopez-Lluch reported decreased oxygen consumption, membrane potential and ROS production in primary hepatocytes, FaO and HeLa cells cultured in serum from 40% CR rats (Lopez-Lluch et al., 2006). CR increased respiratory control ratios (RCRs) in isolated mitochondria suggesting that CR may increase the efficiency of electron transport and oxidative phosphorylation. These cells were able to maintain constant ATP production. CR serum also stimulated mitochondrial proliferation via a peroxisome proliferation-activated receptor co-activator 1 alpha (PGC-1α) signalling mechanism (Lopez-Lluch *et al.*, 2006). Recently, Civitarese *et al.*, (2007) have demonstrated that participants following 25% CR or a combination of 12.5% CR and 12.5% increased energy expenditure program for 6 mo had increased expression of genes coding for proteins involved in mitochondrial function such as PPARGC1A, TFAM, eNOS , SIRT1 and PARL. These increases were in parallel with increase mitochondrial DNA content in both groups. However, the activity of mitochondrial enzymes of the TCA, beta-oxidation and the electron transport chain were unchanged. These results suggest that CR improves mitochondrial biogenesis and efficiency two important factors in the action of CR.

It is currently unclear how improvements in mitochondrial energetics lead to increased lifespan. Over the years, the regulation of lifespan in many species has been suggested to be under the control of a family of class III histone deacetylases called sirtuins. Sirtuins are conserved from bacteria to humans (Blander and Guarente, 2004; Bordone and Guarente, 2005). Recent studies in yeast and flies suggest that the CR-induced increase in lifespan involves the NAD-dependent deacetylase Sir2 gene. NAD is widely used in metabolic reactions, thus Sir2 may be an important factor linking cellular energetics to lifespan (Bordone and Guarente, 2005). The effects of CR on lifespan in yeast and flies

suggest that Sir2 proteins may also be involved in CR effects observed in mammals. SIRT1 is the mammalian homologue to Sir2. Since Sir2 has been shown to mediate the effect of CR in lower animals it has been suggested that SIRT1 may trigger many of the physiological responses to CR. In fact, SIRT1 is up-regulated by CR in humans (Cohen *et al.*, 2004). SIRT1 has been shown to also be an NAD-dependent deacetylase (Imai *et al.*, 2000) with substrates that include histones, and key transcription factors such as p53 and forkhead (Brunet et al., 2004; Luo et al., 2001; Motta et al., 2004; Vaziri et al., 2001). Finally, SIRT1 is involved in the post-translational processing of PGC-1α, an important regulator of mitochondrial biogenesis (Nemoto et al., 2005; Rodgers et al., 2005). Despite the many recent studies examining the specific role of SIRT1 in aging and CR, the mechanisms are still poorly understood.

1.6 UNCOUPLING PROTEIN 3

1.6.1. HISTORICAL PERSPECTIVE

The first member of the uncoupling protein family was cloned and identified in 1985 and was named UCP1 or thermogenin (Bouillaud *et al.*, 1985; Bouillaud *et al.*, 1986). UCP1 a 32kDa protein is abundantly, and solely expressed in brown adipose tissues (BAT), a tissue responsible for non-shivering thermogenesis (NST). NST allows hibernators, cold-adapted rodents and newborn animals to generate heat (thermogenesis) and maintain body temperature (thermoregulation) without shivering (Davis and Mayer, 1955). The thermogenic function of BAT is due to UCP1, which, upon sympathetic activation (by cold

or high-fat diet), mediates a fatty acid induced proton leak across the mitochondrial inner membrane.

The "newer" uncoupling proteins, were discovered by reverse cloning i.e., the genes were cloned before their function was known. Indeed, while it is known that the UCPs are members of the approximately 35-member mitochondrial carrier protein superfamily, their functions are currently still unclear. Members of the UCP subfamily have been found in both animal and plant species and are all mitochondrial inner membrane proteins with molecular mass of 31-34kDa. In mammals, four UCP1 homologues have been identified based on their amino acid similarity to UCP1. The homologues are referred to as UCP2 (Fleury *et al.*, 1997; Gimeno *et al.*, 1997), UCP3 (Boss *et al.*, 1997; Gong *et al.*, 1997; Vidal-Puig *et al.*, 1997), UCP4 (Mao *et al.*, 1999) and UCP5 (Sanchis *et al.*, 1998). Phylogenetic analyses have revealed that UCP2, UCP3 and avian UCPs share a higher similarity to UCP1 than the other homologues and are thus often called the 'novel' UCPs. UCP2 and UCP3 are 50% and 57% homologous to UCP1, respectively. UCP2 and UCP3 are 73% identical to each other. UCP2 and UCP3 also have conserved residues that are thought to be involved in proton transport and nucleotide binding (Klingenberg and Huang, 1999). UCP4 and UCP5 have much lower sequence identity to UCP1 (Borecky *et al.*, 2001).

The 'novel' UCPs were named based on the assumption that they would have the same function as UCP1, thermogenic uncoupling. This naming appears to have been premature since uncoupling may not be their primary function. Almost 10 years after their discovery, the physiological function (s) of the novel UCPs is still unclear. Current ideas include: 1) mediating proton leak; 2) mitigating ROS production; and 3) fatty acid anion

export (Bezaire et al., 2005; Costford et al., 2006). UCPs have become important in the fields of thermogenesis, obesity, diabetes, and free radical biology.

1.6.2 GENE AND PROTEIN STRUCTURE OF UCP3

The human Ucp3 gene is adjacent to the Ucp2 gene on chromosome 11q13, a location linked to hyperinsulinemia and obesity (DeBry and Seldin, 1996; Kleyn *et al.*, 1996; Taylor and Phillips, 1996). The two genes are separated by approximately 7.9kb and 8.3kb of genomic DNA in humans and mice, respectively (Fleury *et al.*, 1997; Solanes *et al.*, 1997). Each exon of the Ucp3 gene encodes one of six transmembrane domains. The UCP3 gene generates two transcripts, UCP3 long form ($UCP3_L$) and UCP3 short form ($UCP3_S$). $UCP3_S$ lacks the last coding exon resulting in a truncated protein missing the sixth transmembrane domain. $UCP3_L$ responds physiologically (e.g., to fasting) however it is not known whether $UCP3_S$ respondes similarly (Boss *et al.*, 1997; Solanes *et al.*, 1997). The transcriptional regulation of UCP3 occurs through three putative peroxisome proliferator elements (PPRE) and one thyroid response element (TRE). The Ucp3 gene also contains muscle specific recognition motifs such as E-box sites and MEF-2 sites (Acin et al., 1999; Gong et al., 1997).

The crystal structure of UCP3 has not yet been elucidated, however, the structure is likely to be similar to other members of the mitochondrial anion carrier family including the ANT and the phosphate carrier (Aquila *et al.*, 1985; Pebay-Peyroula *et al.*, 2003). Some similarities include six transmembrane alpha helices composed of three repeats with each repeat containing two hydrophobic regions. Each helix is attached via a long hydrophilic

loop on the matrix side of the mitochondrial inner membrane. Functional UCPs are thought to be part of a dimer consisting of two identical subunits (Boss et al., 2000).

1.6.3 UCP3 TISSUE EXPRESSION

Unlike UCP1, the gene expression patterns for the novel uncoupling proteins are more diverse. It is now known that UCP2 and UCP3 are present in small amounts, 0.01% and 0.1%, respectively, of membrane protein. The levels of UCP3 in skeletal muscle mitochondrial is approximately 200 fold lower than that for UCP1 in BAT (Esteves and Brand, 2005).

UCP2 mRNA and protein are more ubiquitously expressed, with high levels in the spleen, lung, stomach and pancreas (Pecqueur *et al.*, 2001; Zhang *et al.*, 2001). The protein has not been detected in muscle, heart, kidney, brain and BAT, despite reports of high UCP2 mRNA levels (Pecqueur *et al.*, 2001).

UCP3 mRNA is found in muscle, heart and, brown adipose tissue, however, to date, UCP3 protein has been only found in muscle and heart (Cadenas et al., 2002; Gong et al., 2000; Vidal-Puig et al., 2000). The mRNA and protein levels of UCP3 are higher in type II fibers (fast, glycolytic) than in type I fibers (slow oxidative) in muscle in rodents (Boss et al., 2000; Jimenez et al., 2002) and humans (Hesselink et al., 2001).

1.6.4 HYPOTHESIZED FUNCTION: UCP3 AS A MEDIATOR OF PROTON LEAK?

Due to the relatively high amino acid identity of UCP3 with UCP1, it was originally hypothesized that UCP3 functioned as a true uncoupling protein by causing a proton leak. Several studies have reported increased mitochondrial uncoupling when UCP3 has been

ectopically expressed or entopically overexpressed in a variety of systems including yeast, proteoliposomes, mammalian cells and transgenic mice (Clapham et al., 2000; Gong et al., 1997; Hagen et al., 2000; Hinz et al., 1999a; Hinz et al., 1999b).

Despite the increased uncoupling observed with high levels of UCP3 expression, there is mounting evidence that this hypothesis is incorrect. The first piece of evidence is indicated by cold-intolerance of the *Ucp1*-ablated mouse. In this model, UCP2 and UCP3 mRNA expression was increased but did not substitute for UCP1 in cold-induced non-shivering thermogenesis (Enerback et al., 1997). In addition, UCP2 or UCP3 did not compensate for UCP1 in adrenergic or fatty acid induced thermogenesis in *Ucp1*-ablated brown adipocytes (Matthias et al., 2000). Furthermore, proton leak is not larger in the muscles of fasted rats or mice despite the increased UCP3 expression (Bezaire et al., 2001; Cadenas et al., 1999) (Bezaire et al., 2001). These findings suggest that UCP3 does not cause a physiologically important proton leak. As described below, it was proposed that the uncoupling observed with UCP3 overexpression at supraphysiological levels is artifactual; that is, that the uncoupling is not related to a specific function of UCP3.

In 2001, Stuart *et al.*, used yeast to endogenously or ectopically express UCP1 at low levels. Under these conditions uncoupling by UCP1 was inhibited by purine nucleotides. However, nucleotide inhibition of leak was lost when UCP1 was expressed at higher levels (Stuart et al., 2001a), indicating that this non-GDP sensitive leak was not specific to UCP1 activity. Artifactual uncoupling was similarly detected with high levels of UCP2 or UCP3 expression (Harper et al., 2002; Stuart et al., 2001b). More recently, our laboratory reported that the overexpression of physiologically relevant levels of UCP3 (2.2-2.5 fold) in L6

myotubes did not result in enhanced uncoupling (MacLellan *et al.*, 2005), supporting the conclusion that the uncoupling observed in UCP3 overexpression studies is artifactual.

Gene knockout experiments have been useful for providing further insight into the role of UCP3 as an uncoupler as they avoid the complexities of non-physiological uncoupling that can accompany overexpression. Several groups have characterized the bioenergetic properties of muscle mitochondria of the *Ucp3*-knockout mice (*Ucp3*-KO). These groups have either reported: 1) a decrease in state 4 respiration (Vidal-Puig *et al.*, 2000) or 2) an increase in membrane potential but no change in state 4 respiration (Bezaire et al., 2001; Gong et al., 2000). Another *Ucp3*-KO study did not observe differences in state 4 respiration or membrane potential (Cadenas *et al.*, 1999). These inconsistencies could be a result of experimental differences such as mitochondrial isolation procedures, incubation conditions (*e.g.* presence or absence of fatty acids) and more importantly, the genetic background of the *Ucp3*-KO mice used. In fact, Cadenas *et al.*, (1999) were the only group to conduct their experiments in mice on a congenic background. As a whole these conflicting results do not provide conclusive evidence for the role of UCP3 in skeletal muscle mitochondrial proton leak.

Related to its proposed uncoupling function, UCP3 has also been hypothesized to offer protection from obesity. This is supported by the fact that the UCP3 gene is located near an obesity-related locus. Interestingly, thyroid hormones, which stimulate metabolic rate, also increase UCP3 expression (Barbe et al., 2001; Schrauwen et al., 1999). In addition, the fact that UCP3 is expressed in skeletal muscle, a major contributor to basal metabolic rate, makes it an attractive target for obesity treatment as demonstrated by the lack of obesity in mice overexpressing extremely high levels of the human UCP3 gene (20-fold)

(Clapham *et al.*, 2000). However, a physiological role for UCP3 in thermogenesis and obesity prevention is contradicted by the paradoxal observation that fasting, a condition that conserves energy (*i.e.*, decreases energy expenditure) results in a 4 fold increase in UCP3 mRNA levels without any changes in proton conductance (Bezaire et al., 2001; Cadenas et al., 1999; Samec et al., 1999). Importantly, *Ucp3*-KO mice are not obese as would be expected if UCP3 functions as a true uncoupler (Gong *et al.*, 2000). Thus, the paradoxal effects of fasting on UCP3 expression make it difficult to reconcile the hypothesis that UCP3 is a true uncoupling protein.

1.6.5 HYPOTHESIZED FUNCTION: UCP3 AS A FATTY ACID ANION TRANSPORTER?

Fatty acids are the predominant fuel source for skeletal muscle under certain conditions such as fasting and exercise. The accumulation of fatty acyl CoA molecules or fatty acid anions within the mitochondria is thought to be potentially damaging. Mechanisms to remove these potentially dangerous fatty acid molecules are unknown. In 2001, Himms-Hagen and Harper (2001) proposed such a mechanism. They hypothesized that UCP3 functions to export fatty acid anions out of the mitochondrial matrix, to facilitate high rates of fatty acid oxidation (Figure 4).

The "Himms-Hagen and Harper" model proposes that UCP3, together with mitochondrial acyl-CoA thioesterase-1 (MTE-1), liberate CoASH and fatty acid anions from the hydrolysis of acyl-CoA. The regeneration of CoASH is beneficial as this coenzyme is potentially limiting during high rates of fatty acid oxidation (Bartlett and Eaton, 2004). Its release by MTE-1 increases CoASH availability for β-oxidation and the Krebs cycle. The fatty acid anions generated from MTE-1 would need to be transported back across the inner

membrane by UCP3 to the cytosol, where they can be reesterified by acyl-CoA synthethase and used for other metabolic pathways such as cellular signaling or re-entry into the matrix for oxidation. Thus, UCP3 is suggested to work with MTE-1 to release CoASH and export potentially toxic fatty acid anions out of the matrix (Himms-Hagen and Harper, 2001).

Schrauwen *et al.* (2001b), proposed a somewhat similar hypothesis (Figure 4). He suggested that when fatty acid supply exceeds fatty acid oxidation capacity, cytosolic fatty acids could enter the mitochondria by flip-flopping across the mitochondrial inner membrane. UCP3 would function as a 'flipase' to export these potentially toxic fatty acids from the matrix to the cytosol. However, this model for UCP3 is limited, as it does not integrate UCP3 expression with physiological increases in fatty acid oxidation or MTE-1 expression and relies on mitochondrial fatty acid uptake through a CPT1 independent mechanism (*i.e.*, passive diffusion).

A role for UCP3 in fatty acid anion export is supported by the strong correlation between UCP3 expression and states that are associated with increased fat metabolism such as fasting (Bezaire et al., 2001; Boss et al., 1998a; Cadenas et al., 1999; Millet et al., 1997; Weigle et al., 1998), acute exercise (Cortright et al., 1999; Tsuboyama-Kasaoka et al., 1998), high fat diets (Gong *et al.*, 1999), and Intralipid administration (Weigle et al., 1998), all of which are conditions in which reliance upon fat oxidation in muscle is increased. Conversely, decreased UCP3 mRNA expression has been correlated to situations where fatty acid levels are reduced, such as hypothyroidism (Gong et al., 1997) and chronic starvation (Boss et al., 1998b). Thus, it appears that the expression of skeletal muscle Ucp3 mRNA is associated with a switch towards oxidation of fatty acids, regardless of whether energy expenditure is increased or decreased. The expression of MTE-1, like that of UCP3,

is regulated by PPARs, and recent reports have demonstrated that expression patterns of the two genes are similar (Hunt *et al.*, 1999; Moore *et al.*, 2001; Stavinoha *et al.*, 2004). Expression of MTE-1 mRNA is highest in skeletal muscle, heart, BAT and WAT, which are all tissues with high levels of β-oxidation. Additionally, MTE-1 mRNA expression was increased three-fold in UCP3 overexpressing mice (Moore *et al.*, 2001). Furthermore, a study in db/db mice and db/+ mice showed that UCP3 expression was related to changes in MTE-1 expression in response to treatment with PPAR agonists (Clapham *et al.*, 2001).

It has been reported that fasting and high fat-feeding have a more pronounced effect on UCP3 mRNA in type II fibers in humans (Russell et al., 2003; Schrauwen et al., 2001a). These results are very intriguing as type I muscle fibers, compared to type II fibers, have a greater capacity to shift between glucose and lipid metabolism (i.e., have greater capacity for elevated fatty acid oxidation levels), and have greater mitochondrial contents. Thus, the findings that UCP3 expression is not as pronounced in type I fibers may be a result of the already increased capacity of type I fibers to cope with elevated fatty acid fluxes. Thus adaptive mechanisms (e.g., increased UCP3) would be less urgently required. Altogether, muscle fiber type-specific expression of UCP3 is consistent with the proposal that UCP3 may have a role in facilitating fatty acid oxidation (Himms-Hagen and Harper, 2001) or protection from lipotoxicity (Schrauwen et al., 2001b).

Further evidence for a role of UCP3 in facilitating fat oxidation includes the finding that humans with UCP3 mutations and *Ucp3*-KO mice have higher respiratory quotients, indicating a decreased reliance on lipids as fuels (Argyropoulos *et al.*, 1998; Bezaire *et al.*, 2001). Most recently, Bezaire *et al.*, (2005) observed lower respiratory quotients indicating a shift towards increased fat oxidation in UCP3 overexpressor mice, compared to congenic

control mice. Other observations included increases in plasma membrane fatty acid binding protein content, CPT I, beta-hydroxyacyl-CoA dehydrogenase, citrase synthase, CoA and carnitine, as well as decreases in intramusclar triacylglycerol in UCP3 overexpressors. These findings are consistent for a role of UCP3 in facilitating fatty acid oxidation in skeletal muscle. Despite the substantial amount of indirect evidence that UCP3 may export fatty acid anions out of the matrix, direct evidence has been lacking. Recently, Gerber *et al.*, (2006) demonstrated the existence of a mitochondrial long-chain free fatty acid generation and export system. They also observed that the activity of this system is correlated with MTE-1 and UCP3 levels (Gerber *et al.*, 2006). This is the first report providing direct evidence of such a fatty acid export system in mitochondria, however, more work is needed to directly link the involvement of MTE-1 and UCP3.

1.6.6 HYPOTHESIZED FUNCTION: PROTECTION AGAINST ROS?

As previously mentioned, any means of uncoupling will decrease membrane potential and attenuate ROS production as mitochondrial ROS production is very sensitive to the PMF. UCP3 has been suggested to mitigate excess ROS production by uncoupling processes (Echtay et al., 2002; Vidal-Puig et al., 2000). The proposed mechanism for the UCP3-mediated protection from ROS is shown in Figure 4. Briefly, when membrane potential is high, superoxide production by the ETC is increased. The resulting superoxide may then activate UCP3 through intermediates such as 4-HNE and other reactive alkenals (Echtay et al., 2003). Activation of UCP3 increases proton leak across the mitochondrial inner membrane by transporting a proton from the intermembrane space back into the mitochondrial matrix. In turn, the increase in proton leak causes a decrease in membrane

potential which then limits the production of superoxide in an autoregulatory feedback manner (Brand et al., 2004a).

Support of the UCP3-mediated control of superoxide production comes from the finding that exogenously generated superoxide and lipid peroxidation products such as 4-HNE activate proton leak in isolated mitochondria and in intact cells. This leak was thought to occur in a UCP3-dependent manner as it was inhibited by GDP, a putative inhibitor of UCPs. In addition, this superoxide-activated leak was not present in liver mitochondria, (which do not express UCPs) from wild-type mice and in Ucp3-KO mice (Brand et al., 2004a; Echtay et al., 2002). The effect of mild uncoupling and GDP inhibition on proton leak is consistent with their effect on ROS production (*i.e.,* ROS is lower with mild uncoupling and increased in the presence of GDP) (Brand, 2000; Lambert and Brand, 2004; Miwa et al., 2003; Talbot et al., 2004). Further evidence comes from the fact that superoxide and oxidative damage is increased in skeletal muscle mitochondria from mice lacking UCP3 (Brand et al., 2002; Vidal-Puig et al., 2000). Similarly, UCP2 knockout mice are more resistant to *Toxoplasma gondii* infection through increased macrophage ROS production (Arsenijevic *et al.*, 2000). Moreover, ROS production is elevated when fatty acid oxidation increases (St-Pierre et al., 2002). This provides a potential explanation as to why UCP3 expression is increased during conditions of increased fat oxidation

Despite the supportive evidence described above, it is still unclear what the physiological importance is of UCP3 in prevention of ROS production. The hypothesis for UCP3 in ROS protection is based on the fact that UCP3 acts as an uncoupling protein to decrease ROS production. As illustrated in section 1.6.4, much evidence suggests that UCP3 does not function as a classical uncoupler under physiological conditions. Evidence

against UCP3 in the mitigation of ROS comes from the fact that heart mitochondria, which express UCP3, were found not to be sensitive to exogenous superoxide (Echtay *et al.*, 2002). Similarly other animal models are associated with increased UCP3 expression such as thyroid hormone treated rats which showed no differences in proton conductance despite increased superoxide levels and UCP3 expression (Silvestri et al., 2005). In addition, *Ucp1*-KO mice were also not responsive to the superoxide effect on proton leak as HNE was not able to change the UCP1-dependent proton leak in brown fat mitochondria from wild-type and *Ucp1*- KO mice (Shabalina et al., 2006). Consistent with this notion is the fact that CHO cells stably expressing UCP3 did not show changes in uncoupling after exposure to oligomycin to stimulate endogenous superoxide production (Mozo et al., 2006). Moreover, SOD overexpressing mice did not have differences in fatty acid induced uncoupling despite lower levels of ROS production and damage (Silva et al., 2005). Recently, MacLellan *et al.*, (2005) demonstrated that normal physiological overexpression of UCP3 in L6 myotubes decreased ROS production via a "UCP3 dependent, uncoupling-independent" mechanism. Specifically, ROS production was only decreased via the classical uncoupling mechanism when L6 myotubes were treated with DNP (a chemical uncoupler). In other words, the decrease in ROS production was associated with decreased membrane potential and increased oxygen consumption. In contrast, the decreased ROS production in UCP3 overexpressing myotubes was not associated with changes in oxygen consumption or membrane potential. Therefore, the reduction in ROS production in myotubes occurred by a UCP3- dependent mechanism, but was not mediated by uncoupling (MacLellan *et al.*, 2005). *In vivo*, no differences in oxidative damage were observed in UCP3 overexpressing

mice compared to wild-type mice (Brand *et al.*, 2002) suggesting that mild uncoupling beyond normal basal rates does not provide much protection against ROS and ROS damage.

Recently, David Nicholls published a review on physiological regulation of uncoupling proteins (Nicholls, 2006). In this paper he questioned the physiological importance of the finding by Brand's laboratory that ROS can activate UCP3 through a negative feedback mechanism. Many of the studies supporting this idea have demonstrated that the superoxide activation of UCP3 is inhibitable by GDP. GDP is generally accepted and used to detect the presence endogenous UCPs. Nicholls' major concern is that the *in vivo* concentration of purine nucleotides, including GDP, is greater than the concentration used in many of the *in vitro* studies conducted in Brand's laboratory. Thus in order to be considered physiologically relevant, any putative activator must have an effect even in the presence of physiological concentrations of purine nucleotides (Nicholls, 2006).

It is unclear whether or not endogenous levels of UCP3 protect against ROS production and damage via classical uncoupling or via another mechanism. As a whole, these recent reports suggest that superoxide only regulates UCP3 when present at supra-physiological levels (*i.e.*, endogenous superoxide does not seem to regulate UCP3). However, it cannot be ignored that *Ucp3*-KO mice have increased muscle mitochondrial oxidative damage (Brand et al., 2002; Vidal-Puig et al., 2000). Interestingly, UCP3 overexpression does not lead to additional benefits of protection from ROS (Brand et al., 2002). However, as previously discussed, interpretation of overexpression data must be done with caution as supraphysiological levels of UCP3 lead to artifactual uncoupling. Also, Brand's ROS hypothesis is not specific to UCP3 as even other proteins; UCP1 and ANT are included in this mechanism. All together, more *in vivo* data using physiological

levels of UCP3 overexpression are needed to directly test whether UCP3 plays a role in protection from ROS. Correspondingly, more *in vitro* data are needed to further elucidate the putative mechanism (s) of UCP3-mediated fatty acid translocation.

FIGURE 4: HYPOTHESIZED FUNCTIONS OF UNCOUPLING PROTEIN 3.

Three functions for UCP3 have been proposed. The proposed mechanisms are shown in chronological order of publication. (1) UCP3 exports long-chain fatty acids (LCFA) produced by MTE-1 resulting in the release of mitochondrial matrix CoASH, the rate-limiting coenzyme for β-oxidation and the Krebs cycle. The UCP3-mediated export of LCFA is reactivated by acyl-CoA synthase in the intermembrane space. This model suggests that MTE-1 and UCP3 function together to facilitate fatty acid oxidation. (Himms-Hagen and Harper, 2001). (2) The second hypothesis proposes that UCP3 removes LCFA that have entered the mitochondrial matrix independently of CPT. The export of excess LCFA would remove potentially damaging fatty acid anions from the mitochondrial matrix (Schrauwen et al., 2001b). (3) 4-HNE and other lipid radicals are proposed to activate UCP3-mediated proton leak, which would mitigate ROS production by lowering the mitochondrial membrane potential (Echtay et al., 2003). Figure adapted from (MacLellan et al., 2005).

Abbreviations used in this figure include; MOM, mitochondrial outer membrane; MIM, mitochondrial inner membrane; CPT, carnitine palmitoyltransferase; LCFA, long-chain fatty acid anion; ACS, acyl-coenzyme A synthase; ß-ox, ß-oxidation; MTE-1, mitochondrial thioesterase 1; HNE, hydroxynonenal; H_2O_2, hydrogen peroxide; SOD, superoxide dismutase; OH, hydroxyl radical.

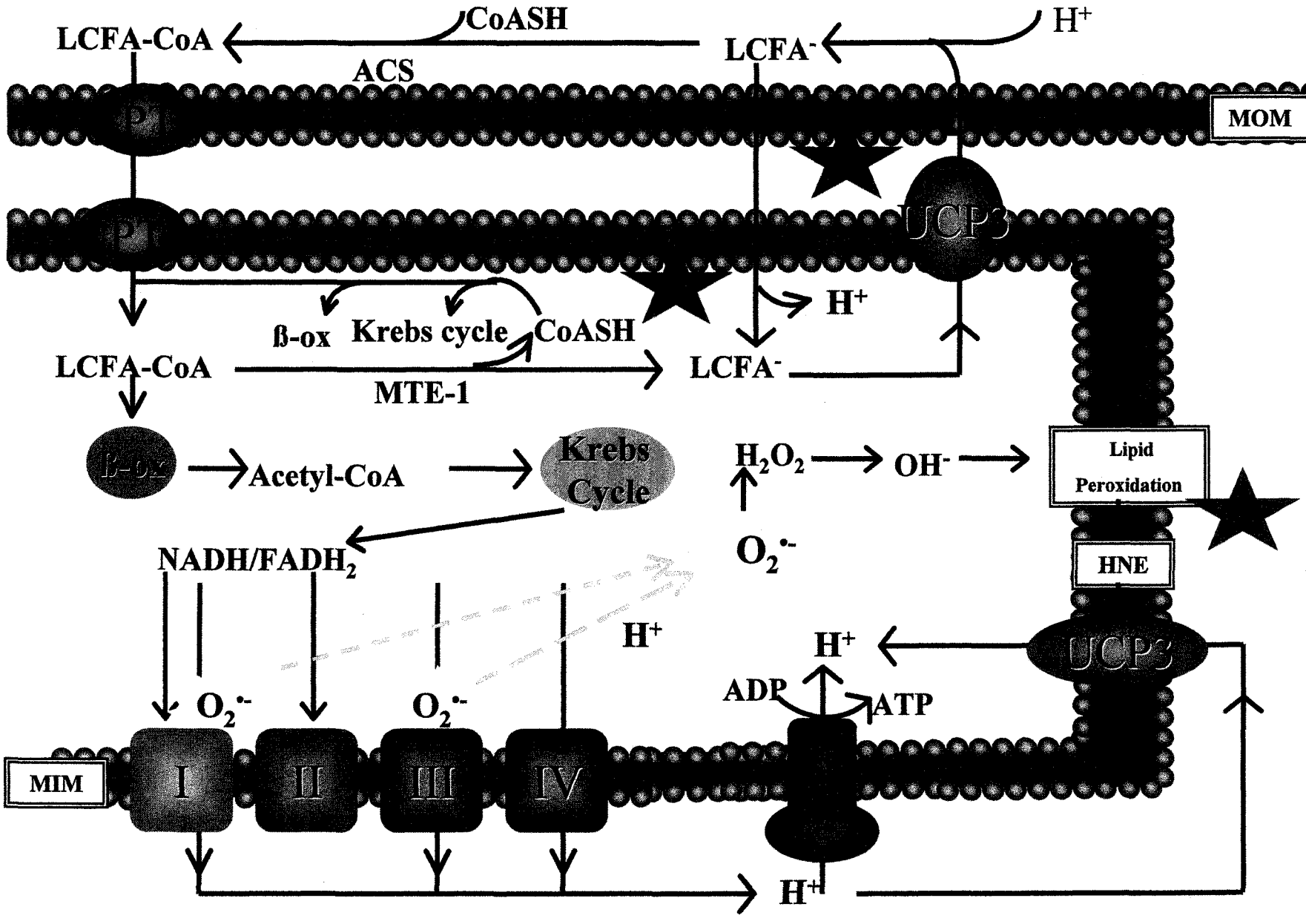

CHAPTER 2
OBJECTIVES

It is well documented that calorie restriction (CR) without malnutrition effectively increases lifespan and stress resistance in a wide variety of species. In addition CR reduces susceptibility to chronic disease and attenuates age-related functional decline. However to date, the mechanisms underlying CR are unclear. In this dissertation we attempted to elucidate the underlying metabolic mechanisms by examining the effects of CR of increasing durations on whole body and mitochondrial energetics. It was hypothesized that CR may attenuate oxidative damage and bioenergetic decline by producing an environment that induces a hypometabolic state characterized by a reduction in whole body and mitochondrial oxygen consumption, decreased ROS production and mitochondrial proton leak with subsequent reduction in damage to cellular macromolecules. We also proposed that the underlying mechanism of a decreased proton leak would involve changes in Uncoupling Protein 3 (UCP3) expression.

To test these hypotheses, we used $FBNF_1$ rats that were either *ad libitum* fed or 40% CR for increasing durations. Furthermore, *Ucp3*-knockout (*Ucp3*-KO) and wild-type mice were studied to determine the potential role of UCP3 in CR-related changes in skeletal muscle mitochondrial energetics. The specific objectives were:

- To evaluate changes in whole body energy metabolism, skeletal muscle mitochondrial proton leak, respiratory control and reactive oxygen species

production with short- (2 wk and 2 mo) and medium- (6 mo) and long-term (12 mo and 18 mo) 40% CR in $FBNF_1$ rats

- To elucidate the implications of increased UCP3 expression in the regulation of whole body energy metabolism and mitochondrial proton leak in response to short-term (2 wk) 40% CR in *Ucp3*- KO mice and wild-type mice.

CHAPTER 3
METHODS AND MATERIALS

3.1 EFFECT OF CALORIE RESTRICTION ON FBNF$_1$ RATS

3.1.1 TREATMENT OF ANIMALS

For all experiments, male FBNF$_1$ rats were obtained from the research laboratory of Dr. J. Ramsey at the University of California, Davis (Davis, CA). FBNF$_1$ rats are the F$_1$ generation of the cross between Fisher 344 rats and Brown Norway rats. This strain is a long-lived rat model that is resistant to the development of several diseases, such as renal failure, that occur commonly in other widely used rat models of aging. Because if this disease resistance, the FBNF$_1$ rat offered a better chance for studying healthy older animals than other strains (e.g., Fisher 344, Sprague-Dawley) (Lipman et al., 1996).

The rats for each study were purchased from the National Institute on Aging (NIA) Aging Rodent Colony (Bethesda, MD) at 4 mo of age. Upon arrival of the rats at the University of Ottawa, daily food intake and body weight measurements were conducted as part of a 3 wk adaptation period. Before the start of the study, the rats were given *ad libitum* access to an AIN-93M purified diet (Research Diets, New Brunswick, NJ). Food intake and body weights were monitored daily until 6 mo of age when the rats were randomly divided into control and CR groups (n = 6-7/group). The initial body weights were approximately in the range of 409-411g. The average daily food intake of the group was taken as the *ad libitum* food intake amount that would be used for all CR adjustments. Animals were cared

for in accordance with guidelines from The Canadian Council on Animal Care and the Institute of Laboratory Animal Resources (National Research Council, Washington, DC)

3.1.2 DIET COMPOSITION

All animals were 6 mo of age at the start of the CR regimens, had free access to water, and were housed at 23°C with lights on from 0700 to 1900. The composition of the control and CR diets used are summarized in Table 1. For the 2 wk and 2 mo time point studies, control animals were allowed *ad libitum* access to AIN-93M purified, defined diet. In the medium and long-term dietary intervention phase, control animals were restricted to 95% of the *ad libitum* intake of the diet to prevent the development of obesity.

For all studies, the CR animals were fed a modified AIN-93M diet (Research Diets, New Brunswick, NJ) at 60% of the calculated *ad libitum* food intake amount. The carbohydrate (corn starch) component of the CR diet was decreased, resulting in an increased amount of protein, fat, vitamins and minerals in the CR diet. This ensured that the control and CR rats had equivalent daily intakes of essential nutrients and avoided nutritional deficiencies in the CR rats. The energy intakes were 61.6 kcal/day for the control and 37.6 kcal/day for the CR rats.

3.1.3 INDIRECT CALORIMETRY

Characteristics of whole body energy expenditure and respiratory exchange ratios were assessed using a customized four-chamber Oxymax open-circuit indirect calorimeter with automatic temperature and light controls (Columbus Instruments, Columbus OH). System settings included an airflow rate of 1.0 L/min, a settle time of 2 min and a

measurement period of 60 s every 12 min. Two to three days prior to sacrifice, rats were individually placed in the respiration chambers (11.7 L / chamber). Data was collected over a 24 h period with a light cycle from 0700 to 1900; temperature was maintained at 23°C.

The data set from each individual rat was plotted, and analyzed using the percent relative cumulative frequency (PRCF) approach as described by Riachi *et al.* (Riachi et al., 2004), and Liu *et al.* (Liu et al., 2003; Riachi et al., 2004). Statistical comparisons of PRCF curves are based on the 50th percentile values and curve slopes (H values). See Appendix 1 for a brief overview PRCF.

3.1.4 ORGAN WEIGHTS MEASUREMENTS

Tissues (heart, kidney, liver epididymal adipose tissue (EWAT)) were removed immediately after the mice were sacrificed and kept on ice until they were weighed (no more than 45 min post-sacrifice).

3.1.5 RATIONALE FOR CHOOSING MUSCLE

This work was completed in skeletal muscle. Skeletal muscle was choosen as it is composed of long-lived, post-mitotic cells that are capable of oxidizing fuels at dramatically increased rates. Muscle is also highly susceptible to oxidative stress, and has been shown to decline in oxidative capacity with age.

TABLE 1: DIET COMPOSITION FOR CONTROL AND CR RATS.

	CONTROL DIET		CR DIET	
	Gm%	**Kcal%**	**Gm%**	**Kcal%**
Protein	14	15	23	24
Carbohydrate	73	76	56	60
Fat	4	9	6	16
Total		100		100
Kcal/gm	3.85		3.76	
Ingredient	**Gm**	**Kcal**	**Gm**	**Kcal**
Casein, 80 Mesh	140	560	140	560
L-Cystine	1.8	7.2	1.8	7.2
Corn starch	495.7	1982.8	112.5	450
Maltodextrin 10	125	500	125	500
Sucrose	100	400	100	400
Cellulose, BW200	50	0	50	0
Soybean Oil	40	360	40	360
t-Butylhydroquione	0.008	0	0.008	0
Mineral Mix (S10022)	35	0	35	0
Vitamin Mix (V10037)	10	40	10	40
Choline Bitarate	2.5	0	2.5	0
TOTAL	1000.008	3850	616.808	2317

3.1.6 ISOLATION OF SKELETAL MUSCLE MITOCHONDRIA

At designated times following the initiation of CR, animals were killed for the collection of tissues and blood. Specifically, animals were euthanized after 2 wk, 2 mo, 6 mo, 12 mo or 18 mo of CR (they were thus 6.5, 8, 12, 18 and 24 mo of age, respectively). Serum was extracted and flash frozen in liquid nitrogen. At the time of sacrifice, heart, liver, kidney and epididymal fat depots, were also removed and weighed. Mitochondria were isolated from the hind limb skeletal muscles of the control and CR rats using a modified method of Bhattacharya *et al.* (Bhattacharya et al., 1991). Specifically, these muscles included the muscles of the lower legs and thigh. The muscle was quickly dissected and placed in ice-cold isolation buffer (100 mM sucrose, 10 mM EDTA, 100 mM Tris-HCl, and 46 mM KCl; pH 7.4 with KOH). The muscle was cleaned of any visible connective tissue and fat, minced with a razor blade and placed in pre-chilled isolation medium containing 0.5% (wt/vol) defatted BSA (see Section 3.4.1 for preparation). The minced tissue was then filtered through 100 μm Nitex mesh and incubated for 2 min with occasional stirring in isolation medium containing 20% (wt/vol) Nagarse (type XVII protease, Sigma®). Thereafter, the minced tissue was homogenized using an ice-cold glass/Teflon Potter-Elvehjem tissue grinder and fractionated by centrifugation at 2,000 rpm (484 *g*) for 10 min at 4°C in a Sorvall® RC2-B centrifuge with a SS-34 rotor. The supernatant was collected and respun at 10,000 rpm (12,000 *g*) for 10 min at 4°C. The resultant supernatant was discarded and the pellet was resuspended in ice-cold isolation medium and respun for a third time at 10,000 rpm for a final 10 min. The final pellet was resuspended in 250 μl of ice-cold suspension buffer (in mM: 120 KCl, 20 sucrose, 20 glucose, 10 KH_2PO_4, 5.0 HEPES, 2.0

$MgCl_2$, 1.0 EDTA, pH 7.2, with KOH). Protein concentration of the mitochondrial suspension was determined using a modified Lowry method with BSA as the standard.

3.1.7 LOWRY DETERMINATION OF PROTEIN CONCENTRATION

Protein concentrations of isolated mitochondrial suspensions were assayed using a modified Lowry method (Lowry et al., 1951). The BSA standard curve ranged in BSA concentration from 0-120 μg (working standard 30 μg BSA/ml ddH_2O made from a 10 mg BSA/ml ddH_2O stock solution). To each of the standards and mitochondrial samples the following amounts of reagents were added as shown in Table 2. Upon the addition of isolation medium, NaOH, copper reagent, standards and samples were mixed and allowed to sit at room temperature for 10 min. Immediately after this incubation, Folin and Ciocalteu phenol reagent (Sigma®) was added and mixed well. Standard and sample tubes were then incubated at 55°C for 5 min and subsequently cooled on ice for 10 min to stop the reaction. Absorbance was read at 550 nm on a Beckman DU-50 spectrophotometer. BSA standard curves were constructed by plotting absorbance as a function of μg protein, and the protein concentration of the mitochondrial suspension was subsequently calculated.

TABLE 2: LIST OF REAGENT VOLUMES USED FOR BSA STANDARDS AND MITOCHONDRIAL SAMPLES.

Protein Content (µg)	Working Standard (µl)	Isolation Medium (µl)	0.5 N NaOH (µl)	Copper Reagent[1] (ml)	Phenol Reagent[2] (ml)
0	0	10	990	1	4
15	50	10	940	1	4
30	100	10	890	1	4
60	200	10	790	1	4
90	300	10	690	1	4
120	400	10	590	1	4
	Mitochondrial Suspension (µl)				
Sample	5	5	990	1	4

[1] 10% Na_2CO_3, 0.1% $K_2C_4H_4O_6 \cdot \frac{1}{2} H_2O$, 0.05% $CuSO_4 \cdot 5 H_2O$

[2] Folin & Ciocalteu phenol reagent (Sigma®) was purchased as a 2N solution and diluted to 0.118N (1/17) with water immediately before use.

3.1.8 MEASUREMENT OF MITOCHONDRIAL O_2 CONSUMPTION

The oxygen consumption of skeletal muscle mitochondria was measured using a Hansatech® Clark-type oxygen electrode (Norfolk, UK). The mitochondrial suspensions (0.5 mg protein/ml) were placed in the incubation chamber maintained at 37°C and magnetically stirred. All respiration rates were determined *simultaneously and in parallel with measurements of protonmotive force* in the chamber. Succinate-driven (*i.e.*, complex II-driven) respiration assessments were performed in the presence of 5.0 μM rotenone to prevent the oxidation of any endogenous NAD-linked substrates. State 3 respiration was defined as the oxygen consumption rate in the presence of 10 mM succinate, 0.65 U/ml of hexokinase, and 100 μM ADP/ATP. State 4 respiration (maximum nonphosphorylating, or leak-dependent respiration) was assessed in the presence of saturating amounts of the ATP synthase inhibitor, oligomycin (12 μg/mg protein). At the end of the experimental day the oxygen electrode was calibrated by equilibrating the incubation medium with air while the temperature was maintained at 37°C for at least 10 min. This value represented 100% air saturation. Zero percent air saturation was obtained by adding a few grams of sodium dithionite ($Na_2S_2O_4$). Upon reaching 0% air saturation, the incubation chamber was rinsed out with water and disassembled. The difference between the 100% air saturated solution and the 0% air saturated solution was then multiplied by 406 nmol O/ml, a previously determined value for oxygen solubility in our buffer (Reynafarje et al., 1985).

3.1.9 MEASUREMENT OF MITOCHONDRIAL PROTONMOTIVE FORCE (PMF)

Mitochondria produce a PMF by pumping protons from the mitochondrial matrix across the inner membrane during electron transport. This PMF drives several important bioenergetic reactions including ATP synthesis, ion transport and proton leak mediated thermogenesis. PMF has two components; an electrical term and a concentration term that are related by the formula:

$$\mathbf{PMF = \Delta\Psi + z\Delta pH}$$

Where $\Delta\Psi$ is the electrical potential difference or membrane potential, z is 2.303RT/F, with values of 59 mV at 25°C and 61.5mV at 37°C, and ΔpH is the difference in pH (mitochondrial intermembrane space –matrix). When measuring PMF, one must always take into account both the membrane potential and the pH gradient. To measure total PMF, ΔpH was clamped to zero by the addition of nigericin (0.4 μg/ml) to the incubation medium. Nigericin is an electroneutral H+-K+ antiporter (Nicholls, D. G. (1982). Bioenergetics: An Introductrion to the Chemiosmotic Theory. Academic Press, London) that collapses the transmembrane ΔpH and thus increases $\Delta\Psi$. Thus the whole PMF can be measured in units of membrane potential i.e., millivolts (mV) (Brown, 1995).

PMF is measured by quantifying the distribution of a lipophilic organic ion (triphenylmethylphosphonium, $TPMP^+$) across the mitochondrial inner membrane. The distribution of $TPMP^+$ was monitored using a $TPMP^+$-sensitive electrode (Kwik-Tip™) which was constructed using the methods described by Kamo *et al.,* (Kamo et al., 1979; Lal et al., 2001). Mitochondrial PMF was measured in duplicate and in parallel with

mitochondrial oxygen consumption determinations. The outputs from the $TPMP^+$ electrode and the O_2 electrode were transferred to two voltmeters whose reference sockets were connected together; data were then fed into a data analysis software package (Duo 18™ data recording system), which allowed real-time monitoring and recording of data on a personal computer.

3.1.9.1 CALIBRATION AND USE OF THE $TPMP^+$ - SENSITIVE ELECTRODE.

The $TPMP^+$ electrode is calibrated before the start of each titration. Mitochondria (0.5 μg protein) were added to the electrode chamber, which contained 1.0 ml of suspension medium, nigericin (0.4 μg/ml) and rotenone (5.0 μM). The $TPMP^+$ electrode was then inserted and the incubation chamber sealed. Once the trace was steady, 1 μl of $TPMP^+$ (final concentration, 1 μM) was added. When the trace reached a new steady state value (5-30 s) a second addition of 1μM aliquot of $TPMP^+$ was added and a new steady state was achieved. These additions were repeated until the total final $TPMP^+$ concentration was 5 μM. Succinate (10 μM) was then added and the mitochondria were allowed to accumulate the $TPMP^+$ until an equilibrium distribution was achieved and the extramitochondrial $TPMP^+$ concentration was stable (~1 min). Subsequent additions of various inhibitors, ionophores, or other compounds were then made, with the new steady state values being obtained within approximately one minute of each addition. At the end of the run, 0.1 μM of FCCP (carbonylcyanide p-trifluoromethoxyphenylhydrazone) was added to dissipate the PMF. At this point all the $TPMP^+$ should have been released by the mitochondria, returning the external concentration back to 5 μM. To determine electrode drift, the signal after FCCP addition was compared with the signal after the last $TPMP^+$ addition (*i.e.*, at 5 μM). If the

drift was mild then it was assumed that it was constant during the experiment. If the drift was severe then the cause of the drift was determined and adjusted before the next experiment (Brown, 1995).

3.1.9.2 CALCULATION OF PMF FROM $TPMP^+$ ELECTRODE DATA

The deflection caused by each 1 μm $TPMP^+$ addition in chart units from the baseline recording was measured and plotted against the logarithm of the final $TPMP^+$ concentration to produce a calibration graph. To measure the external $TPMP^+$ concentration ($TPMP^+_e$), for any given electrode signal, the deflection from the baseline (in chart units) to the new steady state was determined. $TPMP^+_e$ was then read directly off the calibration graph. The concentration of the $TPMP^+$ in the mitochondrial matrix ($TPMP^+_m$) was determined as follows:

$$[TPMP^+_m] = \frac{[TPMP]_{added} - [TPMP]_e}{(0.001 * MV * \text{mg protein/ml})}$$

The MV factor represents the mitochondrial matrix volume, and the value used was 0.33μl/mg protein (Lal et al., 2001). The PMF was then calculated using the Nernst equation as follows:

$$PMF = 61.5 * \log (a_m \cdot TPMP^+_m / TPMP^+_e)$$

Where a_m represent the correction factor for non-specific $TPMP^+$ binding to the mitochondrial membrane that occurs due to the highly hydrophobic character of $TPMP^+$. The value used for a_m was 0.35 μl/mg protein (Lal et al., 2001).

3.1.10 TOP-DOWN METABOLIC CONTROL ANALYSIS: A BRIEF OVERVIEW

Metabolic control analysis (MCA) was originally developed in 1973, as a practical and theoretical approach for analysis of the distribution of control within metabolic pathways (Heinrich and Rapoport, 1973; Kacser and Burns, 1973). It allows quantitative descriptions of the importance of reactions, or blocks of reactions, in the control of metabolic variables such as fluxes and metabolite concentration within a pathway. MCA assumes that there is not one rate limiting step within a pathway, but that control is distributed throughout the pathway (Brown et al., 1990; Hafner et al., 1990; Harper and Brand, 1995). When analyzing a system by MCA two approaches can be used: the traditional approach (or bottom-up approach) or the top-down approach. The traditional approach involves the manipulation of individual enzyme activities within a metabolic pathway using specific inhibitors for each enzymatic step. This approach is limited because it requires manipulating each and every enzyme in a pathway. In certain cases, a full set of very specific inhibitors are often not available (Harper and Brand, 1995).

The second approach, top-down metabolic control analysis, determines the distribution of control between blocks of enzymatic reactions instead of individual reactions. This approach produces flux control coefficients and concentration control coefficients for blocks of reactions in a metabolic pathway. The flux control coefficient is the quantification of how much control a block of reactions has over the flux through the entire pathway. Concentration control coefficients describe the distribution of control by the reaction blocks over the metabolite concentrations in the system under study. The top-down approach involves breaking down a metabolic pathway into two or three blocks of reactions centered around one of its intermediates (Brown *et al.*, 1990; Hafner *et al.*, 1990). The intermediate

is a component or metabolite of the system under investigation that is generated by one or more pathway (s) and is consumed by the subsequent pathway (s). To study flux and control, the concentration of the intermediate is manipulated by titrating each of the blocks of reactions with inhibitors or activators. This results in variable degrees of change of each reaction block to the concentration of the intermediate. The change in the flux through a block of reactions that is caused by changes in the concentration of the intermediate is termed as the *elasticity* (*i.e.,* overall kinetics) of that block of reactions (Harper and Brand, 1995). Elasticity is interchangeably referred to as an elasticity coefficient, and is used to determine the flux and control coefficients (see Appendix 2 for more definitions and equations).

The metabolic system that has been the focus of my research is oxidative phosphorylation. For the application of the MCA approach, the oxidative phosphorylation system has been broken down into three blocks of reactions: the substrate oxidation reactions (including cellular catabolic reactions, Krebs cycle, and the ETC), the phosphorylation reactions (ATP synthesis and consumption) and the proton leak (Figure 5). The intermediate used in this system is the protonmotive force. Protonmotive force is produced by the ETC reactions and consumed by the subsequent pathways, the phosphorylation reactions and the proton leak reactions. Flux through the pathway, measured as oxygen consumption is the ultimate step in the ETC. Distribution of control and sites of regulation within the system can be measured by manipulating the concentration of protonmotive force by titrating each block of reactions with various inhibitors (Brown et al., 1990; Hafner et al., 1990; Harper and Brand, 1995) .

FIGURE 5: SCHEMATIC DIAGRAM OF THE TRIPARTITE OXIDATIVE PHOSPHORYLATION SYSTEM.

The oxidative phosphorylation system is divided into three blocks or branches of reactions centered around protonmotive force (PMF). PMF is produced by the "substrate oxidation reactions" that comprises all of the reactions including and following the oxidation of glucose, lactate, pyruvate, and endogenous substrates. The PMF is consumed both the "phosphorylation reactions" and the "proton leak reactions". The phosphorylation branch includes PMF-dependent mitochondrial ATP synthesis and all cellular ATP-consuming reactions. Proton leak reactions include the leakage of protons and any cation cycles across the mitochondrial inner membrane. Figure adapted from (Harper and Brand, 1995).

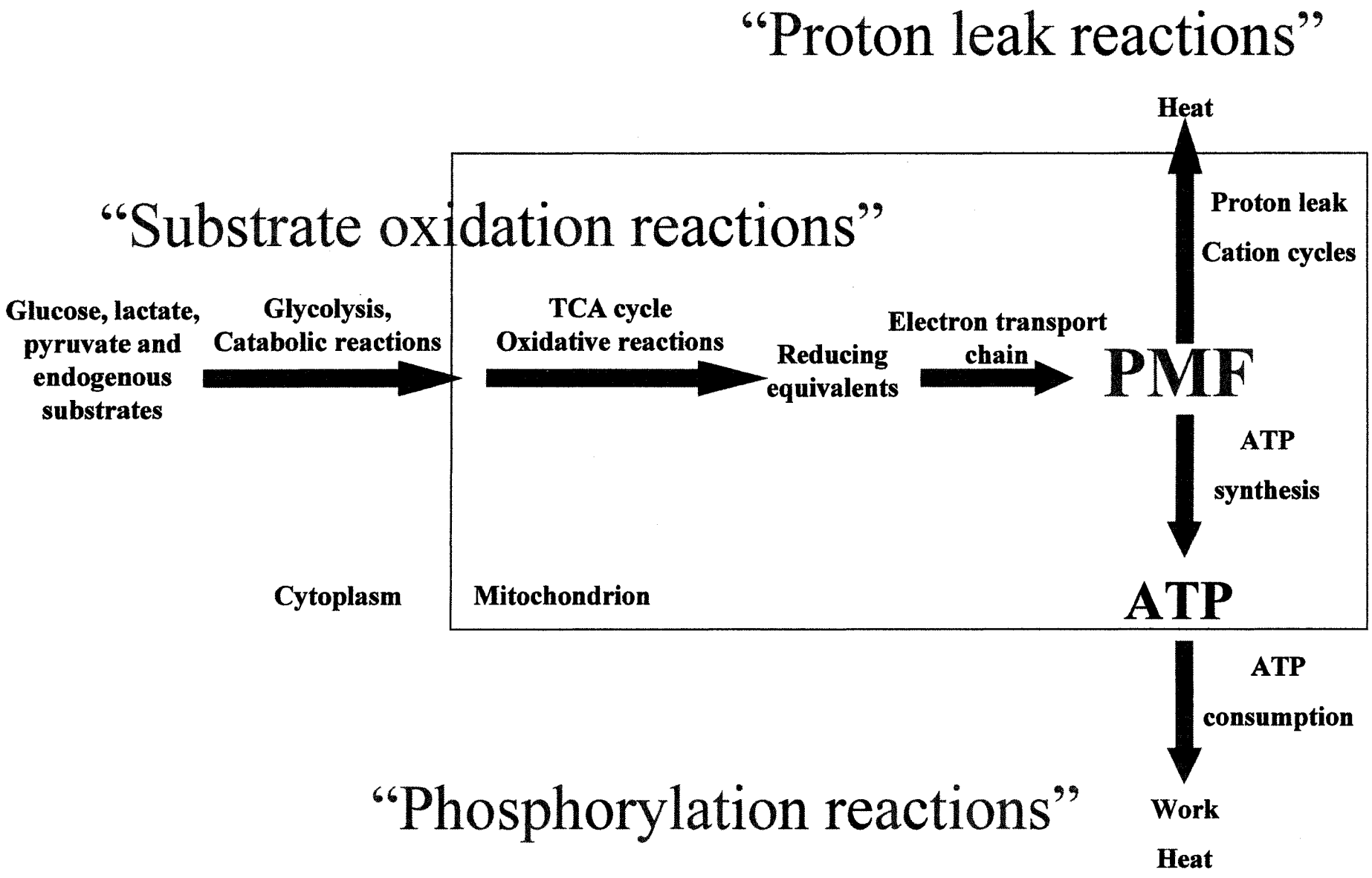

3.1.11 APPLICATION OF TOP-DOWN CONTROL ANALYSIS

To identify CR-induced changes in the control of oxidative phosphorylation in mitochondria, we used the top-down elasticity and metabolic control analyses (Brand, 1990; Harper and Brand, 1995). As described in the previous sectionwe defined the oxidative phosphorylation system as a tripartite system. The kinetic response to changes in PMF was measured for each of the three subsystems by using various inhibitors while measuring oxygen consumption through the pathway (Table 3). Specifically, the kinetics (or elasticity) of proton leak to changes in PMF was assessed by inhibiting proton return through ATP synthase using saturating concentrations of the specific ATP synthase inhibitor, oligomycin (12 μg/ml) followed by titrating the electron chain reactions with incremental additions of malonate (0-10 mM), a competitive inhibitor of complex II of the respiratory chain. The kinetic response of the substrate oxidation reactions was determined in the presence of 10 mM succinate, 10 mM ATP, 10 mM ADP, and 0.65 U/ml of hexokinase followed by incremental additions of oligomycin. The kinetic response of the phosphorylation reactions was assessed using 10 mM succinate, 10 mM ATP, 10 mM ADP, 0.65 U/ml hexokinase and incremental additions of malonate. Because this measurement contains components of both phosphorylation and proton leak, a correction was subsequently made for the proton leak-related oxygen consumption at each measured PMF value. Using this top-down approach, we are able to graph oxygen consumption as a function of PMF and examine the kinetics of each of the oxidative phosphorylation branches (see Appendix 2).

TABLE 3: SUBSTRATES AND INHIBITORS USED FOR TOP-DOWN METABOLIC CONTROL ANALYSIS.

SUBSTRATE/INHIBITOR	CONCENTRATION
All experiments	
Nigericin[a]	0.4 μg/ml
Rotenone[b]	5.0 μM
$TPMP^+$ Calibration	5 - 1 μM additions of 1mM stock = f.c. 5 μM
Proton Leak Reactions	
Succinate	10 mM
Oligomycin[c]	12 μg/ml
Malonate[d]	0-10 mM (incremental additions)
Substrate Oxidation Reactions	
Succinate	10 mM
ADP/ATP	10 mM/10 mM
Hexokinase	0.65 U/ml
Oligomycin[c]	0-12 μg/ml (incremental additions)
Phosphorylation Reactions	
Succinate	10 mM
ADP/ATP	10 mM/10 mM
Hexokinase	0.65 U/ml
Malonate[d]	0-10 mM (incremental additions)

[a]Nigericin: Ionophore used to collapse the ΔpH
[b]Rotenone: Inhibitor for NADH dehydrogenase (Complex I)
[c]Oligomycin: Inhibitor for ATP Synthase (Complex V)
[d]Malonate: Inhibitor for succinate dehydrogenase (Complex II)

3.1.12 DETERMINATION OF MITOCHONDRIAL H_2O_2 PRODUCTION

H_2O_2 production was determined using a p-hydroxyphenylacetate (PHPA) fluorometric assay as described by Hyslop and Sklar (Hyslop and Sklar, 1984). In the presence of horseradish peroxidase, PHPA is oxidized by H_2O_2 to a fluorescent dimerized product (excitation at 320 nm, emission at 400 nm). Briefly, 500 μg of PHPA, 4 U of horseradish peroxidase (type II, Sigma®) and freshly isolated mitochondria (0.25 mg/ml) were added to the assay buffer (10 mM potassium phosphate buffer, pH 7.4, containing 154 mM KCl, 0.1 mM EGTA, and 3 mM $MgCl_2$) with a final volume of 3 ml. Samples were maintained at 37°C and protected from light whenever possible. After an initial baseline reading was obtained (~1-2 min), 10 μM succinate was added and the fluorescence was monitored for 10 min. To calculate H_2O_2 production, the initial baseline reading was subtracted from the reading after 10 min. An H_2O_2 standard curve was used to covert the intensity reading to nanomoles H_2O_2 that was then divided by the μg of protein and reaction time used to obtain nmoles H_2O_2/min/mg.

3.1.13 QUANTIFICATION OF SERUM NONESTERIFIED FATTY ACIDS

Blood was collected at the time of sacrifice and was allowed to clot on ice for 15 min. Serum was separated by centrifugation at 5,000 rpm (2000*g*) for 15 min. Following centrifugation serum was collected, flash frozen in liquid nitrogen and stored at minus 80°C. At the time of analysis samples were thawed on ice. Nonesterified fatty acid (NEFA) levels were assessed with a NEFA C microtitre procedure (Wako Chemicals®, Richmond, VA). Briefly, working colour reagents (Wako Chemicals®) and standards were prepared according

to the package insert instructions. Samples, blanks and standards were pipetted (5 µL) into a 96 microwell plate. Colour reagent solution A (Wako Chemicals®) was added (100 µL) to each well. The plate was mixed well and incubated at 37°C for 5 min. Immediately after, absorbance of each well was read at 550nm (Sub:660nm) on a Tecan® microplate reader (model A-5002). Colour reagent solution B (Wako Chemicals®) was added to each well and subsequently incubated for 5 min at 37°C. Absorbance was read at the same wavelength described above. A calibration curve of absorbance vs. concentration was plotted and used to determine NEFA concentrations were read from this curve. NEFA content was calculated from the following equation:

$$C_{sample}\ (mEq/L) = \frac{A_{sample}}{A_{standard}} \times C_{standard}\ (mEq/L)$$

Where A is absorbance at 550nm and C is the NEFA concentration (mEq/L).

3.1.14 WESTERN BLOTS OF UNCOUPLING-PROTEIN-3

3.1.14.1 SAMPLE PREPARATION

UCP3 was detected in isolated mitochondria using polyacrylamide gel electrophoresis (PAGE) and western blotting. Mitochondrial samples were prepared by diluting samples to 2 mg protein/ml in 1X PBS (phosphate buffered saline; 1.8 mM KH_2PO_4, 137 mM NaCl, 2.7 mM KCl; 10 mM Na_2HP0_4 pH 7.4), and combining 4:1 with sample loading buffer (2% SDS, 50 mM Tris-HCl (pH 6.8), 25% glycerol (w/v), 0.2% bromophenol blue (w/v), and 14.4 mM β-mercaptoethanol). Additionally, Rainbow™ colour protein molecular weight markers (Amersham Pharmacia Biotech®), Santa Cruz®

biotinylated molecular weight markers, and recombinant murine UCP3 (prepared in our laboratory by Dr Martin Gerrits) were also prepared and loaded onto the gel. The Rainbow markers™ were prepared by combining them with 1X PBS and sample loading buffer in a ratio of 1:3:1. Before loading, mitochondrial samples, Santa Cruz® markers, and UCP3 fusion control protein were boiled for approximately 5 min. Rainbow markers™ were boiled for 1 min. On each blot, muscle mitochondrial proteins from *Ucp3*-knockout mice (from our mouse colonies) and recombinant murine UCP3 were used as a negative and positive control, respectively. Three western blots were performed per mitochondrial sample from each of 3-4 rats in each group.

3.1.14.2 RESOLUTION OF MITOCHONDRIAL PROTEIN SAMPLES BY SDS-PAGE

The Protean II Mini Electrophoresis® Cell (Bio-Rad®) was used for casting and running of the gels. The 12% separation gel was prepared by mixing 40% acrylamide/bis-acrylamide, 1.5 M Tris-base (pH 8.8), 0.4% SDS, 10% ammonim persulfate, and TEMED. After the gel was poured, it was overlayed with ddH_2O to prevent drying, and left to polymerize for 30 min at room temperature.

Upon polymerization, the water was removed by inversion of the assembly apparatus. The 4% stacking gel (40% acrylamide/bis-acrylamide, 0.5M Tris base, 0.4% SDS, 10% ammonium persulfate and TEMED) was poured on top of the separation gel. Combs were carefully inserted avoiding bubbles and centering carefully. The gel was left for 30 min at room temperature for polymerization. After the gels had polymerized the combs were carefully removed, the wells were dried with pieces of filter paper, and the gels

were placed in the electrophoresis cell. The gel assembly was clamped onto the electrode. Electrophoresis buffer (25 mM Tris base, 192 mM glycine, and 0.1% SDS) was added to the inner and outer electrode chamber, sample wells were rinsed with electrophoresis buffer prior to loading samples. Subsequently, 25 µl of the samples and markers were loaded. Electrophoresis was conducted for 1 hr at 150V.

Following electrophoresis, the gels were removed from between the glass plates and placed in gel buffer (96 mM glycine, 12.5 mM Tris base, 0.05% SDS) to equilibrate for 5 min at room temperature with gentle shaking (Speed 4) on a Belly Dancer® (Stovall Life Science Inc.). A Mini Trans-Blot® Cell (Bio-Rad®) was used for the transferring of the proteins. The gels were set up in the transferring cassettes as follows: sponge fiber pad, 2 piece of filter paper, equilibrated gel, nitrocellulose membrane (0.45 micron, Bio-Rad®), 2 pieces of filter paper (Whatman® grade No.1), sponge fiber pad. The 2 pieces of filter paper were equilibrated in gel buffer for 5 min. All other components of the transfer were pre-soaked in transfer buffer (96mM glycine, 12.5mM% Tris base, and 20% iso-propanol(v/v) for 5 min before assembly, with the exception of the nitrocellulose membrane which was pre-soaked for 30 min. The assembled cassette was placed into the Trans-blot cell with the nitrocellulose membrane facing the anode. A magnetic stir bar was placed in the chamber, and the transfer was conducted at 120V for exactly 30 min. Once the transfer was complete, the nitrocellulose membrane was carefully separated from the filter paper, wrapped in Fisher® all-purpose laboratory wrap (polyvinyl-chloride) and stored at -20°C until further processing (no more than two days after transfer).

3.1.14.3 WESTERN BLOTTING WITH UCP3 ANTIBODIES

The blot was removed from its plastic wrap and placed in 100 ml of blocking solution (PBS, 0.1% (v/v) Tween-20 and 5% (w/v) skim milk powder) for 1 hr at room temperature with gentle shaking (speed 4) on a Belly Dancer® Shaker (Stovall Life Science Inc.). After blocking, the membrane was washed in a solution containing PBS and 0.1% Tween-20 (v/v). This was followed by three quick rinses, each with approximately 50 ml of washing solution (fresh solution between each wash) at room temperature.

The washed membrane was incubated in 1:1000 dilution with a polyclonal rabbit antibody to the COOH terminus of human uncoupling protein-3 (AB-3046; Chemicon International Inc.), for 1 hr at room temperature with gentle shaking (speed 4) on a Belly Dancer® Shaker (Stovall Life Science Inc.). After incubation, 3 quick rinses were performed. The membrane was then incubated with the secondary antibody (goat anti-rabbit IgG horseradish peroxidase conjugate, 200 μg/0.5 ml, Santa Cruz Inc.), diluted 1:5,00 in PBS and 5% (w/v) skim milk powder solution for one hour at room temperature with gentle shaking (Speed 4 on Belly Dancer®). Three ten min washes in 1X PBS were completed as described above.

3.1.14.4 CHEMILUMINESCENT DETECTION OF SECONDARY ANTIBODY

Detection of the secondary antibody conjugate was carried out using an ECL™ RPN 2109 Western blotting detection kit (Amersham Pharmacia Biotech®). This is a light emitting non-radioactive method for detection of immobilized specific antigens, conjugated directly or indirectly with horseradish peroxidase-labelled antibodies. After taking the blot

out of the PBS solution, it was laid flat on a piece of plastic wrap, and its entire surface was covered with 1 ml of the ECL™ kit reagents (1 ml Reagent #1 and 1 ml Reagent #2, mixed immediately before pouring). The blot was then left undisturbed for 1 min, after which time, the solution was tipped and poured off. The blot was then placed face down in the camera dish and any air bubbles were carefully manually excluded.

Visualization of the blot was carried out by exposing it to Polaroid™ Polapan-667 black and white instant film using an Amersham® ECL Mini-camera. Exposure times varied from experiment to experiment. After the film was removed from the camera, it was left for 30 s before the film cover was removed.

3.1.15 DETERMINATION OF MITOCHONDRIAL LIPID PEROXIDATION

Mitochondrial lipid peroxidation levels (or thiobarbituric acid reactive substances; TBARS) were determined as malondialdehyde-thiobarbituric acid adducts according to Buege and Aust (Buege and Aust, 1978). Briefly, sucrose (which interferes with the assay) was removed from the isolated mitochondria through centrifugation at 11,500 rpm (12,000*g*) for 2 min at 4°C. The supernatant was carefully removed and discarded. A volume of cold 0.1M potassium phosphate buffer (KPB; pH 7.4) equal in volume to that of the discarded supernatant was added. The protein concentration of the sample was determined using the modified Lowry method. Aliquots (0.1-2 mg of protein) were taken and brought to a final volume of 1ml with KPB. The blank was composed of 1ml KPB and treated as the sample. Samples were mixed with butylated hydroxytoluene (BHT; 0.07mM final concentration.) to prevent formation of artifactual peroxidized lipids during the assay. Two ml of the TCA-

TBA-HCl Reagent (14% trichloroactetic acids, 0.375% (w/v) thiobarbituric acid and 0.25M HCl) was added and mixed thoroughly. Samples were heated in a boiling bath for 15 min then cooled at room temperature. Thereafter samples were centrifuged at 2100 rpm (1000*g*) for 10min, at RT, on a bench centrifuge. The resulting supernatants were collected and placed into clean tubes. Absorbance was read at 535 nm and a molar extinction coefficient of $1.56 \times 10^5\ M^{-1} \times cm^{-1}$ was used to calculate TBARS concentration.

3.2 EFFECT OF CALORIE RESTRICTION ON WILD TYPE AND *UCP3*-KNOCKOUT MICE

3.2.1 TREATMENT OF ANIMALS

Two month old male C57BL/6 wild-type (WT) and *Ucp3*-knockout (*Ucp3*-KO) mice were housed individually from weaning and given free access to water and allowed *ad libitum* intake of rodent chow (5% fat by weight; Harlan 2018). The *Ucp3*-KO mice used in this study were on a mixed genetic background and have been backcrossed 10 generations in C57BL/6 background. Daily individual food intake was measured over a period of two weeks. These data were used to determine the amount of food to give the animals during the CR phase of the study. At this point the mice were randomly assigned into control or CR treatment groups. The control mice were restricted 95% of *ad libitum* intake of the rodent chow to prevent the development of obesity. The CR mice were provided with 60% of the *ad libitum* energy intakes of the fed control mice. The treatment period for this study was 2 wk. Throughout the study all animals were allowed free access to water, and were kept at 23°C with lights at 0700-1900. The mice were cared for in accordance with the principles and guidelines of the Canadian Council on Animal Care and the Institute of Laboratory Animal Resources (National Research Council). The Animal Care Committee of the University of Ottawa approved the study.

3.2.2 DIET COMPOSITION

See section 3.1.2 for the diet composition of the control and CR groups. The energy intakes were 11.6 kcal/day for the control and 7.1 kcal/day for the restricted mice.

3.2.3 ORGAN WEIGHTS MEASUREMENTS

Tissues (heart, kidney, liver epididymal adipose tissue) were removed immediately after the mice were sacrificed and kept on ice until they were weighed (no more than 45 min post-sacrifice).

3.2.4 INDIRECT CALORIMETRY

Whole body oxygen consumption and respiratory exchange ratios were measured using a customized four-chamber Oxymax open-circuit indirect calorimeter with automatic temperature and light controls (Columbus Instruments, Columbus, OH). System settings included a flow rate of 0.5 L/min, a sample line-purge time of 2 min, and a measurement period of 60 s every 12 min. Two days prior to sacrifice, mice were individually placed in the respiration chambers (2.5 L/chamber). Data was collected over a 24-hour period with the temperature maintained at 24°C, with light on from 0700 to 1900. The respiratory exchange ratios were calculated as the ratio of VCO_2 divided by VO_2. The data set from each individual mouse was plotted and analyzed using the percent relative cumulative frequency (PRCF) as previously described (Riachi et al., 2004). The curves from each individual mouse were compared statistically using the 50th percentile values and curve slopes (H values). See Appendix 1 for a brief overview of PRCF.

3.2.5 SKELETAL MUSCLE MITOCHONDRIAL ISOLATION

Animals were sacrificed after 2 wk of treatment (CR or CON). Hind limb skeletal muscle mitochondria were isolated using a protocol adapted from (Chappell and Perry, 1954; Makinen et al., 1968). All media and procedures were kept at and performed at 0-4°C

respectively. Freshly dissected hind limb skeletal muscle was placed in ice-cold basic medium (140 mM KCl, 20 mM HEPES, 5 mM $MgCl_2$, 1 mM EGTA, pH 7.0). Connective and adipose tissue was immediately removed. The skeletal muscle was blotted dry and placed in pre-weighed ice-cold fresh basic medium to obtain a tissue weight. The muscle was then finely minced for 2 min on a pre-chilled Teflon cutting board. The minced muscle was resuspended in 5 volumes of homogenization medium (140 mM KCl, 20 mM HEPES, 5 mM $MgCl_2$, 2 mM EGTA, 1 mM di-potassium ATP, and 1% w/v defatted BSA, pH 7.0). Two Units of subtilisin A/g tissue (Type VIII, Sigma®) was added and the mixture was incubated on ice with constant manual swirling for 2 min. The mixture was then diluted 6-fold with subtilisin A-free homogenization medium and centrifuged at 9,000 rpm (9, 681g_{max}) for 10 min. For all centrifugations, a Sorvall® RC-5B refrigerated centrifuge with a SS-34 rotor was used. The supernatant was removed and the pellet was resuspended in fresh was homogenization medium. Homogenization was performed at approximately 350 RPM; twice with a loose (TC = 300μm) and twice with a medium (TC=120μm) fit Teflon pestle using a Potter-Elvehjem-type homogenizer. The homogenate was then centrifuged at 2,000 rpm (484 g_{max}) for 10 min. The supernatant was removed and respun at 9,000 rpm (9,681 g_{max}) for 10 min. The pellet was retained and resuspended in Wash One Medium (140 mM KCl, 20 mM HEPES, 5 mM $MgCl_2$, 1 mM EGTA and 1% w/v BSA, pH 7.0). The mixture was mixed well and incubated on ice for 10 min to allow for myofibrillar re-polymerization. This was followed by centrifugation of the sample at 2,000 rpm (484 g_{max}). The supernatant was retained and re-spun at 9,000 rpm (9,681 g_{max}) for 10 min to obtain the pellet. The pellet was resuspended in basic medium and re-centrifuged at the same speed for another for 10 min. The final pellet was retained and resuspended in approximately 300-250

µl of basic medium. The protein concentration of the pellet was assayed using a modified Lowry method using BSA as the standard.

3.2.6 MEASUREMENT OF MITOCHONDRIAL O_2 CONSUMPTION

Mitochondrial oxygen consumption was assayed using a Hansatech Clark-type oxygen electrode (Norfolk, UK) with an incubation chamber maintained at 37°C as described in section 3.1.6. All measurements used 0.5 mg/ml of mitochondrial protein in incubation medium (120 mM KCl, 5 mM HEPES, 5 mM $MgCl_2$, 1 mM EGTA, 5 mM KH_2PO_4, 0.3% defatted BSA, pH 7.4). State 3 (phosphorylating) respiration was determined in the presence of 5 mM pyruvate, 2.5 mM malate and 100 µM ADP. State 4 (non-phosphorylating) respiration was determined following the addition of saturating amounts of oligomycin (8 µg/mg protein).

3.2.7 MEASUREMENT OF MITOCHONDRIAL PROTONMOTIVE FORCE

As outlined in section 3.1.9.

3.2.8 MEASUREMENT OF PROTON LEAK KINETICS

Proton leak measurements were determined as described in section 3.1.11.

3.2.9 EFFECTS OF CAT ON SKELETAL MUSCLE PROTON LEAK KINETICS

Mitochondria were isolated from 8 *Ucp3*-KO (4 mice on either CON or CR regimen) and 8 wild-type (4 mice on either CON or CR regimen) mice as described above in section 3.3.5. Oxygen consumption and mitochondrial PMF were measured for each individual preparation of mitochondria as outlined in sections 3.1.6 and 3.1.7. The effects of carboxyatractylate (CAT) on the kinetics of leak were determined by titrating mitochondrial incubations with saturating amounts of oligomycin (8 μg/ml) and increasing amounts of malonate (0.25-5 mM) in the presence of 0.3% defatted BSA and 10 μM CAT (final concentration).

3.2.10 WESTERN BLOTTING OF ANT AND UCP3

Western blotting was completed as described in section 3.1.12 with the exception of the following. Thirty-five micrograms of mitochondrial protein were loaded onto the gel for both ANT and UCP3 blots. The primary used was a rabbit polyclonal antibody to human UCP3 (ab3477; AbCam®). A 1:500 dilution was used. The secondary antibody (goat anti-rabbit IgG horseradish peroxidase conjugate, 200 μg/0.5 ml, Santa Cruz Biotechnology®), diluted 1:2000 in PBS and 5% (w/v) skim milk powder.

The primary antibody for ANT was affinity purified goat polyclonal raised against the N-terminus of human ANT (sc-9299 Santa Cruz Biotechnology®) and was used at a 1:500 dilution. The secondary antibody (donkey anti-goat IgG horseradish peroxidase conjugate, 200 μg/0.5 ml, Santa Cruz Biotechnology), was diluted 1:2000 in PBS and 5%

(w/v) skim milk powder. An ANT peptide (sc-9299P, Santa Cruz Biotechnology®) was used as the positive control.

3.3 GENERAL METHODS

3.3.1 DEFATTING BOVINE SERUM ALBUMIN (BSA)

Defatted BSA is used to bind fatty acids released from the isolation of skeletal muscle mitochondria. For the rat studies, BSA was defatted by the method described by Chen (Chen, 1967). Briefly, BSA (50g of fraction V, Sigma®) was dissolved in 250 ml of ddH_2O and magnetically stirred. While the BSA was dissolving a suspension of 25 g of activated charcoal (acid washed BDH® 33033) in 100 ml of ddH_2O was prepared. This solution was mixed for approximately 15 min, and fines were removed with a tissue. The activated charcoal was added to the BSA solution that had been stirring for approximately an hour. The charcoal-BSA suspension was then brought to a pH of 3.0 with 10M HCl (added dropwise) and stirred on ice for 1 h. The solution was spun at 11,300 rpm (20,000g) for 20 min at 4°C using a Beckman® J2-21M centrifuge with a JA14 rotor. The resulting supernatant was carefully poured off into a 500 ml beaker and brought to a pH of 7.0 with 10 M NaOH, and the spin was repeated. The supernatant was carefully pour into another 500 ml beaker and vacuumed filtered with a 0.45μm filter (Millipore® HA type) and then through a 0.22μm filter (GS type). The filtrate collected was then dialyzed in 153mM NaCl and 10.8 mM KCl twice for an hour and once overnight at 4°C (magnetically stirred). Prior to dialysis, the dialysis tubing was boiled in 75mM ethylenediamine tetraactetic acid

(Na_2EDTA; disodium salt) for 5 min and then in ddH_2O for 5min. Approximately 250ml of the last dialysis medium was retained for dilutions. The following morning, the protein concentration of the defatted BSA was determined using a modified Lowry (Lowry et al., 1951). The BSA suspension was diluted in the final dialysis media to give a final stock concentration of 9% BSA (w/v) and then stored at approximately -20°C in 10 ml aliquots. These aliquots were later used for additions to media.

3.4 MATERIALS

Oligomycin, malonate, FCCP, BSA (fraction V), Nagarse (type XXVII), Subtilisin (type VIII), hexokinase (type III), succinic acid, ATP, ADP, rotenone, nigericin, TPMP, PHPA, Folin-Ciocalteau, H_2O_2 and horseradish peroxidase were purchased from Sigma-Aldrich® (St. Louis, MO). Tris-base, SDS, Tween-20, PMSF, B-mercaptoethanol, bromophenol, acrylaminde/bisacyrlamide and ammonium persulfate were purchased from Bio-Rad Laboratories (Hercules, CA).

3.5 STATISTICAL ANALYSIS

To determine differences between two individual means data were analyzed using a one- or two- way analysis of variance (one- or two- way ANOVA), or a one-way ANOVA with Tukey's post-hoc tests, when determining significance between more than three groups. Statistics were performed using Prism® 4.1 for Windows (Graph Pad, San Diego, CA). Statistical significant was defined as a P value less than 0.05. All results are presented as means ± SEM.

CHAPTER 4
RESULTS

4.1. EFFECTS OF CALORIE RESTRICTION ON WHOLE BODY ENERGY EXPENDITURE AND SKELETAL MUSCLE MITOCHONDRIA BIOENERGETICS IN FBNF$_1$ RATS

The results described in the following section were published in the American Journal of Physiology: Endocrinology and Metabolism (Bevilacqua et al., 2004; Bevilacqua et al., 2005). Author contributions: M.E.H. and J.J.R. designed research; L.B. performed research; L.B. analyzed data; and L.B. and M.E.H wrote the paper.

4.1.1 WHOLE BODY ENERGETICS

The objective of this study was to determine the effect of CR on whole body and mitochondrial energetics. It has been suggested that CR may attenuate oxidative damage and bioenergetic decline by producing an environment that favors a hypometabolic state involving a reduction in whole-body and mitochondrial oxygen consumption and/or decreased reactive oxygen species (ROS) production (Ramsey et al., 2000). The exact role of hypometabolism is unclear. Several studies have yielded contradictory results as to whether or not CR increases, decreases or has no effect on whole animal metabolism (see Ramsey et al., 2006 for review). As a result, we decided to assess energy expenditure to better understand the role energy metabolism plays in the actions of CR. Figures 6 and 7 summarize energy expenditure results collected over 24 h time periods. The results were plotted using a PRCF approach that allows quantitative analysis of

large sets of indirect calorimetry data (Riachi et al., 2004). When results are expressed as whole body oxygen consumption (Figure 6, graphs on *left*), mean 50th percentile values were 14, 19, and 39% lower in CR rats than in control rats at the 2 wk, 2 mo, and 6 mo time points (each $P < 0.01$), respectively. Mean 50th percentile values of whole body oxygen consumption after long-term CR were 34.6 ($P<0.01$) and 35.6% ($P<0.001$) lower in CR rats than in their respective controls at the 12 and 18 mo CR time points (Figure 7, panel A and C), and this was also equivalent to the magnitude of CR between groups.

Mean oxygen consumption values normalized for body weight (VO_2/g Bwt) were not different ($P>0.05$) between CR and control groups at 2 wk, and 2 mo CR ($P<0.05$), whereas after 6 mo of CR there was a 40% decrease ($P < 0.05$) compared with control rats, a percentage equivalent to the reduction in caloric intake (Figure 6, graphs on *right*). With long-term CR, reductions in mass-adjusted oxygen consumption were also observed. Adjusted oxygen consumption (per gram body wt; (Figure 7, panel B and D), was 11.1 ($P>0.05$) and 29.5% lower ($P<0.05$) in the CR rats than in the controls at the 12 or 18 mo CR time points. Interestingly, the percent reduction in mass-adjusted oxygen consumption were smaller than the 6 mo CR study and may be a result of whole body adaptation to CR once an initial drop in energy metabolism occurs. The lack of difference between the controls and CR rats at the 12 mo time point may be a result of seasonal or environmental effects. Respiratory exchange ratios were determined to estimate the mix of fuel substrates being oxidized by the rats. The mean respiratory exchange ratio (RER) decreased with the CR rats compared with controls after 12 and 18 mo of CR, respectively (Figure 8). The overall pattern of these whole body analyses indicates that CR results in a hypometabolic state.

FIGURE 6: PERCENT RELATIVE CUMULATIVE FREQUENCY (PRCF) PLOTS OF WHOLE BODY AND MASS-ADJUSTED OXYGEN CONSUMPTION ($\dot{V}O_2$) FOR CONTROL AND 40% CR RATS (N=7 RATS/GROUP).

A: 2 wk study; B: 2 mo study; C: 6 mo study. For each panel, the graph on the left represents whole body $\dot{V}O_2$ (*i.e.,* per rat), and curve on the right represents mass-adjusted $\dot{V}O_2$ (*i.e.,* per gram Bwt). For each graph, the solid and dashed lines represent the lines of best fit for the control and CR rats, respectively. The equations for the lines of best fit are shown and provide the 50^{th} percentile values and the H (slope) values for each group.

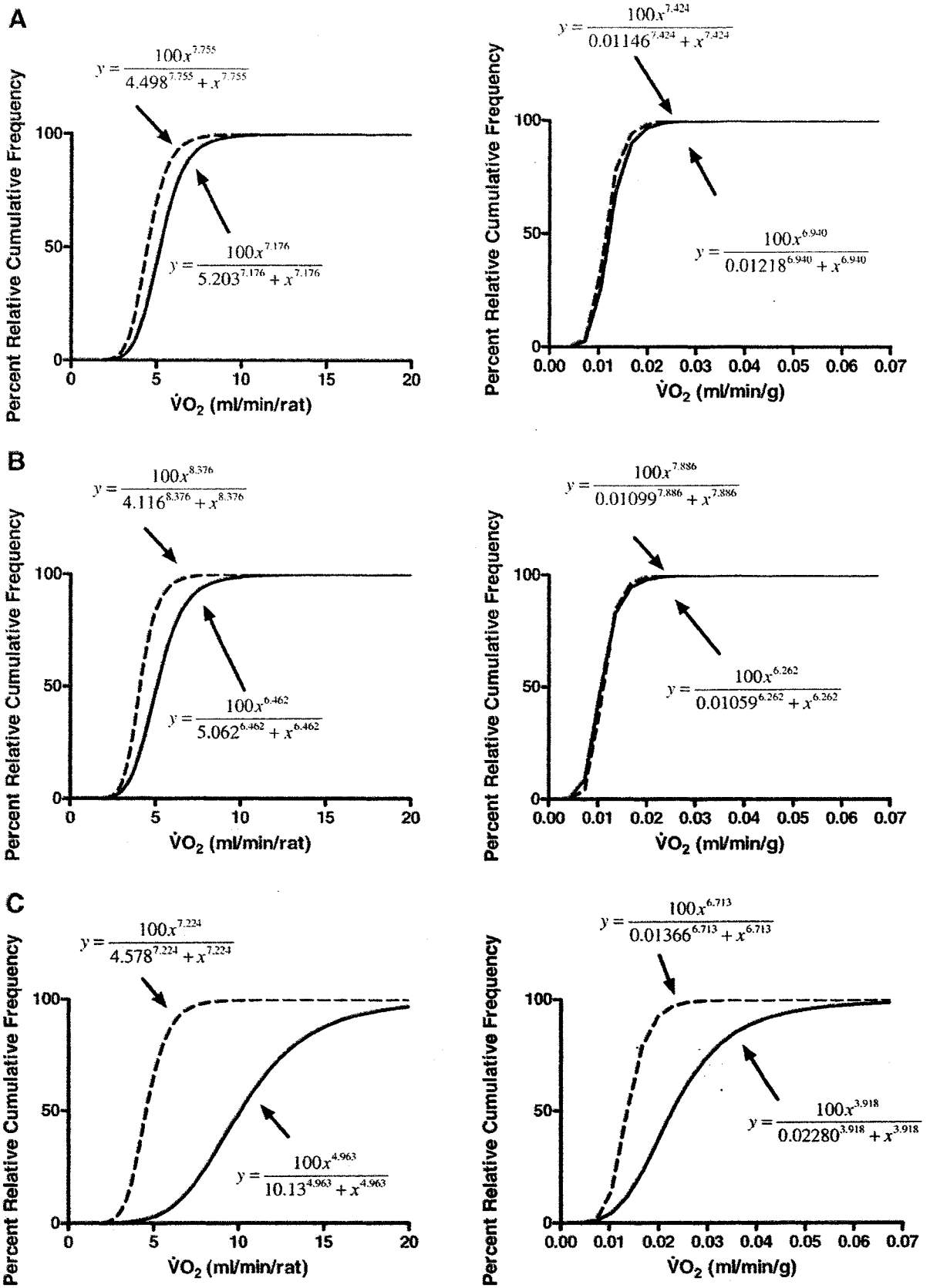

FIGURE 7: PERCENT RELATIVE CUMULATIVE FREQUENCY PLOTS OF WHOLE BODY AND MASS-ADJUSTED O_2 CONSUMPTION ($\dot{V}O_2$) FOR CONTROL AND 40% CR RATS (N= 6 RATS/GROUP).

A and B: 12 mo study; C and D: 18 mo study. For each panel, the top graph represents whole body $\dot{V}O_2$ (*i.e.,* per rat), and the bottom graph represents mass-adjusted $\dot{V}O_2$ (*i.e.,* per gram Bwt). For each graph, the solid and dashed lines represent the lines of best fit for the control and CR rats, respectively. The equations for the lines of best fit are shown and provide the 50^{th} percentile values and the H value (slope) values for each group. Note: the equations of the line for panel B are reversed.

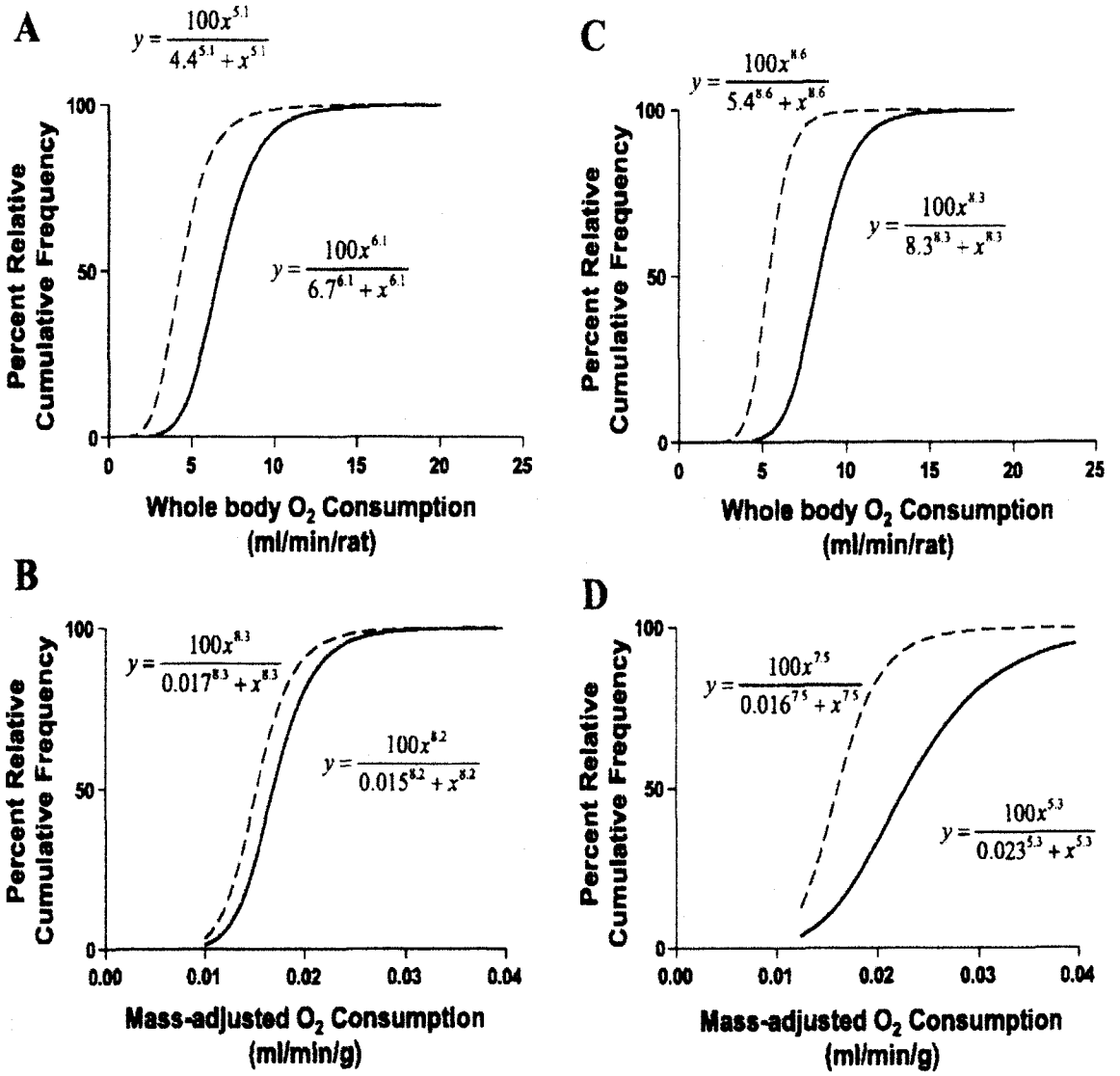

FIGURE 8: PERCENT RELATIVE CUMULATIVE FREQUENCY (PRCF) PLOTS OF RESPIRATORY EXCHANGE RATIOS FOR CONTROL AND 40% CR RATS (N= 6 RATS/GROUP).

A: 12 mo study and B: 18 mo study. The equations for the lines of best fit are shown and provide the 50^{th} percentile values and the H (slope) values for each group. For each graph, the solid and dashed lines represent the lines of best fit for the control and CR rats, respectively.

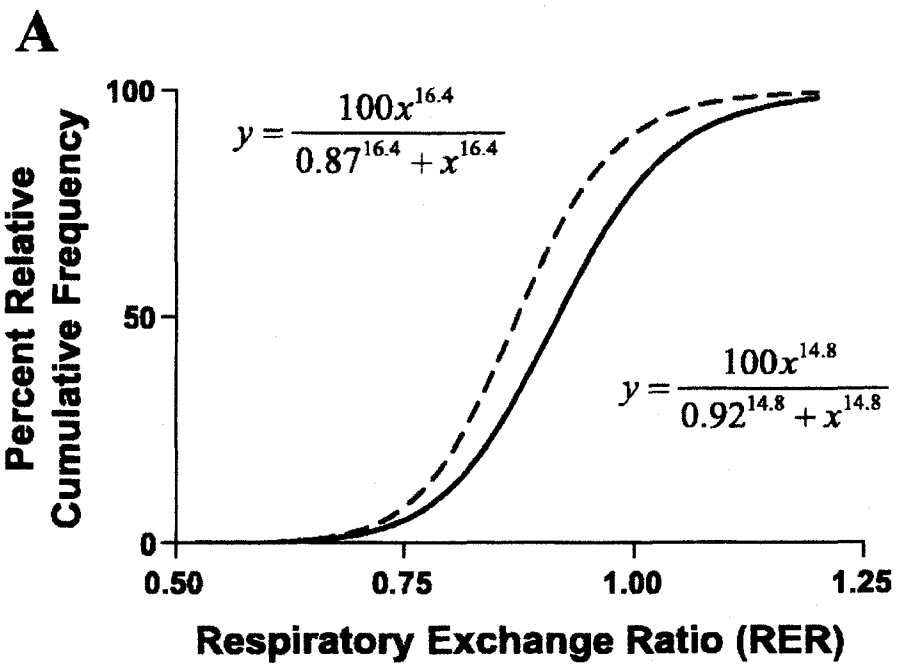

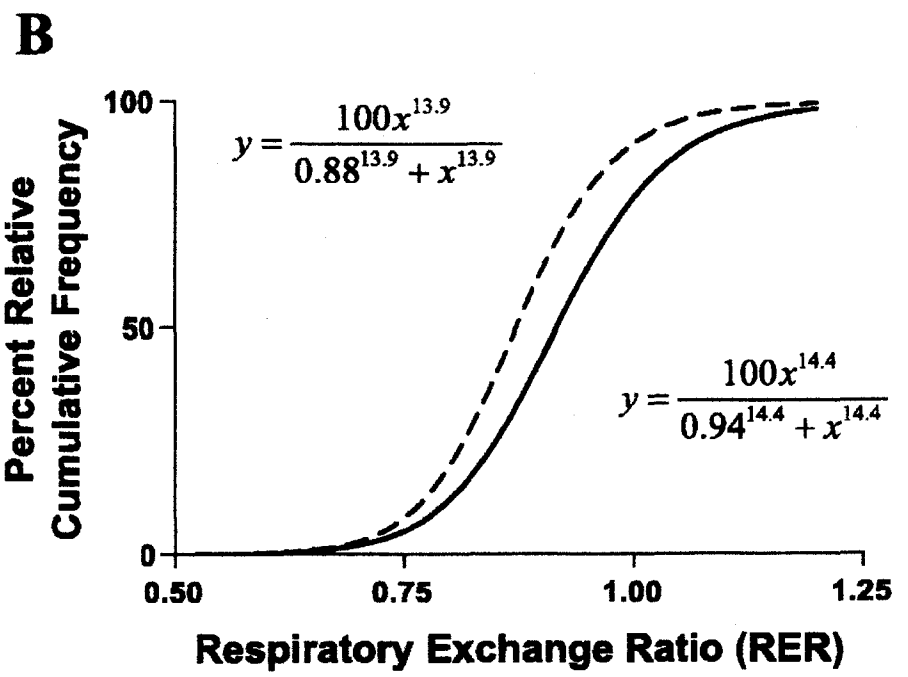

4.1.2 FOOD INTAKE, BODY AND ORGAN WEIGHTS

To better understand body composition changes with CR and how these changes contribute to alterations in energy expenditure, organ weights were measured in both control and CR animals. These data are summarized in Tables 4-8. Initial daily food intake and body weights were similar between groups ($P > 0.05$, data not shown). After 2 wk of CR, mean body weight was not significantly different between CR and *ad libitum*-fed controls. Epididymal adipose tissue (EWAT; a crude indicator of adiposity) and organ weights were also not significantly different between 2 wk CR rats and controls (Table 4). At 2 mo of CR, mean body weight was decreased 17% ($P < 0.001$) in CR rat compared to their control counterparts. At this time point, however, EWAT weight was 47% ($P<0.01$) lower in the CR rats. Significant decreases in liver and heart weights were also observed at the 2 mo time point, 30% ($P < 0.001$) and 13% ($P < 0.05$), respectively (Table 5). The only tissue not to show a significant decrease in weight at 2 mo CR was the kidney. At 6 mo of CR, body weight was 32% lower ($P < 0.001$) compared with the controls. After 6 mo of CR, there were significant reductions in the weights of all organs assessed. EWAT weight was reduced 70% ($P < 0.001$). Liver, kidney, and heart exhibited decreases of 38% ($P < 0.001$), 20% ($P < 0.001$), and 17% ($P < 0.01$), respectively (Table 6).

Body and organ weights in response to long-term CR are summarized in Table 7 and 8. After 12 mo of CR, there was a 35.7% decrease in mean body weight between the CR and the age-matched control groups. There were decreases in all measured organ weights following 12 mo of CR. Liver weight decreased to the greatest extent, with a 44.3% decrease ($P<0.01$). Thereafter, the greatest proportional decreases were in the kidneys and heart, which decreased 26.9 ($P<0.01$) and 20.7% ($P<0.001$), respectively. EWAT weight

decreased 78.8% ($P<0.001$) following 12 mo CR. After 18 mo of CR, animals had smaller liver, kidneys, and hearts; decreases were 45.5 ($P<0.001$), 31.6 ($P<0.001$), and 29.1% ($P<0.001$), respectively. After 18 mo of CR, the decrease in EWAT weight was 75.6% ($P<0.001$), similar to that after 12 mo of CR indicating these rats had reached weight stability.

Results support the conclusion that CR does not result in a uniform change in organ weights. These non-uniform alterations in body composition complicate whole animal comparisons between control and CR groups, and, therefore, measurements of cellular energy-consuming processes are required to accurately determine the role that alterations in energy expenditure may play in the actions of CR.

TABLE 4: AVERAGE BODY AND ORGAN WEIGHTS FOR CONTROL AND 40% CR FBNF$_1$ RATS AFTER 2 WK OF CR.

Organ	2 WK STUDY		
	Control	CR	% Change (CR vs. Control)
Liver (g)	10.7 ± 0.4	8.89 ± 0.22	-16.9
Kidney (g)	1.97 ± 0.03	2.02 ± 0.06	+0.03
Heart (g)	1.02 ± 0.04	0.98 ± 0.03	-3.9
EWAT (g)	5.99 ± 0.55	4.94 ± 0.37	-17.5
Body Weight (g)	409 ± 10	375 ± 12	-8.3

Body weights were measured prior to sacrificing the animals for metabolic studies. Tissues were removed immediately after sacrifice and kept on ice until they were weighed (no more than 45 min post-sacrifice). Results are expressed as means ± SEM of 7 rats/group. Statistical differences were analysed using a one-way ANOVA. CR, calorie restricted; EWAT, epididymal white adipose tissues.

TABLE 5: AVERAGE BODY AND ORGAN WEIGHTS FOR CONTROL AND 40% CR FBNF$_1$ RATS AFTER 2 MO OF CR.

Organ	2 MO STUDY		
	Control	CR	% Change (CR vs. Control)
Liver (g)	12.5 ± 0.57	8.74 ± 0.69	-30.0***
Kidney (g)	2.21 ±0.07	1.96 ± 0.05	-11.3
Heart (g)	1.12 ± 0.04	0.97 ± 0.03	-13.3*
EWAT (g)	7.51 ± 0.64	4.00 ± 0.19	-46.7**
Body Weight (g)	437 ± 17	364 ± 5	-16.7***

Body weights were measured prior to sacrificing the animals for metabolic studies. Tissues were removed immediately after sacrifice and kept on ice until they were weighed (no more than 45 min post-sacrifice). Results are expressed as means ± SEM of 7 rats/group. * denotes a statistically significant difference at $P<0.05$, ** $P<0.01$, and *** $P<0.001$, as determined by a one-way ANOVA with Tukey's post hoc test. CR, calorie restricted; EWAT, epididymal white adipose tissues.

TABLE 6: AVERAGE BODY AND ORGAN WEIGHTS FOR CONTROL AND 40% CR FBNF$_1$ RATS AFTER 6 MO OF CR.

Organ	6 MO STUDY		
	Control	CR	% Change (CR vs. Control)
Liver (g)	13.4 ± 0.54	8.36 ± 0.28	-37.6***
Kidney (g)	2.41 ± 0.10	1.93 ± 0.07	-19.9***
Heart (g)	1.07 ± 0.03	0.89 ± 0.05	-16.8**
EWAT (g)	11.4 ± 0.99	3.48 ± 1.05	-69.5***
Body Weight (g)	480 ± 11	326 ± 8	-32.1***

Body weights were measured prior to sacrificing the animals for metabolic studies. Tissues were removed immediately after sacrifice and kept on ice until they were weighed (no more than 45 min post-sacrifice). Results are expressed as means ± SEM of 7 rats/group. * denotes a statistically significant difference at $P<0.05$, ** $P<0.01$, and *** $P<0.001$, as determined by a one-way ANOVA with Tukey's post hoc test. CR, calorie restricted; EWAT, epididymal white adipose tissues.

TABLE 7: AVERAGE BODY AND ORGAN WEIGHTS FOR CONTROL AND 40% CR FBNF$_1$ RATS AFTER 12 MO OF CR.

Organ	12 MO STUDY		
	Control	CR	% Change (CR vs. Control
Liver (g)	14.2 ± 0.25	7.91 ± 0.19	44.3***
Kidney (g)	2.66 ± 0.06	2.11 ± 0.07	29.6***
Heart (g)	1.19 ± 0.02	0.87 ± 0.16	20.7*
EWAT (g)	11.3 ± 1.02	2.39 ± 0.21	78.8***
Body Weight (g)	483 ± 10	320 ± 8	35.7**

Body weights were measured prior to sacrificing the animals for metabolic studies. Tissues were removed immediately sacrifice and kept on ice until they were weighed (no more than 45 min post-sacrifice). Results are expressed as means ± SEM of 6 rats/group. Statistical significance was determined using a one-way ANOVA with Tukey's post hoc test. * denotes a significant difference at $P<0.05$, ** $P<0.01$, and *** $P<0.001$. CR, calorie restricted; EWAT, epididymal white adipose tissues.

TABLE 8: AVERAGE BODY AND ORGAN WEIGHTS FOR CONTROL AND 40% CR FBNF$_1$ RATS AFTER 18 MO OF CR.

Organ	18 MO STUDY		
	Control	CR	% Change (CR vs. Control
Liver (g)	15.1 ± 1.95	8.23 ± 0.56	45.5***
Kidney (g)	3.06± 0.17	2.10 ± 0.07	31.6***
Heart (g)	1.36 ± 0.02	0.97 ± 0.16	29.1*
EWAT (g)	10.8 ± 1.7	2.63 ± 0.64	75.6***
Body Weight (g)	515 ± 16	315 ± 3	38.8**

Body weights were measured prior to sacrificing the animals for metabolic studies. Tissues were removed immediately after the rats were sacrificed and kept on ice until they were weighed (no more than 45 min post-sacrifice). Results are expressed as means ± SEM of 6 rats/group. Statistical significance was determined using 1-way ANOVA with Tukey's post hoc test. * denotes a significant difference between the means of the paired columns at $P<0.05$, $**P<0.01$, and $***P<0.001$. CR, calorie restricted; EWAT, epididymal white adipose tissues.

4.1.3 COMPARISON OF THE KINETIC RESPONSE OF PROTON LEAK, SUBSTRATE OXIDATION, AND PHOSPHORYLATION REACTIONS IN SKELETAL MUSCLE MITOCHONDRIA FROM CONTROL AND CR FBNF$_1$ RATS

To accurately determine the role that energy metabolism may play in the actions of CR, it was necessary to investigate specific cellular energy consuming pathways. One of the major cellular energy-consuming pathways is the mitochondrial proton leak. This process has been estimated to be responsible for approximately 20-25% of the resting metabolic rate in rats (Rolfe and Brown, 1997). Thus, mitochondrial proton leak was measured in skeletal muscle mitochondria from control and CR rats at each time point. We also assessed the kinetics of oxidative phosphorylation to determine if CR alters the distribution of control over the oxidative phosphorylation system.

Results shown in Figures 9-10 are the product of top-down elasticity analysis performed to assess differences in the kinetics of the proton leak reactions in skeletal muscle mitochondria isolated from 2 wk, 2 mo, 6 mo, 12 mo and 18 mo CR and control rats. The kinetic response of the proton leak reaction is shown in Figure 9. These results demonstrate that state 4 respiration rates (maximal leak-dependent respiration, represented by the points on the *far right* of each curve) were decreased by 26% ($P < 0.01$), 42% ($P < 0.001$) and 53% ($P < 0.001$), respectively, for the 2 wk, 2 mo, and 6 mo CR animals compared to controls. Unexpectedly, state 4 PMF values for the 2 wk and 2 mo CR animals were 6% ($P < 0.05$) and 9% ($P < 0.01$) lower than their respective controls. However, after 6 mo of CR, PMF was increased 6% ($P < 0.05$). At each time point, there were also distinct differences in proton leak kinetics (i.e., the overall characteristics of the curves in Figure 8) between CR and control groups. The fact that state 4 oxygen consumption is lower despite lower state 4 PMF values in short-term CR vs. control mitochondria is unusual; the decreased state 4

oxygen consumption with increased PMF observed following 6 mo of CR is typical of decreased proton leak reactions.

At the 12 mo CR assessment point, the CR rats had a 40% lower ($P<0.001$) maximal proton leak-dependent respiration compared with the control-fed rats. The kinetics of proton leak was affected by 12 mo CR such that leak-dependent respiration was lower in the CR mitochondria at PMF values exceeding 170 mV, but no below this PMF value. After 18 mo of CR, there were no differences ($P>0.05$) in maximal leak-dependent respiration rates between CR and control rats. Such differences between short- medium- and long-term CR are presumably due to differences in metabolic adaptations between short- and medium-term CR (see *DISCUSSION*).

FIGURE 9: THE OVERALL KINETIC RESPONSE OF THE PROTON LEAK REACTIONS IN SKELETAL MUSCLE MITOCHONDRIA FROM CONTROL (■) AND CR (▲) RATS AFTER 2 WK (A), 2 MO (B), AND 6 MO (C) OF 40% CR.

The farthest point on the *right* represents state 4 (maximal nonphosphorylating) respiration and was determined by the addition of saturating amounts of oligomycin (12μg/ml) to mitochondria respiring on 10mM succinate. The kinetic response of the proton leak block was determined by incremental additions of the complex II inhibitor, malonate (0.33-10 mM) to the mitochondria at state 4. Each point represents the mean ± SEM of 7 duplicate assays (*i.e.*, 7 rats/group). Statistical significance of state 4 respiration and PMF was determined using a one-way ANOVA with a Tukey's post hoc test.

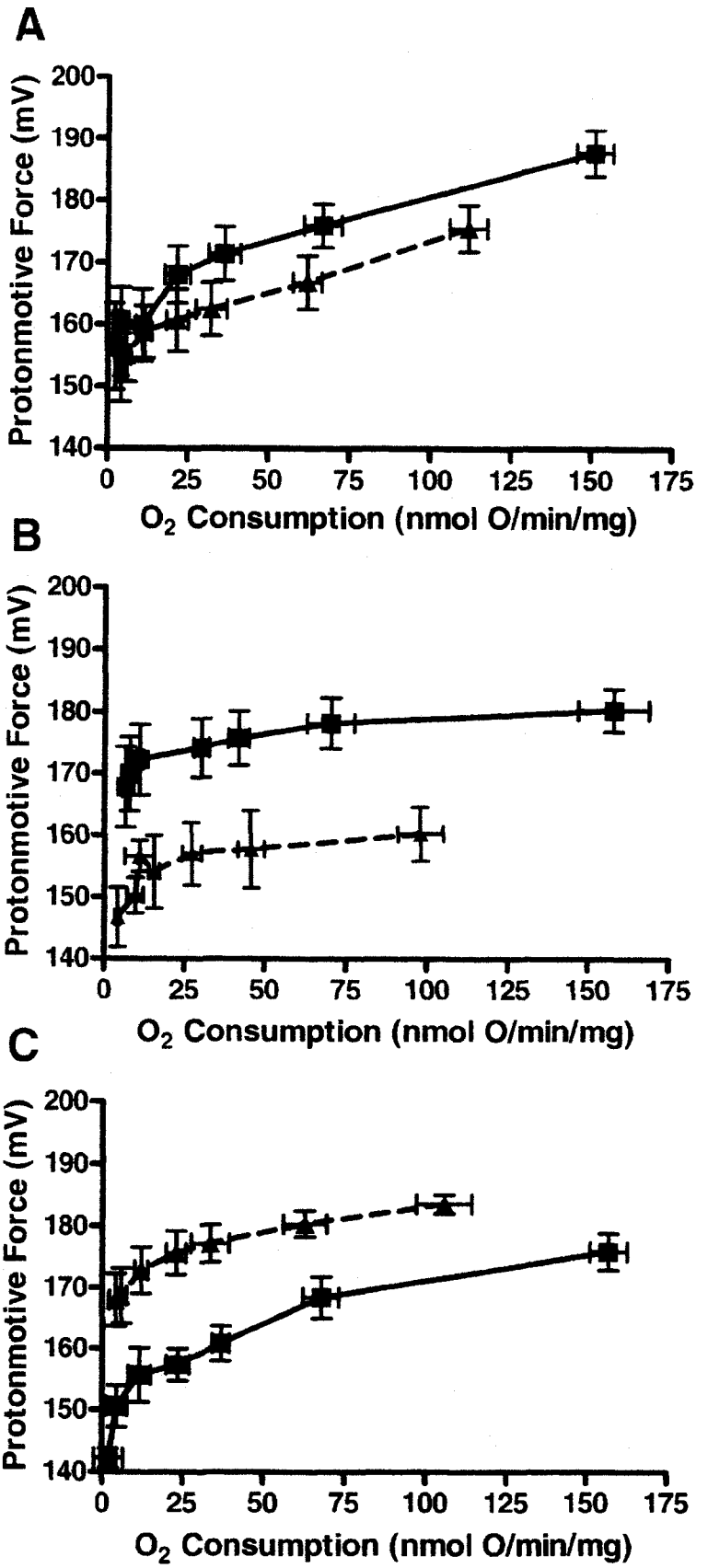

FIGURE 10: THE OVERALL KINETIC RESPONSE OF THE PROTON LEAK REACTIONS IN SKELETAL MUSCLE MITOCHONDRIA FROM CONTROL (■) AND CR (▲) RATS AFTER 12 MO (A) AND 18 MO (B) 40% CR.

The farthest point on the *right* represents state 4 (maximal nonphosphorylating) respiration and was determined by the addition of saturating amounts of oligomycin (12μg/ml) to mitochondria respiring on 10mM succinate. The kinetic response of the proton leak block was determined by incremental additions of the complex II inhibitor, malonate (0.33-10 mM) to the mitochondria at state 4. Each point represents the mean ± SEM of 6 duplicate assays (*i.e.,* 6 rats/group). Statistical significance of state 4 respiration and PMF was determined using a one-way ANOVA with a Tukey's post hoc test.

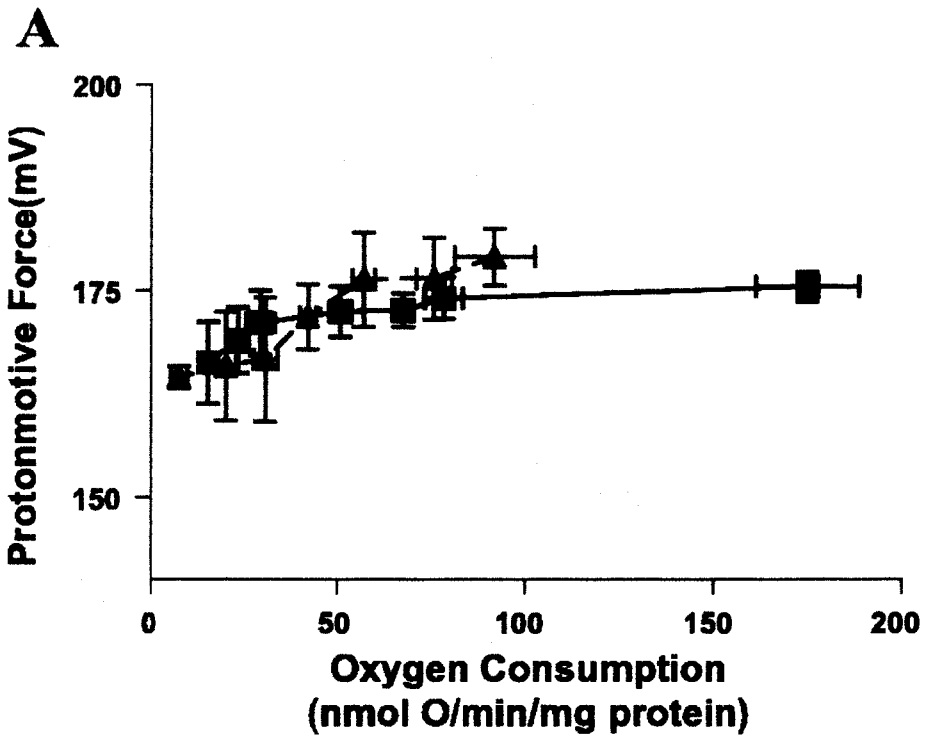

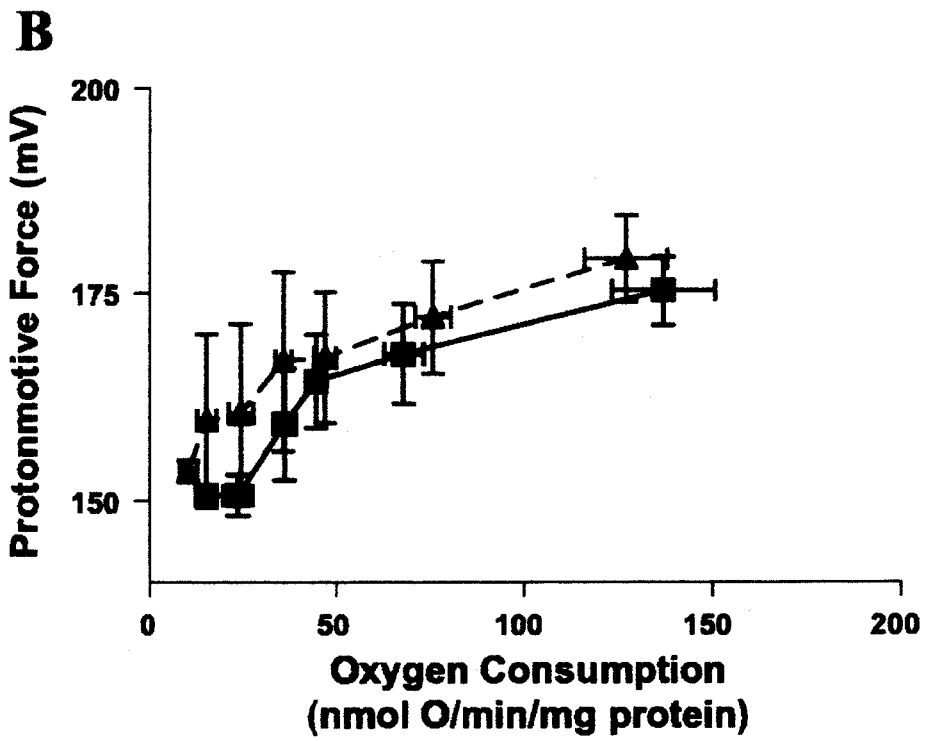

Top-down metabolic control analysis and its extension, elasticity analysis, were used to determine the response of the substrate oxidation reactions to CR. Figure 11 summarizes the kinetics of the substrate oxidation reactions for each time point. The substrate oxidation reactions measured in these isolated mitochondria involve the activities of the complexes of the ETC chain subsequent to complex II. At 2 wk of CR, state 3 (maximal phosphorylating) oxygen consumption and PMF were significantly lower than in controls (each $P < 0.05$). Results show that, for any given value of PMF, the oxygen consumed to support the activity of substrate oxidation reactions was lower in mitochondria from CR rats. At the 2 mo time-point, state 3 oxygen consumption remained lower in mitochondria from CR animals compared with their respective controls ($P < 0.004$). Here again, over a range of PMF values, the oxygen used to support substrate oxidation was lower in CR than in controls. After 6 mo of CR, state 3 oxygen consumption and PMF were no longer significantly different. It is also interesting to note that the large differences in kinetics at the 2 wk time point were diminished at 2 mo and were absent by the 6 mo time point.

The overall kinetics of the substrate oxidation reactions for the 12 and 18 mo CR time points are summarized in Figure 12. State 3 oxygen consumption and the slope of the line were not significantly ($P > 0.05$) different between mitochondria from the 12 mo CR rats and their control counterparts, whereas, at 18 mo CR we did observe a significant decrease in state 3 oxygen consumption compared with control rats ($P < 0.001$). The overall kinetics (i.e., the slopes of the lines) did not significantly change following 18 mo CR. However, at both the 12 and 18 mo CR time points, the amount of oxygen used to support the substrate oxidation reactions at any PMF value was lower in mitochondria of CR rats compared with controls. Moreover, there were no age-related differences in State 3 oxygen

consumption, but the slopes of the lines (representing the kinetics of the substrate oxidation reactions, i.e., squares in Figure 12 A and B significantly differed ($P < 0.01$) with age.

The kinetics of the phosphorylation reactions is summarized in Figure 13. The phosphorylation reactions include ATP synthase, ANT and the phosphate carrier. At the 2 wk and 6 mo time points, there were no differences in the overall kinetics of the phosphorylation reactions between CR and control animals. However, at the 2 mo time point, the oxygen used to support phosphorylation reactions was lower over a range of PMF values in CR animals compared with controls. Given that these differences were absent at the 6 mo time point, the effect appears to be transient.

Figure 14 summarizes the overall kinetics of the phosphorylation reactions. There were no differences ($P > 0.05$) in kinetics between the CR and the control-fed rats at either the 12 or the 18 mo assessment points. Moreover, there were no age-related differences in the overall kinetics of the phosphorylation reactions (*i.e.*, between control fed rats at the 12 and 18 mo time points).

FIGURE 11: THE OVERALL KINETIC RESPONSE OF THE SUBSTRATE OXIDATION REACTIONS IN SKELETAL MUSCLE MITOCHONDRIA FROM CONTROL (■) AND CR (▲) RATS AFTER 2 WK (A), 2 MO (B), AND 6 MO (C) 40% CR.

The overall kinetic response of the substrate oxidation reactions was determined by titration of mitochondria respiring at state 3 (phosphorylating) with increasing amounts of oligomycin (0-12 μg/ml). Each point represents the mean ± SEM of 7 duplicate assays (*i.e.*, 7 rats/group). Statistical significance of state 3 respiration and PMF was determined using a one-way ANOVA with a Tukey's post hoc test.

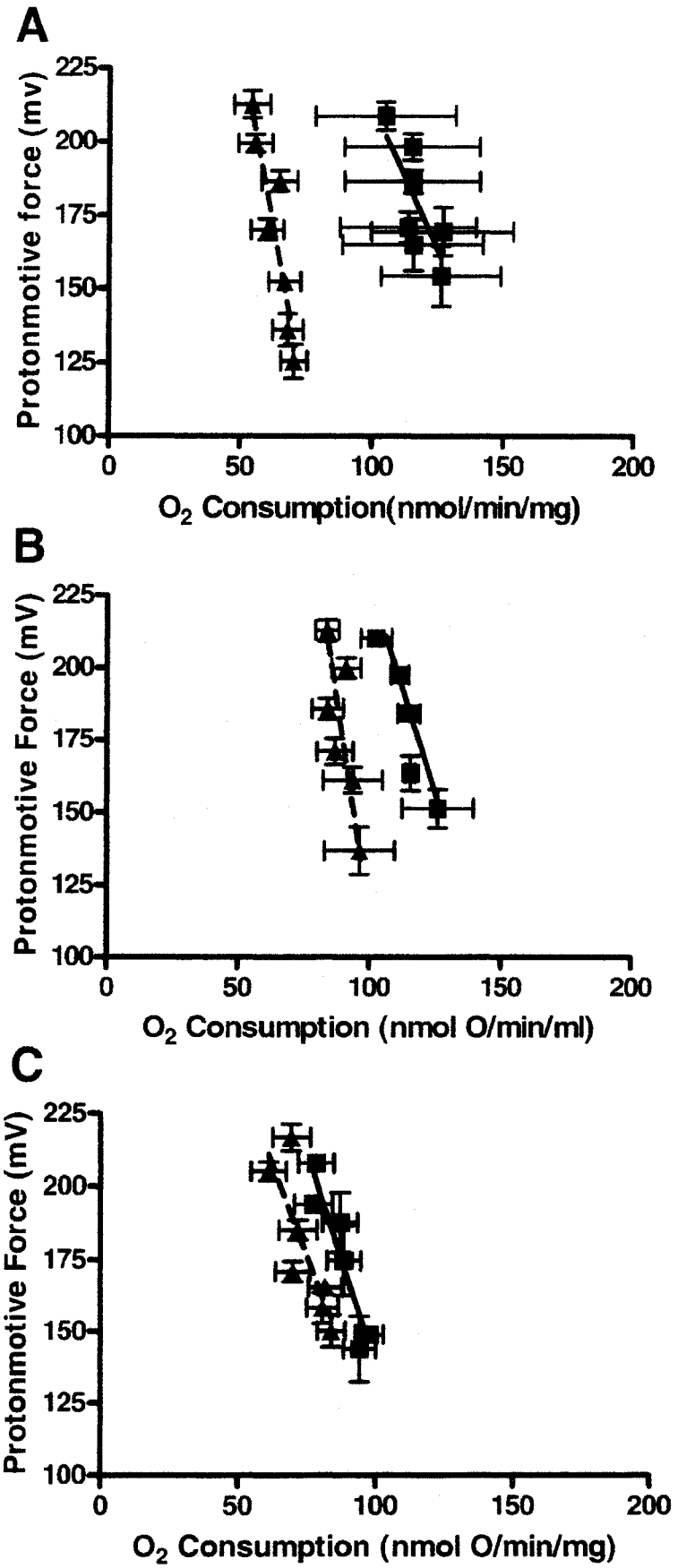

FIGURE 12: THE OVERALL KINETIC RESPONSE OF THE SUBSTRATE OXIDATION REACTIONS IN SKELETAL MUSCLE MITOCHONDRIA OF CONTROL (■) AND CR (▲) RATS AFTER 12 MO (*A*) AND 18 MO (*B*) OF 40% CR.

The overall kinetic response of the substrate oxidation reactions was determined by titration of mitochondria respiring at state 3 (phosphorylating) with increasing amounts of oligomycin (0-12μg/ml). Each point represents the mean ± SEM of 6 duplicate assays (*i.e.*, 6 rats/group). Statistical significance of state 3 respiration and PMF was determined using a one-way ANOVA with a Tukey's post hoc test.

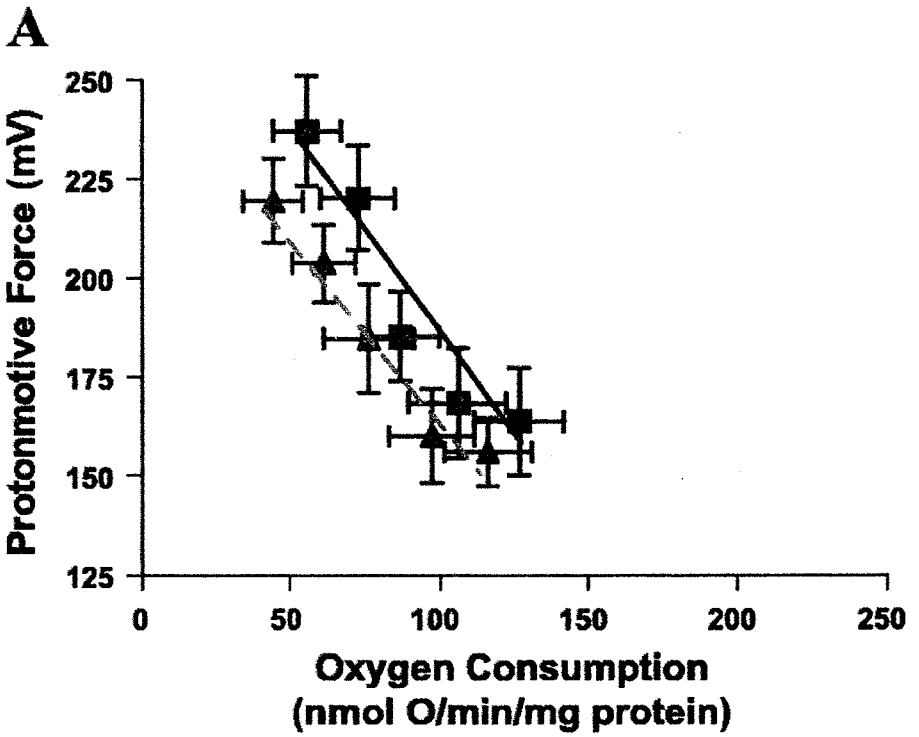

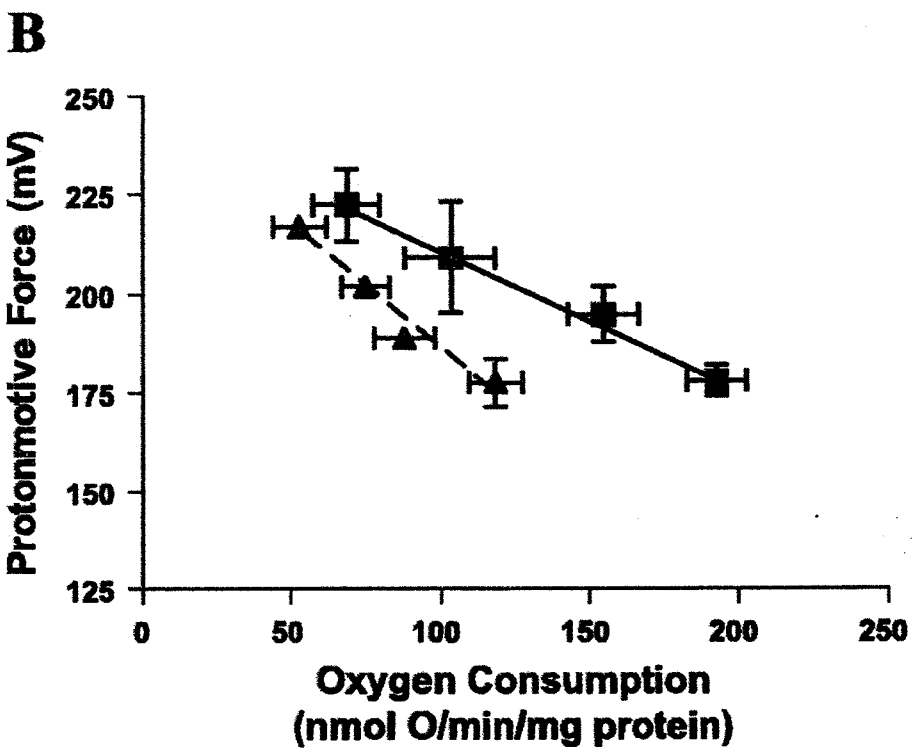

FIGURE 13: THE KINETIC RESPONSE OF THE PHOSPHORYLATION REACTIONS IN SKELETAL MUSCLE OF CONTROL (■) AND CR (▲) RATS FOLLOWING 2 WK (A), 2 MO (B), AND 6 MO (C) OF 40% CR.

The kinetic response of the phosphorylation block was determined by titration of mitochondria in state 3 (phosphorylating) with incremental additions of malonate. Each point represents the mean ± SEM of 7 duplicate assays (*i.e.,* 7 rats/group). Statistical significance of state 3 respiration and PMF was determined using a one-way ANOVA with a Tukey's post hoc test.

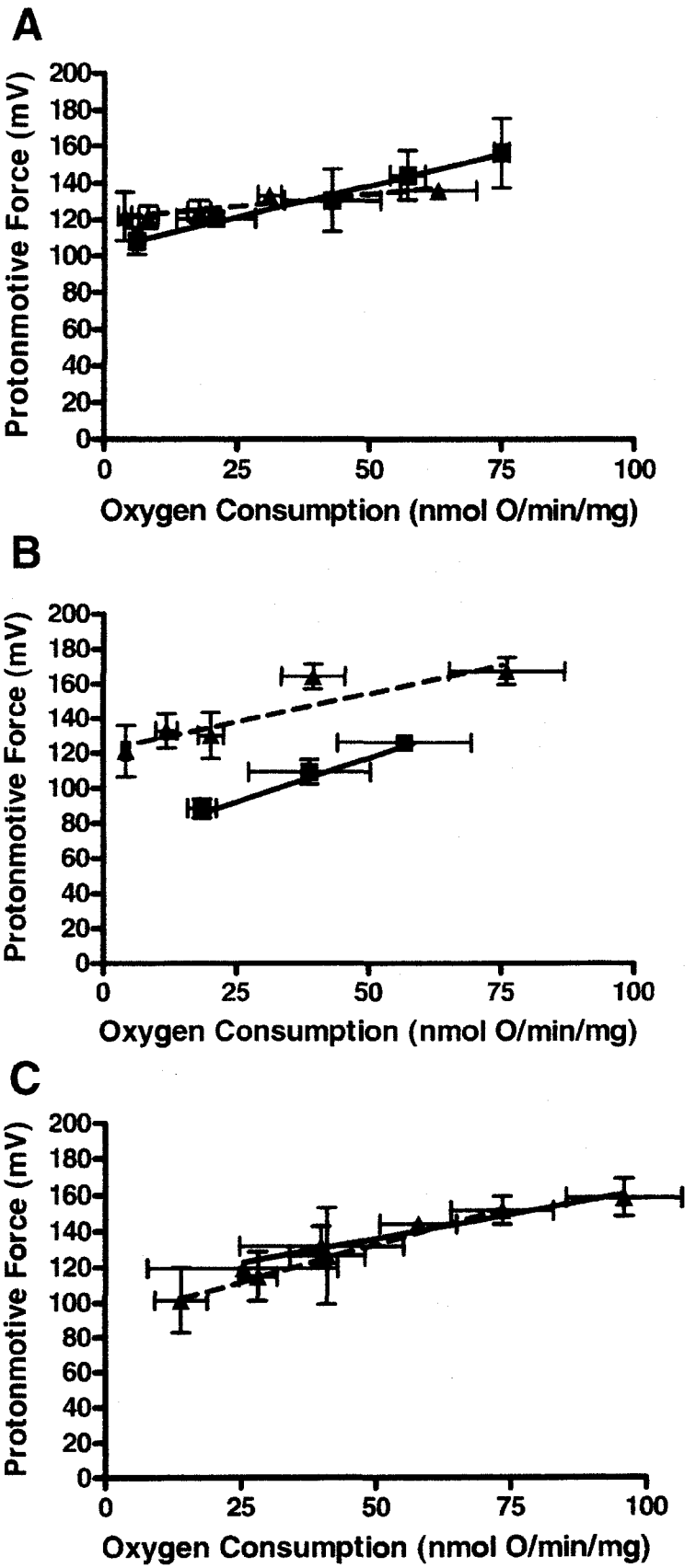

FIGURE 14: THE KINETIC RESPONSE OF PHOSPHORYLATION REACTIONS IN SKELETAL MUSCLE MITOCHONDRIA OF CONTROL (■) AND CR (▲) RATS AFTER 12 MO (*A*) AND 18 MO (*B*) OF 40% CR.

The kinetic response of the phosphorylation block was determined by titration of mitochondria in state 3 (phosphorylating) with incremental additions of malonate. Each point represents the mean ± SEM of 6 duplicate assays (*i.e.,* 6 rats/group). Statistical significance of state 3 respiration and PMF was determined using a one-way ANOVA with a Tukey's post hoc test.

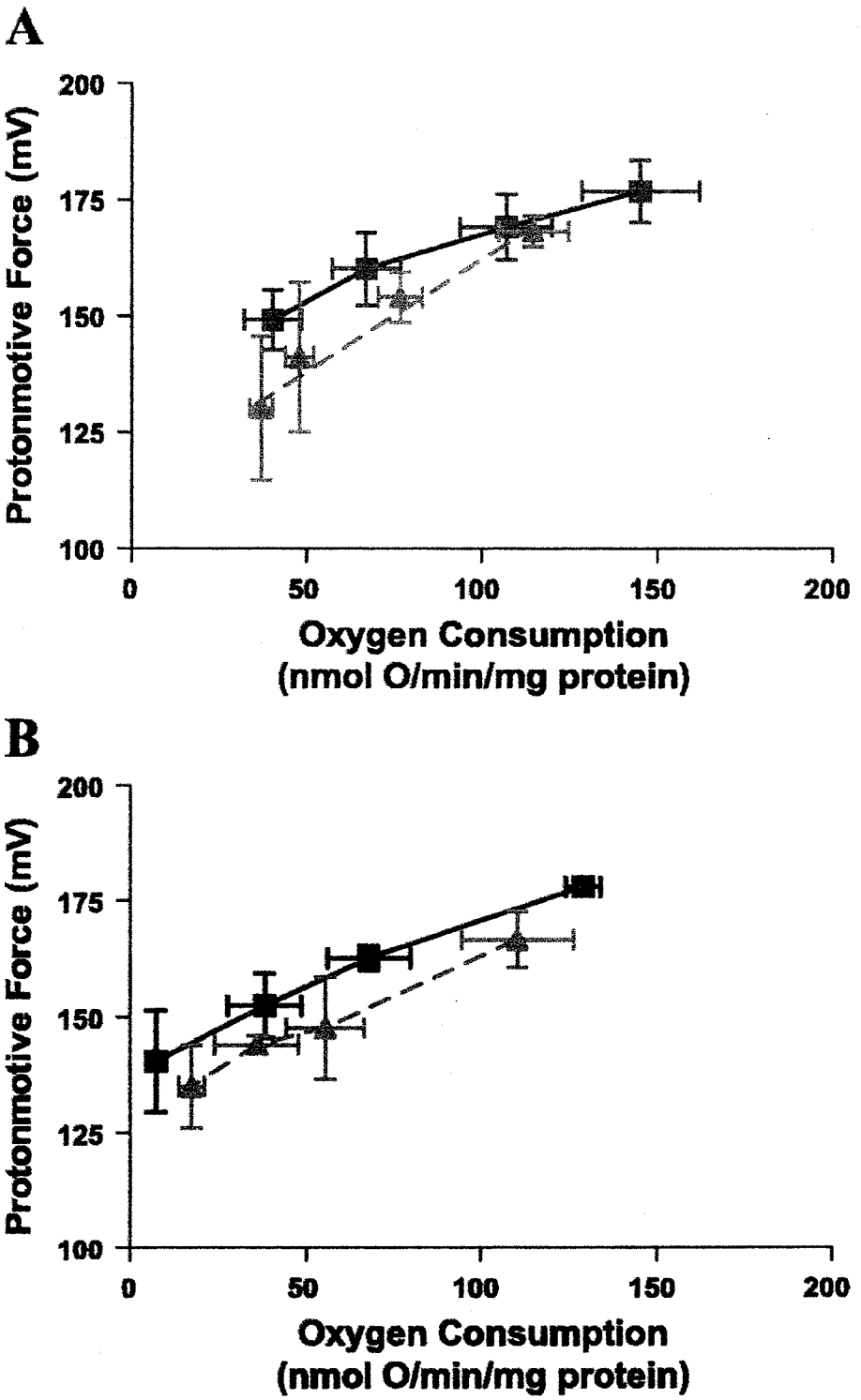

4.1.4 METABOLIC CONTROL ANALYSIS

Metabolic control analysis was used to quantify changes induced by CR on the distribution of control over oxidative phosphorylation reactions and over PMF. Tables 9-10 summarize the flux and concentration control coefficients of the three subsystems for short- and medium-term CR assessment points. The concentration control coefficients show that PMF is controlled primarily by substrate oxidation reactions under state 3 conditions. The lower concentration control coefficients in the CR compared with the control animals at all time points indicate a tighter degree of control over PMF in the CR mitochondria at both states 3 and 4. In general, control over the three subsystems by proton leak was reduced in the CR mitochondria under state 3 conditions. At all three time points, control of phosphorylation reactions was shifted toward increased control by phosphorylation reactions and decreased control by substrate oxidation and proton leak reactions in CR rats under state 3 conditions. Under state 4 conditions, control over flux through the subsystems was somewhat similar between groups. However, the degree of control by proton leak over fluxes through the substrate oxidation and leak pathways was decreased and increased, respectively, in CR compared with control rats.

Tables 11 and 12 summarize the results of the metabolic control analyses for long-term CR (12 and 18 mo). At 12 mo, the only substantive shift in control by proton leak over the three branches of the oxidative phosphorylation system appears to be the increased control over phosphorylation reactions. The decreased control over proton leak reactions by substrate oxidation reactions and the increased control over phosphorylation flux by the phosphorylation reactions however, also are substantial. At 18 mo, shifts in the control by the substrate oxidation and the proton leak reactions over the flux through all blocks of

reactions are similar. During State 4 respiration, there were no consistent CR-induced changes in the control of the oxidative phosphorylation system.

Concentration control coefficient results (Tables 9-12, *bottom*) demonstrate that PMF is primarily controlled by substrate oxidation reactions under State 3 conditions. CR did not result in any consistent changes in the distribution of control over PMF. Under state 4 conditions, control is balanced between substrate oxidation and leak pathways, and again there were no consistent changes in the distribution of control over PMF after 12 and 18 mo of CR. In the control group, the increase in the magnitude of the concentration control coefficients indicates that the protonmotive force becomes more sensitive to changes in substrate oxidation or phosphorylation system fluxes with age.

The overall pattern in the kinetic curves of each of the oxidative phosphorylation subsystems, as well as the findings from the metabolic control analysis, suggest that CR shifts the control of the phosphorylation reactions away from leak and substrate oxidation reactions toward increased control by the phosphorylation reactions. CR also appears to have induced a tighter degree of control over protonmotive force in isolated mitochondria. These results are consistent with the idea that CR produces a more efficient mitochondrial environment.

TABLE 9: STATE 3 FLUX CONTROL COEFFICIENTS FOR EACH OF THE 3 SUBSYSTEMS AND CONCENTRATION COEFFICIENTS OVER PMF IN SKELETAL MUSCLE MITOCHONDRIA FROM 2 WK, 2 MO, AND 6 MO CR AND CONTROL RATS

	2 WK STUDY		2 MO STUDY		6 MO STUDY	
Flux control coefficients	**CON**	**CR**	**CON**	**CR**	**CON**	**CR**
Substrate Oxidation Reactions						
C_S^{JS}	0.84	0.84	0.78	0.93	0.91	0.89
C_P^{JS}	0.07	0.04	0.08	0.03	0.03	0.04
C_L^{JS}	0.09	0.06	0.14	0.04	0.06	0.07
Phosphorylation Reactions						
C_S^{JP}	0.81	0.69	0.63	0.20	1.77	0.90
C_P^{JP}	0.64	0.74	0.77	0.92	0.43	0.67
C_L^{JP}	-0.45	-0.41	-0.40	-0.12	-1.20	-0.57
Proton Leak Reactions						
C_S^{JL}	0.87	1.02	0.86	1.31	0.82	0.88
C_P^{JL}	-0.37	-0.39	-0.32	-0.54	-0.27	-0.32
C_L^{JL}	0.52	0.37	0.46	0.23	0.45	0.44
Concentration Control Coefficients						
$C^{\Delta P}{}_S$	0.094	0.20	0.68	0.36	0.45	0.30
$C^{\Delta P}{}_P$	-0.042	-0.08	-0.25	-0.15	-0.15	-0.11
$C^{\Delta}{}_L$	-0.052	-0.12	-0.43	-0.21	-0.30	-0.19

Δp, protonmotive force; C, coefficient; S, substrate oxidation; P, phosphorylation; L, proton leak; J_S, flux through substrate oxidation reaction; J_P, flux through phosphorylation reactions; J_L, flux through proton leak reactions.

TABLE 10: STATE 4 FLUX CONTROL COEFFICIENTS FOR EACH OF THE 3 SUBSYSTEMS AND CONCENTRATION COEFFICIENTS OVER PMF IN SKELETAL MUSCLE MITOCHONDRIA FROM 2 WK, 2 MO, AND 6 MO CR AND CONTROL RATS.

	2 WK STUDY		2 MO STUDY		6 MO STUDY	
Flux control coefficients	**CON**	**CR**	**CON**	**CR**	**CON**	**CR**
Substrate Oxidation Reactions						
C_S^{JS}	0.87	0.86	0.71	0.91	0.85	0.83
C_P^{JS}*						
C_L^{JS}	0.13	0.14	0.29	0.09	0.15	0.17
Phosphorylation Reactions*						
C_S^{JP}						
C_P^{JP}						
C_L^{JP}						
Proton Leak Reactions						
C_S^{JL}	0.13	0.14	0.29	0.09	0.15	0.17
C_P^{JL}*						
C_L^{JL}	0.87	0.86	0.71	0.91	0.85	0.83
Concentration Control Coefficients						
$C^{\Delta P}{}_S$	0.006	0.16	0.62	0.26	0.53	0.30
$C^{\Delta P}{}_P$*						
$C^{\Delta P}{}_L$	-0.006	-0.16	-0.62	-0.26	-0.53	-0.30

*Flux and control coefficients cannot be calculated, as no ATP synthesis occurs in St 4.

Δp, protonmotive force; C, coefficient; S, substrate oxidation; P, phosphorylation; L, proton leak; J_S, flux through substrate oxidation reaction; J_P, flux through phosphorylation reactions; J_L, flux through proton leak reactions.

TABLE 11: STATE 3 FLUX CONTROL COEFFICIENTS FOR EACH OF THE 3 SUBSYSTEMS AND CONCENTRATION COEFFICIENTS OVER PMF IN SKELETAL MUSCLE MITOCHONDRIA FROM 12 AND 18 MO 40% CR AND CONTROL RATS.

	12 MO STUDY		18 MO STUDY	
Flux control coefficients	**CON**	**CR**	**CON**	**CR**
Substrate Oxidation Reactions				
C_S^{JS}	0.88	0.87	0.61	0.74
C_P^{JS}	0.07	0.01	0.06	0.04
C_L^{JS}	0.05	0.12	0.33	0.22
Phosphorylation Reactions				
C_S^{JP}	0.24	0.27	0.40	0.51
C_P^{JP}	0.81	0.98	0.99	0.95
C_L^{JP}	-0.05	-0.25	-0.39	-0.46
Proton Leak Reactions				
C_S^{JL}	0.87	0.72	0.65	0.39
C_P^{JL}	-0.16	-0.08	-0.36	-0.06
C_L^{JL}	0.29	0.32	0.71	0.67
Concentration Control Coefficients				
$C^{\Delta P}{}_S$	0.05	0.08	0.09	0.06
$C^{\Delta P}{}_P$	-0.03	-0.02	-0.08	-0.03
$C^{\Delta}{}_L$	-0.02	-0.06	-0.01	-0.03

Δp, protonmotive force; C, coefficient; S, substrate oxidation; P, phosphorylation; L, proton leak; J_S, flux through substrate oxidation reaction; J_P, flux through phosphorylation reactions; J_L, flux through proton leak reactions.

TABLE 12: STATE 4 FLUX CONTROL COEFFICIENTS FOR EACH OF THE 3 SUBSYSTEMS AND CONCENTRATION COEFFICIENTS OVER PMF IN SKELETAL MUSCLE MITOCHONDRIA FROM 12 AND 18 MO 40% CR AND CONTROL RATS

	12 MO STUDY		18 MO STUDY	
Flux control coefficients	**CON**	**CR**	**CON**	**CR**
Substrate Oxidation Reactions				
C_S^{JS}	0.95	0.86	0.64	0.88
C_P^{JS}*				
C_L^{JS}	0.05	0.14	0.36	0.11
Phosphorylation Reactions*				
C_S^{JP}				
C_P^{JP}				
C_L^{JP}				
Proton Leak Reactions				
C_S^{JL}	0.69	0.71	0.65	0.46
C_P^{JL}*				
C_L^{JL}	0.33	0.29	0.35	0.54
Concentration Control Coefficients				
$C^{\Delta P}{}_S$	0.02	0.05	0.09	0.07
$C^{\Delta P}{}_P$*				
$C^{\Delta}{}_L$	-0.02	-0.05	-0.09	-0.07

* Flux and control coefficients cannot be calculated, as no ATP synthesis occurs in State 4.

Δp, protonmotive force; C, coefficient; S, substrate oxidation; P, phosphorylation; L, proton leak; JS, flux through substrate oxidation reaction; JP, flux through phosphorylation reactions; JL, flux through proton leak reactions.

4.1.5 MITOCHONDRIAL H_2O_2 PRODUCTION

The oxidative stress hypothesis suggests that CR results in decreased production of ROS. To test this idea, mitochondrial production of ROS was estimated indirectly from measurements of H_2O_2 production. After 2 wk of CR, H_2O_2 production was decreased by 53% ($P < 0.01$; Figure 15). Reductions at 2 mo and 6 mo of CR were 57 and 74% (both $P < 0.001$), respectively, compared with control groups. At the 12 mo and 18 mo CR time points, mitochondrial H_2O_2 production in CR rats decreased 51 ($P<0.01$) and 49% ($P<0.01$), respectively, compared with controls (Figure 15). We also observed an age-related increase in the rate of H_2O_2 production; it was 29% higher ($P<0.01$) in the 24 mo old (18 mo on CR) compared with the 6.5 mo old (2 wk on CR) control rats. Therefore these results support the oxidative stress hypothesis of aging.

4.1.6 LIPID PEROXIDATION

To determine if the decrease in H_2O_2 was accompanied by a decrease in mitochondrial oxidative damage we assessed lipid peroxidation via a TBARS assay. After 12 mo of CR, there was a 46% decrease in mitochondrial lipid peroxidation compared with controls ($P < 0.05$; Figure 16). Eighteen months of CR resulted in a 52% decrease in peroxidation ($P < 0.01$). Moreover, with regard to age-related changes in mitochondrial lipid damage, there was a 24.4% increase in lipid peroxidation in the 24 mo old compared with the 18 mo old control rats ($P < 0.05$). Similarly to H_2O_2 production the reduction in lipid peroxidation further supports the oxidative stress theory of aging.

FIGURE 15: EFFECT OF SHORT- (2 WK AND 2 MO), MEDIUM-TERM (6 MO) AND LONG- (12 MO AND 18 MO) TERM CR ON H_2O_2 PRODUCTION IN SKELETAL MUSCLE MITOCHONDRIA FROM CONTROL AND 40% CR RATS.

Oxidant production was measured using a fluorometric *p*-hydroxyphenylacetate assay (Hyslop and Sklar, 1984). Results shown are expressed as means ± SEM of 6-7 rats per group. Open bars and filled bars depict results from the control and CR animals, respectively. Statistical significance was determined using a two-way ANOVA with a Tukey's post hoc test. ** Denotes statistically significant difference between CR and CON at $P < 0.01$ and ***$P < 0.001$. ## Denotes statistically significant difference at $P<0.01$ between 24 Mo CON (18 Mo Study) vs. 6.5 Mo CON (2 Wk Study).

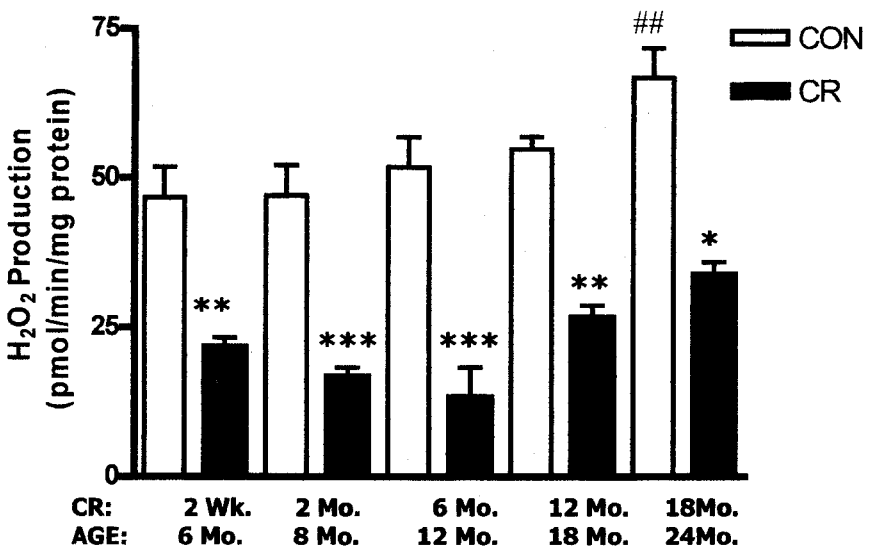

FIGURE 16: LIPID PEROXIDATION IN SKELETAL MUSCLE MITOCHONDRIA FOLLOWING 12 MO AND 18 MO 40% CR.

Lipid peroxidation was measured by the TBARS (thiobarbituric acid reactive substances) assay. TBARS are a measure of lipid oxidation and oxidative stress. Open and filled bars depict control and CR results, respectively. Statistical significance was determined using one-way ANOVA with a Tukey's post hoc test. * denotes a statistically significant difference at $*P < 0.05$; $**P < 0.001$

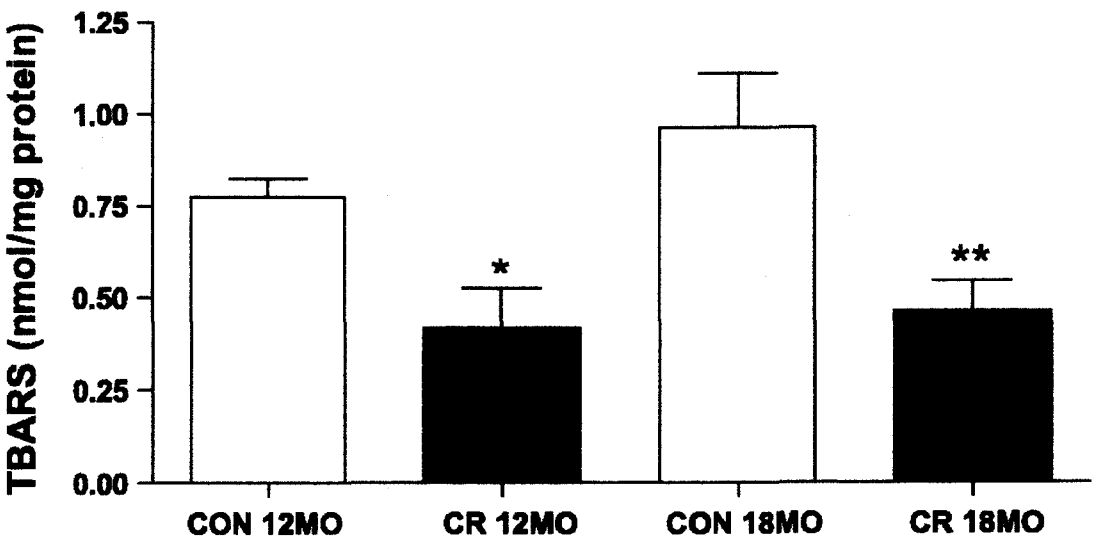

4.1.7 SERUM NEFA LEVELS

To aid in the interpretation of adaptive responses to CR, circulating levels of NEFA were analyzed at each time point. Moreover, *Ucp3* gene expression in muscle correlates with situations where there are increased circulating levels of fatty acids (Himms-Hagen and Harper, 2001). Results are summarized in Figure 17. Average NEFA concentrations were significantly higher ($P < 0.001$) in CR animals compared with controls at the 2 wk time point. There were no significant differences between CR and control values at the 2 mo and 6 mo time points. These results suggest that CR increases rates of fatty acid oxidation.

4.1.8 WESTERN BLOTS OF UCP3

Because proton leak and ROS have been associated with the uncoupling proteins, we assessed the expression of the UCP3. Results in Figure 18 indicate an approximately two-fold increased protein expression with 6 mo CR (average increase was 2-fold, based on densitometry). Western blots of mitochondrial samples remaining from analyses at 2 wk and 2 mo of CR were not possible, given the small amounts of mitochondria remaining and the possible degradation of protein during freezing and thawing. UCP3 protein content was increased in muscle mitochondria at both 12 and 18 CR time points compared with controls. A representative immunoblot is shown in Figure 19. UCP3 protein content was also consistently lower in the 24 mo old control-fed rats compared with the 18 mo old control rats. The increase in UCP3 content provides further evidence for the link between increased UCP3 and situations with increased rats of fatty acid oxidation.

FIGURE 17: SERUM NONESTERIFIED FATTY ACID LEVELS FOLLOWING 2 WK (*A*), 2 MO (*B*), AND 6 MO (*C*) OF 40% CR.

Each point represents the mean ± SEM of three duplicate assays (*i.e.*, 3 rats/group). Filled bars and open bars depict results from control and CR rats, respectively. Statistical significance was determined using a one-way ANOVA with Tukey's post hoc test. ***denotes a statistically significant difference at $P < 0.001$.

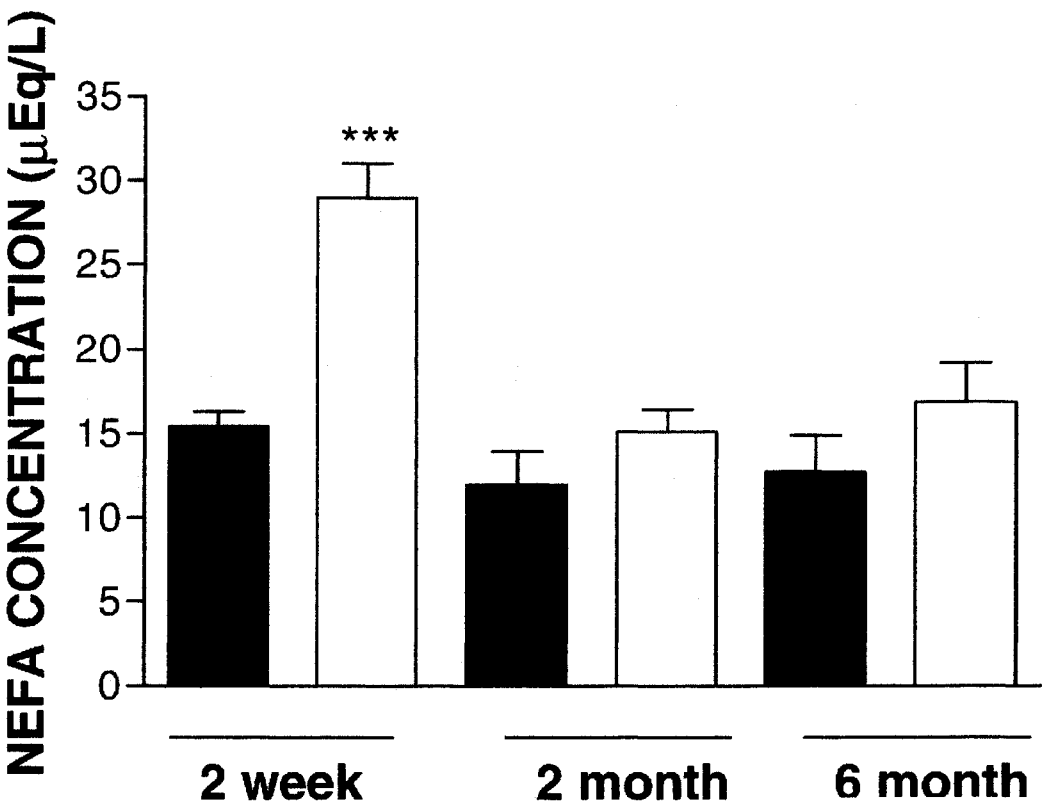

FIGURE 18: A REPRESENTATIVE WESTERN BLOT OF SKELETAL MUSCLE MITOCHONDRIAL PREPARATIONS FROM 6 MO CR AND CONTROL RATS PROBED USING A RABBIT ANTIBODY AGAINST HUMAN UCP3.

Mitochondrial protein (50 mg) from 6 mo CR rats and controls was loaded per lane. Recombinant mouse UCP3 served as a positive control; it migrates at a molecular mass of 39–40 kDa due to a 5-kDa-fusion protein. Mitochondrial protein (50 g) from *Ucp3*-knockout mice served as a negative control. UCP3 migrates at 34 kDa; the band below that for UCP3 is due to nonspecific interactions and is often observed in muscle mitochondrial proteins.

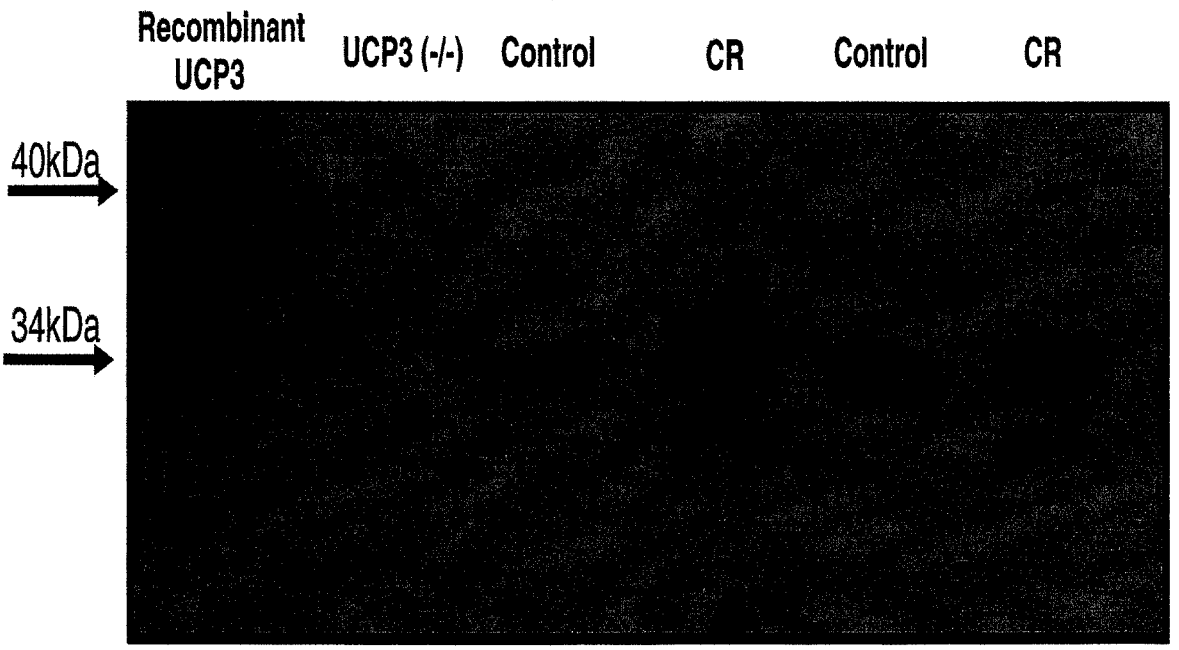

FIGURE 19: A REPRESENTATIVE WESTERN BLOT OF SKELETAL MUSCLE MITOCHONDRIAL PREPARTIONS FROM 12 AND 18 MO CR AND CONTROL RATS PROBED USING A RABBIT ANTIBODY AGAINST HUMAN UCP3.

Mitochondrial protein (75 mg) from 12 and 18 mo CR rats and controls was loaded per lane. Recombinant mouse UCP3 served as a positive control; it migrates at a molecular mass of 39–40 kDa due to a 5-kDa-fusion protein. Mitochondrial protein (75 mg) from *Ucp3*-knockout mice served as a negative control. UCP3 migrates at 34 kDa; the band below that for UCP3 is due to nonspecific interactions and is often observed in muscle mitochondrial proteins.

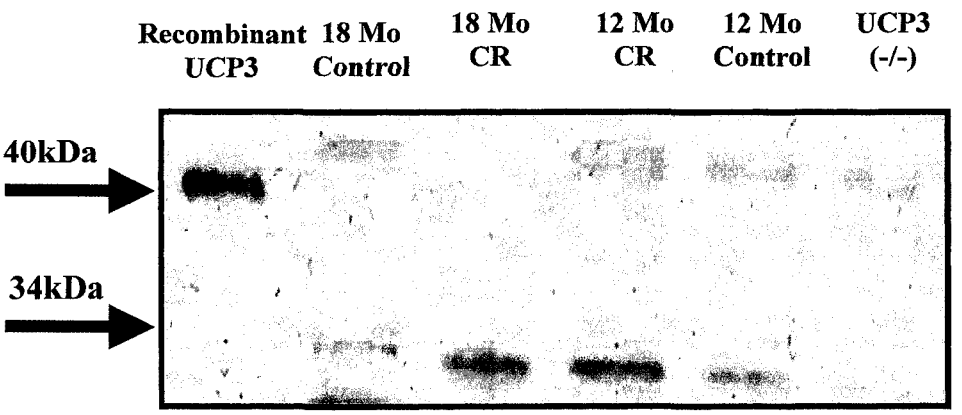

4.2 INFLUENCE OF CALORIE RESTRICTION ON WHOLE BODY AND MUSCLE MITOCHONDRIAL ENERGETICS FROM WILD-TYPE AND UCP3-KNOCKOUT MICE

The results described in the following section are in preparation and will be submitted to the American Journal of Physiology: Endocrinology and Metabolism. Author contributions: M.E.H. and L.B. designed research; L.B. performed research; L.B. analyzed data; and L.B. and M.E.H will write the paper.

4.2.1 WHOLE BODY OXYGEN CONSUMPTION AND RESPIRATORY EXCHANGE RATIOS

Indirect calorimetry was used to assess *in vivo* 24 h energy expenditure and respiratory exchange ratio (RER) (Figure 20-22). Data were collected over a 24 h period that was 2 d prior to sacrifice and muscle collection. There were no significant differences in the mean RER between over the 24 h period with 2 wk of CR in both the wild-type and the *Ucp3*-KO animals. However, the wild-type mice displayed a trend for lower RER with 2 wk CR (P=0.0675; Figure 20, *Panel A*). The actual mean values were 0.870 ± 0.038, 0.783 ± 0.024, 0.826 ± 0.018, 0.789 ± 0.027 for wild-type control, CR and *Ucp3*-KO control, CR, respectively. CR significantly reduced whole body oxygen consumption by 19.9 and 35.4% in both the wild-type and Ucp3-KO mice, respectively, compared to their fed control counterparts (P<0.05; Figure 21). We found that there were no differences in whole body oxygen consumption between wild-type and knockout control groups consistent with findings from Bezaire et al., (2001) and Gong et al., (2000). The mean values of whole body oxygen consumption in ml/min/mouse were 1.606 ± 0.069, 1.286 ± 0.100, 1.775 ± 0.086, 1.146 ± 0.053 for wild-type control, CR, and *Ucp3*-KO control, CR, respectively.

These differences in whole body oxygen consumption disappeared when the values were adjusted for body weight in both groups of mice (Figure 22). Mean mass-adjusted oxygen consumption values for wild-type control and CR, respectively, were 0.058 ± 0.001 and 0.057 ± 0.005 in ml/min/g bwt. For the *Ucp3*-KO control and CR, the mean values were 0.055 ± 0.001 and 0.051 ± 0.027 in ml/min/g bwt. Although the statistical tests did not indicate a significance difference between the values, it is still possible that there are some physiological differences between the WT and KO (as some of the curves appeared to be different at the lower and higher PRCF values). Previous studies have demonstrated differences in metabolic efficiency despite no differences in indirect calorimetry data as there is approximately 5% error associated with indirect calorimetry (Costford et al., 2006).

4.2.2 BODY AND TISSUE WEIGHTS

Food intake and body weights were measured daily to accurately determine the energy intake to be given thereafter to the CR animals. Mean body weights after 2 wk CR, were decreased 16.9% and 26.7% for wild-type and *Ucp3*-KO mice, respectively ($P<0.001$; Table 13 and 14). Heart tissue weights were not different with 2 wk CR in both the wild-type and *Ucp3*-KO mice. Kidney mass was only significantly lower in the CR *Ucp3*-KO animals, but not the CR wild-type animals, although a trend for decreased mass was observed. Both wild-type and *Ucp3*-KO mice had reduced epididymal adipose tissue depots mass of 41.0 and 60.2 % following 2 wk of CR (Table 13 and 14). Liver weights were significantly reduced with 2 wk of CR in the wild-type mice (28.6%; $P<0.001$) and *Ucp3*-KO (33.3%; $p<0.001$). These results agree with the idea that CR does not result in a miniaturized version of the control animal.

FIGURE 20: PERCENT RELATIVE CUMULATIVE FREQUENCY (PRCF) PLOTS OF RESPIRATORY EXCHANGE RATIO (RER) FOR WILD-TYPE AND *UCP3* KNOCKOUT MICE FOLLOWING 2 WK CR (N=6 MICE/GROUP).

A: Wild-type mice and B: *Ucp3*-knockout mice. For each graph, the solid and dashed lines represent the lines of best fit for the control and CR mice, respectively. The equations for the lines of best fit are shown and provide the 50^{th} percentile values and the H (slope) values for each group.

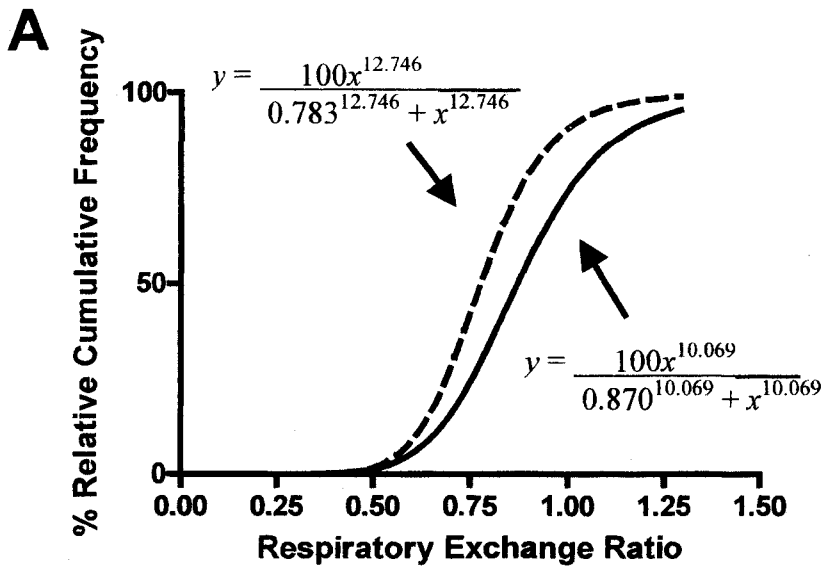

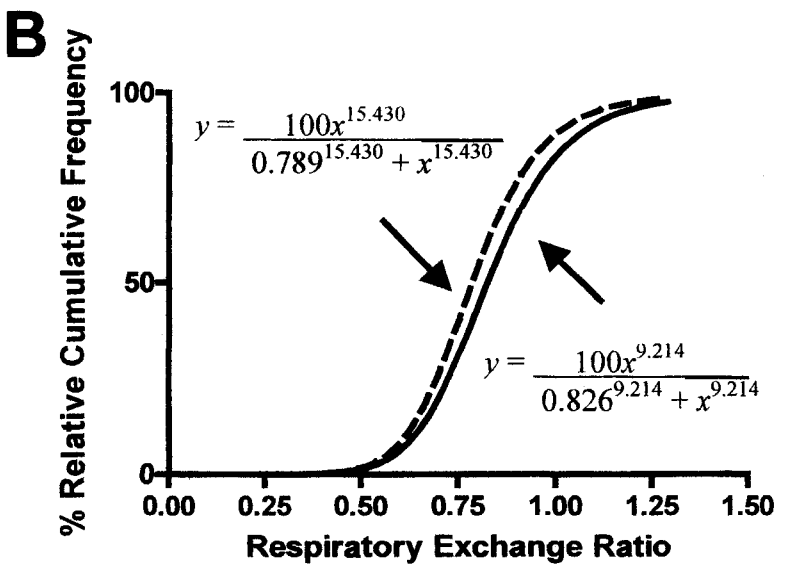

FIGURE 21: PERCENT RELATIVE CUMULATIVE FREQUENCY (PRCF) PLOTS OF WHOLE BODY O_2 CONSUMPTION (VO_2) FOR WILD-TYPE AND *UCP3* KNOCKOUT MICE FOLLOWING 2 WK CR (N= 6 MICE/GROUP).

A: Wild-type mice and B: *Ucp3*-knockout mice. For each graph, the solid and dashed lines represent the lines of best fit for the control and CR mice. The equations for the lines of best fit are shown and provide the 50^{th} percentile values and the H (slope) values for each group.

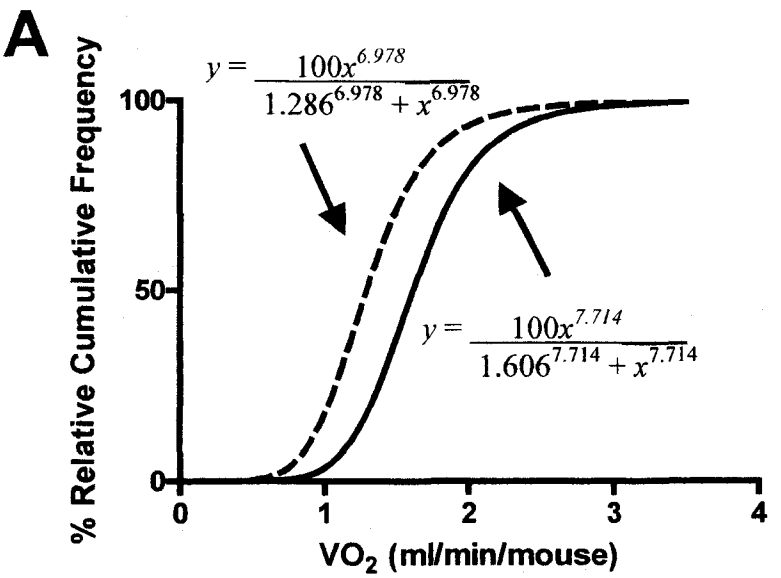

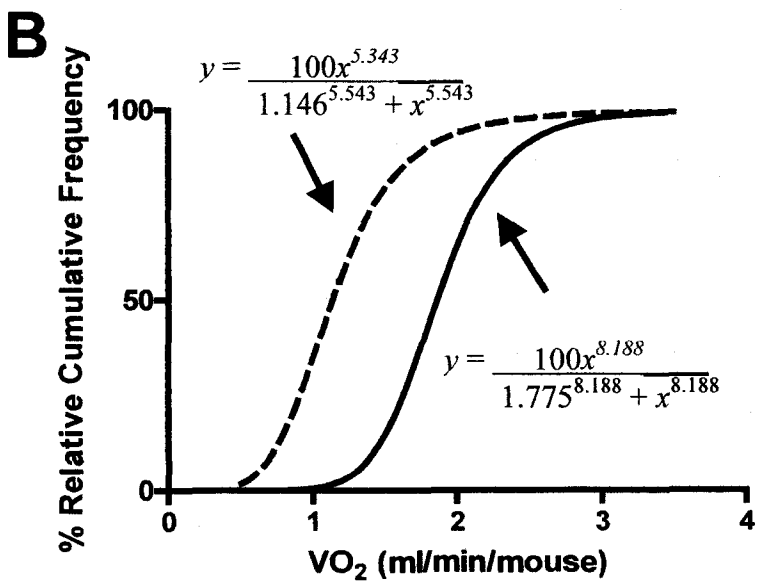

FIGURE 22: PERCENT RELATIVE CUMULATIVE FREQUENCY (PRCF) PLOTS OF MASS-ADJUSTED O_2 CONSUMPTION (VO_2) FOR WILD-TYPE AND *UCP3* KNOCKOUT MICE FOLLOWING 2 WK CR (N=6 MICE/GROUP).

A: Wildtype mice and B: *Ucp3*-knockout mice. For each graph, the solid and dashed lines represent the lines of best fit for the control and CR mice. The equations for the lines of best fit are shown and provide the 50^{th} percentile values and the H (slope) values for each group.

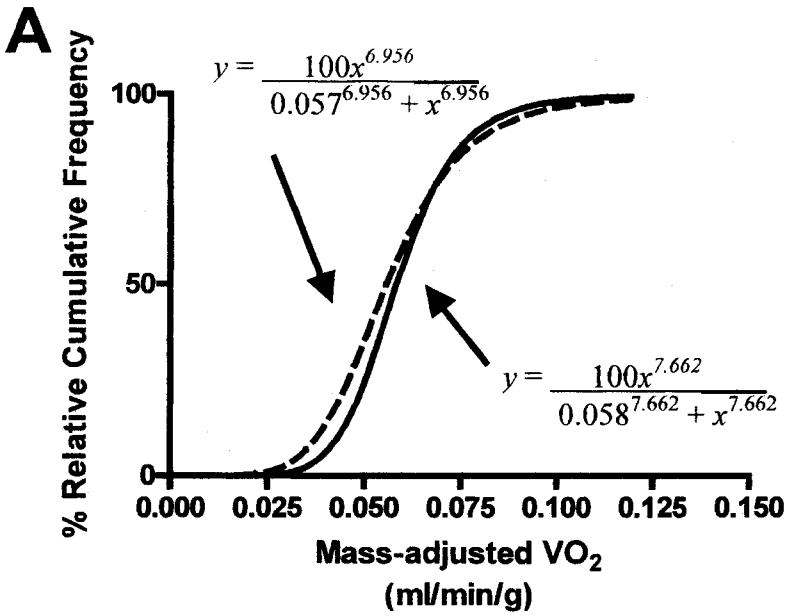

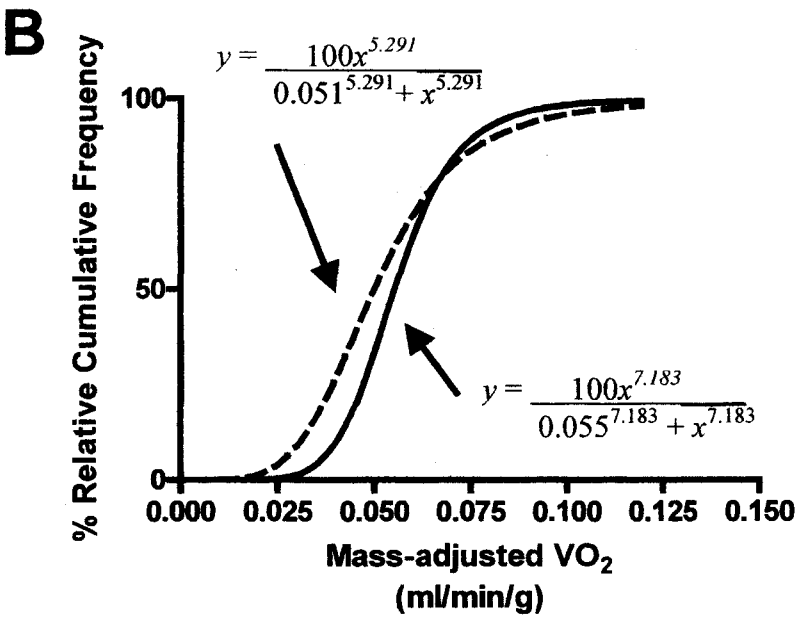

TABLE 13: AVERAGE BODY AND ORGAN WEIGHTS FOR WILD-TYPE (WT) MICE AFTER 2 WK OF 40% CR.

	WT CON	WT CR	% Change (Control vs. CR)
Body Weight (g)	25.9 ± 0.8	21.5 ± 0.6	-20.5 % ***
Liver (g)	1.12 ± 0.05	0.80 ± 0.03	-28.3 % ***
Heart (g)	0.16 ± 0.01	0.15 ± 0.01	-5.06 %
Kidney (g)	0.30 ± 0.01	0.26 ± 0.01	-13.8 %
EWAT (g)	0.78 ± 0.07	0.46 ± 0.1	-17.0 % *

Body weights were measured prior to sacrificing the animals for metabolic studies. Tissues were removed immediately after sacrifice and kept on ice until they were weighed (no more than 45 min post-sacrifice). Results are expressed as means ± SEM of 6 mice/group. Statistical significance was determined using a one-way ANOVA with a Tukey's post hoc test. * denotes a significant difference between the means of the paired columns at $P<0.05$, ** $P<0.01$, and *** $P<0.001$. CR, calorie restricted; EWAT, epididymal white adipose tissues.

TABLE 14: AVERAGE BODY AND ORGAN WEIGHTS FOR *UCP3*-KNOCKOUT MICE AFTER 2 WK OF 40% CALORIE RESTRICTION (CR).

	Ucp3-KO CON	*Ucp3*-KO CR	% Change (Control vs. CR)
Body Weight (g)	28.8 ± 0.5	21.1 ± 0.5	-26.7 % ***
Liver (g)	1.05 ± 0.04	0.70 ± 0.04	-32.7 % ***
Heart (g)	0.15 ± 0.01	0.14 ± 0.01	-9.67 %
Kidney (g)	0.33 ± 0.01	0.26 ± 0.01	-19.9 % ***
EWAT (g)	0.75 ± 0.05	0.30 ± 0.03	-60.2 % ***

Body weights were measured prior to sacrificing the animals for metabolic studies. Tissues were removed immediately after sacrifice and kept on ice until they were weighed (no more than 45 min post-sacrifice). Results are expressed as means ± SEM of 6 mice/group. Statistical significance was determined using a one-way ANOVA with a Tukey's post hoc test. * denotes a significant difference between the means of the paired columns at $P<0.05$, ** $P<0.01$, and *** $P<0.001$. CR, calorie restricted; EWAT, epididymal white adipose tissues.

4.2.3 COMPARISON OF THE KINETIC RESPONSE OF PROTON LEAK IN SKELETAL MUSCLE MITOCHONDRIA FROM WILD-TYPE AND *UCP3*-KNOCKOUT MICE

The results from rat skeletal muscle demonstrated that CR induced a consistent decrease in maximum proton leak dependent respiration. However the mechanism through which this reduction in leak-dependent respiration was achieved differed between short- and long-term CR. With short-term CR, the reduction in leak-dependent respiration was associated with an increase in leak conductance. We hypothesized that this result could be partially explained by increased UCP3 content. To test this idea we measured the effect of CR on the overall kinetics of skeletal muscle mitochondrial proton leak in wild-type (WT) mice and *Ucp3*-knockout (*Ucp3*-KO) mice. Results from these assessments are shown in Figure 23. In mitochondria from wild-type mice, maximum proton leak dependent respiration was 24.4% lower with CR ($P<0.05$). Protonmotive force at state 4 for both CR and control WT mice were not statistically different (-4.9% control vs. CR, $P>0.05$). Similarly, there were no apparent differences in the kinetics of the proton leak curves between the wild-type control and CR mice (Figure 23, Panel A). Maximum proton leak-dependent respiration was 11% lower in the *Ucp3*-KO CR mice compared to their respective controls, but this was not statistically significant using a one-way ANOVA. State 4 PMF was 6.5% lower in the CR *Ucp3*-KO compared to fed control *Ucp3*-KO ($P<0.05$). Figure 23, Panel B demonstrates that the proton leak kinetics for *Ucp3*-KO CR were quite different than their control counterparts. The overall proton leak kinetics over a range of oxygen consumption values show that PMF is lower in the *Ucp3*-KO CR mice. Oxygen consumption over a range of PMF values is higher for the CR *Ucp3*-KO mice. These results indicate that the oxygen used to balance the leak over a range of PMF is higher (i.e., the leak

is higher) in mitochondria from *Ucp3*-KO CR mice compared to *Ucp3*-KO controls. These results suggested that the increased leak conductance observed with short-term CR is indepenent of UCP3.

4.2.4 EFFECT OF CAT ON SKELETAL MUSCLE MITOCHONDRIAL PROTON LEAK KINETICS IN WILD-TYPE AND UCP3-KNOCKOUT MICE AFTER 2 WK OF 40% CALORIE RESTRICTION

The increase in leak conductance in the Ucp3-KO CR mice could be due to increased ANT activity or content. ANT has recently been shown to catalyze basal and inducible proton leak (Brand et al., 2005; Shabalina et al., 2006). To test this idea skeletal muscle mitochondria were incubated with carboxyatracylate (CAT), a known ANT inhibitor (Figure 24 and 25). In both the control and CR wild-type mice, CAT increased protonmotive force and had a tendency for decreased maximum leak dependent respiration. State 4 respiration values in the wild-type controls and *Ucp3*-KO CON mice were decreased 15.2% and 13.6% with CAT (P>0.05). In the CR animals, state 4 respiration was 21.2% and 13.1% lower for WT CR and *Ucp3*-KO CR respectively (P>0.05). In the presence of CAT, State 4 PMF was increased 5.0% and 2.2% in the wild-tyep CON and *Ucp3*-KO CON mice, respectively. For the CR mice, PMF was 5.0% and 5.1% higher with CAT in the wild-type CR and *Ucp3*-KO CR mice. The overall proton leak kinetics over a range of oxygen consumption values show that PMF is higher with CAT in all groups studied. Conversly, oxygen consumption over a range of PMF values is lower with CAT for all groups studied. These results indicate that the oxygen used to balance the leak over a range of PMF is lower (i.e., the leak is lower) with CAT inhibition. This is consistent with the idea that ANT catalyzes proton leak.

Recently, Brand *et al.*, have demonstrated that CAT can also inhibit UCP3 in addition to ANT (personal communication; M-E Harper). To determine this CAT sensitive

respiration, oxygen consumption at a common membrane potential (170mV) was compared between the proton leak curves with and without CAT (Figure 26). We found that the *Ucp3*-KO CON mice, responded less to CAT compared to their wild-type CON counterparts ($P<0.05$). Conversely with CR, *Ucp3*-KO mice had a larger CAT-sensitive respiration compared to their respective controls ($P<0.05$). These results are consistent with an increase in ANT activity and/or content with CR in the *Ucp3*-KO. The significance of this will be discussed in Chapter 5.

4.2.5 WESTERN BLOTTING OF ANT AND UCP3

Western blotting of ANT was completed to determine if the differences in CAT-sensitivity observed in Figure 27 were due to differences in ANT content (Figure 27). We did not observe any differences in ANT content in any of the genotypes or diet groups. To confirm our previous results in rats, UCP3 content was probed and was found to increase with CR (Figure 28). These results suggest that the increased CAT response in the CR *Ucp3*-KO is independent of ANT content. However this does not rule out that there may be changes in ANT activity.

FIGURE 23: THE OVERALL KINETIC RESPONSE OF THE PROTON LEAK REACTIONS IN SKELETAL MUSCLE MITOCHONDRIA FROM CONTROL (■) AND CR (▲) MICE AFTER 2 WK OF 40% CR.

A: Wild=type mice (n=6) and B: U*cp3*-knockout mice (n=6). The farthest point on the *right* represents state 4 (maximal nonphosphorylating) respiration and was determined by the addition of saturating amounts of oligomycin (8μg/ml) to mitochondria respiring on 10mM succinate. The kinetic response of the proton leak block was determined by incremental additions of the complex II inhibitor, malonate (0.33-10 mM) to the mitochondria at state 4. Each point represents the mean ± SEM of 6 duplicate assays (*i.e.,* 6 mice/group). Statistical significance of state 4 respiration and PMF was determined using a one-way ANOVA with a Tukey's post hoc test.

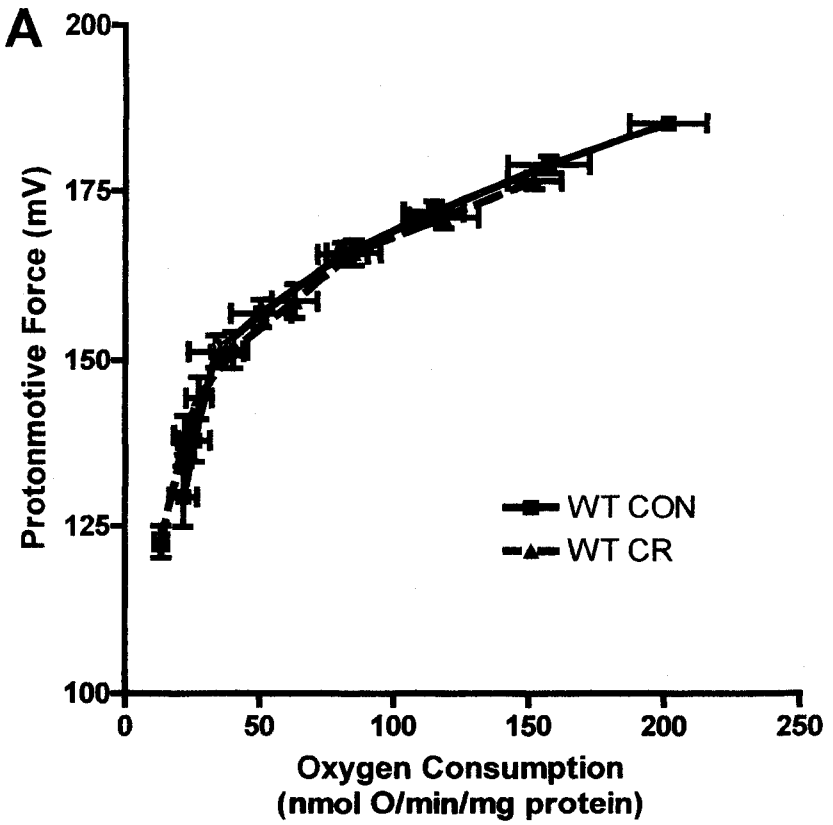

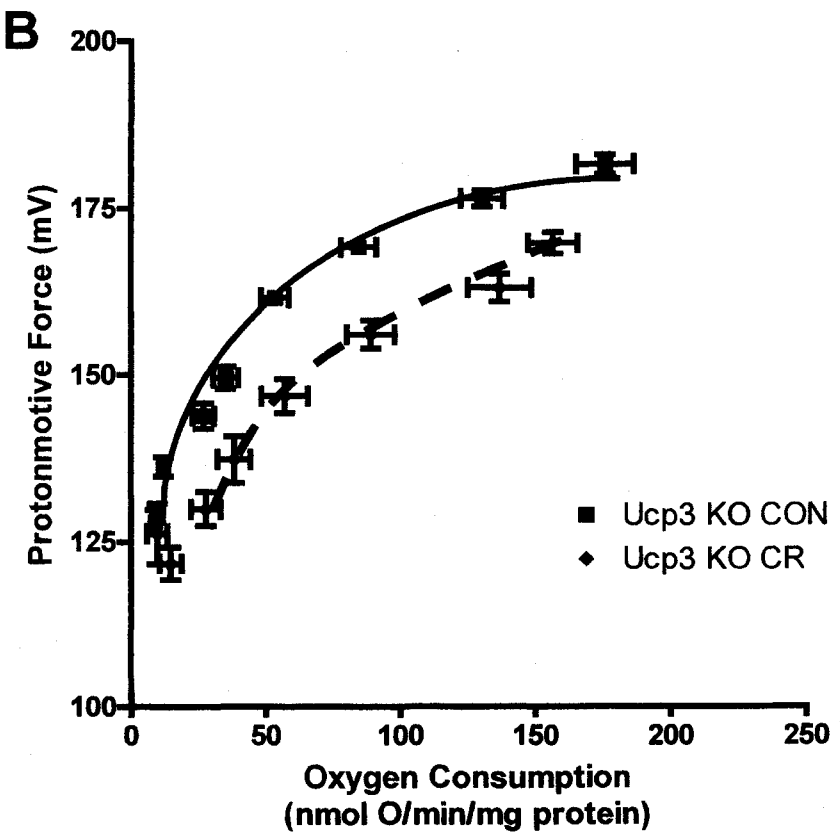

FIGURE 24: THE EFFECT OF CAT ON THE OVERALL KINETIC RESPONSE OF THE PROTON LEAK REACTIONS IN WILD-TYPE SKELETAL MUSCLE MITOCHONDRIA FROM CONTROL (■) AND CR (▲) MICE AFTER 2 WK OF 40% CR.

A: Control mice and B: CR mice. For each panel (■) represents no CAT addition (n=6) and (▲) represent incubations with CAT (n=4). The farthest point on the *right* represents state 4 (maximal nonphosphorylating) respiration and was determined by the addition of saturating amounts of oligomycin (8μg/ml) to mitochondria respiring on 10mM succinate. The kinetic response of the proton leak block was determined by incremental additions of the complex II inhibitor, malonate (0.33-10 mM) to the mitochondria at state 4. Each point represents the mean ± SEM of 6 duplicate assays (*i.e.*, 6 mice/group). Statistical significance of state 4 respiration and PMF was determined using a one-way ANOVA with a Tukey's post hoc test.

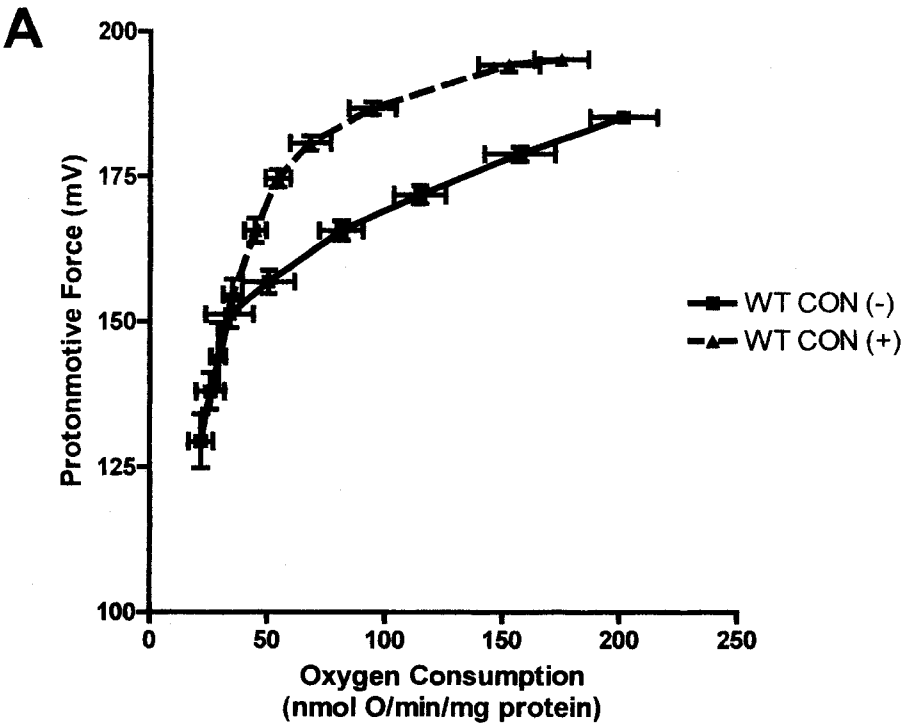

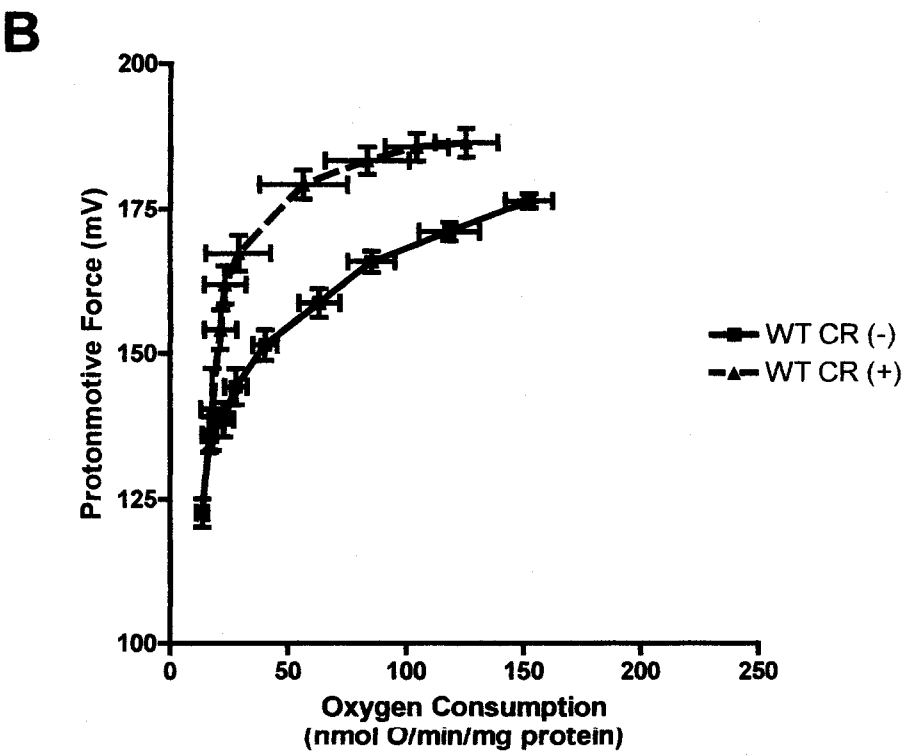

FIGURE 25: THE EFFECT OF CAT ON THE OVERALL KINETIC RESPONSE OF THE PROTON LEAK REACTIONS IN *UCP3*-KNOCKOUT SKELETAL MUSCLE MITOCHONDRIA FROM CONTROL (■) AND CR (▲) MICE AFTER 2 WK OF 40% CR.

A: Control mice and B: CR mice. For each panel (■) represents no CAT addition (n=6) and (▲) represent incubations with CAT (n=4). The farthest point on the *right* represents state 4 (maximal nonphosphorylating) respiration and was determined by the addition of saturating amounts of oligomycin (8μg/ml) to mitochondria respiring on 10mM succinate. The kinetic response of the proton leak block was determined by incremental additions of the complex II inhibitor, malonate (0.33-10 mM) to the mitochondria at state 4. Each point represents the mean ± SEM of 6 duplicate assays (*i.e.*, 6 mice/group). Statistical significance of state 4 respiration and PMF was determined using a one-way ANOVA with a Tukey's post hoc test.

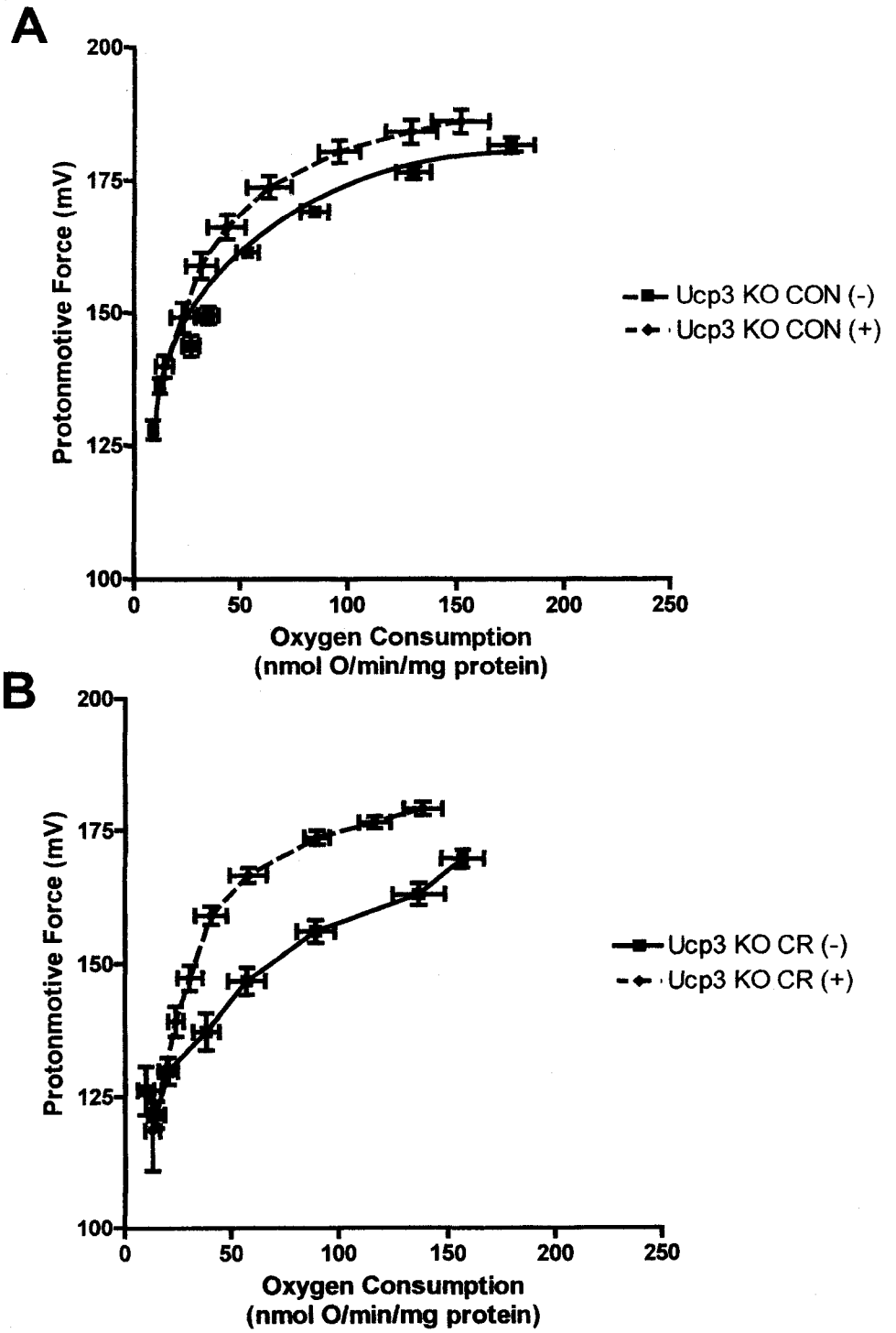

FIGURE 26: THE CAT-SENSITIVE RESPIRATION RATE IN SKELETAL MUSCLE MITOCHONDRIA FROM WILD-TYPE AND *UCP3* KNOCKOUT MICE FOLLOWING 2 WK CR.

Respiration rates at a common membrane potential (170mV) from the proton leak curves with and without CAT were compared between each genotype and diet group. Each point represents the mean ± SEM of 6 duplicate experiments (*i.e.*, 6 mice/group). Statistical significance was determined using one-way ANOVA with a Tukey post-hoc test. * Denotes a statistically significant difference at the level of $P<0.05$.

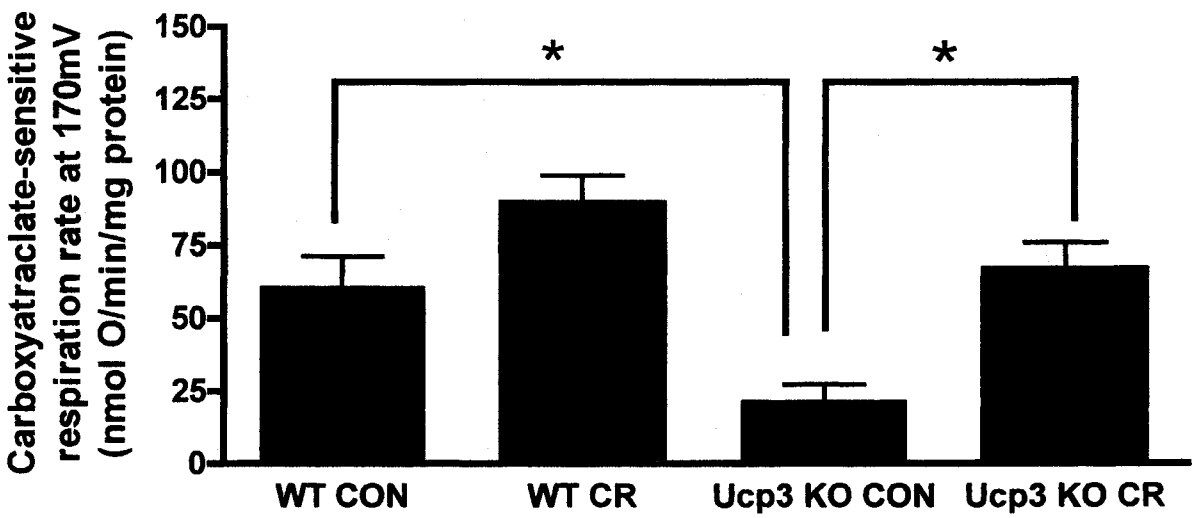

FIGURE 27: A REPRESENTATIVE WESTERN BLOT PROBING FOR ANT CONTENT IN SKELETAL MUSCLE MITOCHONDRIAL PREPARATIONS FROM WILD-TYPE AND UCP3-KNOCKOUT MICE AFTER 2 WK CR.

Mitochondrial protein (35mg) from wild-type (CON and CR), and *Ucp3*-KO (CON and CR), were loaded per lane. The location and size of the molecular weight markers are indicated on the left hand side of the blot. Mitochondrial samples from the wild-type CON and wildtype CR mice are found in lanes 2-3 and 4-5, respectively. Mitochondrial samples from *Ucp3*-KO CON mice are found in lanes 6 and 7, whereas, lanes 8 and 9 contain samples from *Ucp3*-KO CR mice. The positive control was the ANT peptide (Lane 10) and migrates at 32kDa.

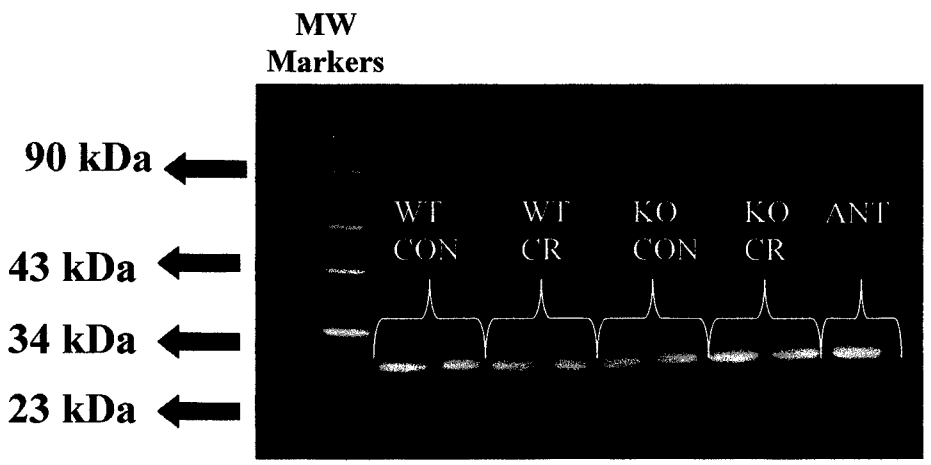

FIGURE 28: A REPRESENTATIVE WESTERN BLOT PROBING FOR UCP3 CONTENT IN SKELETAL MUSCLE MITOCHONDRIAL PREPARATIONS FROM WILD-TYPE AND UCP3-KNOCKOUT MICE AFTER 2 WK CR

Mitochondrial protein (35mg) from wild-type (CON and CR), and *Ucp3*-KO (CON and CR), were loaded per lane. The location and size of the - molecular weight markers are indicated on the left hand side of the blot. Mitochondrial samples from the wild-type CON and wild-type CR mice are found in lanes 2-3 and 3-5, respectively. Mitochondrial samples from *Ucp3*-KO CON mice are found in lanes 6-8, whereas, lanes 9-11 contain samples from *Ucp3*-KO CR mice. Recombinant mouse UCP3 served as a positive control (lane 12); it migrates at a molecular mass of 39–40 kDa due to a 5-kDa-fusion protein. UCP3 migrates at 34 kDa.

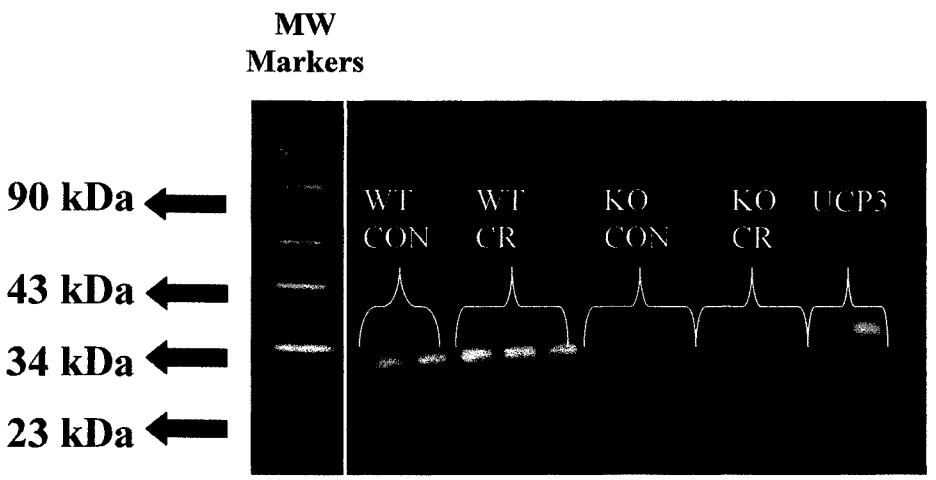

CHAPTER 5
DISCUSSION AND CONCLUSIONS

It has long been known that calorie restriction (CR), without malnutrition, is the only intervention to consistently increase maximum lifespan by delaying the rate of aging in a wide variety of animal species, including insects, fish, spiders, rats and mice (Weindruch and Sohal, 1997). CR has also been shown to attenuate many age-related functional declines and age-related diseases, including loss of skeletal muscle mass and incidence of cancer, respectively. To date, the mechanism(s) responsible for the anti-aging effects of CR are unknown, and are actively being currently investigated. Two theories of aging, the rate of living theory, and the oxidative stress theory, support the idea that CR may attenuate oxidative damage and bioenergetic decline by producing an environment that favors a reduction in cellular oxygen consumption and/or decreased mitochondrial reactive oxygen species (ROS) production (Harper et al., 2004; Ramsey et al., 2000). The exact role of hypometabolism is unclear, as many whole-body and organ-specific energy expenditure (EE) studies have yielded contradictory results (Ramsey and Hagopian, 2006; Ramsey et al., 2000). On a cellular level, CR clearly mitigates age-associated increases in ROS production and damage to biomolecules, including DNA, proteins and lipids in many tissues such as heart, liver and skeletal muscle (Bevilacqua et al., 2004; Bevilacqua et al., 2005; Harper et al., 1998; Lopez-Torres et al., 2002; Zainal et al., 2000). CR also affects mitochondria, which are responsible for approximately 90 % of cellular oxygen consumption and are also a major source of ROS. Several studies have demonstrated that alterations in mitochondrial

energy metabolism play an important role in the aging process and in the anti-aging effects of CR (Hagen et al., 1997; Harper et al., 1998; Sastre et al., 1996).

Under resting conditions, the mitochondrial proton leak pathway is a major cellular energy expending process as it accounts for about 20-25 % of resting cellular oxygen consumption (Rolfe and Brown, 1997). Since this pathway is a major contributor to resting energy expenditure we thought that it's characterization within context of CR would be fundamental to of the underlying mechanism(s) of CR, and influence of cellular ROS production on the aging process. We have proposed that CR may act, in part, by inducing a hypometabolic state of decreased oxygen consumption, ROS production and mitochondrial proton leak.

In light of the unknown mechanism (s) underlying the action of CR, a major objective of my dissertation was to elucidate the metabolic mechanism(s) behind CR. The effects of CR of increasing durations on whole body energetics and skeletal muscle mitochondrial proton leak, respiratory control, and ROS production were examined across the lifespan of rats. To further understand the mechanism underlying CR we examined the effect of short-term CR on whole body energetics and skeletal muscle mitochondrial proton leak in wild-type and *Ucp3*-knockout mice (*Ucp3*-KO). The fundamental questions addressed were: What are the responses of skeletal muscle mitochondrial proton leak to CR of variable durations? And, how is this related to mitigated ROS production?

5.1 SUMMARY OF RESULTS

We have examined the effects of short (2 wk and 2 mo)-, medium (6 mo)- and long- (12 and 18 mo) term CR on whole body energy expenditure (as assessed by indirect calorimetry), the oxidative phosphorylation system in muscle mitochondria (proton leak, substrate oxidation and phosphorylation), H_2O_2 production, and UCP3 protein content in $FBNF_1$ rats (section 4.1). Whole body oxygen consumption decreased with CR at all time points, whereas mass-adjusted oxygen consumption was not changed with short-term CR (2 wk and 2 mo; Figure 6). However, large decreases in mass-adjusted oxygen consumption were observed with 6 mo and 18 mo CR (Figure 6 and 7). CR of short-, medium- and long-term duration resulted in consistent reductions in skeletal muscle mitochondrial ROS production (Figure 15). Similarly, maximum proton leak-dependent oxygen consumption was lower in skeletal muscle mitochondria isolated from CR animals until 12 mo of CR, compared with controls; however, after 18 months of CR, there was a slight but not statistically significant decrease in maximum proton-leak dependent respiration (Figure 9 and 10). Interestingly, the kinetics of proton leak suggested that mechanisms of the response to CR were different between short-, medium- and long- term treatment. With short-term CR there was an unexpected increase in leak-dependent oxygen consumption for a given PMF (Figure 9, Panel A and B). Conversely, leak-dependent oxygen consumption for a given PMF was decreased with medium-term CR (Figure 9, Panel C). The differences were no longer apparent with long-term CR (Figure 10). These unexpected differences in leak conductance with CR of various durations were hypothesized to be due to changes in the content of uncoupling protein 3 (UCP3), a putative mediator of proton leak. Thus, muscle mitochondrial UCP3 protein content was determined after CR of 6, 12 and 18 mo.

Following these time points, UCP3 content in CR mitochondria was increased compared to mitochondria isolated from control rats (Figure 18 and 19). The implication of this result is that proton leak is not the primary function of UCP3 (i.e., the increase in UCP3 was not associated with an increase in proton leak). Metabolic control analysis was used to investigate the effects of CR on the distribution of metabolic control within the oxidative phosphorylation system. Overall, we demonstrated that the strength of the control by proton leak over flux through the substrate oxidation and phosphorylation branches of the system was decreased with CR at all time points studied, whereas, CR increased the strength of the control by the phosphorylation reactions. Moreover, the application of metabolic control analysis revealed that ATP turnover reactions become a stronger controlling factor, and proton leak a weaker controlling factor, in muscle mitochondrial oxidative phosphorylation following CR (Tables 7-8 and 11-12). *Ucp3*-KO mice were used to further examine the possibility that UCP3 may play a role in the altered proton leak kinetics observed with 2 wk CR (Section 4.2). CR resulted in a reduction in whole body oxygen consumption in both genotypes (Figure 21). However, mass-adjusted oxygen consumption was not significantly changed with CR (Figure 22). With CR, maximum proton leak-dependent respiration was lower in the wild-type mice but not in the *Ucp3*-KO mice compared to their respective controls (Figure 23). PMF was not statistically different between control and CR mice in the wildtype mice (Figure 23, Panel A). However there was a downward shift in the overall kinetics of the proton leak reactions for the *Ucp3*-KO CR mice compared to their respective counterparts (Figure 23, Panel B). These results indicate that proton leak is higher in mitochondria isolated from the CR *Ucp3*-KO mice compared to *Ucp3*-KO controls.

5.2. DOES CR INDUCE HYPOMETABOLISM?

Pathways that are central to energy expenditure (EE) are potentially important players in the aging process. Despite the numerous studies in rodents, non-human primates, and humans, there is still no clear consensus on the effect of CR on mass-adjusted energy expenditure. Overall, whole body EE studies have reported either a decrease or no change in mass-adjusted EE after CR durations ranging from 4.5 to 22.5 months, as reviewed by Ramsey *et al.*, (2000). Reports of no difference in mass-adjusted EE between control and CR rats have been used as evidence to argue against the idea that a reduction in EE may have a role in the actions of CR. However, the discrepancies originate from the use of inappropriate normalization methods to adjust EE for changes in body size and composition. A common approach to adjust EE data for body mass differences involves dividing EE by total body mass (kg or g), lean body mass, fat-free mass, metabolic body size ($kg^{0.75}$), or body surface area ($kg^{0.67}$). Adjusting data using this approach may have limited benefit, but it does not fully account for the influence of body composition and may hide many important changes that may occur at a cellular level (Allison et al., 1995). Often procedures used to normalize for body size assume that the composition of body mass (or lean mass) is similar between the CR and the control animal. However, this is usually not the case. Changes in organ weights are usually not identical to the decreases in body weight and energy intake. This is important because different tissues and organs do not have uniform rates of EE. In fact, the internal organs, including the liver, brain, heart, kidneys, intestines, and pancreas contribute approximately 70% of resting EE, even though they represent less than 10% of total body weight (Holliday et al., 1967; Ramsey and Hagopian, 2006). This suggests that it is important to examine EE in different organs. Selman et al., (2005)

assessed daily EE in rats using doubly labeled water, in conjunction with comprehensive assessments of organ and tissue weights. They used a statistical stepwise multiple regression approach to determine the best-fit normalization method to estimate daily energy expenditure. Using mathematical models they compared the measured and predicted EE based on morphological assessments. From this it was concluded that the mass-adjusted EE of CR rats was higher than predicted based on changes to body composition (Selman et al., 2005). It was unclear in this study, if the researchers were truly investigating the effect of long-term CR on EE in animals that were weight-stable instead of animals not in energy balance, as they used either old or young animals that were CR for only a short period of time (i.e., 2 mo). The limitations of this particular study preclude any conclusions that CR results in hypermetabolism.

Another report, compared results from multiple studies involving humans, monkeys, and rodents. Data were combined and analyzed using a regression based approach (ANCOVA) to determine if CR affected EE independent of body weight (Blanc et al., 2003). The results suggested that CR does in fact lead to a reduction in total EE and resting EE when corrected for body weight and fat-free mass respectively. More recently, Heilbronn et al., (2006) reported decreases in energy expenditure that were larger than expected based on the loss of metabolic mass in human subjects who were subjected to 6 mo of 25 % CR. In these human subjects, CR resulted in lower core body temperatures and lower plasma thyroid concentrations, consistent with a reduction in energy expenditure. Similarly, EE was reduced in a subgroup of patients following a combined regimen of CR and exercise, which caused an equivalent level of calorie restriction (i.e., a total of 25 %).

However, it is unclear if the decreased EE in this particular group was due to the energy deficit or CR itself (Heilbronn et al., 2006).

The results in this dissertation support an important role for hypometabolism in the mechanisms of CR. The overall pattern of our short- and long-term results demonstrates that whole body oxygen consumption decreases in response to CR. However, these values reflect the integrated sum of changes occurring at the tissue and cellular level. When the EE data were normalized for body weight, only medium- and long- term CR resulted in reduced mass-adjusted oxygen consumption. The decreased mass-adjusted EE with 6 and 18 mo CR may reflect changes in body composition (i.e., organ mass variation in response to CR). As mentioned above, CR does not result in uniform rates of change in the weight of internal organs and the degree of change are not always proportional to the reductions in body weight and energy intake (Weindruch and Sohal, 1997). In our 6 mo and 18 mo studies, only body and liver weights showed a reduction similar to the magnitude of CR (~40% decrease), with the degree of liver weight reduction slightly exceeding the level of CR 18 mo (~45%; Table 8-9). The weight of EWAT was significantly reduced with medium- and long-term CR (the reduction was similar for the 6, 12 and 18 mo CR rats, indicating that they had reached weight stability). Unfortunately, skeletal muscle mass was not weighed. Thus, its contribution to EE could not be determined. However, the weights of heart muscle and kidney mass were determined and found to decrease with medium and long-term CR. Interestingly changes to kidney and heart weights were lower than the extent of the magnitude of the calorie restriction (i.e., ~20-30% vs. 40%). Therefore, medium- and long-term CR produced a decrease in body weight that matched the level of CR. However, this weight loss was achieved primarily by loss of adipose tissue; thus heart and kidney weights

became accounted for a greater component of body weight in the CR animals. However, the proportional contribution of weights of metabolically active organs to body weight is nearly equal between control and CR animals when liver weight is included in the calculation. With CR, rapid and large decreases in liver weight may reflect water loss secondary to glycogen depletion, and it is not certain that a 45% decrease in liver mass with long-term CR truly reflects a 45% decrease in metabolically active tissue. Therefore, in our studies the maintenance of relatively high internal organ weight with CR may explain the decrease in mass-adjusted EE and may be indicative of a decrease in tissue EE. EE and organ mass provide only an estimate of EE at the cellular level, and integration of EE and organ mass measures with measures of energy metabolism at the biochemical level are required to determine more accurately whether animals adapt to sustained CR with a decrease in EE. This issue was a focus of the research presented in this dissertation.

5.3 DOES CR RESULT IN LOWER ROS PRODUCTION AND DAMAGE?

Findings presented in this dissertation are the first to reveal that CR is associated with rapid and consistent reductions in skeletal mitochondrial ROS production, assessed as net H_2O_2 release We also observed lower levels of mitochondrial lipid peroxidation following long-term CR. While our studies did not include measurements of the content and activity of antioxidant enzymes such as MnSOD, other groups have conducted such analyses. CR has not been shown to consistently alter the activities of antioxidant enzymes. For example, Lass *et al.*, (1998) reported no changes in SOD and glutathione peroxidase activities in skeletal muscle homogenates with CR. Catalase activity was increased with CR, however, the activity level of catalase itself was very low, which may argue against the idea that

catalase is important in delaying the age-related increase in oxidative damage (Lass et al., 1998). Similarly, Cu/ZnSOD and catalase protein levels were not altered in FaO cells and Hela cells treated will serum isolated from CR rats (Lopez-Lluch et al., 2006). The results of this study and others do not provide strong supporting evidence that CR causes alterations in MnSOD, or other antioxidants, with CR (Lopez-Lluch et al., 2006; Sohal and Weindruch, 1996).

Our results of decreased ROS production at all CR time-points assessed are in line with previous long-term studies in muscle and heart. Specifically, H_2O_2 production was decreased in the vastus lateralis muscle of 17- to 23- mo old rhesus monkeys after 10 mo of 30% CR compared to age-matched controls (Zainal et al., 2000). Furthermore Drew *et al.*, (2003) reported decreased H_2O_2 production from gastrocnemius muscle mitochondria following long-term (21 mo) CR (40%) in Fisher 344 rats compared to *ad libitum* fed controls. Gredilla *et al.*, (2004) also reported a decrease in rat heart mitochondria H_2O_2 production with 1 yr of 40% CR, but not following 6 wk or 4 mo of 40% CR. In isolated liver mitochondria, H_2O_2 production and mtDNA oxidative damage was lower following 1 yr of 40% CR (Lopez-Torres et al., 2002). Our collaborators at the University of California (Davis) did not report any differences in liver mitochondrial H_2O_2 production with CR after 1, 6 or 12 mo of 40% CR. However, they did observe a decrease in H_2O_2 production after 18 mo of CR (Hagopian et al., 2005; Ramsey et al., 2004). Additionally, Lopez–Lluch *et al.*, (2006) observed decreases in H_2O_2 production in isolated hepatocytes, HeLa cells and FaO cells after being incubated in serum from CR rats (Lopez-Lluch et al., 2006). Differences in the tissue- and time- specific H_2O_2 production in these studies may be, in part, due to differences in experimental conditions, such as substrates used, the duration and

degree of CR, and differences between mitotic and post-mitotic tissues. Interestingly, we also observed an age-related increase in the rate of H_2O_2 production in skeletal muscle mitochondria in our rat studies. Recently Mansouri *et al.*, (2006) have confirmed this age-related increase in H_2O_2 production in skeletal muscle mitochondria. This is the first study to show such rapid decreases in skeletal muscle mitochondrial H_2O_2 production. Our findings are consistent, overall, with the oxidative stress theory of aging as we observed that CR, which clearly extends lifespan, consistently lowers rates of mitochondrial free radical production and damage.

5.4 DOES CR ALTER PROTON LEAK?

It is still unclear what method is most appropriate for normalizing and expressing whole body EE. To avoid complications associated with normalizing EE data, and to accurately determine the role of EE in the actions of CR, assessments of energy consuming cellular processes are required. In non-exercising humans, resting EE is responsible for a majority of total energy expenditure; therefore processes that contribute to this are the largest contributors to total EE. The three main processes of resting cellular EE include mitochondrial proton leak, Na^+K^+ ATPase, and protein turnover, and are roughly estimated to account for 20-25 %, 20-28 % and 20-30 % of rat resting cellular energy expenditure, respectively (Rolfe and Brown, 1997). To better understand the effect of CR on cellular EE, we focused on the mitochondrial proton leak in our investigations.

Proton leak is a process that uncouples oxidative phosphorylation by allowing protons to return back into the mitochondrial matrix via a route that bypasses ATP synthase. This process is not an artifact of mitochondrial damage that may occur during mitochondrial

isolation; it has been measured in isolated mitochondria, intact cells and in tissues (Nobes et al., 1990). However, the mechanism of proton leak is still not completely understood.

Our initial hypothesis that CR may function in part by inducing a rapid and sustained state of decreased mitochondrial proton leak (i.e., decreased leak-dependent O_2 consumption for a given value of PMF) and decreased ROS production runs counter to the currently accepted "Uncoupling-to-Survive" hypothesis (Brand, 2000). This hypothesis originates from studies reporting decreased ROS production during metabolic states in which mitochondria are exposed to chemical uncoupling agents (e.g., FCCP or dinitrophenol). In such situations, uncoupling decreases ROS production by increasing electron flux through the respiratory chain, thus preventing the components of the chain from elevated states of reduction (Brand, 2000). Also, recent findings have shown that superoxide or oxidized lipid products, such as hydroxynonenal, can activate UCPs. This is consistent with the idea that UCPs may offer protection against ROS production by an uncoupling dependent mechanism (Echtay et al., 2003; Echtay et al., 2002). The physiological significance of the latter has not as yet been demonstrated, and some researchers have expressed concern about the experimental conditions used (e.g., the high concentrations of GDP required to demonstrate a UCP effect (Nicholls, 2006). It seems unlikely, however, that UCP3-mediated amelioration of ROS is the sole, or even the primary, defense mechanism against increased levels of cellular ROS production. Additionally, the "Uncoupling to Survive" hypothesis does not address many studies that support the idea that "long-term uncoupling" is associated with increased ROS production and potentially with decreased lifespan; this will be discussed further in section 5.7.4.

Our results demonstrate that the relationship between proton leak and ROS may be more complex than the fundamentals of the "Uncoupling-to-Survive" hypothesis. The research findings reported herein are the first to describe in detail the response of proton leak to CR in muscle over increasing spans of treatment duration. Our results demonstrate that CR alters proton leak in a duration-specific manner. Interestingly, short-term CR (2 wk and 2 mo) resulted in decreased maximum proton leak-dependent respiration, concomitantly with decreased maximum proton leak-dependent PMF. Furthermore, PMF values in the CR rats were significantly lower over a range of oxygen consumption values. Our short-term results are not consistent with those of a recent study by Johnson et al., (2006) that demonstrated decreases in proton leak rate and basal proton conductance in both intermyofibrillar and subsarcolemmal mitochondria isolated from quadriceps and gastrocnemius of rats following 3 d of 50% food restriction (Johnson et al., 2006). However, there are several important differences in experimental design between this study and our own. What is clear from this study, in addition to ours is that there is a rapid response in skeletal muscle mitochondrial energetics to CR. The changes in state 4 respiration that we observed with 6 mo and 12 mo CR are consistent with the findings of Lal *et al.*, (2001) who observed a 23% decrease in maximal leak-dependent respiration in rats after 23 mo of 33 % CR. However, differences in maximum leak-dependent respiration were lost at the longest CR time point (18 mo) used in our research. This difference may be due to the fact that we used a different rat strain. $FBNF_1$ rats in our study are resistant to the development of several diseases, such as renal failure, which are common in other rat models of aging. This strain allows the study of healthier older animals, which often is not possible with other strains (Lipman et al., 1996). These rats have a mean lifespan of 34 mo

compared to 24 mo for F344 rats. It is unknown if the effect of CR is less in these rats than other rats due to their resistance to disease. Other differences between studies include the age of CR initiation (10 mo compared to 6 mo of age). Also contributing to the discrepancy with long-term CR, is the observation that mitochondria from old rats appear to be more fragile than those from young rats and are perhaps more easily damaged during isolation (Hagen et al., 1997).

We observed intriguing differences in the response of skeletal muscle proton leak to CR of increasing duration. The decrease in PMF with decreased maximum proton leak-dependent respiration following short-term CR is not consistent with our overall hypothesis. Our results indicate that the mechanisms of mitochondrial adaptations to CR may be distinct for short- medium- and long- term CR (See section 5.7 for suggested mechanism).

Another important outcome from our findings and those of our collaborators is that we have demonstrated tissue-specific differences in the mitochondrial bioenergetic responses to CR. Specifically the CR-induced responses we observed in skeletal muscle mitochondria were rapid whereas, findings from the laboratory of our collaborators did not finding any CR-related changes in liver mitochondria until much later 18 mo CR despite the fact that the liver mitochondria was isolated from the same rat strain ($FBNF_1$) and subjected to the same CR diet and degree of restriction as in our studies in skeletal muscle. Ramsey et al., (2004) demonstrated that proton leak was not substantially altered following short- (1 mo) or medium- (6 mo) term CR, but was significantly decreased following 18 mo CR (Hagopian et al., 2005). Similarly, another study of the effects of food restriction on liver mitochondrial energetics also demonstrated that proton leak was not altered after 3 days of food restriction (Dumas et al., 2004).

These tissue-specific differences may be related to the fact that skeletal muscle is post-mitotic and is highly susceptible to oxidative stress and atrophy with aging. Liver however is a mitotic tissue that is apparently less affected by aging and tends to show signs of oxidative damage only at advanced ages. Moreover, we consistently observed that liver weight is rapidly reduced with CR, whereas changes in skeletal muscle weight occur at much slower rates. The acute response of liver to CR is thus a reduction in weight without significant alterations in mitochondrial bioenergetics, whereas skeletal muscle apparently responds by altering the activity of energy consuming processes, such as proton leak. However, given enough time, CR eventually induces changes in liver mitochondrial energetics, as demonstrated by the long-term CR effects on proton leak, H_2O_2 production and oxidative damage (Hagopian et al., 2005). In summary our results demonstrate that CR alters proton leak in a time and tissue dependent manner.

5.5 DOES CR AFFECT UCP3 CONTENT?

We hypothesized that the bioenergetic effect of CR on skeletal muscle mitochondria might be related to changes in UCP3 protein expression. UCP3 is a 34kDa protein in the mitochondrial inner membrane of skeletal muscle, BAT and sometimes, heart. The physiological function of UCP3 is unknown, however many studies have demonstrated that its expression correlates strongly with conditions where fatty acid oxidation is high (Bezaire et al., 2001; Cadenas et al., 1999; Cortright et al., 1999; Gong et al., 1999). Our results of reduced NEFA levels with 2 wk CR are also consistent with this idea (Figure 17). Thus the correlation of free fatty acid levels with UCP3 mRNA expression is consistent with a role for UCP3 in the regulation of fatty acid metabolism rather than uncoupling oxidative

phosphorylation. Specifically, UCP3 has been proposed to enhance fatty acid handling and oxidation by functioning as a mitochondrial fatty acid anion exporter (Himms-Hagen and Harper, 2001). It has also been suggested that UCP3 may play an important role in protection from ROS-mediated cellular damage (Echtay et al., 2002; Vidal-Puig et al., 2000). Evidence for the latter stems from the early observation of higher levels of ROS damage in isolated skeletal muscle of *Ucp3*- KO mice (Vidal-Puig et al., 1997). In our studies, 6 mo of CR increased UCP3 protein content approximately 2-fold, consistent with results of gene expression profiling which demonstrated increased UCP3 mRNA expression in heart and muscle of CR mice (Lee et al., 2002). This increase in UCP3 content at 6 mo of CR was concurrent with decreased maximal proton leak-dependent respiration, decreased proton conductance and is inconsistent with the hypothesis that UCP3 contributes to proton leak. Fundamentally however, it is also consistent with an increased reliance on fatty acid metabolism, and corroborates several other studies demonstrating that increased UCP3 expression (e.g., with fasting) was not associated with increased proton leak (Bezaire et al., 2001; Cadenas et al., 1999). Thus, mitochondrial proton leak does not seem to be inextricably linked to levels of UCP3 expression. The hypothesized function of UCP3 as a regulator of proton leak was initially supported by many *in vivo* and *in vitro* studies in which UCP3 was expressed at supra-physiological levels. However, it is currently agreed that the uncoupling observed in these studies may have been artifactual; via disruption of the structure or integrity of the mitochondrial inner membrane (Stuart et al., 2001). Thus, we hypothesized that the reduction in PMF with short-term CR was not due to UCP3-mediated increase in proton leak. The decreases in PMF with CR suggested to us that UCP3 may be altering PMF through processes that are distinct from proton leak reactions (e.g.,

translocation of another ionic species, such as a fatty acid anion, across the membrane). Consistent with the hypothesis of Himms-Hagen and Harper (2001), the decrease in PMF over a range of oxygen consumption values observed with short-term CR may be related to increased fatty acid anion export from the mitochondria. Under these conditions, the export of a fatty acid anion from the matrix to the cytosol would have the same effect on PMF as the import of a proton into the matrix, all else remaining equal. It was thus necessary in the latter stages of this research to compare the effects of CR on proton leak and ROS production in the absence and in the presence of UCP3 in muscle.

5.6 IS UCP3 RESPONSIBLE FOR CR-RELATED CHANGES IN SKELETAL MUSCLE MITOCHONDRIAL ENERGETICS?

If UCP3 was responsible for the initial CR-related changes in skeletal muscle mitochondrial PMF, then the responses to short-term CR, such as the decreases in PMF would be absent in mitochondria from *Ucp3*-KO mice. To test this possibility, we measured proton leak in wild-type and *Ucp3*-KO mice after short term (2 wk) CR. Top-down metabolic control analysis was used to study the metabolic differences in skeletal muscle mitochondria isolated from wild-type and *Ucp3*-KO mice. Maximum proton leak-dependent respiration was lower in the wild-type mice following 2 wk of CR (Figure 23A). This response is consistent with our short-term rat data. Interestingly, there was no difference in maximum proton-leak dependent respiration in response to short-term CR in the *Ucp3*-KO mice. There were no differences in the wild-type proton leak curves with 2 wk CR. However, the proton leak kinetics for the restricted *Ucp3*-KO were shifted downwards, indicating an increase proton conductance (Figure 23B). The lack of effect of CR on proton

leak kinetics in wild-type mice is not consistent with our findings in rats. A possible reason for this discrepancy may be related to metabolic differences between rats and mice. For example, both wild-type and *Ucp3* KO mice weighed much more than other mice our laboratory has used in past studies (i.e., these mice weighed 25g vs. 17g in a study by Bezaire et al., (2005). Another important difference between our rat and mouse studies is the fact that CR was initiated at different ages (6 mo in the rats vs. 2 mo in the mice). Interestingly, both our studies demonstrate that short-term CR reduces maximum proton leak-dependent respiration. We originally proposed that the difference in rat skeletal muscle proton leak kinetics with short-term CR was due to increased UCP3 protein levels. This idea is not supported by our current findings as the restricted *Ucp3*-KO displayed altered leak kinetics (Figure 23B). However, caution should be applied when interpreting these results, as the PMF response to short-term CR in mitochondria from wild-type mice was not consistent with the rat data we collected however this may be a result of the age at which CR was initiated. Our short-term results in *Ucp3*-KO mice indicate that the observed effects are independent, at least to some extent, of UCP3. Other mechanisms may involve changes in ANT content and/or activity. ANT is a 32kDa mitochondrial inner membrane protein that exchanges ADP for ATP across the membrane. ANT mediates a carboxyatracylate (CAT)-sensitive proton leak when activated by fatty acids (Andreyev et al., 1989), AMP (Cadenas et al., 2000), and alkenals (Echtay et al., 2003). Recently it has been demonstrated that ANT may catalyze one-half to two-thirds of basal proton leak (i.e., fatty acid independent leak) (Brand et al., 2005). We thus speculated that the increased proton conductance in *Ucp3*-KO CR animals may be due to increases in ANT content and/or activity. To test this idea, mitochondria were isolated from the four groups of mice to assess CAT-sensitive and -

insensitive leak kinetics. We documented a CAT-sensitive proton leak in mitochondria from all four groups of mice (Figure 24 and 25). In our study, the *Ucp3*-KO control mice had lower CAT-sensitive respiration rates compared to wild-type control mice (Figure 27), demonstrating that CAT can inhibit UCP3 or a UCP3-related process. These results are consistent with Brand's laboratory, which have demonstrated that CAT fully inhibits UCP3 in addition to ANT (Personal communication, M-E. Harper).

Interestingly, we observed that the *Ucp3*-KO CR group had the highest sensitivity to CAT, consistent with the idea that *Ucp3*-KO mice respond to CR by increasing ANT activity and/or content or possibly increased ANT/bilayer interactions (Figure 26). To further examine the effect of short-term CR on ANT, we used western blotting to analyze ANT content in our muscle mitochondrial preparations. Interestingly we did not observe any differences in ANT content in any of the genotypes or treatment groups (Figure 27). Our western blot results are consistent with the results from Brand's group to the extent that there were no differences in ANT protein levels between the wild type and *Ucp3*-KO mice that were fed *ad libitum* (personal communication between MD Brand and ME Harper).

With respect to the effects of short-term CR, our novel findings indicate that ANT-mediated proton leak is increased with CR despite the lack of effect on ANT protein content. Recently it has been shown that the ANT contribution to basal leak is ANT isoform specific. Specifically, ANT1 may mediate leak, but not ANT2 (Shabalina et al., 2006). Thus, the lack of change in ANT content may be a result of the fact that the antibody used to probe for ANT was not isoform-specific. Also, it may be a reflection of an additional level of regulatory control for ANT.

It is clear from our results that the ANT-mediated proton leak is 3.2- fold higher in muscle mitochondria of *Ucp3*-KO CR mice compared to the *Ucp3*-KO CON mice (Figure 26). Similarly, there appears to be a trend for a 1.5-fold increase in CR-induced ANT-mediated proton leak in the wild-type mice. *Ucp3*-KO mice have been shown to have higher levels of ROS and oxidative stress (Vidal-Puig et al., 2000). Thus, the greater ANT activity in *Ucp3*-KO CR mitochondria could potentially be a protective mechanism to further compensate the lack of UCP3 defense from ROS. In comparison, the wild-type animals in general may be in a less oxidative state and therefore may not require such defenses. It is also interesting that the *Ucp3*-KO mice lost a greater amount of weight on CR than the wild-type mice. This finding also supports the idea that the increased ANT activity in these mice is protective. Perhaps the increased weight loss was another way to further prevent any extra lipid peroxidation that could occur as a result of the higher levels of oxidative stress in these knockout mice. Therefore, the increased ANT activity and extra weight loss could be an extra adaptation to CR for an already "damaged" mouse.

5.7. A PROPOSED MECHANISM UNDERLYING CR

The overall goal of my research has been to understand the importance of mitochondrial proton leak in response to CR of increasing duration, and how alterations in proton leak are related to decreases in oxidative stress. The results of this dissertation overall, demonstrate that the response of proton leak to CR is time- and tissue- dependent. In rats, 6 mo- and 18 mo CR resulted in decreased mass-adjusted EE, decreased maximum proton leak dependent respiration and ROS production in skeletal muscle mitochondria. The response of the PMF component of proton leak, which has been shown to influence ROS

production, varied depending on our experimental conditions. Overall, our findings of decreased maximum proton leak dependent respiration and H_2O_2 production support the possibility that they are related as suggested by previous studies (see section 5.7.1). A review of the literature reveals, that this relationship is also observed within cross-species comparisons; comparisons of altered thyroid status; and comparisons of young versus old hepatocytes, as described in the following sections.

5.7.1 CROSS SPECIES COMPARISONS OF PROTON LEAK, LONGEVITY AND ROS

Cross-species comparisons support the idea that maximum leak-dependent respiration is inversely related to longevity. When compared across species, proton leak rates are inversely related to body size. Liver mitochondria from small mammals such as mice had higher maximum proton leak dependent respiration and proton conductance than larger animals such as horses and sheep (Porter and Brand, 1993). In fact, liver mitochondria from mice were 4-fold more permeable to protons than liver mitochondria from horses. A follow-up study using isolated hepatocytes from large and small mammals demonstrated similar results (Porter and Brand, 1995). Thus, mitochondrial proton leak is inversely related to body size when compared across species, as is cellular EE. Interestingly, there is an inverse relationship between H_2O_2 production in liver sub-mitochondrial particles, body mass and lifespan when compared within the same species and across different species (Sohal et al., 1990; Sohal et al., 1989). In summary these studies generally suggest that animals with a high proton leak rate and greater ETC capacity such as rats and mice have higher rates of ROS production. Conversely, animals with low rates of

proton leak such as horses have low rates of ROS production. Our data of reduced maximum leak-dependent respiration and ROS production with CR is consistent with this correlative evidence, which predicts that an intervention that extends lifespan would be associated with decreased rates of proton leak.

5.7.2 PROTON LEAK AND THYROID HORMONES

Thyroid hormone studies provide further support for the idea that CR results in decreased leak and ROS production. It is well known that thyroid hormones affect oxidative phosphorylation by decreasing its coupling efficiency (Harper et al., 1993; Harper and Brand, 1993; Harper and Brand, 1994; Maley and Lardy, 1955). It has been reported that hepatocytes isolated from hypothyroid rats had lower rates of oxygen consumption due to a 50% reduction in proton leak (Harper and Brand, 1994). Conversely, hepatocytes from hyperthyroid rats consumed more oxygen due to a 50% increase in proton leak (Harper and Brand, 1993; Harper and Brand, 1994; Harper and Brand, 1995). Thus, if proton leak increases with age and thyroid hormones then it would be expected that lifespan would increase with hypothyroidism. In fact, Ooka and Shinkai (1986) demonstrated this idea by making rats hyperthyroid by adding exogenous T_4 to their drinking water. The hyperthyroid and hypothyroid rats had shorter and longer lifespans, respectively, compared to their respective controls animals (Ooka and Shinkai, 1986). As mentioned in section 1.4.5 circulating thyroid hormone levels are known to decrease with CR in rats (Herlihy *et al.*, 1990), monkeys (Roth *et al.*, 2002) and humans (Heilbronn *et al.*, 2006). Similarly mice on a methionine-deficient diet also had lower levels of thyroid hormones and increased lifespan compared to controls (Miller *et al.*, 2005). Interestingly, long-lived mouse models such as

the Snell and Ames mice or growth hormone receptor/binding protein knockout mouse have low levels of circulating thyroid hormones (Hauck and Bartke, 2001; Tatar *et al.*, 2003).

ROS and RNS production is also affected by thyroid levels, as discussed by Venditti and Di Meo (2006). Production is increased with hyperthyroidism and decreased with hypothyroidism (Silvestri et al., 2005; Venditti et al., 2006; Venditti et al., 2003). Furthermore, thyroid hormones alter membrane fatty acid composition, which has also been suggested to regulate proton leak. Linoleic acid composition, which is negatively correlated with proton leak, is increased with hypothyroidism and decreased with hyperthyroidism (Saha et al., 1998). Docosahexaenoic acid, which is positively correlated with proton leak, is increased by hyperthyroidism and decreased by methimazole-induced hypothyroidism (Saha *et al.*, 1998). Thus, thyroid hormones may play a role in the regulation of CR-induced changes in leak and these findings overall support the idea that CR results in decreased in maximum leak-dependent respiration, ROS production, and increased longevity.

5.7.3 MITOCHONDRIAL PROTON LEAK AND MEMBRANE COMPOSITION

As described to some extent in the previous section, mitochondrial inner membrane lipid composition can effect mitochondrial proton leak rates. Many studies have provided correlative evidence between proton leak and mitochondrial inner membrane phopholipid/acyl chain composition. Again, proton leak has been positively correlated with docosahexaenoic acid (C22:6n3) and negatively correlated with linoleic acid (C18:2n6) (Brand et al., 1994; Brookes et al., 1998; Porter et al., 1996). Moreover, as mentioned in Section 1.5.3, aging is associated with changes in fatty acid composition of the inner

membrane. Specifically, linoleic acid content decreases and docosahexaenoic acid increases with age. In fact, the 'Membrane Pacemaker' theory of aging proposes that longevity is determined by membrane fatty acid composition (Hulbert, 2003). This theory is supported by the fact that maximum lifespan is inversely correlated with the degree of membrane fatty acid desaturation and is associated with a higher ratio of membrane n-3 to n-6 PUFA (Hulbert, 2003; Pamplona et al., 2002) This theory also suggests that aging is associated with increased peroxidation of long-chain fatty acids (Pamplona *et al.*, 2002; Yu, 2005).

Long-term CR leads to increased mitochondrial linoleic acid content and decrease docosahexaenoic acid content (Laganiere and Yu, 1993). Thus, CR may be expected to decrease maximum leak-dependent respiration. Ramsey *et al.* (2005) investigated the role of fatty acid regulation of leak and ROS. In this study rats were fed purified diets with either corn oil (high C18:2n-6) or fish oil (high C22:6n-3) as the fat source. In liver, no differences were observed in proton leak between the different diets but mitochondrial hydrogen peroxide production was lower in the fish oil compared to the corn oil diet. However, caution must be applied when interpreting the results of this study as the fatty acid manipulations did not mimic the fatty acid changes that have been described in long-term studies of CR as the increase in linoleic acid content were lower than those in other reports. Furthermore, two studies have demonstrated that dietary lipid source can alter membrane oxidative damage (Bhattacharya *et al.*, 2003; Ochoa *et al.*, 2003). For example, lifelong feeding of sunflower oil (n-6 PUFA) had a greater effect on lipid peroxidation in post-mitotic tissue (heart and skeletal muscle) compared to mitotic tissue. Conversely, less peroxidation was observed in both tissues with lifelong feeding of virgin olive oil (monounsaturated fatty acids) compared to sunflower oil (Ochoa *et al.*, 2003). Thus, further

studies are needed with an appropriate diet composition to assess directly the effect of fat source on proton leak rates.

5.7.4 WHY WOULD MITOCHONDRIA RESPOND DIFFERENTLY TO CR OF INCREASING DURATION?

As discussed above, our overall findings; cross-species comparisons; comparisons of altered thyroid status; and comparisons of hepatocytes from young versus old rats support the possibility that maximum proton leak-dependent respiration and ROS production are related. The relationship between the CR- induced changes in skeletal muscle proton leak and ROS production may be through distinct but not mutually exclusive mechanisms (i.e., short-term mechanisms may still occur with long-term CR but may not be as prominent).

A possible mechanism short-term CR on ROS may involve an improvement in the efficiency of energy transduction by conditioning the mitochondria to rapidly mitigate ROS production by increasing proton leak. Such a scenario could result in a decreased PMF, and limit the amount of time that the components of the ETC remain in reduced states. This would allow the mitochondria to switch rapidly, and safely, from states of low and high ATP turnover. While safe (i.e., low ROS production), this may be energetically costly. It seems counter-intuitive that skeletal muscle of a CR animal would shift energy resources toward a reduction in ROS generation. However this may be a quick mechanism for short-term CR as energy can be drawn from fat depots. This would not occur with long-term CR and is not supported by studies showing that animals with high rates of proton leak produce more ROS. Given the associated energetic costs, it is possible that this sort of mechanism only occurs with short-term CR.

Although we did not measure ATP content directly, results from our metabolic control analyses suggest that ATP turnover becomes a stronger controlling factor following CR when compared to control animals. Specifically, top down metabolic control analyses indicated that short-term CR resulted in increased control by the phosphorylation reactions (under State 3 conditions). Also, control by proton leak over substrate oxidation and phosphorylation reactions tended to be lower in the CR mitochondria at all time points. In other words, CR decreased control by proton leak and increased control by phosphorylation reactions over components of the oxidative phosphorylation system. Our results are therefore consistent with the idea that, as one might expect, CR causes changes in the distribution of control over ATP production.

Another possible mechanism may explain our findings with short-term CR and may involve a coordinated decrease in oxygen consumption and increase in proton permeability. The increase in leak conductance could explain the decreased ROS but it does not explain the reduction in maximum proton leak dependent respiration (which normally does not accompany decreased PMF). It is possible that the decrease in oxygen consumption we observed is due to an inhibition of respiration by other factors such as increased mtNOS. Mitochondrial NO has been shown to play a role in the regulation of mitochondrial respiration and energy metabolism. NO inhibits oxygen consumption by reversibly inhibiting Complex IV (cytochrome oxidase). Thus the decrease in maximum leak dependent respiration could be due to increased mtNOS activity, which would produce NO to inhibit respiration and ETC flux. The effects of decreased flux through the ETC could be counteracted by decreased PMF that would minimize the formation of ROS.

The mechanism of short-term CR may also involve up-regulation of the expression of UCP3. As described above, UCP3 has been proposed to facilitate high rates of fatty acid oxidation by exporting fatty acid anions out of the mitochondrial matrix (Himms-Hagen and Harper, 2001). Hypothetically, the export of a fatty acid anion from the matrix to the cytosol would reduce the PMF as would a UCP3-mediated influx of protons. Thus, increased UCP3 could alter ROS production in a process that is distinct from uncoupling (i.e., increased oxygen consumption and leak conductance). Indeed, MacLellan *et al.*, (2005) recently demonstrated that the overexpression of physiological levels of UCP3 in L6 myotubes resulted in decreased ROS production in the absence of any evidence of uncoupling. While the addition of dinitrophenol (a chemical uncoupler) to untransfected cells also decreased ROS production, it increased oxygen consumption and decreased PMF, characteristic of true uncoupling. These results suggest that UCP3 may be involved in the protection from ROS via a *UCP3*-dependent but uncoupling-independent mechanism (MacLellan et al., 2005). Although we did not measure UCP3 expression with short-term CR we did measure circulating NEFA levels, which were increased and would likely be associated with increased UCP3 expression in muscle. Moreover, many other studies of short-term CR have clearly demonstrated increased UCP3 expression in muscle of rats, mice, and humans (Lee et al., 2002; Lee et al., 1999). We also measured UCP3 protein content with medium and long-term restriction and documented increases in UCP3 content. Recall that with medium- and long- term CR, we observed an increase or no change in PMF. Our results suggest that UCP3 may play little or no role in long-term adaptations to CR. Our assessments of the overall kinetics of proton leak reactions in muscle mitochondria of wild-type and *Ucp*3-KO mice also do not support a role for exclusively UCP3-dependent

decrease in PMF in the short-term bioenergetic adaptation to CR. No differences were observed in the kinetics of proton leak in the wild-type CR mice whereas there was increased proton conductance in the *Ucp*3-KO CR mice compared to their respective controls. The decreased PMF in the *Ucp*3-KO CR mice was thought to be a result of changes in ANT content - as the *Ucp*3-KO CR had a larger response to CAT. While our western blot results do not support this idea, it is possible that there are other regulatory control factors that may be governing ANT activity in situ. Our study is the first to examine the effect of CR on ANT-mediated proton leak.

Long-term CR may inhibit ROS production through mechanisms that are distinct from those that are mechanistically related to decreases in PMF described above. Thus, it remains possible that alterations in ROS production are not the primary function of proton leak. Instead ROS production may be controlled through other, as yet unknown, mechanisms that regulate ETC flux under resting conditions (e.g., ROS production can be mitigated by reductions in the content of complex I and/or III. Overall, it thus seems very unlikely that such CR-induced changes occur without significant mitochondrial adaptations. Adaptations could include decreases in mitochondrial inner membrane surface area or ETC complexes. Mitochondrial inner membrane surface area has been positively associated with proton leak. For example, surface area is decreased in mammals with increasing body size (Else and Hulbert, 1985b), and increased in mammals compared to reptiles (Else and Hulbert, 1985a). Also, mitochondrial inner membrane surface area has also been shown to be increased in hyperthyroid compared to hypothyroid rats (Jakovcic et al., 1978). A decrease in surface area would provide less area and less ETC proteins for ROS production;

and could explain the decreased ROS with long-term CR. To date, the effect of CR on mitochondrial surface area has not been investigated.

The effect of CR on substrate oxidation pathways has been assessed in liver. Several studies have shown that 40% CR reduced the activity of liver glycolytic enzymes (Hagopian et al., 2003) Our collaborators have also demonstrated that long-term CR differentially regulates enzymes of the Krebs cycle. Specifically, CR decreased activities of citrate synthase, aconitase, and isocitrate dehydrogenase. The remaining enzymes in the Krebs cycle had increased activity with long-term CR (Hagopian et al., 2003). These changes are consistent with an increased capacity for gluconeogenesis and decreased capacity for substrate oxidation. Our top-down metabolic control analysis of the substrate oxidation reactions indicated that flux through the ETC was lower in the long-term CR compared to the control rats (i.e., the oxygen consumption used to support substrate oxidation at a given membrane potential was lower), whereas, no differences were observed in the kinetics of the phosphorylation reactions. Similarly, the flux control coefficients for the substrate oxidation reactions indicated that control exerted by the substrate oxidation reactions over proton leak was lower. These results suggest CR may cause changes in the substrate oxidation pathways.

Several groups have examined the effect of CR on enzymes involved in substrate oxidation pathways in skeletal muscle. One study in skeletal muscle has reported that activities of mitochondrial ETC complexes I, III and IV were decreased by 33-64% in mice consuming a long-term 40% CR diet compared to *ad libitum* fed mice (Desai et al., 1996), indicating that CR could limit the capacity for substrate oxidation pathways (e.g., glycolysis, Krebs and ETC). Similarly, citrate synthase and complex IV activities were lower in the

plantaris and gastrocnemius muscle of young adult male CR rats compared to age-matched controls (Baker et al., 2006). The down-regulation of the ETC could result in lowered ROS production by decreasing ETC sites available for ROS production (e.g., at complexes I and III). This type of mechanism is consistent with our observed increases in protonmotive force following medium and long-term CR. Moreover, it is also consistent with the findings of decreased ETC content in hypothyroidism and increased ETC content with hyperthyroidism (Venditti et al., 2003); ROS production is decreased in hypothyroid states and increased in hyperthyroid states (Ramsey et al., 2000).

Changes in processes related to mitochondrial biogenesis are also possible. Recent studies in isolated hepatocytes, HeLa cells and FaO cells have demonstrated that long-term CR may result in increased in mitochondrial biogenesis via increased expression of PGC-1α and PPARs. This study also reported reduced oxygen consumption, PMF and ROS production in the cells treated with serum isolated from CR rats. Interestingly, ATP content of the CR cells did not change, suggesting that CR resulted in more efficient mitochondria or mitochondria or cells with lower ATP demands (Lopez-Lluch et al., 2006).

Recently Civitarese et al., (2007) have demonstrated in human skeletal muscle cells that 6 mo 25% CR or 12.5% CR in combination with exercise increased the expression of genes encoding proteins involved in mitochondrial function such as PPARGC1A, TFAM, eNOS, SIRT1 and PARL in parallel with increased mitochondrial DNA content and reduced DNA damage. However, the activity of key mitochondrial enzymes of the TCA cycle (citrate synthase), beta-oxidation (beta-hydroxyacyl-CoA dehydrogenase), and electron transport chain (cytochrome C oxidase II) were unchanged per mitochondrial mass (Civitarese et al., 2007). The increased mitochondrial biogenesis observed in these studies

may be used as an argument against the idea of decreased ETC content however the findings that activity of reduced activity of mitochondrial enzymes per mitochondrial mass is very intriguing and supportive of our ideas. Further studies are required to specifically examine the effects of CR of increasing duration on skeletal muscle ETC content and activity of the ETC complexes. Results from this dissertation suggest that mechanisms underlying the action of CR are extremely complex. Further study is merited to better understand the effect of CR on mitochondrial bioenergetics and biogenesis.

5.8 FUTURE WORK

Further research is required to better understand the role of mitochondrial energetics in oxidative stress, aging and calorie restriction. The findings herein demonstrate that the effects of CR on proton leak are dependent in part on the duration of CR. These time dependent differences are important to keep in mind for further mechanistic studies addressing the poorly understood relationships between proton leak, H_2O_2 production and CR. Specifically in skeletal muscle, attention should be directed toward the effect of CR of various durations on the content and activity of the components of the ETC. Additional research examining the effect of CR on skeletal muscle mitochondrial biogenesis (i.e., mtNOS, PGC-1α and SIRT1 expression) with long-term CR is required, as most studies to date have been conducted with short-term CR.

The results of this dissertation and work from the laboratory of our collaborators have also demonstrated that there are tissue-specific differences in the response to CR. Thus, further comparisons of the effect of CR on other mitotic (e.g., kidney) and post-mitotic (e.g., heart, brain) tissues are also required. Post-mitotic tissues appear to be more

susceptible to the cumulative effects of oxidative stress, and be subject to considerable oxidative damage with age. Whereas, mitotic tissues such as liver appear to be less affected by aging take longer to demonstrate any CR-related changes (Hagopian et al., 2005). Several studies have demonstrated that age-related oxidative damage is lower in liver compared to skeletal muscle and brain (Ku and Sohal, 1993). Similarly, CR has been shown to decrease H_2O_2 production and oxidative damage in heart and non-synaptic brain mitochondria (Gredilla et al., 2002; Barja, 1999). The effect of CR on mitochondrial proton leak has never been investigated in kidney, heart and brain. Thus, further examination of various other tissues is merited to determine the importance of proton leak in the net mechanism of CR. For accurate comparisons between post-mitotic and mitotic tissues, similar dietary interventions (i.e., 40% CR) and experimental designs (e.g., metabolic control analysis) as those used in previously published work should be used.

5.9 CONCLUSIONS

In summary, this dissertation provides new information regarding the effects of CR on skeletal muscle energetics and ROS production. We have shown unequivocally that there are dramatic changes in skeletal muscle ROS production with CR. Specifically, we are the first group to report such rapid and sustained decreases in ROS with short- medium and long-term CR. We are also the first to describe in detail the response of proton leak in skeletal muscle to CR of increasing duration. The intriguing differences in the response of proton leak to CR indicate that the mechanisms of mitochondrial adaptations to CR are different between short- medium- and long- term CR. We also reinforced the view that

UCP3 does not cause basal proton leak, as we observed decreased maximal proton leak-dependent respiration and decreased proton conductance despite increased UCP3 expression. Our results in *Ucp3*-KO mice subjected to CR are also consistent with the idea that UCP3 is not involved in CR-induced increases in proton conductance. Our findings in rats and in mice suggest that alterations in proton leak kinetics with short-term CR occur via a UCP3-independent mechanism that, to some extent, involves ANT. We also demonstrated that CR-related changes in proton leak are different between skeletal muscle and liver mitochondria. In the liver, the effects of CR on proton leak are detectable only with long-term CR, and not with short-term CR. Together, this work enhances our understanding of the effect of CR on whole-body energetics and mitochondrial energetics. The conclusions that can be made from this work include: (1) the duration of CR is an important variable; that is, CR has time-dependent bioenergetic effects, and therefore the underlying mechanisms may differ with CR duration. (2) There are important tissue-specific bioenergetic effects for a given duration of CR. In summary, these findings clearly demonstrate a complex and time-dependent response of mitochondrial energetics to CR that includes a hypometabolism and alterations in mitochondrial function. These findings provide further insights into the metabolic mechanisms underlying the phenomenon of CR and may lead to the development of interventions aimed at improving human health during aging.

FIGURE 29: A PROPOSED MECHANISM FOR THE EFFECT OF CR OF VARIABLE DURATIONS ON WHOLE BODY AND SKELETAL MUSCLE METABOLISM.

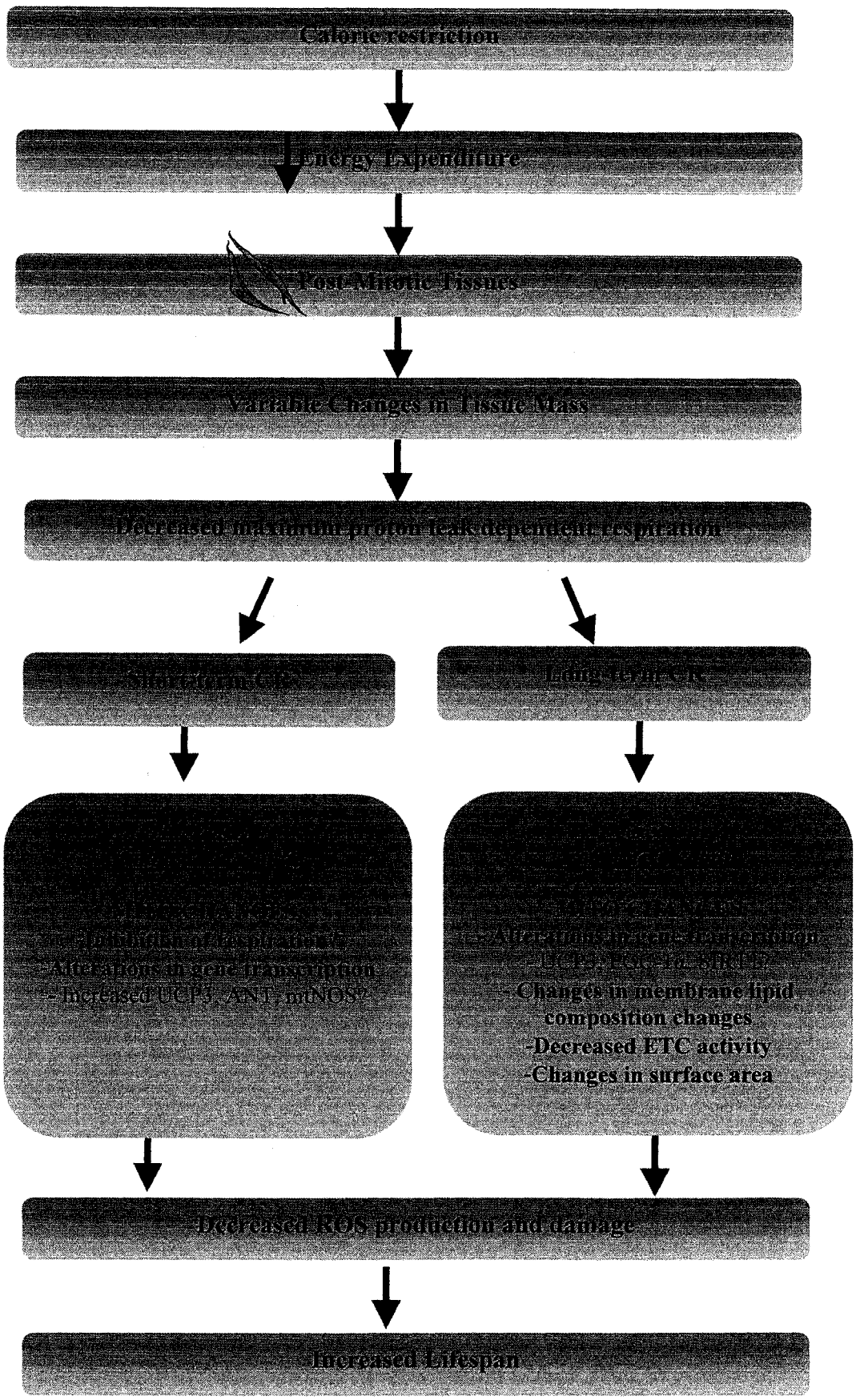

CHAPTER 6
REFERENCES

Acin, A., Rodriguez, M., Rique, H., Canet, E., Boutin, J. A., and Galizzi, J. P. (1999). Cloning and characterization of the 5' flanking region of the human uncoupling protein 3 (UCP3) gene. Biochem Biophys Res Commun *258*, 278-283.

Aguilaniu, H., Gustafsson, L., Rigoulet, M., and Nystrom, T. (2003). Asymmetric inheritance of oxidatively damaged proteins during cytokinesis. Science *299*, 1751-1753.

Andreyev, A., Bondareva, T. O., Dedukhova, V. I., Mokhova, E. N., Skulachev, V. P., Tsofina, L. M., Volkov, N. I., and Vygodina, T. V. (1989). The ATP/ADP-antiporter is involved in the uncoupling effect of fatty acids on mitochondria. Eur J Biochem *182*, 585-592.

Andreyev, A., Bondareva, T. O., Dedukhova, V. I., Mokhova, E. N., Skulachev, V. P., and Volkov, N. I. (1988). Carboxyatractylate inhibits the uncoupling effect of free fatty acids. FEBS Lett *226*, 265-269.

Aquila, H., Link, T. A., and Klingenberg, M. (1985). The uncoupling protein from brown fat mitochondria is related to the mitochondrial ADP/ATP carrier. Analysis of sequence homologies and of folding of the protein in the membrane. Embo J *4*, 2369-2376.

Argyropoulos, G., Brown, A. M., Willi, S. M., Zhu, J., He, Y., Reitman, M., Gevao, S. M., Spruill, I., and Garvey, W. T. (1998). Effects of mutations in the human uncoupling protein 3 gene on the respiratory quotient and fat oxidation in severe obesity and type 2 diabetes. J Clin Invest *102*, 1345-1351.

Armario, A., Montero, J. L., and Jolin, T. (1987). Chronic food restriction and the circadian rhythms of pituitary-adrenal hormones, growth hormone and thyroid-stimulating hormone. Ann Nutr Metab *31*, 81-87.

Arsenijevic, D., Onuma, H., Pecqueur, C., Raimbault, S., Manning, B. S., Miroux, B., Couplan, E., Alves-Guerra, M. C., Goubern, M., Surwit, R., *et al.* (2000). Disruption of the uncoupling protein-2 gene in mice reveals a role in immunity and reactive oxygen species production. Nat Genet *26*, 435-439.

Aspnes, L. E., Lee, C. M., Weindruch, R., Chung, S. S., Roecker, E. B., and Aiken, J. M. (1997). Caloric restriction reduces fiber loss and mitochondrial abnormalities in aged rat muscle. Faseb J *11*, 573-581.

Austad, S. N. (1989). Life extension by dietary restriction in the bowl and doily spider, Frontinella pyramitela. Exp Gerontol *24*, 83-92.

Balaban, R. S., Nemoto, S., and Finkel, T. (2005). Mitochondria, oxidants, and aging. Cell *120*, 483-495.

Barbe, P., Larrouy, D., Boulanger, C., Chevillotte, E., Viguerie, N., Thalamas, C., Oliva Trastoy, M., Roques, M., Vidal, H., and Langin, D. (2001). Triiodothyronine-mediated up-regulation of UCP2 and UCP3 mRNA expression in human skeletal muscle without coordinated induction of mitochondrial respiratory chain genes. Faseb J *15*, 13-15.

Barja, G. (1999). Mitochondrial oxygen radical generation and leak: sites of production in states 4 and 3, organ specificity, and relation to aging and longevity. J Bioenerg Biomembr *31*, 347-366.

Barja, G., and Herrero, A. (2000). Oxidative damage to mitochondrial DNA is inversely related to maximum life span in the heart and brain of mammals. Faseb J *14*, 312-318.

Barrows, C. H., Jr., and Kokkonen, G. (1975). Protein synthesis, development, growth and life span. Growth *39*, 525-533.

Bartke, A., Brown-Borg, H., Mattison, J., Kinney, B., Hauck, S., and Wright, C. (2001). Prolonged longevity of hypopituitary dwarf mice. Exp Gerontol *36*, 21-28.

Bartke, A., Chandrashekar, V., Dominici, F., Turyn, D., Kinney, B., Steger, R., and Kopchick, J. J. (2003). Insulin-like growth factor 1 (IGF-1) and aging: controversies and new insights. Biogerontology *4*, 1-8.

Bartlett, K., and Eaton, S. (2004). Mitochondrial beta-oxidation. Eur J Biochem *271*, 462-469.

Barzilai, N., and Gupta, G. (1999). Revisiting the role of fat mass in the life extension induced by caloric restriction. J Gerontol A Biol Sci Med Sci *54*, B89-96; discussion B97-88.

Beckman, K. B., and Ames, B. N. (1998). The free radical theory of aging matures. Physiol Rev *78*, 547-581.

Bertrand, H. A., Lynd, F. T., Masoro, E. J., and Yu, B. P. (1980). Changes in adipose mass and cellularity through the adult life of rats fed ad libitum or a life-prolonging restricted diet. J Gerontol *35*, 827-835.

Bezaire, V., Hofmann, W., Kramer, J. K., Kozak, L. P., and Harper, M. E. (2001). Effects of fasting on muscle mitochondrial energetics and fatty acid metabolism in Ucp3(-/-) and wild-type mice. Am J Physiol Endocrinol Metab *281*, E975-982.

Bezaire, V., Spriet, L. L., Campbell, S., Sabet, N., Gerrits, M., Bonen, A., and Harper, M. E. (2005). Constitutive UCP3 overexpression at physiological levels increases mouse skeletal muscle capacity for fatty acid transport and oxidation. Faseb J *19*, 977-979.

Blanc, S., Schoeller, D., Kemnitz, J., Weindruch, R., Colman, R., Newton, W., Wink, K., Baum, S., and Ramsey, J. (2003). Energy expenditure of rhesus monkeys subjected to 11 years of dietary restriction. J Clin Endocrinol Metab *88*, 16-23.

Blander, G., and Guarente, L. (2004). The Sir2 family of protein deacetylases. Annu Rev Biochem *73*, 417-435.

Bluher, M., Kahn, B. B., and Kahn, C. R. (2003). Extended longevity in mice lacking the insulin receptor in adipose tissue. Science *299*, 572-574.

Boffoli, D., Scacco, S. C., Vergari, R., Solarino, G., Santacroce, G., and Papa, S. (1994). Decline with age of the respiratory chain activity in human skeletal muscle. Biochim Biophys Acta *1226*, 73-82.

Bohr, V. A. (2002). Repair of oxidative DNA damage in nuclear and mitochondrial DNA, and some changes with aging in mammalian cells. Free Radic Biol Med *32*, 804-812.

Bordone, L., and Guarente, L. (2005). Calorie restriction, SIRT1 and metabolism: understanding longevity. Nat Rev Mol Cell Biol *6*, 298-305.

Borecky, J., Maia, I. G., and Arruda, P. (2001). Mitochondrial uncoupling proteins in mammals and plants. Biosci Rep *21*, 201-212.

Boss, O., Bobbioni-Harsch, E., Assimacopoulos-Jeannet, F., Muzzin, P., Munger, R., Giacobino, J. P., and Golay, A. (1998a). Uncoupling protein-3 expression in skeletal muscle and free fatty acids in obesity. Lancet *351*, 1933.

Boss, O., Hagen, T., and Lowell, B. B. (2000). Uncoupling proteins 2 and 3: potential regulators of mitochondrial energy metabolism. Diabetes *49*, 143-156.

Boss, O., Samec, S., Kuhne, F., Bijlenga, P., Assimacopoulos-Jeannet, F., Seydoux, J., Giacobino, J. P., and Muzzin, P. (1998b). Uncoupling protein-3 expression in rodent skeletal muscle is modulated by food intake but not by changes in environmental temperature. J Biol Chem *273*, 5-8.

Boss, O., Samec, S., Paoloni-Giacobino, A., Rossier, C., Dulloo, A., Seydoux, J., Muzzin, P., and Giacobino, J. P. (1997). Uncoupling protein-3: a new member of the mitochondrial carrier family with tissue-specific expression. FEBS Lett *408*, 39-42.

Bouillaud, F., Ricquier, D., Thibault, J., and Weissenbach, J. (1985). Molecular approach to thermogenesis in brown adipose tissue: cDNA cloning of the mitochondrial uncoupling protein. Proc Natl Acad Sci U S A *82*, 445-448.

Bouillaud, F., Weissenbach, J., and Ricquier, D. (1986). Complete cDNA-derived amino acid sequence of rat brown fat uncoupling protein. J Biol Chem *261*, 1487-1490.

Boveris, A., and Chance, B. (1973). The mitochondrial generation of hydrogen peroxide. General properties and effect of hyperbaric oxygen. Biochem J *134*, 707-716.

Boveris, A., Oshino, N., and Chance, B. (1972). The cellular production of hydrogen peroxide. Biochem J *128*, 617-630.

Brand, M. D. (2000). Uncoupling to survive? The role of mitochondrial inefficiency in ageing. Exp Gerontol *35*, 811-820.

Brand, M. D. (2005). The efficiency and plasticity of mitochondrial energy transduction. Biochem Soc Trans *33*, 897-904.

Brand, M. D., Affourtit, C., Esteves, T. C., Green, K., Lambert, A. J., Miwa, S., Pakay, J. L., and Parker, N. (2004a). Mitochondrial superoxide: production, biological effects, and activation of uncoupling proteins. Free Radic Biol Med *37*, 755-767.

Brand, M. D., Buckingham, J. A., Esteves, T. C., Green, K., Lambert, A. J., Miwa, S., Murphy, M. P., Pakay, J. L., Talbot, D. A., and Echtay, K. S. (2004b). Mitochondrial superoxide and aging: uncoupling-protein activity and superoxide production. Biochem Soc Symp, 203-213.

Brand, M. D., Couture, P., and Hulbert, A. J. (1994). Liposomes from mammalian liver mitochondria are more polyunsaturated and leakier to protons than those from reptiles. Comp Biochem Physiol Biochem Mol Biol *108*, 181-188.

Brand, M. D., Pakay, J. L., Ocloo, A., Kokoszka, J., Wallace, D. C., Brookes, P. S., and Cornwall, E. J. (2005). The basal proton conductance of mitochondria depends on adenine nucleotide translocase content. Biochem J *392*, 353-362.

Brand, M. D., Pamplona, R., Portero-Otin, M., Requena, J. R., Roebuck, S. J., Buckingham, J. A., Clapham, J. C., and Cadenas, S. (2002). Oxidative damage and phospholipid fatty acyl composition in skeletal muscle mitochondria from mice underexpressing or overexpressing uncoupling protein 3. Biochem J *368*, 597-603.

Brdiczka, D., Bucheler, K., Kottke, M., Adams, V., and Nalam, V. K. (1990). Characterization and metabolic function of mitochondrial contact sites. Biochim Biophys Acta *1018*, 234-238.

Brookes, P. S., Hulbert, A. J., and Brand, M. D. (1997a). The proton permeability of liposomes made from mitochondrial inner membrane phospholipids: no effect of fatty acid composition. Biochim Biophys Acta *1330*, 157-164.

Brookes, P. S., Land, J. M., Clark, J. B., and Heales, S. J. (1998). Peroxynitrite causes proton leak in brain mitochondria. Biochem Soc Trans *26*, S332.

Brookes, P. S., Rolfe, D. F., and Brand, M. D. (1997b). The proton permeability of liposomes made from mitochondrial inner membrane phospholipids: comparison with isolated mitochondria. J Membr Biol *155*, 167-174.

Brown-Borg, H. M., Borg, K. E., Meliska, C. J., and Bartke, A. (1996). Dwarf mice and the ageing process. Nature *384*, 33.

Brown, G. C. (1992). The leaks and slips of bioenergetic membranes. Faseb J *6*, 2961-2965.

Brown, G. C., and Brand, M. D. (1986). Changes in permeability to protons and other cations at high proton motive force in rat liver mitochondria. Biochem J *234*, 75-81.

Brunet, A., Sweeney, L. B., Sturgill, J. F., Chua, K. F., Greer, P. L., Lin, Y., Tran, H., Ross, S. E., Mostoslavsky, R., Cohen, H. Y., *et al.* (2004). Stress-dependent regulation of FOXO transcription factors by the SIRT1 deacetylase. Science *303*, 2011-2015.

Bua, E. A., McKiernan, S. H., Wanagat, J., McKenzie, D., and Aiken, J. M. (2002). Mitochondrial abnormalities are more frequent in muscles undergoing sarcopenia. J Appl Physiol *92*, 2617-2624.

Buttgereit, F., Brand, M. D., and Muller, M. (1992). ConA induced changes in energy metabolism of rat thymocytes. Biosci Rep *12*, 381-386.

Buttgereit, F., Muller, M., and Rapoport, S. M. (1991). Quantification of ATP-producing and consuming processes in quiescent pig spleen lymphocytes. Biochem Int *24*, 59-67.

Cabelof, D. C., Yanamadala, S., Raffoul, J. J., Guo, Z., Soofi, A., and Heydari, A. R. (2003). Caloric restriction promotes genomic stability by induction of base excision repair and reversal of its age-related decline. DNA Repair (Amst) *2*, 295-307.

Cadenas, S., Buckingham, J. A., Samec, S., Seydoux, J., Din, N., Dulloo, A. G., and Brand, M. D. (1999). UCP2 and UCP3 rise in starved rat skeletal muscle but mitochondrial proton conductance is unchanged. FEBS Lett *462*, 257-260.

Cadenas, S., Buckingham, J. A., St-Pierre, J., Dickinson, K., Jones, R. B., and Brand, M. D. (2000). AMP decreases the efficiency of skeletal-muscle mitochondria. Biochem J *351 Pt 2*, 307-311.

Cadenas, S., Echtay, K. S., Harper, J. A., Jekabsons, M. B., Buckingham, J. A., Grau, E., Abuin, A., Chapman, H., Clapham, J. C., and Brand, M. D. (2002). The basal proton conductance of skeletal muscle mitochondria from transgenic mice overexpressing or lacking uncoupling protein-3. J Biol Chem *277*, 2773-2778.

Cavallini, G., Donati, A., Gori, Z., Pollera, M., and Bergamini, E. (2001). The protection of rat liver autophagic proteolysis from the age-related decline co-varies with the duration of anti-ageing food restriction. Exp Gerontol *36*, 497-506.

Chacon, F., Cano, P., Jimenez, V., Cardinali, D. P., Marcos, A., and Esquifino, A. I. (2004). 24-hour changes in circulating prolactin, follicle-stimulating hormone, luteinizing hormone, and testosterone in young male rats subjected to calorie restriction. Chronobiol Int *21*, 393-404.

Chance, B., Sies, H., and Boveris, A. (1979). Hydroperoxide metabolism in mammalian organs. Physiol Rev *59*, 527-605.

Chang, T. S., Cho, C. S., Park, S., Yu, S., Kang, S. W., and Rhee, S. G. (2004). Peroxiredoxin III, a mitochondrion-specific peroxidase, regulates apoptotic signaling by mitochondria. J Biol Chem *279*, 41975-41984.

Chen, J. J., and Yu, B. P. (1994). Alterations in mitochondrial membrane fluidity by lipid peroxidation products. Free Radic Biol Med *17*, 411-418.

Choe, M., Jackson, C., and Yu, B. P. (1995). Lipid peroxidation contributes to age-related membrane rigidity. Free Radic Biol Med *18*, 977-984.

Choi, J. H., and Yu, B. P. (1995). Brain synaptosomal aging: free radicals and membrane fluidity. Free Radic Biol Med *18*, 133-139.

Civitarese, A. E., Carling, S., Heilbronn, L. K., Hulver, M. H., Ukropcova, B., Deutsch, W. A., Smith, S. R., and Ravussin, E. (2007). Calorie Restriction Increases Muscle Mitochondrial Biogenesis in Healthy Humans. PLoS Med *4*, e76.

Clapham, J. C., Arch, J. R., Chapman, H., Haynes, A., Lister, C., Moore, G. B., Piercy, V., Carter, S. A., Lehner, I., Smith, S. A., *et al.* (2000). Mice overexpressing human uncoupling protein-3 in skeletal muscle are hyperphagic and lean. Nature *406*, 415-418.

Clapham, J. C., Coulthard, V. H., and Moore, G. B. (2001). Concordant mRNA expression of UCP-3, but not UCP-2, with mitochondrial thioesterase-1 in brown adipose tissue and skeletal muscle in db/db diabetic mice. Biochem Biophys Res Commun *287*, 1058-1062.

Cohen, H. Y., Miller, C., Bitterman, K. J., Wall, N. R., Hekking, B., Kessler, B., Howitz, K. T., Gorospe, M., de Cabo, R., and Sinclair, D. A. (2004). Calorie restriction promotes mammalian cell survival by inducing the SIRT1 deacetylase. Science *305*, 390-392.

Comfort, A. (1963). Effect Of Delayed And Resumed Growth On The Longevity Of A Fish (Lebistes Reticulatus, Peters) In Captivity. Gerontologia *49*, 150-155.

Conley, K. E., Jubrias, S. A., and Esselman, P. C. (2000). Oxidative capacity and ageing in human muscle. J Physiol *526 Pt 1*, 203-210.

Cortright, R. N., Zheng, D., Jones, J. P., Fluckey, J. D., DiCarlo, S. E., Grujic, D., Lowell, B. B., and Dohm, G. L. (1999). Regulation of skeletal muscle UCP-2 and UCP-3 gene expression by exercise and denervation. Am J Physiol *276*, E217-221.

Costford, S. R., Chaudhry, S. N., Salkhordeh, M., and Harper, M. E. (2006). Effects of the presence, absence, and overexpression of uncoupling protein-3 on adiposity and fuel metabolism in congenic mice. Am J Physiol Endocrinol Metab *290*, E1304-1312.

Davis, T. R., and Mayer, J. (1955). Demonstration and quantitative determination of the contributions of physical and chemical thermogenesis on acute exposure to cold. Am J Physiol *181*, 675-678.

de la Asuncion, J. G., Millan, A., Pla, R., Bruseghini, L., Esteras, A., Pallardo, F. V., Sastre, J., and Vina, J. (1996). Mitochondrial glutathione oxidation correlates with age-associated oxidative damage to mitochondrial DNA. Faseb J *10*, 333-338.

DeBry, R. W., and Seldin, M. F. (1996). Human/mouse homology relationships. Genomics *33*, 337-351.

DeLany, J. P., Hansen, B. C., Bodkin, N. L., Hannah, J., and Bray, G. A. (1999). Long-term calorie restriction reduces energy expenditure in aging monkeys. J Gerontol A Biol Sci Med Sci *54*, B5-11; discussion B12-13.

Desai, V. G., Weindruch, R., Hart, R. W., and Feuers, R. J. (1996). Influences of age and dietary restriction on gastrocnemius electron transport system activities in mice. Arch Biochem Biophys *333*, 145-151.

Donati, A., Cavallini, G., Paradiso, C., Vittorini, S., Pollera, M., Gori, Z., and Bergamini, E. (2001). Age-related changes in the autophagic proteolysis of rat isolated liver cells: effects of antiaging dietary restrictions. J Gerontol A Biol Sci Med Sci *56*, B375-383.

Drew, B., Phaneuf, S., Dirks, A., Selman, C., Gredilla, R., Lezza, A., Barja, G., and Leeuwenburgh, C. (2003). Effects of aging and caloric restriction on mitochondrial energy production in gastrocnemius muscle and heart. Am J Physiol Regul Integr Comp Physiol *284*, R474-480.

Droge, W. (2002). Free radicals in the physiological control of cell function. Physiol Rev *82*, 47-95.

Duffy, P. H., Feuers, R. J., Leakey, J. A., Nakamura, K., Turturro, A., and Hart, R. W. (1989). Effect of chronic caloric restriction on physiological variables related to energy metabolism in the male Fischer 344 rat. Mech Ageing Dev *48*, 117-133.

Dulloo, A. G., and Girardier, L. (1993). 24 hour energy expenditure several months after weight loss in the underfed rat: evidence for a chronic increase in whole-body metabolic efficiency. Int J Obes Relat Metab Disord *17*, 115-123.

Echtay, K. S., Esteves, T. C., Pakay, J. L., Jekabsons, M. B., Lambert, A. J., Portero-Otin, M., Pamplona, R., Vidal-Puig, A. J., Wang, S., Roebuck, S. J., and Brand, M. D. (2003). A signalling role for 4-hydroxy-2-nonenal in regulation of mitochondrial uncoupling. Embo J *22*, 4103-4110.

Echtay, K. S., Roussel, D., St-Pierre, J., Jekabsons, M. B., Cadenas, S., Stuart, J. A., Harper, J. A., Roebuck, S. J., Morrison, A., Pickering, S., *et al.* (2002). Superoxide activates mitochondrial uncoupling proteins. Nature *415*, 96-99.

Enerback, S., Jacobsson, A., Simpson, E. M., Guerra, C., Yamashita, H., Harper, M. E., and Kozak, L. P. (1997). Mice lacking mitochondrial uncoupling protein are cold-sensitive but not obese. Nature *387*, 90-94.

Esteves, T. C., and Brand, M. D. (2005). The reactions catalysed by the mitochondrial uncoupling proteins UCP2 and UCP3. Biochim Biophys Acta *1709*, 35-44.

Fanestil, D. D., and Barrows, C. H., Jr. (1965). Aging in the rotifer. J Gerontol *20*, 462-469.

Finkel, T. (2003). Ageing: a toast to long life. Nature *425*, 132-133.

Finkel, T., and Holbrook, N. J. (2000). Oxidants, oxidative stress and the biology of ageing. Nature *408*, 239-247.

Fleury, C., Neverova, M., Collins, S., Raimbault, S., Champigny, O., Levi-Meyrueis, C., Bouillaud, F., Seldin, M. F., Surwit, R. S., Ricquier, D., and Warden, C. H. (1997). Uncoupling protein-2: a novel gene linked to obesity and hyperinsulinemia. Nat Genet *15*, 269-272.

Flurkey, K., Papaconstantinou, J., and Harrison, D. E. (2002). The Snell dwarf mutation Pit1(dw) can increase life span in mice. Mech Ageing Dev *123*, 121-130.

Fontana, L., Meyer, T. E., Klein, S., and Holloszy, J. O. (2004). Long-term calorie restriction is highly effective in reducing the risk for atherosclerosis in humans. Proc Natl Acad Sci U S A *101*, 6659-6663.

Forsmark-Andree, P., Lee, C. P., Dallner, G., and Ernster, L. (1997). Lipid peroxidation and changes in the ubiquinone content and the respiratory chain enzymes of submitochondrial particles. Free Radic Biol Med *22*, 391-400.

Garthwaite, S. M., Cheng, H., Bryan, J. E., Craig, B. W., and Holloszy, J. O. (1986). Ageing, exercise and food restriction: effects on body composition. Mech Ageing Dev *36*, 187-196.

Genova, M. L., Ventura, B., Giuliano, G., Bovina, C., Formiggini, G., Parenti Castelli, G., and Lenaz, G. (2001). The site of production of superoxide radical in mitochondrial Complex I is not a bound ubisemiquinone but presumably iron-sulfur cluster N2. FEBS Lett *505*, 364-368.

Gerber, L. K., Aronow, B. J., and Matlib, M. A. (2006). Activation of a novel long-chain free fatty acid export system in mitochondria of diabetic rat hearts. Am J Physiol Cell Physiol *291*, C1198-1207.

Gimeno, R. E., Dembski, M., Weng, X., Deng, N., Shyjan, A. W., Gimeno, C. J., Iris, F., Ellis, S. J., Woolf, E. A., and Tartaglia, L. A. (1997). Cloning and characterization of an uncoupling protein homolog: a potential molecular mediator of human thermogenesis. Diabetes *46*, 900-906.

Gong, D. W., He, Y., Karas, M., and Reitman, M. (1997). Uncoupling protein-3 is a mediator of thermogenesis regulated by thyroid hormone, beta3-adrenergic agonists, and leptin. J Biol Chem *272*, 24129-24132.

Gong, D. W., He, Y., and Reitman, M. L. (1999). Genomic organization and regulation by dietary fat of the uncoupling protein 3 and 2 genes. Biochem Biophys Res Commun *256*, 27-32.

Gong, D. W., Monemdjou, S., Gavrilova, O., Leon, L. R., Marcus-Samuels, B., Chou, C. J., Everett, C., Kozak, L. P., Li, C., Deng, C., *et al.* (2000). Lack of obesity and normal response to fasting and thyroid hormone in mice lacking uncoupling protein-3. J Biol Chem *275*, 16251-16257.

Gonzales-Pacheco, D. M., Buss, W. C., Koehler, K. M., Woodside, W. F., and Alpert, S. S. (1993). Energy restriction reduces metabolic rate in adult male Fisher-344 rats. J Nutr *123*, 90-97.

Goodrick, C. L. (1978). Body weight increment and length of life: the effect of genetic constitution and dietary protein. J Gerontol *33*, 184-190.

Goto, S., Takahashi, R., Araki, S., and Nakamoto, H. (2002). Dietary restriction initiated in late adulthood can reverse age-related alterations of protein and protein metabolism. Ann N Y Acad Sci *959*, 50-56.

Hagen, T., Zhang, C. Y., Vianna, C. R., and Lowell, B. B. (2000). Uncoupling proteins 1 and 3 are regulated differently. Biochemistry *39*, 5845-5851.

Hagen, T. M., Yowe, D. L., Bartholomew, J. C., Wehr, C. M., Do, K. L., Park, J. Y., and Ames, B. N. (1997). Mitochondrial decay in hepatocytes from old rats: membrane potential declines, heterogeneity and oxidants increase. Proc Natl Acad Sci U S A *94*, 3064-3069.

Hagopian, K., Harper, M. E., Ram, J. J., Humble, S. J., Weindruch, R., and Ramsey, J. J. (2005). Long-term calorie restriction reduces proton leak and hydrogen peroxide production in liver mitochondria. Am J Physiol Endocrinol Metab *288*, E674-684.

Han, D., Williams, E., and Cadenas, E. (2001a). Mitochondrial respiratory chain-dependent generation of superoxide anion and its release into the intermembrane space. Biochem J *353*, 411-416.

Hansford, R. G., Hogue, B. A., and Mildaziene, V. (1997). Dependence of H2O2 formation by rat heart mitochondria on substrate availability and donor age. J Bioenerg Biomembr *29*, 89-95.

Harman, D. (1956). Aging: a theory based on free radical and radiation chemistry. J Gerontol *11*, 298-300.

Harman, D. (1972). The biologic clock: the mitochondria? J Am Geriatr Soc *20*, 145-147.

Harper, J. A., Stuart, J. A., Jekabsons, M. B., Roussel, D., Brindle, K. M., Dickinson, K., Jones, R. B., and Brand, M. D. (2002). Artifactual uncoupling by uncoupling protein 3 in yeast mitochondria at the concentrations found in mouse and rat skeletal-muscle mitochondria. Biochem J *361*, 49-56.

Harper, M. E., and Brand, M. D. (1993). The quantitative contributions of mitochondrial proton leak and ATP turnover reactions to the changed respiration rates of hepatocytes from rats of different thyroid status. J Biol Chem *268*, 14850-14860.

Harper, M. E., Monemdjou, S., Ramsey, J. J., and Weindruch, R. (1998). Age-related increase in mitochondrial proton leak and decrease in ATP turnover reactions in mouse hepatocytes. Am J Physiol *275*, E197-206.

Harrison, D. E., Archer, J. R., and Astle, C. M. (1984). Effects of food restriction on aging: separation of food intake and adiposity. Proc Natl Acad Sci U S A *81*, 1835-1838.

Heilbronn, L. K., de Jonge, L., Frisard, M. I., DeLany, J. P., Larson-Meyer, D. E., Rood, J., Nguyen, T., Martin, C. K., Volaufova, J., Most, M. M., *et al.* (2006). Effect of 6-month calorie restriction on biomarkers of longevity, metabolic adaptation, and oxidative stress in overweight individuals: a randomized controlled trial. Jama *295*, 1539-1548.

Heilbronn, L. K., and Ravussin, E. (2003). Calorie restriction and aging: review of the literature and implications for studies in humans. Am J Clin Nutr *78*, 361-369.

Herrero, A., and Barja, G. (1997). Sites and mechanisms responsible for the low rate of free radical production of heart mitochondria in the long-lived pigeon. Mech Ageing Dev *98*, 95-111.

Hesselink, M. K., Keizer, H. A., Borghouts, L. B., Schaart, G., Kornips, C. F., Slieker, L. J., Sloop, K. W., Saris, W. H., and Schrauwen, P. (2001). Protein expression of UCP3 differs between human type 1, type 2a, and type 2b fibers. Faseb J *15*, 1071-1073.

Higami, Y., Pugh, T. D., Page, G. P., Allison, D. B., Prolla, T. A., and Weindruch, R. (2004). Adipose tissue energy metabolism: altered gene expression profile of mice subjected to long-term caloric restriction. Faseb J *18*, 415-417.

Himms-Hagen, J., and Harper, M. E. (2001). Physiological role of UCP3 may be export of fatty acids from mitochondria when fatty acid oxidation predominates: an hypothesis. Exp Biol Med (Maywood) *226*, 78-84.

Hinz, W., Faller, B., Gruninger, S., Gazzotti, P., and Chiesi, M. (1999a). Recombinant human uncoupling protein-3 increases thermogenesis in yeast cells. FEBS Lett *448*, 57-61.

Hinz, W., Gruninger, S., De Pover, A., and Chiesi, M. (1999b). Properties of the human long and short isoforms of the uncoupling protein-3 expressed in yeast cells. FEBS Lett *462*, 411-415.

Hudson, E. K., Hogue, B. A., Souza-Pinto, N. C., Croteau, D. L., Anson, R. M., Bohr, V. A., and Hansford, R. G. (1998). Age-associated change in mitochondrial DNA damage. Free Radic Res *29*, 573-579.

Hunt, M. C., Nousiainen, S. E., Huttunen, M. K., Orii, K. E., Svensson, L. T., and Alexson, S. E. (1999). Peroxisome proliferator-induced long chain acyl-CoA thioesterases comprise a highly conserved novel multi-gene family involved in lipid metabolism. J Biol Chem *274*, 34317-34326.

Hunt, N. D., Hyun, D. H., Allard, J. S., Minor, R. K., Mattson, M. P., Ingram, D. K., and de Cabo, R. (2006). Bioenergetics of aging and calorie restriction. Ageing Res Rev *5*, 125-143.

Imai, S., Johnson, F. B., Marciniak, R. A., McVey, M., Park, P. U., and Guarente, L. (2000). Sir2: an NAD-dependent histone deacetylase that connects chromatin silencing, metabolism, and aging. Cold Spring Harb Symp Quant Biol *65*, 297-302.

Itoh, K., Wakabayashi, N., Katoh, Y., Ishii, T., Igarashi, K., Engel, J. D., and Yamamoto, M. (1999). Keap1 represses nuclear activation of antioxidant responsive elements by Nrf2 through binding to the amino-terminal Neh2 domain. Genes Dev *13*, 76-86.

Iwata, S., Lee, J. W., Okada, K., Lee, J. K., Iwata, M., Rasmussen, B., Link, T. A., Ramaswamy, S., and Jap, B. K. (1998). Complete structure of the 11-subunit bovine mitochondrial cytochrome bc1 complex. Science *281*, 64-71.

Jezek, P., and Hlavata, L. (2005). Mitochondria in homeostasis of reactive oxygen species in cell, tissues, and organism. Int J Biochem Cell Biol *37*, 2478-2503.

Jimenez, M., Yvon, C., Lehr, L., Leger, B., Keller, P., Russell, A., Kuhne, F., Flandin, P., Giacobino, J. P., and Muzzin, P. (2002). Expression of uncoupling protein-3 in subsarcolemmal and intermyofibrillar mitochondria of various mouse muscle types and its modulation by fasting. Eur J Biochem *269*, 2878-2884.

Johnson, P. R., Stern, J. S., Horwitz, B. A., Harris, R. E., Jr., and Greene, S. F. (1997). Longevity in obese and lean male and female rats of the Zucker strain: prevention of hyperphagia. Am J Clin Nutr *66*, 890-903.

Kagawa, Y. (1978). Impact of Westernization on the nutrition of Japanese: changes in physique, cancer, longevity and centenarians. Prev Med *7*, 205-217.

Kalant, N., Stewart, J., and Kaplan, R. (1988). Effect of diet restriction on glucose metabolism and insulin responsiveness in aging rats. Mech Ageing Dev *46*, 89-104.

Kang, K. A., Lee, K. H., Park, J. W., Lee, N. H., Na, H. K., Surh, Y. J., You, H. J., Chung, M. H., and Hyun, J. W. (2007). Triphlorethol-A induces heme oxygenase-1 via activation of ERK and NF-E2 related factor 2 transcription factor. FEBS Lett *581*, 2000-2008.

Kayo, T., Allison, D. B., Weindruch, R., and Prolla, T. A. (2001). Influences of aging and caloric restriction on the transcriptional profile of skeletal muscle from rhesus monkeys. Proc Natl Acad Sci U S A *98*, 5093-5098.

Kemnitz, J. W., Roecker, E. B., Weindruch, R., Elson, D. F., Baum, S. T., and Bergman, R. N. (1994). Dietary restriction increases insulin sensitivity and lowers blood glucose in rhesus monkeys. Am J Physiol *266*, E540-547.

Kirk, K. L. (2001). Dietary restriction and aging: comparative tests of evolutionary hypotheses. J Gerontol A Biol Sci Med Sci *56*, B123-129.

Klass, M. R. (1977). Aging in the nematode Caenorhabditis elegans: major biological and environmental factors influencing life span. Mech Ageing Dev *6*, 413-429.

Kleyn, P. W., Fan, W., Kovats, S. G., Lee, J. J., Pulido, J. C., Wu, Y., Berkemeier, L. R., Misumi, D. J., Holmgren, L., Charlat, O., *et al.* (1996). Identification and characterization of the mouse obesity gene tubby: a member of a novel gene family. Cell *85*, 281-290.

Klingenberg, M., and Huang, S. G. (1999). Structure and function of the uncoupling protein from brown adipose tissue. Biochim Biophys Acta *1415*, 271-296.

Kumaran, S., Subathra, M., Balu, M., and Panneerselvam, C. (2004). Age-associated decreased activities of mitochondrial electron transport chain complexes in heart and skeletal muscle: role of L-carnitine. Chem Biol Interact *148*, 11-18.

Kushnareva, Y., Murphy, A. N., and Andreyev, A. (2002). Complex I-mediated reactive oxygen species generation: modulation by cytochrome c and NAD(P)+ oxidation-reduction state. Biochem J *368*, 545-553.

Laganiere, S., and Yu, B. P. (1993). Modulation of membrane phospholipid fatty acid composition by age and food restriction. Gerontology *39*, 7-18.

Lal, S. B., Ramsey, J. J., Monemdjou, S., Weindruch, R., and Harper, M. E. (2001). Effects of caloric restriction on skeletal muscle mitochondrial proton leak in aging rats. J Gerontol A Biol Sci Med Sci *56*, B116-122.

Lambert, A. J., and Brand, M. D. (2004). Superoxide production by NADH:ubiquinone oxidoreductase (complex I) depends on the pH gradient across the mitochondrial inner membrane. Biochem J *382*, 511-517.

Lambert, A. J., Wang, B., and Merry, B. J. (2004). Exogenous insulin can reverse the effects of caloric restriction on mitochondria. Biochem Biophys Res Commun *316*, 1196-1201.

Lambeth, J. D. (2004). NOX enzymes and the biology of reactive oxygen. Nat Rev Immunol *4*, 181-189.

Lane, M. A., Baer, D. J., Rumpler, W. V., Weindruch, R., Ingram, D. K., Tilmont, E. M., Cutler, R. G., and Roth, G. S. (1996). Calorie restriction lowers body temperature in rhesus monkeys, consistent with a postulated anti-aging mechanism in rodents. Proc Natl Acad Sci U S A *93*, 4159-4164.

Lane, M. A., Baer, D. J., Tilmont, E. M., Rumpler, W. V., Ingram, D. K., Roth, G. S., and Cutler, R. G. (1995a). Energy balance in rhesus monkeys (Macaca mulatta) subjected to long-term dietary restriction. J Gerontol A Biol Sci Med Sci *50*, B295-302.

Lane, M. A., Ball, S. S., Ingram, D. K., Cutler, R. G., Engel, J., Read, V., and Roth, G. S. (1995b). Diet restriction in rhesus monkeys lowers fasting and glucose-stimulated glucoregulatory end points. Am J Physiol *268*, E941-948.

Lass, A., Sohal, B. H., Weindruch, R., Forster, M. J., and Sohal, R. S. (1998). Caloric restriction prevents age-associated accrual of oxidative damage to mouse skeletal muscle mitochondria. Free Radic Biol Med *25*, 1089-1097.

Lee, C. K., Allison, D. B., Brand, J., Weindruch, R., and Prolla, T. A. (2002). Transcriptional profiles associated with aging and middle age-onset caloric restriction in mouse hearts. Proc Natl Acad Sci U S A *99*, 14988-14993.

Lee, C. K., Klopp, R. G., Weindruch, R., and Prolla, T. A. (1999a). Gene expression profile of aging and its retardation by caloric restriction. Science *285*, 1390-1393.

Lee, C. K., Weindruch, R., and Prolla, T. A. (2000). Gene-expression profile of the ageing brain in mice. Nat Genet *25*, 294-297.

Lee, J., Yu, B. P., and Herlihy, J. T. (1999b). Modulation of cardiac mitochondrial membrane fluidity by age and calorie intake. Free Radic Biol Med *26*, 260-265.

Leeuwenburgh, C., Wagner, P., Holloszy, J. O., Sohal, R. S., and Heinecke, J. W. (1997). Caloric restriction attenuates dityrosine cross-linking of cardiac and skeletal muscle proteins in aging mice. Arch Biochem Biophys *346*, 74-80.

Leto, S., Kokkonen, G. C., and Barrows, C. H., Jr. (1976). Dietary protein, life-span, and biochemical variables in female mice. J Gerontol *31*, 144-148.

Lippe, G., Comelli, M., Mazzilis, D., Sala, F. D., and Mavelli, I. (1991). The inactivation of mitochondrial F1 ATPase by H2O2 is mediated by iron ions not tightly bound in the protein. Biochem Biophys Res Commun *181*, 764-770.

Liu, R., Li, B., Flanagan, S. W., Oberley, L. W., Gozal, D., and Qiu, M. (2002a). Increased mitochondrial antioxidative activity or decreased oxygen free radical propagation prevent mutant SOD1-mediated motor neuron cell death and increase amyotrophic lateral sclerosis-like transgenic mouse survival. J Neurochem *80*, 488-500.

Liu, Y., Fiskum, G., and Schubert, D. (2002b). Generation of reactive oxygen species by the mitochondrial electron transport chain. J Neurochem *80*, 780-787.

Longo, V. D., and Fabrizio, P. (2002). Regulation of longevity and stress resistance: a molecular strategy conserved from yeast to humans? Cell Mol Life Sci *59*, 903-908.

Lopez-Lluch, G., Hunt, N., Jones, B., Zhu, M., Jamieson, H., Hilmer, S., Cascajo, M. V., Allard, J., Ingram, D. K., Navas, P., and de Cabo, R. (2006). Calorie restriction induces mitochondrial biogenesis and bioenergetic efficiency. Proc Natl Acad Sci U S A *103*, 1768-1773.

Lopez-Torres, M., Gredilla, R., Sanz, A., and Barja, G. (2002). Influence of aging and long-term caloric restriction on oxygen radical generation and oxidative DNA damage in rat liver mitochondria. Free Radic Biol Med *32*, 882-889.

Loschen, G., Flohe, L., and Chance, B. (1971). Respiratory chain linked H(2)O(2) production in pigeon heart mitochondria. FEBS Lett *18*, 261-264.

Luo, J., Nikolaev, A. Y., Imai, S., Chen, D., Su, F., Shiloh, A., Guarente, L., and Gu, W. (2001). Negative control of p53 by Sir2alpha promotes cell survival under stress. Cell *107*, 137-148.

MacLellan, J. D., Gerrits, M. F., Gowing, A., Smith, P. J., Wheeler, M. B., and Harper, M. E. (2005). Physiological increases in uncoupling protein 3 augment fatty acid oxidation and

decrease reactive oxygen species production without uncoupling respiration in muscle cells. Diabetes *54*, 2343-2350.

Mair, W., Piper, M. D., and Partridge, L. (2005). Calories do not explain extension of life span by dietary restriction in Drosophila. PLoS Biol *3*, e223.

Mannella, C. A. (2006). The relevance of mitochondrial membrane topology to mitochondrial function. Biochim Biophys Acta *1762*, 140-147.

Mannella, C. A., Marko, M., and Buttle, K. (1997). Reconsidering mitochondrial structure: new views of an old organelle. Trends Biochem Sci *22*, 37-38.

Mansouri, A., Muller, F. L., Liu, Y., Ng, R., Faulkner, J., Hamilton, M., Richardson, A., Huang, T. T., Epstein, C. J., and Van Remmen, H. (2006). Alterations in mitochondrial function, hydrogen peroxide release and oxidative damage in mouse hind-limb skeletal muscle during aging. Mech Ageing Dev *127*, 298-306.

Mao, W., Yu, X. X., Zhong, A., Li, W., Brush, J., Sherwood, S. W., Adams, S. H., and Pan, G. (1999). UCP4, a novel brain-specific mitochondrial protein that reduces membrane potential in mammalian cells. FEBS Lett *443*, 326-330.

Marcinek, D. J., Schenkman, K. A., Ciesielski, W. A., Lee, D., and Conley, K. E. (2005). Reduced mitochondrial coupling in vivo alters cellular energetics in aged mouse skeletal muscle. J Physiol *569*, 467-473.

Masoro, E. J. (1990). Assessment of nutritional components in prolongation of life and health by diet. Proc Soc Exp Biol Med *193*, 31-34.

Masoro, E. J. (1995). Antiaging action of caloric restriction: endocrine and metabolic aspects. Obes Res *3 Suppl 2*, 241s-247s.

Masoro, E. J. (2002). Calorie Restriction: A Key to Understanding and Modulating Aging, Vol 1, First edn (Charleston, South Carolina: Elsevier).

Masoro, E. J., McCarter, R. J., Katz, M. S., and McMahan, C. A. (1992). Dietary restriction alters characteristics of glucose fuel use. J Gerontol *47*, B202-208.

Matthias, A., Ohlson, K. B., Fredriksson, J. M., Jacobsson, A., Nedergaard, J., and Cannon, B. (2000). Thermogenic responses in brown fat cells are fully UCP1-dependent. UCP2 or UCP3 do not substitute for UCP1 in adrenergically or fatty scid-induced thermogenesis. J Biol Chem *275*, 25073-25081.

McCarter, R. J., and Palmer, J. (1992). Energy metabolism and aging: a lifelong study of Fischer 344 rats. Am J Physiol *263*, E448-452.

McCay, C. M., Crowell, M.F., & Maynard, L.A. (1935). The effect of retarded growth upon the length of life and upon the ultimated body size. Journal of Nutrition *10*, 63-79.

McCay, C. M., Dilley, W.E., & Crowell, M.F. (1929). Growth rates of brook trout reared upon purified rations, upon dry skim milk diets and upon feel combinations of cereal grains. Journal of Nutrition *1*, 233-246.

McCay, C. M., Maynard, L.A., Sperling, G., & Barnes, L.L. (1939). Retarded growth, lifespan, ultimate body size, and age changes in the albino rat after feeding diets restricted in calories. Journal of Nutrition *18*, 1-13.

Mecocci, P., Fano, G., Fulle, S., MacGarvey, U., Shinobu, L., Polidori, M. C., Cherubini, A., Vecchiet, J., Senin, U., and Beal, M. F. (1999). Age-dependent increases in oxidative damage to DNA, lipids, and proteins in human skeletal muscle. Free Radic Biol Med *26*, 303-308.

Miller, R. A., Buehner, G., Chang, Y., Harper, J. M., Sigler, R., and Smith-Wheelock, M. (2005). Methionine-deficient diet extends mouse lifespan, slows immune and lens aging, alters glucose, T4, IGF-I and insulin levels, and increases hepatocyte MIF levels and stress resistance. Aging Cell *4*, 119-125.

Millet, L., Vidal, H., Andreelli, F., Larrouy, D., Riou, J. P., Ricquier, D., Laville, M., and Langin, D. (1997). Increased uncoupling protein-2 and -3 mRNA expression during fasting in obese and lean humans. J Clin Invest *100*, 2665-2670.

Miwa, S., and Brand, M. D. (2003). Mitochondrial matrix reactive oxygen species production is very sensitive to mild uncoupling. Biochem Soc Trans *31*, 1300-1301.

Miwa, S., St-Pierre, J., Partridge, L., and Brand, M. D. (2003). Superoxide and hydrogen peroxide production by Drosophila mitochondria. Free Radic Biol Med *35*, 938-948.

Moore, G. B., Himms-Hagen, J., Harper, M. E., and Clapham, J. C. (2001). Overexpression of UCP-3 in skeletal muscle of mice results in increased expression of mitochondrial thioesterase mRNA. Biochem Biophys Res Commun *283*, 785-790.

Motta, M. C., Divecha, N., Lemieux, M., Kamel, C., Chen, D., Gu, W., Bultsma, Y., McBurney, M., and Guarente, L. (2004). Mammalian SIRT1 represses forkhead transcription factors. Cell *116*, 551-563.

Mozo, J., Ferry, G., Studeny, A., Pecqueur, C., Rodriguez, M., Boutin, J. A., and Bouillaud, F. (2006). Expression of UCP3 in CHO cells does not cause uncoupling, but controls mitochondrial activity in the presence of glucose. Biochem J *393*, 431-439.

Nemoto, S., Fergusson, M. M., and Finkel, T. (2005). SIRT1 functionally interacts with the metabolic regulator and transcriptional coactivator PGC-1{alpha}. J Biol Chem *280*, 16456-16460.

Nicholls, D. G. (1974). The influence of respiration and ATP hydrolysis on the proton-electrochemical gradient across the inner membrane of rat-liver mitochondria as determined by ion distribution. Eur J Biochem *50*, 305-315.

Nicholls, D. G. (2002a). Mitochondrial function and dysfunction in the cell: its relevance to aging and aging-related disease. Int J Biochem Cell Biol *34*, 1372-1381.

Nicholls, D. G. (2004). Mitochondrial membrane potential and aging. Aging Cell *3*, 35-40.

Nicholls, D. G. (2006). The physiological regulation of uncoupling proteins. Biochim Biophys Acta *1757*, 459-466.

Nicholls, D. G., and Locke, R. M. (1984). Thermogenic mechanisms in brown fat. Physiol Rev *64*, 1-64.

Nicholls, D. G. a. F., S.J. (2002b). Bioenergetics 3, 3 edn: Elsevier Science).

Nicolay, K., Rojo, M., Wallimann, T., Demel, R., and Hovius, R. (1990). The role of contact sites between inner and outer mitochondrial membrane in energy transfer. Biochim Biophys Acta *1018*, 229-233.

Nobes, C. D., Brown, G. C., Olive, P. N., and Brand, M. D. (1990). Non-ohmic proton conductance of the mitochondrial inner membrane in hepatocytes. J Biol Chem *265*, 12903-12909.

Nohl, H., and Stolze, K. (1992). Ubisemiquinones of the mitochondrial respiratory chain do not interact with molecular oxygen. Free Radic Res Commun *16*, 409-419.

Pak, J. W., Herbst, A., Bua, E., Gokey, N., McKenzie, D., and Aiken, J. M. (2003). Mitochondrial DNA mutations as a fundamental mechanism in physiological declines associated with aging. Aging Cell *2*, 1-7.

Pamplona, R., Barja, G., and Portero-Otin, M. (2002). Membrane fatty acid unsaturation, protection against oxidative stress, and maximum life span: a homeoviscous-longevity adaptation? Ann N Y Acad Sci *959*, 475-490.

Park, S. K., and Prolla, T. A. (2005). Gene expression profiling studies of aging in cardiac and skeletal muscles. Cardiovasc Res *66*, 205-212.

Payne, A. M., Dodd, S. L., and Leeuwenburgh, C. (2003). Life-long calorie restriction in Fischer 344 rats attenuates age-related loss in skeletal muscle-specific force and reduces extracellular space. J Appl Physiol *95*, 2554-2562.

Pebay-Peyroula, E., Dahout-Gonzalez, C., Kahn, R., Trezeguet, V., Lauquin, G. J., and Brandolin, G. (2003). Structure of mitochondrial ADP/ATP carrier in complex with carboxyatractyloside. Nature *426*, 39-44.

Pecqueur, C., Alves-Guerra, M. C., Gelly, C., Levi-Meyrueis, C., Couplan, E., Collins, S., Ricquier, D., Bouillaud, F., and Miroux, B. (2001). Uncoupling protein 2, in vivo distribution, induction upon oxidative stress, and evidence for translational regulation. J Biol Chem *276*, 8705-8712.

Petersen, K. F., Befroy, D., Dufour, S., Dziura, J., Ariyan, C., Rothman, D. L., DiPietro, L., Cline, G. W., and Shulman, G. I. (2003). Mitochondrial dysfunction in the elderly: possible role in insulin resistance. Science *300*, 1140-1142.

Porter, R. K., and Brand, M. D. (1993). Body mass dependence of H+ leak in mitochondria and its relevance to metabolic rate. Nature *362*, 628-630.

Porter, R. K., Hulbert, A. J., and Brand, M. D. (1996). Allometry of mitochondrial proton leak: influence of membrane surface area and fatty acid composition. Am J Physiol *271*, R1550-1560.

Radi, R., Turrens, J. F., Chang, L. Y., Bush, K. M., Crapo, J. D., and Freeman, B. A. (1991). Detection of catalase in rat heart mitochondria. J Biol Chem *266*, 22028-22034.

Ramsey, J. J., and Hagopian, K. (2006). Energy expenditure and restriction of energy intake: could energy restriction alter energy expenditure in companion animals? J Nutr *136*, 1958S-1966S.

Ramsey, J. J., Hagopian, K., Kenny, T. M., Koomson, E. K., Bevilacqua, L., Weindruch, R., and Harper, M. E. (2004). Proton leak and hydrogen peroxide production in liver mitochondria from energy-restricted rats. Am J Physiol Endocrinol Metab *286*, E31-40.

Ramsey, J. J., Roecker, E. B., Weindruch, R., and Kemnitz, J. W. (1997). Energy expenditure of adult male rhesus monkeys during the first 30 mo of dietary restriction. Am J Physiol *272*, E901-907.

Richie, J. P., Jr., Leutzinger, Y., Parthasarathy, S., Malloy, V., Orentreich, N., and Zimmerman, J. A. (1994). Methionine restriction increases blood glutathione and longevity in F344 rats. Faseb J *8*, 1302-1307.

Rodgers, J. T., Lerin, C., Haas, W., Gygi, S. P., Spiegelman, B. M., and Puigserver, P. (2005). Nutrient control of glucose homeostasis through a complex of PGC-1alpha and SIRT1. Nature *434*, 113-118.

Rolfe, D. F., and Brand, M. D. (1997). The physiological significance of mitochondrial proton leak in animal cells and tissues. Biosci Rep *17*, 9-16.

Rolfe, D. F., and Brown, G. C. (1997). Cellular energy utilization and molecular origin of standard metabolic rate in mammals. Physiol Rev *77*, 731-758.

Rolfe, D. F., Hulbert, A. J., and Brand, M. D. (1994). Characteristics of mitochondrial proton leak and control of oxidative phosphorylation in the major oxygen-consuming tissues of the rat. Biochim Biophys Acta *1188*, 405-416.

Ross, M. H. (1961). Length of life and nutrition in the rat. J Nutr *75*, 197-210.

Ross, M. H., and Bras, G. (1965). Tumor incidence patterns and nutrition in the rat. J Nutr *87*, 245-260.

Russell, A. P., Wadley, G., Hesselink, M. K., Schaart, G., Lo, S., Leger, B., Garnham, A., Kornips, E., Cameron-Smith, D., Giacobino, J. P., *et al.* (2003). UCP3 protein expression is lower in type I, IIa and IIx muscle fiber types of endurance-trained compared to untrained subjects. Pflugers Arch *445*, 563-569.

Sabatino, F., Masoro, E. J., McMahan, C. A., and Kuhn, R. W. (1991). Assessment of the role of the glucocorticoid system in aging processes and in the action of food restriction. J Gerontol *46*, B171-179.

Samec, S., Seydoux, J., and Dulloo, A. G. (1999). Post-starvation gene expression of skeletal muscle uncoupling protein 2 and uncoupling protein 3 in response to dietary fat levels and fatty acid composition: a link with insulin resistance. Diabetes *48*, 436-441.

Sanchis, D., Fleury, C., Chomiki, N., Goubern, M., Huang, Q., Neverova, M., Gregoire, F., Easlick, J., Raimbault, S., Levi-Meyrueis, C., *et al.* (1998). BMCP1, a novel mitochondrial carrier with high expression in the central nervous system of humans and rodents, and respiration uncoupling activity in recombinant yeast. J Biol Chem *273*, 34611-34615.

Sanz, A., Caro, P., Ayala, V., Portero-Otin, M., Pamplona, R., and Barja, G. (2006). Methionine restriction decreases mitochondrial oxygen radical generation and leak as well as oxidative damage to mitochondrial DNA and proteins. Faseb J *20*, 1064-1073.

Sastre, J., Pallardo, F. V., Pla, R., Pellin, A., Juan, G., O'Connor, J. E., Estrela, J. M., Miquel, J., and Vina, J. (1996). Aging of the liver: age-associated mitochondrial damage in intact hepatocytes. Hepatology *24*, 1199-1205.

Sawada, M., and Carlson, J. C. (1987). Association between lipid peroxidation and life-modifying factors in rotifers. J Gerontol *42*, 451-456.

Saxton, J. A., Jr. & Kimball, G.C. (1941). Relation to nephrosis and other diseases of albino rat to age and to modification of diet. Arch Path *32*, 951-965.

Saxton, J. A., Jr., Boon, M.C., & Furth, J. (1944). Observations on the inhibition of development of spontaneous leukemia in mice by underfeeding. Cancer Res *4*, 401-409.

Schagger, H., de Coo, R., Bauer, M. F., Hofmann, S., Godinot, C., and Brandt, U. (2004). Significance of respirasomes for the assembly/stability of human respiratory chain complex I. J Biol Chem *279*, 36349-36353.

Schagger, H., and Pfeiffer, K. (2000). Supercomplexes in the respiratory chains of yeast and mammalian mitochondria. Embo J *19*, 1777-1783.

Scholes, T. A., and Hinkle, P. C. (1984). Energetics of ATP-driven reverse electron transfer from cytochrome c to fumarate and from succinate to NAD in submitochondrial particles. Biochemistry *23*, 3341-3345.

Schrauwen, P., Hoppeler, H., Billeter, R., Bakker, A. H., and Pendergast, D. R. (2001a). Fiber type dependent upregulation of human skeletal muscle UCP2 and UCP3 mRNA expression by high-fat diet. Int J Obes Relat Metab Disord *25*, 449-456.

Schrauwen, P., Saris, W. H., and Hesselink, M. K. (2001b). An alternative function for human uncoupling protein 3: protection of mitochondria against accumulation of nonesterified fatty acids inside the mitochondrial matrix. Faseb J *15*, 2497-2502.

Schrauwen, P., Xia, J., Bogardus, C., Pratley, R. E., and Ravussin, E. (1999). Skeletal muscle uncoupling protein 3 expression is a determinant of energy expenditure in Pima Indians. Diabetes *48*, 146-149.

Selman, C., Phillips, T., Staib, J. L., Duncan, J. S., Leeuwenburgh, C., and Speakman, J. R. (2005). Energy expenditure of calorically restricted rats is higher than predicted from their altered body composition. Mech Ageing Dev *126*, 783-793.

Shabalina, I. G., Petrovic, N., Kramarova, T. V., Hoeks, J., Cannon, B., and Nedergaard, J. (2006). UCP1 and defense against oxidative stress. 4-Hydroxy-2-nonenal effects on brown fat mitochondria are uncoupling protein 1-independent. J Biol Chem *281*, 13882-13893.

Shigenaga, M. K., Hagen, T. M., and Ames, B. N. (1994). Oxidative damage and mitochondrial decay in aging. Proc Natl Acad Sci U S A *91*, 10771-10778.

Short, K. R., Bigelow, M. L., Kahl, J., Singh, R., Coenen-Schimke, J., Raghavakaimal, S., and Nair, K. S. (2005). Decline in skeletal muscle mitochondrial function with aging in humans. Proc Natl Acad Sci U S A *102*, 5618-5623.

Silva, J. P., Shabalina, I. G., Dufour, E., Petrovic, N., Backlund, E. C., Hultenby, K., Wibom, R., Nedergaard, J., Cannon, B., and Larsson, N. G. (2005). SOD2 overexpression: enhanced mitochondrial tolerance but absence of effect on UCP activity. Embo J *24*, 4061-4070.

Silvestri, E., Moreno, M., Lombardi, A., Ragni, M., de Lange, P., Alexson, S. E., Lanni, A., and Goglia, F. (2005). Thyroid-hormone effects on putative biochemical pathways involved in UCP3 activation in rat skeletal muscle mitochondria. FEBS Lett *579*, 1639-1645.

Skulachev, V. P. (1998). Uncoupling: new approaches to an old problem of bioenergetics. Biochim Biophys Acta *1363*, 100-124.

Sohal, R. S., Agarwal, S., Candas, M., Forster, M. J., and Lal, H. (1994a). Effect of age and caloric restriction on DNA oxidative damage in different tissues of C57BL/6 mice. Mech Ageing Dev *76*, 215-224.

Sohal, R. S., and Dubey, A. (1994). Mitochondrial oxidative damage, hydrogen peroxide release, and aging. Free Radic Biol Med *16*, 621-626.

Sohal, R. S., Ku, H. H., Agarwal, S., Forster, M. J., and Lal, H. (1994b). Oxidative damage, mitochondrial oxidant generation and antioxidant defenses during aging and in response to food restriction in the mouse. Mech Ageing Dev *74*, 121-133.

Sohal, R. S., and Sohal, B. H. (1991). Hydrogen peroxide release by mitochondria increases during aging. Mech Ageing Dev *57*, 187-202.

Sohal, R. S., and Weindruch, R. (1996). Oxidative stress, caloric restriction, and aging. Science *273*, 59-63.

Solanes, G., Vidal-Puig, A., Grujic, D., Flier, J. S., and Lowell, B. B. (1997). The human uncoupling protein-3 gene. Genomic structure, chromosomal localization, and genetic basis for short and long form transcripts. J Biol Chem *272*, 25433-25436.

Sreekumar, R., Unnikrishnan, J., Fu, A., Nygren, J., Short, K. R., Schimke, J., Barazzoni, R., and Nair, K. S. (2002). Effects of caloric restriction on mitochondrial function and gene transcripts in rat muscle. Am J Physiol Endocrinol Metab *283*, E38-43.

St-Arnaud J., B. M. P., Tully PO (2005). Life expectancy, In Health Reports (Statistics Canada, Catalogue No. 82-003-X1E), A. Lacroix, ed. (Government of Canada), pp. 1-68.

St-Pierre, J., Buckingham, J. A., Roebuck, S. J., and Brand, M. D. (2002). Topology of superoxide production from different sites in the mitochondrial electron transport chain. J Biol Chem *277*, 44784-44790.

Staniek, K., and Nohl, H. (2000). Are mitochondria a permanent source of reactive oxygen species? Biochim Biophys Acta *1460*, 268-275.

Stavinoha, M. A., RaySpellicy, J. W., Essop, M. F., Graveleau, C., Abel, E. D., Hart-Sailors, M. L., Mersmann, H. J., Bray, M. S., and Young, M. E. (2004). Evidence for mitochondrial thioesterase 1 as a peroxisome proliferator-activated receptor-alpha-regulated gene in cardiac and skeletal muscle. Am J Physiol Endocrinol Metab *287*, E888-895.

Stuart, J. A., Harper, J. A., Brindle, K. M., Jekabsons, M. B., and Brand, M. D. (2001a). A mitochondrial uncoupling artifact can be caused by expression of uncoupling protein 1 in yeast. Biochem J *356*, 779-789.

Stuart, J. A., Harper, J. A., Brindle, K. M., Jekabsons, M. B., and Brand, M. D. (2001b). Physiological levels of mammalian uncoupling protein 2 do not uncouple yeast mitochondria. J Biol Chem *276*, 18633-18639.

Stuart, J. A., Karahalil, B., Hogue, B. A., Souza-Pinto, N. C., and Bohr, V. A. (2004). Mitochondrial and nuclear DNA base excision repair are affected differently by caloric restriction. Faseb J *18*, 595-597.

Talbot, D. A., Lambert, A. J., and Brand, M. D. (2004). Production of endogenous matrix superoxide from mitochondrial complex I leads to activation of uncoupling protein 3. FEBS Lett *556*, 111-115.

Tatar, M., Bartke, A., and Antebi, A. (2003). The endocrine regulation of aging by insulin-like signals. Science *299*, 1346-1351.

Taylor, B. A., and Phillips, S. J. (1996). Detection of obesity QTLs on mouse chromosomes 1 and 7 by selective DNA pooling. Genomics *34*, 389-398.

Taylor, S. W., Fahy, E., Zhang, B., Glenn, G. M., Warnock, D. E., Wiley, S., Murphy, A. N., Gaucher, S. P., Capaldi, R. A., Gibson, B. W., and Ghosh, S. S. (2003). Characterization of the human heart mitochondrial proteome. Nat Biotechnol *21*, 281-286.

Tsuboyama-Kasaoka, N., Tsunoda, N., Maruyama, K., Takahashi, M., Kim, H., Ikemoto, S., and Ezaki, O. (1998). Up-regulation of uncoupling protein 3 (UCP3) mRNA by exercise training and down-regulation of UCP3 by denervation in skeletal muscles. Biochem Biophys Res Commun *247*, 498-503.

Turrens, J. F. (1997). Superoxide production by the mitochondrial respiratory chain. Biosci Rep *17*, 3-8.

Turrens, J. F., Alexandre, A., and Lehninger, A. L. (1985). Ubisemiquinone is the electron donor for superoxide formation by complex III of heart mitochondria. Arch Biochem Biophys *237*, 408-414.

Van Remmen, H., and Richardson, A. (2001). Oxidative damage to mitochondria and aging. Exp Gerontol *36*, 957-968.

Vaziri, H., Dessain, S. K., Ng Eaton, E., Imai, S. I., Frye, R. A., Pandita, T. K., Guarente, L., and Weinberg, R. A. (2001). hSIR2(SIRT1) functions as an NAD-dependent p53 deacetylase. Cell *107*, 149-159.

Vidal-Puig, A., Solanes, G., Grujic, D., Flier, J. S., and Lowell, B. B. (1997). UCP3: an uncoupling protein homologue expressed preferentially and abundantly in skeletal muscle and brown adipose tissue. Biochem Biophys Res Commun *235*, 79-82.

Vidal-Puig, A. J., Grujic, D., Zhang, C. Y., Hagen, T., Boss, O., Ido, Y., Szczepanik, A., Wade, J., Mootha, V., Cortright, R., *et al.* (2000). Energy metabolism in uncoupling protein 3 gene knockout mice. J Biol Chem *275*, 16258-16266.

Votyakova, T. V., and Reynolds, I. J. (2001). DeltaPsi(m)-Dependent and -independent production of reactive oxygen species by rat brain mitochondria. J Neurochem *79*, 266-277.

Walford, R. L., Mock, D., MacCallum, T., and Laseter, J. L. (1999). Physiologic changes in humans subjected to severe, selective calorie restriction for two years in biosphere 2: health, aging, and toxicological perspectives. Toxicol Sci *52*, 61-65.

Walford, R. L., Mock, D., Verdery, R., and MacCallum, T. (2002). Calorie restriction in biosphere 2: alterations in physiologic, hematologic, hormonal, and biochemical parameters in humans restricted for a 2-year period. J Gerontol A Biol Sci Med Sci *57*, B211-224.

Walford, R. L., Weber, L., and Panov, S. (1995). Caloric restriction and aging as viewed from Biosphere 2. Receptor *5*, 29-33.

Wei, Y. H., Ma, Y. S., Lee, H. C., Lee, C. F., and Lu, C. Y. (2001). Mitochondrial theory of aging matures--roles of mtDNA mutation and oxidative stress in human aging. Zhonghua Yi Xue Za Zhi (Taipei) *64*, 259-270.

Weigle, D. S., Selfridge, L. E., Schwartz, M. W., Seeley, R. J., Cummings, D. E., Havel, P. J., Kuijper, J. L., and BeltrandelRio, H. (1998). Elevated free fatty acids induce uncoupling protein 3 expression in muscle: a potential explanation for the effect of fasting. Diabetes *47*, 298-302.

Weindruch, R. (1996). The retardation of aging by caloric restriction: studies in rodents and primates. Toxicol Pathol *24*, 742-745.

Weindruch, R., Keenan, K. P., Carney, J. M., Fernandes, G., Feuers, R. J., Floyd, R. A., Halter, J. B., Ramsey, J. J., Richardson, A., Roth, G. S., and Spindler, S. R. (2001). Caloric restriction mimetics: metabolic interventions. J Gerontol A Biol Sci Med Sci *56 Spec No 1*, 20-33.

Weindruch, R., Walford, R. L., Fligiel, S., and Guthrie, D. (1986). The retardation of aging in mice by dietary restriction: longevity, cancer, immunity and lifetime energy intake. J Nutr *116*, 641-654.

Weinert, B. T., and Timiras, P. S. (2003). Invited review: Theories of aging. J Appl Physiol *95*, 1706-1716.

Welle, S., Brooks, A. I., Delehanty, J. M., Needler, N., Bhatt, K., Shah, B., and Thornton, C. A. (2004). Skeletal muscle gene expression profiles in 20-29 year old and 65-71 year old women. Exp Gerontol *39*, 369-377.

Welle, S., Brooks, A. I., Delehanty, J. M., Needler, N., and Thornton, C. A. (2003). Gene expression profile of aging in human muscle. Physiol Genomics *14*, 149-159.

Weyer, C., Walford, R. L., Harper, I. T., Milner, M., MacCallum, T., Tataranni, P. A., and Ravussin, E. (2000). Energy metabolism after 2 y of energy restriction: the biosphere 2 experiment. Am J Clin Nutr *72*, 946-953.

Yagi, T., and Matsuno-Yagi, A. (2003). The proton-translocating NADH-quinone oxidoreductase in the respiratory chain: the secret unlocked. Biochemistry *42*, 2266-2274.

Yakes, F. M., and Van Houten, B. (1997). Mitochondrial DNA damage is more extensive and persists longer than nuclear DNA damage in human cells following oxidative stress. Proc Natl Acad Sci U S A *94*, 514-519.

Yan, L. J., Levine, R. L., and Sohal, R. S. (1997). Oxidative damage during aging targets mitochondrial aconitase. Proc Natl Acad Sci U S A *94*, 11168-11172.

Yan, L. J., and Sohal, R. S. (1998). Mitochondrial adenine nucleotide translocase is modified oxidatively during aging. Proc Natl Acad Sci U S A *95*, 12896-12901.

Yu, B. P. (1996). Aging and oxidative stress: modulation by dietary restriction. Free Radic Biol Med *21*, 651-668.

Yu, B. P., Lim, B. O., and Sugano, M. (2002). Dietary restriction downregulates free radical and lipid peroxide production: plausible mechanism for elongation of life span. J Nutr Sci Vitaminol (Tokyo) *48*, 257-264.

Yu, B. P., Masoro, E. J., Murata, I., Bertrand, H. A., and Lynd, F. T. (1982). Life span study of SPF Fischer 344 male rats fed ad libitum or restricted diets: longevity, growth, lean body mass and disease. J Gerontol *37*, 130-141.

Yu, B. P., Wong, G., Lee, H. C., Bertrand, H., and Masoro, E. J. (1984). Age changes in hepatic metabolic characteristics and their modulation by dietary manipulation. Mech Ageing Dev *24*, 67-81.

Zhang, C. Y., Baffy, G., Perret, P., Krauss, S., Peroni, O., Grujic, D., Hagen, T., Vidal-Puig, A. J., Boss, O., Kim, Y. B., *et al.* (2001). Uncoupling protein-2 negatively regulates insulin secretion and is a major link between obesity, beta cell dysfunction, and type 2 diabetes. Cell *105*, 745-755.

Zhang, Z., Huang, L., Shulmeister, V. M., Chi, Y. I., Kim, K. K., Hung, L. W., Crofts, A. R., Berry, E. A., and Kim, S. H. (1998). Electron transfer by domain movement in cytochrome bc1. Nature *392*, 677-684.

Zhu, M., de Cabo, R., Lane, M. A., and Ingram, D. K. (2004). Caloric restriction modulates early events in insulin signaling in liver and skeletal muscle of rat. Ann N Y Acad Sci *1019*, 448-452.

APPENDIX 1
PRCF ANALYSIS

A1.1 PRCF IN INDIRECT CALORIMETRY

Indirect calorimetry is a noninvasive technique used to measure characteristics of energy metabolism at the level of the whole body. The term "indirect calorimetry" originates from the fact that energy expenditure is measured indirectly from respiratory gas exchanges (*i.e., in vivo* measurements of oxygen consumption ($\dot{V}O_2$) and carbon dioxide production ($\dot{V}CO_2$), rather than measuring heat production, or thermogenesis, directly. The O_2 consumed and the CO_2 produced stem from the oxidation of fuel substrates such as carbohydrates, lipids and proteins (Even et al., 1994). In addition to metabolic rate determinations, indirect calorimetry can be used to assess the respiratory exchange ratio (RER) (*i.e.*, the ratio of $\dot{V}CO_2/\dot{V}O_2$). The amount of CO_2 released in relation to the amount of O_2 consumed varies depending on the substrate being metabolized by a subject. Values typically range between 0.7 and 1.0. An RER value close to 0.7 indicates that fat is the major fuel source being oxidized; an RER close to 1.0 indicates that the preferred fuel source is glucose. The approximate RER value for protein oxidation is 0.82; the exact RER value depends on the specific amino acids being oxidized. RER values of less than 0.7 are thought to be related to carbohydrate synthesis or ketone body metabolism; values greater than 1.0 are thought to represent lipid synthesis (Blaxter, 1989; Riachi et al., 2004).

A1.2 DATA ANALYISIS

Indirect calorimetry typically yields very large sets of data (approximately 150 data points/mouse/24 h). The PRCF approach makes the analysis of these large data sets more manageable. For analysis, the $\dot{V}O_2$ and RER data points collected from each respiration chamber, are transferred into a Microsoft Excel spreadsheet using the delimited text option. The raw data from each subject (mouse or rat in the work reported herein) is placed into one column of the spreadsheet. An example of the steps for the transformation of the raw data is shown in Table 15. In this particular example, $\dot{V}O_2$ data are used; however the same transformations are also used with RER data. The raw data points (Column A) are first sorted in ascending order (Column B). In the adjacent column (Column C), a starting value of 1.10 is used as it corresponds to the lowest value in the sorted list (Column B). This value is used as the lowest value on the x-axis graph. The other values in Column C are obtained by adding an increment of 0.01 to the value in the preceding row until the entire range of raw data is collected. The frequency of each $\dot{V}O_2$ increment in the sorted raw data is calculated by counting. The cumulative frequency is determined by counting the number of times that values in each row of Column C are observed in the sorted data set (Column D). The cumulative sum (Column E) is determined by the addition of the values each $\dot{V}O_2$ increment in Column D to the value in its preceding row. Finally, the percent relative cumulative frequency (PRCF; Column F) is calculated by the dividing the individual cumulative frequency at each $\dot{V}O_2$ increment by the sum of the frequencies (sum of column D) and multiplying by 100%. Conversion of the data to PRCF allows for the correction of slight differences in the number of data points collected between subjects and allows the comparison of data sets from experiment to experiment. The range of $\dot{V}O_2$ values (*i.e.*, $\dot{V}O_2$

increments in Column C) is then plotted on the x-axis and the PRCF values are then plotted on the y-axis. The resulting curve is a sigmoidal in shape, with a minimum plateau at zero and maximum plateau at 100%. The PRCF curves will always reach 100% regardless of the number or data points collected as the individual curves are scaled up or down to that percent (Riachi et al., 2004). Each curve will also have an inflection point where the largest slope is observed. This point corresponds to the 50^{th} percentile value. Determining the equation-of-best-fit allows the quantitative comparison of the PRCF curves. The PRCF data is regressed using a nonlinear regression (curve fit) similar to dose response curves used in pharmacology, with the exception that the x-axis is linear, and not logarithmic (Riachi et al., 2004). The equation for the PRCF curve is the following.

$$Y = \frac{B + (T-B)x^H}{EC50^H + x^H}$$

In this equation, B is the bottom plateau, T is the top plateau, x is the $\dot{V}O_2$ (or RER) values plotted on the x-axis, H is the slope of the curve between 10%ile and 90%ile y-axis values, and EC50 is the x-axis value corresponding to the 50 % ile value on the y axis. With the PRCF approach, B is always 0 and T is always 100% reducing the equation to:

$$Y = \frac{100x^H}{EC50^H + x^H}$$

TABLE 15: PARTIAL DATA SET OF $\dot{V}O_2$ TO DEMONSTRATE THE PRCF APPROACH

A	B	C	D	E	F
Raw $\dot{V}O_2$ data (ml O_2/min/rat)	**Sorted $\dot{V}O_2$ data**	**Interval Increment**	**Frequency**	**Cumulative Frequency**	**PRCF (%)**
1.16	1.10	1.10	1	1	1/14 = 7.14
1.10	1.12	1.11	0	1	1/14 = 7.14
1.21	1.14	1.12	1	2	2/14 = 14.3
1.17	1.15	1.13	0	2	2/14 =14.3
1.22	1.16	1.14	1	3	3/14 = 21.4
1.15	1.16	1.15	1	4	4/14 = 28.5
1.20	1.17	1.16	2	6	6/14 = 42.9
1.22	1.17	1.17	2	8	8/14 = 57.1
1.21	1.20	1.18	0	8	8/14 = 57.1
1.14	1.20	1.19	0	8	8/14 =57.1
1.17	1.21	1.20	2	10	10/14 = 71.4
1.20	1.21	1.21	2	12	12/14 = 85.7
1.12	1.22	1.22	2	14	14/14 = 100
1.16	1.22	1.23	0	14	14/14 = 100

A1.3 STATISTICAL ANALYSIS OF THE DATA

If the data are normally distributed, then the 50%ile value represents the mean, and statistical tests for comparison of the means are possible (*e.g.*, paired or unpaired t tests). If the data are skewed and do not follow the normal distribution, then nonparametric tests for differences in the 50%ile (*i.e.*, the median) can be conducted. The differences in the slopes (H values) of the curves can also be compared. To conduct the statistical comparison of the curves, a PRCF curve is derived for each subject. PRCF values at "X" percentiles are calculated for each individual subject. Means and errors are then calculated and analyzed using the appropriate statistical tests.

APPENDIX 2
TOP-DOWN METABOLIC CONTROL ANALYSIS

A2.1 DEFINITIONS AND EQUATIONS

As described in Chapter 3, Section 3.1.8, top-down metabolic control analysis was used to study the oxidative phosphorylation system. The flux through each of the blocks of reactions was required to determine control within this system.

There are three fluxes (*J*) through the oxidative phosphorylation system:

(1) J_S = flux leading to the production of PMF by substrate oxidation (or ETC in isolated mitochondria)
(2) J_P = flux due to the dissipation of PMF by the ATP-synthesizing (phosphorylation) reactions
(3) J_L = flux due to the dissipation of PMF by proton leak reactions

Where the subscript refers to a block of reactions in the oxidative phosphorylation system:
S= substrate oxidation
P = phosphorylation
L = leak

Each of these fluxes is measured directly as rates of oxygen consumption. Each experiment was performed in the non-phosphorylating respiration state (*State 4*), and in the maximal phosphorylating state (*State 3*).

A2.1.1 ELASTICITY COEFFICIENTS

The ***elasticity*** (*i.e.*, overall kinetics) expresses how the flux through a reaction block varies with the change in the concentration/amount of the intermediate. In the oxidative phosphorylation system PMF (also referred to as Δp) is the intermediate.

Elasticity is determined from the normalized slope of a plot of respiration rate against Δp. The slope of the graph is scaled by the values of the respiration rate and Δp at the reference state (*i.e.*, State 4 or 3).

Elasticities are described quantitatively in the form of elasticity coefficients. The following equations are used to calculate an elasticity coefficient (ε^{Y}_{X}), where ε is elasticity, Y= the block of reaction (S= substrate oxidation, P=phosphorylating and L=leak), and X is Δp.

- **Elasticity of the substrate oxidation reactions to changes in Δp:**

$$*\varepsilon^{S}_{\Delta p} = \frac{dJs}{d\Delta p} \cdot \frac{\Delta p}{J_S}$$

- **Elasticity of the leak reactions to changes in Δp :**

$$*\varepsilon^{L}_{\Delta p} = \frac{dJ_L}{d\Delta p} \cdot \frac{\Delta p}{J_L}$$

- **Elasticity of the phosphorylation reactions to changes in Δp**

$$*\varepsilon^{P}_{\Delta p} = \frac{d(Js\text{-}J_L)}{d\Delta p} \cdot \frac{\Delta p}{J_S\text{-}J_L}$$

A2.1.2 FLUX CONTROL COEFFICIENTS

A **Flux Control Coefficient (C)** describes the extent to which changes in the activities of the blocks of reactions affect the flux through each of the blocks in the metabolic system being studied. These coefficients can be calculated using the elasticity values. The sum of all of the flux control coefficients for a given pathway is always 1.0. Thus if one block of reactions has a high value (e.g., near 1.0) it indicates that the block of reactions has a great degree of control over the flux through the entire system. Conversely, a value close to 0 indicates that the block has little control over flux through the system.

In the following equations, C^{Y}_{Z} C refers to the flux control coefficient, Y = J_X and refers to the flux a particular the block of reactions, and Z refers to the particular block of reactions for which the control strength is being determined.

- **Control exerted by substrate oxidation over substrate oxidation flux:**

$$*C^{Js}_{S} = \frac{(J_P \cdot *\varepsilon^{P}_{\Delta p} + J_L \cdot *\varepsilon^{L}_{\Delta p})}{(J_P \cdot *\varepsilon^{P}_{\Delta p} + J_L \cdot *\varepsilon^{L}_{\Delta p} - J_S \cdot *\varepsilon^{S}_{\Delta p})}$$

- **Control exerted by phosphorylation over substrate oxidation flux:**

$$*C^{Js}_{P} = \frac{J_P \cdot (1 - *C^{Js}_{S})}{J_S}$$

- **Control exerted by proton leak over substrate oxidation flux:**

$$*C^{Js}_{L} = \frac{J_L \cdot (1 - *C^{Js}_{S})}{J_S}$$

- **Control exerted by substrate oxidation over phosphorylation flux:**

$$*C^{Jp}_{S} = \frac{(J_S \cdot *\varepsilon^{P}_{\Delta p})}{(J_P \cdot *\varepsilon^{P}_{\Delta p} + J_L \cdot *\varepsilon^{L}_{\Delta p} - J_S \cdot *\varepsilon^{S}_{\Delta p})}$$

- **Control exerted by phosphorylation over phosphorylation flux:**

$$*C^{Jp}{}_{P} = (1 - J_P) \cdot \frac{*C^{Jp}{}_{S}}{J_S}$$

- **Control exerted by proton leak over phosphorylation flux:**

$$*C^{Jp}{}_{L} = -J_L \cdot \frac{*C^{Jp}{}_{S}}{J_S}$$

- **Control exerted by substrate oxidation over proton leak:**

$$*C^{JL}{}_{S} = \frac{(J_S \cdot *\varepsilon^{L}{}_{\Delta p})}{(J_P \cdot *\varepsilon^{P}{}_{\Delta p} + J_L \cdot *\varepsilon^{L}{}_{\Delta p} - J_S \cdot *\varepsilon^{S}{}_{\Delta p})}$$

- **Control exerted by phosphorylation over proton leak flux:**

$$*C^{JL}{}_{P} = -J_P \cdot \frac{*C^{JL}{}_{S}}{J_S}$$

- **Control exerted by proton leak over proton leak flux:**

$$*C^{JL}{}_{L} = (1 - J_L) \cdot \frac{*C^{JL}{}_{S}}{J_S}$$

A2.1.3 CONCENTRATION CONTROL COEFFICIENTS

A **Concentration Control Coefficient ($C^{Y}{}_{Z}$)** describes the proportional control by the blocks of reactions in a system over the amount of intermediate in the system. The concentration control coefficients add up to zero, the components exerting the greatest control will have the largest absolute values.

In the following equations, $C^{Y}{}_{Z}$ C refers to the concentration control coefficient, Y = Δp (i.e., the intermediate in the system) and Z refers to the particular block of reactions for which the control strength is being determined.

- **Control exerted by substrate oxidation reactions to PMF:**

$$*C^{\Delta p}{}_{S} = \frac{J_S}{(J_P \cdot *\varepsilon^{P}{}_{\Delta p} + J_L \cdot *\varepsilon^{L}{}_{\Delta p} - J_S \cdot *\varepsilon^{S}{}_{\Delta p})}$$

- **Control exerted by phosphorylation reactions to PMF:**

$$*C^{\Delta p}{}_{P} = -J_P \cdot \frac{*C^{\Delta p}{}_{S}}{J_S}$$

- **Control exerted by the leak reactions to PMF:**

$$*C^{\Delta p}{}_{L} = -J_L \cdot \frac{*C^{\Delta p}{}_{S}}{J_S}$$

May 2001 – Aug 2001 **Research Assistant**
University of Ottawa, Faculty of Medicine, Department of BMI
Supervisor: Dr. Mary-Ellen Harper

ACADEMIC AWARDS

Sept 2006 **Health Canada Postdoctoral Fellowship**
- Research Grant ($ 43,000)
- Declined

May 2006 – Dec 2006 **University of Ottawa Excellence Scholarship**
- Full tuition coverage (~$6,000)

May 2004 – April 2006 **NSERC Postgraduate Scholarship (PGS D)**
- Research Grant ($42,000/2 years)

May 2003– April 2006 **University of Ottawa Excellence Scholarship**
- Full tuition coverage (~$5,000)

May 2003 – April 2004 **Ontario Graduate Scholarship**
- Research Grant ($ 15,000)

Sept 1997 – May 2001 **Metropolitan Life Merit Scholarship**
- Educational Grant ($1,800/year)

Sept 2007 – May 1998 **University of Ottawa Excellence Scholarship**
- Tuition coverage ($1,800)

HONOURS AND RESEARCH AWARDS

May 2005 **Canadian Institutes of Health Research**
- Certificate of Merit for outstanding volunteer in science promotion

April 2004 **Dept. Biochemistry, Microbiology and Immunology**
Graduate Student Poster Day
- Best Ph.D. Poster Presentation

June 2003 **Canadian Society for Nutritional Sciences (CSNS)**
Nestle Nutrition Graduate Student Oral Presentation Competition
- 2nd Place

June 2003 **Christine Gagnon Memorial Travel Award**
- Sponsored by the CSNS

May 2003 **Canadian Institutes of Health Research**
- Certificate of Merit for outstanding volunteer in science promotion

June 2002 **Canadian Society for Nutritional Sciences (CSNS)**
Nestle Nutrition Graduate Student Oral Presentation Competition
- FINALIST

June 2002 **Christine Gagnon Memorial Travel Award**
- Sponsored by the CSNS

May 2002 **Canadian Institutes of Health Research**
- Certificate of Merit for outstanding volunteer in science promotion

Nov 2001 **Center for Catalysis Research and Innovation**
- Best Poster Presentation

April 2001 **Faculty of Science, University of Ottawa**
- Dean's Honour List

VOLUNTEER EXPERIENCE

LEADERSHIP/INIITATIVE

Jan 2006-present **BMI Graduate Students' Association**
- Vice-President Finance

Sept 2002 – Dec 2005 **BMI Graduate Students' Association**
- Co-President

June 2002 – June 2005 **Canadian Society for Nutritional Sciences**
- Student Representative

Sept 2001 – June 2004 **University of Ottawa Graduate Students' Association**
- Director without portfolio and council member

POLICY

Aug 2005 – Aug 2005 **Health Sciences Research Ethics Board Member**
University of Ottawa
- Responsible for reviewing ethics applications

COMMUNICATION/SCIENCE PROMOTION

Sept 2001 – Aug 2005 **Let's Talk Science Representative**
University of Ottawa

June 2004 - Jan 2005 **CHIN Radio (97.9 FM)**
Morning Italian Program "Espresso Corretto"
- Health Correspondent

COMMUNITY

Sept 1996 –present **St. Anthony's Youth Choir**

ORAL PRESENTATIONS

June 2003 **Canadian Federation for Biological Societies**
Annual Meeting; Ottawa, ON

June 2002 **Canadian Federation for Biological Societies**
Annual Meeting; Montreal, QC

POSTER PRESENTATIONS

June 2006 **American Aging Association**
Annual Meeting; Boston MA

June 2005 **Canadian Federation for Biological Sciences**
Annual Meeting; Guelph, ON

Nov 2004 **Aging and Human Disease Workshop organized by Cell Press and University of California (San Diego)**
Tuscany, Italy

April 2004 **Experimental Biology**
Annual Meeting; Washington, DC

June 2003 **Canadian Federation for Biological Societies**
Annual Meeting; Ottawa, ON

June 2002 **Canadian Federation for Biological Societies**
Annual Meeting; Montreal, QC

April 2004 **Experimental Biology**
Annual Meeting; San Diego, CA

RESEARCH PUBLICATIONS

BOOK CHAPTER

Harper ME, Doucet L, **BEVILACQUA L**, Costford S and Gerrits M. Uncoupling Protein 3 (UCP3) and Fatty Acid Metabolism in Muscle. In: Progress in Obesity Research: 9. Eds. G. Mederios-Neta, A. Halpern and C. Bouchard. John Libbey&Co. Eastleigh, England.

PEER-REVIEWED ARTICLES

Costford S, Seifert EL, Bezaire V, Gerrits M, **BEVILACQUA L**, Harper ME. The energetic implications of Uncoupling Protein-3 in skeletal muscle. Journal of Applied Physiology, Nutrition and Metabolism. Submitted Oct 17 2006, Under revision.

Scime A, Grenier G, Huh MS, Gillespie MA, **BEVILACQUA L**, Harper ME, Rudnicki MA. Rb and p107 Regulate Preadipocyte Differentiation into White versus Brown Fat through Repression of PGC-1α. Cell Metabolism,2(5):283-95. 2005

BEVILACQUA L, Ramsey JJ, Hagopian K, Weindruch R, Harper ME. Long-term caloric restriction increases UCP3 content but decreases proton leak and reactive oxygen species production in rat skeletal muscle mitochondria. Am J Physiol Endocrinol Metab. 2005 Sep;289(3):E429-38. Epub 2005 May 10.

Ramsey JJ, Harper ME, Humble SJ, Koomson EK, Ram JJ, **BEVILACQUA L**, Hagopian K. Influence of mitochondrial membrane fatty acid composition on proton leak and H2O2 production in liver. Comp Biochem Physiol B Biochem Mol Biol. 2005 Jan;140(1):99-108.

Harper ME, **BEVILACQUA L**, Hagopian K, Weindruch R, Ramsey JJ. Ageing, oxidative stress, and mitochondrial uncoupling. Acta Physiol Scand. 2004 Dec;182(4):321-31. Review

BEVILACQUA L, Ramsey JJ, Hagopian K, Weindruch R, Harper ME. Effects of short- and medium-term calorie restriction on muscle mitochondrial proton leak and reactive oxygen species production. Am J Physiol Endocrinol Metab. 2004 May;286(5):E852-61. Epub 2004 Jan 21.

Son C, Hosoda K, Ishihara K, **BEVILACQUA L**, Masuzaki H, Fushiki T, Harper ME, Nakao K. Reduction of diet-induced obesity in transgenic mice overexpressing uncoupling protein 3 in skeletal muscle. Diabetologia. 2004 Jan;47(1):47-54. Epub 2003 Dec 12.

Ramsey JJ, Hagopian K, Kenny TM, Koomson EK, **BEVILACQUA L**, Weindruch R, Harper ME. Proton leak and hydrogen peroxide production in liver mitochondria from energy-restricted rats. Am J Physiol Endocrinol Metab. 2004 Jan;286(1):E31-40.

Harper ME, Antoniou A, **BEVILACQUA L**, Bezaire V, Monemdjou S. Cellular energy expenditure and the importance of uncoupling. J. Ani Sci. 2002 Jan 80: 1-8.